Synthesis, GC–MS, GC–MS/MS, GC–IR and chromatographic studies on cathinone derivatives related to methylenedioxypyrovalerone (MDPV)

by

Younis Faraj Hamad Abiedalla

A dissertation submitted to the Graduate Faculty of
Auburn University
in partial fulfillment of the
requirements for the degree of
Doctor of Philosophy

Auburn, Alabama
December 15, 2018

Keywords: designer drugs, bath salts, GC–MS, GC–IR, MS/MS, regioisomers.

Approved by

C. Randall Clark, Chair, Professor of Medicinal Chemistry
Jack DeRuiter, Professor of Medicinal Chemistry
Forrest Smith, Associate Professor of Medicinal Chemistry
Angela Calderon, Associate Professor of Medicinal Chemistry

Abstract

This project will address issues of resolution and discriminatory capabilities for cathinone derivatives (regioisomeric and homologous groups) providing additional reliability and selectivity for forensic evidence and analytical data on new analytes of the so-called bath salt-type drugs of abuse. A number of aminoketones have appeared on the illicit drug market in recent years including methcathinone, mephedrone, methylone and MDPV (3,4-methylenedioxypyrovalerone). These substances represent a variety of aromatic ring substituent, hydrocarbon side-chain and amino group modifications of the basic cathinone molecular skeleton.

Exploration and designer development in the aminoketone drugs using models based on substituted amphetamines and related phenethylamines is likely to continue for many years. Current clandestine designer drug development concepts used for amphetamine-type molecules can be applied directly for aminoketone analogues. Production of these drugs can be based on common readily available precursor chemicals. These numerous precursor substances are commercially available and would not prevent the further clandestine/designer exploration of this group of compounds. It could be argued that isomer differentiation is not necessary in forensic drug science because of the Controlled Substance Analogue Act. However, the courts should expect forensic drug chemistry to be able to identify a substance as an individual compound, not report it as an unknown member of a large group of isomeric substances. Furthermore, the forensic chemist must identify the compound in order to know if it is an analogue of a controlled substance.

These circumstances all point to the strong need for a thorough and systematic investigation of the forensic chemistry of these substituted aminoketones.

The broad objective of this research is to improve the specificity, selectivity and reliability of the analytical methods used to identify ring substituted aminoketones and related compounds. This improvement will come from methods, which allow the forensic analyst to identify specific regioisomeric forms of substituted aminoketones among many isomers of mass spectral equivalence. Mass spectrometry is the most common method of confirmation in forensic analysis. This project will provide methodology and analytical data to discriminate between those regioisomeric molecules having the same molecular weight and major fragments of equivalent mass (i.e. identical mass spectra). Furthermore, this work will anticipate the future appearance of some designer aminoketones and develop analytical reference data and analytical reference standards for these compounds.

The initial phase of this work is the organic synthesis of aminoketones of varying aromatic ring substituents, hydrocarbon side-chains and amino groups. In this phase of the work more than 60 substituted aminoketones of potential forensic interest will be evaluated. The analytical phases will consist of chemical characterization, using tools common to forensic science labs such as MS and IR and these studies will be carried out on each of the compounds. The chromatographic retention properties for each series of isomers will be evaluated by gas chromatographic techniques on a variety of stationary phases. These studies will establish a structure-retention relationship for the regioisomers aminoketones on selected chromatographic stationary phases.

The results of this project will significantly increase the forensic drug chemistry knowledge base for aminoketone-type designer drugs. When compounds exist which produce the same mass

spectrum (same MW and fragments of equivalent mass) as the drug of interest, the identification by GC–MS must be based entirely upon the ability of the chromatographic system to resolve these substances. Chromatographic co-elution of compounds having identical mass spectra can lead to misidentification. This is a critical issue when some of the MS equivalent compounds are controlled substances. This project involves the synthesis and generation of complete analytical profiles as well as methods of differentiation for those homologous and regioisomeric substances related to MDPV.

Acknowledgments

First and foremost, my thanks and all praise go to Allah (SWT) without Whom this life is nonexistent and absolutely meaningless. I thank Him for giving me the ability and patience to persevere through this process and I ask for His Guidance in becoming someone who continually seeks useful knowledge and delivers it to others.

To my chair, Dr. Randall Clark, who regardless of how busy I know he was, always made me feel that I was the top priority as soon as I walked in his office. Without his constructive feedback, guidance, support and patience, I would not have been able to complete my dissertation.

To the rest of my committee, Dr. Jack DeRuiter, Dr. Forrest Smith and Dr. Angela Calderon, have each provided helpful feedback and have been great teachers who have prepared me to get to this place in my academic life. This project would not be nearly as good without their help. I would also like to thank former postdoctoral fellows, Dr. Karim Hafiz and Dr. Amber Thaxton for their sincere help and support in the lab.

We gratefully acknowledge the National Institute of Justice, Office of Justice Programs, U. S. Department of Justice (Award No. 2013-DN-BX-K022) for supporting portions of this research project.

To my father, Faraj (May Allah bless him), who has been the driving force behind my motivation to excel as an academician, and more importantly, as a human being. To my mother, Mabroka, whose devotion to her seven sons and two daughters and her sincere desire for our success has been immeasurable. I would especially like to thank my family. My wife, Azeza has been extremely supportive of me throughout this entire process and has made countless sacrifices to help me get to this point. My children, Faraj and Saad, have continually provided the requisite breaks from philosophy and the motivation to finish my degree with expediency.

Finally yet importantly, I would like to thank my sponsor, The Ministry of Higher Education in Libya, and the administrator of the sponsorship program, Canadian Bureau for International Education (CBIE) in Canada, for giving me this opportunity and for their support and help throughout the duration of my study.

Table of Contents

List of Tables

List of Figures

List of Schemes

List of Abbreviations

MDPV	3,4-methylenedioxypyrovalerone
MS	Mass spectrometry
IR	Infrared
MW	Molecular weight
GC–MS	Gas chromatography–mass spectrometry
NDIC	National Drug Intelligence Center
4-MMC	4-methylmethcathinone
4-FMC	4-fluoromethcathinone
MDMC	3,4-methylenedioxy-*N*-methylcathinone
EMCDDA	European Monitoring Center for Drugs and Drug Addiction
CNS	Central nervous system
MPPP	4-methyl- α-pyrrolidinopropiophenone
MOPPP	4-methoxy- α-pyrrolidinopropiophenone
3,4-DMMC	3,4-dimethylmethcathinone
α-PVP	α-pyrrolidinovalerophenone
NPS	New psychoactive substances
UNODC	United Nations Office on Drugs and Crime
AAPCC	American Association of Poison Control Centers
DEA	Drug Enforcement Administration

MDPPP	3',4'-methylenedioxy-α-pyrrolidinopropiophenone
MDPBP	3',4'-methylenedioxy-α-pyrrolidinobutiophenone
NRG-1	(Neuregulin-1)
BBB	Blood-brain barrier
MDMA	Methylenedioxymethamphetamine
CYP2D6	Cytochrome- P450 (2D6)
LC–MS	Liquid chromatography–mass spectrometry
COMT	Catechol *O*-methyltransferase
MAO	Monoamine oxidase
DAT	Dopamine transporter
NET	Norepinephrine transporter
SERT	Serotonin transporter
LC–MS/MS	Liquid chromatography–mass spectrometry/mass spectrometry
LC–HR-MS	Liquid chromatography–high-resolution-mass spectrometry
m/z	Mass/charge ratio
EI	Electron ionization
eV	Electron volt
GC–MS/MS	Gas chromatography–mass spectrometry/mass spectrometry
GC–IR	Gas chromatography–infrared
EI-MS	Electron ionization-mass spectrometry
cm^{-1}	Centimeter (wavenumber)
NMR	Nuclear magnetic resonance
D	Deuterium

$[M+H]^+$	Protonated molecular ion
TLC	Thin layer chromatography
cm	Centimeter
µm	Micrometer
nm	Nanometer
DMF	Dimethylformamide
°C	Degree centigrade
m	Meter
mm	Millimeter
i.d.	Internal diameter
CI-MS	Chemical ionization-mass spectrometry
MS-MS	Mass spectrometry-mass spectrometry
GC–CI-MS	Gas chromatography–chemical ionization-mass spectrometry
CI	Chemical ionization
Da	Dalton
AMD	Automated Method Development
P-2-P	1-phenyl-2-propanone
P-1-P	1-phenyl-1-propanone
LAH	Lithium aluminum hydride
DMPV	Dimethoxypyrrovalerone
HPLC	High-performance liquid chromatography
THF	Tetrahyrdofuran
s	Second

ml	Milliliter
psi	Pound-force per square inch
µl	Microliter
IRD-3	Infrared detector-Model 3
f.d.	Film depth
TP	Temperature program
mol	Mole
N	Normal (normality)

1. Review of relevant literature

1.1. Introduction

Cathinone is a major naturally occurring psychoactive substance found in the leaves of *Catha edulis* plant, commonly known as khat. For centuries, "khat sessions" have played a very important role in the social and cultural traditions around Saudi Arabia and most East African countries. The identification of cathinone (a Schedule I controlled substance) as the main psychoactive component of the khat leaves with amphetamine like pharmacological effects has led to the synthesis of several derivatives, which are structurally similar to this so-called natural amphetamine [Valente *et al*, 2014].

The first cathinone derivatives were originally synthesized at the beginning of the 20th century for therapeutic purposes. However, the recreational use of these synthetic compounds only gained public attention in the last decade [Kelly, 2011]. These cathinones emerged in the recreational drug markets as legal alternatives ("legal highs") to amphetamine and cocaine. They are included in a large group of psychoactive substances generally designated by "legal highs". These derivatives are abused indiscriminately for their cocaine and amphetamine-like effects. Furthermore, these synthetic cathinones are typically marketed as "**bath salts**" or "plant food" and are sold under various names (Ivory Wave, Blizzard, etc.) labeled "not for human consumption" in order to bypass legislative restrictions in several countries [Bretteville-Jensen *et al*, 2013; Fass *et al*, 2012; Van Hout and Brennan, 2011].

Based on a report from The National Drug Intelligence Center (U. S. Department of Justice), there has been a significant increase in the production, distribution and use of synthetic cathinones or "bath salt" drugs across the U. S. and abroad over the past several years [U. S. DOJ-NDIC, 2011]. The synthetic cathinones that have appeared in clandestine samples to date include a number of aromatic aminoketones (shown in Figure 1) such as 3,4-methylenedioxypyrovalerone (MDPV), 4-methylmethcathinone (mephedrone, 4-MMC), *N*-methylcathinone (also known as methcathinone, ephedrone or CAT), 4-fluoromethcathinone (also known as flephedrone or 4-FMC), and 3,4-methylenedioxy-*N*-methylcathinone (also known as methylone, MDMC, β-keto MDMA, or M1). These drugs are also structurally related to several Schedule IV and V prescription drugs including bupropion (Zyban®, Wellbutrin®), diethylpropion (Tenuate®), and pyrovalerone (Centroton®) [German *et al*, 2014; Lewin *et al*, 2014; Katz *et al*, 2014].

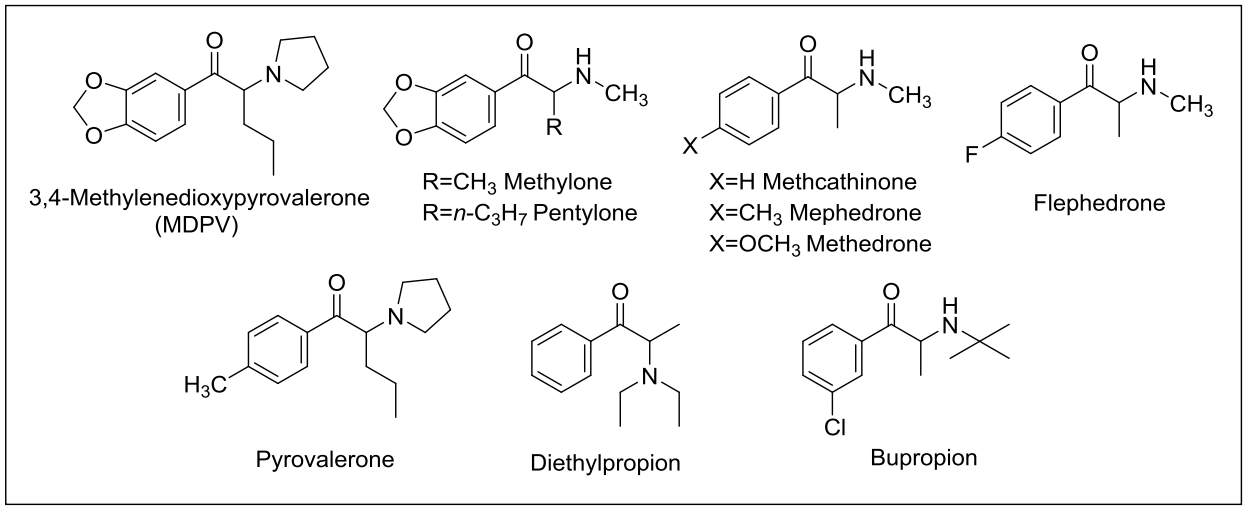

Figure 1. Structures of common cathinone/bath salts reported in recent forensic samples and their similarity to Schedule IV and V prescription drugs.

Ephedrone and mephedrone were the first two derivatives to be produced by the pharmaceutical industry in the late 1920's. Recently, mephedrone, methylone and MDPV rapidly emerged in recreational drug markets as the main ingredients of "bath salts". These were generally sold in retail establishments such as adult stores, independently owned convenience stores, gas

stations, head shops, and smart shops. The synthetic cathinone products, as well as their synthetic precursors, are also sold on many Internet sites, including popular Internet auction sites [Valente *et al*, 2014].

By the end of 2011, MDPV, mephedrone and methylone were provisionally scheduled in the United States under drug legislation for further analysis of their potential harm. Nonetheless, the legal control of these substances like cathinones is hard to attain success since they are easily replaced by novel compounds by minor structural modifications, which consequently leads to new and powerful analogues reaching the licit drug market [Jerry *et al*, 2012; Kelly, 2011; Prosser and Nelson, 2012]. The 2018 European Drug Report describes the synthetic cathinones as the second largest group of new substances monitored by The European Monitoring Center for Drugs and Drug Addiction (EMCDDA), with a total of 130 different substances identified from 2008–2018 in clandestine drug samples [EMCDDA, 2018].

1.2. Historical background

Khat is a flowering evergreen plant that grows in Africa and the southwestern of Arabian Peninsula. For centuries, the chewing of fresh khat leaves for their stimulant effects has been a tradition in cultural ceremonies at the so-called khat sessions [Balint *et al*, 2009]. The fresh leaves contain over 40 compounds, including alkaloids, tannins, flavonoids, vitamins and minerals [Cox and Rampes, 2003]. In the first attempts to identify the active constituents of khat, the psychoactive compound named *katin* was detected by [Fluckiger and Gerock, 1887] which was later identified by [Wolfes, 1930] as (+)-norpseudoephedrine and commonly named cathine in the next decades. Cathine was believed to be the main active component of khat even though it was not sufficient for the stimulant effect of khat. A β-keto analogue of cathine (cathinone) was isolated in the United

Nations' Narcotics Laboratory [UN, 1975] and early studies demonstrated that cathinone is 10-fold more potent than cathine and undergoes degradation rapidly which, explains the chewing of fresh leaves [Kalix and Khan, 1984].

Methcathinone (ephedrone, EPH) and 4-methylmethcathinone (mephedrone, MEPH) were synthesized by optimized methods in 1928/1929 in a study attempting to prepare a series of ephedrine homologues [Hyde *et al*, 1928]. These derivatives as well as other analogues were developed for therapeutic purposes due to their CNS stimulant effects [Canning *et al*, 1979]. However, due to their addictive potential (especially EPH) with cocaine-like stimulant effect, this has led to the abuse of EPH in the former Soviet Union and later in the U. S. [Young and Glennon, 1993; Emerson and Cisek, 1993]. Several cases of intoxications have been reported in the early 1990's which typically manifest as a Parkinsonism-like syndrome induced by manganese ingestion [Iqbal *et al*, 2012; Varlibas *et al*, 2009]. This is attributed to the easy synthesis of ephedrone at home through the oxidation of available pharmaceuticals that contain ephedrine or pseudoephedrine by potassium permanganate in the presence of acetic acid. In 1996, methylone was synthesized as an antidepressant but it never reached the legitimate pharmaceutical market [Dal Cason *et al*, 1997]. 4-Methyl-α-pyrrolidinopentanophenone (pyrovalerone) was synthesized in the 1970's for clinical use to treat obesity and chronic fatigue [Gardos and Cole, 1971] and was withdrawn due to its strong addiction potential [Sauer *et al*, 2009]. Unlike pyrovalerone, other psychoactive substances from the pyrrolidinophenone family such as 4-methyl- α-pyrrolidinopropiophenone (MPPP), 4-methoxy- α-pyrrolidinopropiophenone (MOPPP) and MDPV were never intended for clinical use [Peters *et al*, 2005].

Recreationally, the first-generation cathinones sold on the black market includes methylone in the mid-2000's under the name of explosion, first in Netherlands and Japan, and later in Australia and New Zealand [Zaitsu *et al*, 2011]. Mephedrone was first identified in Finland in 2008 and reported to The European Monitoring Center for Drugs and Drug Addiction (EMCDDA), another five synthetic cathinones were reported beside MEPH in 2008 [EMCDDA-Europol, 2009]. The fluorinated derivatives flephedrone and 3-fluoromethcathinone were the next to reach the black market in 2009, followed by butylone (β-keto-*N*-methylbenzodioxolylbutanamine) and ethylone (3,4-methylenedioxy-*N*-ethylcathinone) and finally MDPV [Archer, 2009; EMCDDA-Europol, 2009].

Due to the continuous search for new, legal and more powerful highs by the drug users, the synthesis of novel cathinone derivatives became a fruitful industry leading to the rapid emergence of new alternative derivatives every year. The first of the second-generation derivatives to be reported was naphyrone in 2010 by EU early-warning system (EMCDDA-Europol, 2011]. The third-generation cathinones such as 3,4-dimethylmethcathinone (3,4-DMMC) and α-pyrrolidinovalerophenone (α-PVP) started to show up at the same time [EMCDDA-Europol, 2010, 2011]. In 2017, 12 new cathinone derivatives were reported for the first time [EMCDDA, 2018]. Figure 2 summarizes the time line of the main events related to the khat plant and synthetic cathinones.

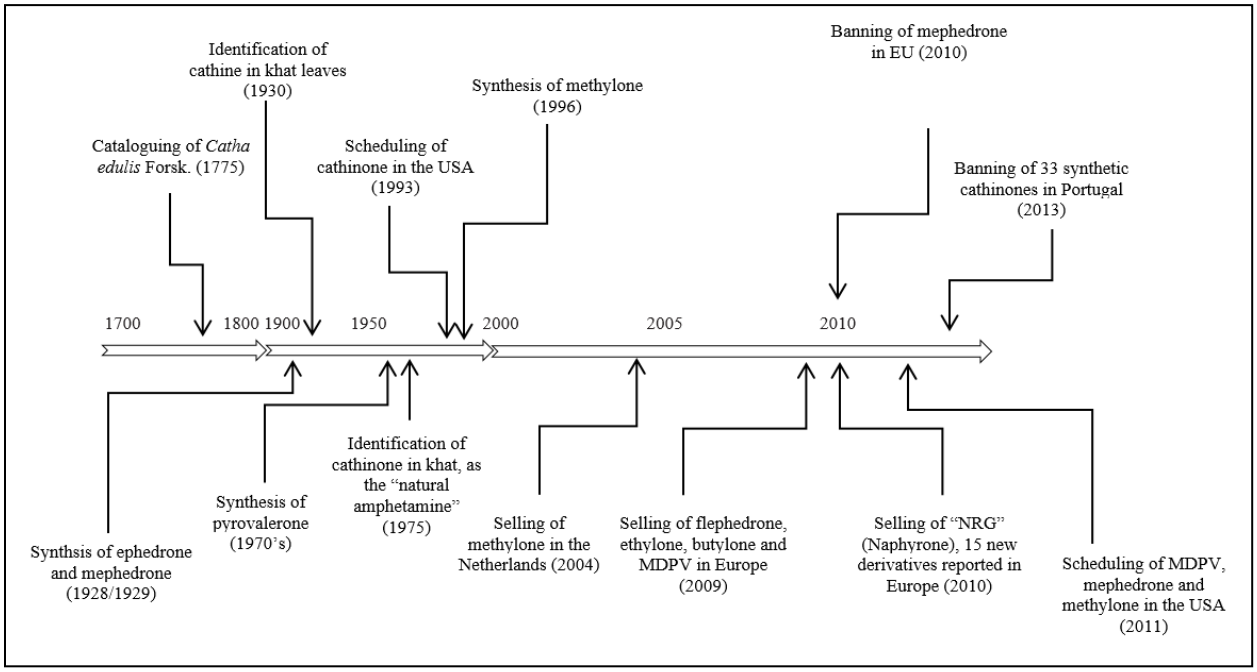

Figure 2. The major historical events associated with khat and synthetic cathinone derivatives [Valente *et al*, 2014].

1.3. Prevalence, patterns of use and legal status

The majority of khat consumers are located in Yemen and many East African countries like Somalia and Ethipoia [Al-Mugahed, 2008]. The use of khat leaves has been local to where these plants grow. However, improving distribution routes has led to the distribution of the leaves in Europe and U. S. and their costs depend on the freshness of these leaves [Alem *et al*, 1999; Klein *et al*, 2012].

In 1993, cathinone was placed into Schedule I of the Controlled Substance Act. Khat's legal status is often challenging and depends on the detectable amounts of cathinone. Currently, khat is illegal in U. S. and Canada and was banned in several European countries [Gezon, 2012]. In Europe, over 150 new psychoactive substances (NPS) were reported to the EMCDDA from

2005 to 2011, 34 were synthetic cathinones [EMCDDA-Europol, 2011]. Cathinone analogues together with cannabinoids represent two-thirds of these NPS that are included in a large group of so-called "legal highs" [EMCDDA, 2012]. The rapid proliferation of new psychoactive substances has led to the development of drug analogue laws attempting to control unspecified drug molecules not yet known to exist. In a recent report from The United Nations Office on Drugs and Crime, approximately 650 new psychoactive substances have been reported by 102 countries and territories since 2008 [UNODC, 2016]. Additionally, by the end of 2017, the EMCDDA was monitoring more than 670 new psychoactive substances that have been identified in Europe [EMCDDA, 2018]. A total of 75 new psychoactive substances appearing for the first time in 2015 according to the 2016 World Drug Report [UNODC, 2016]. This represents an increase from the 66 new psychoactive substances from clandestine samples reported during the previous year. A total of 20 of these first time reports in 2015 represented new synthetic cathinone derivatives and for the first time in history, the number of new synthetic cathinones rivaled the number of reported new synthetic cannabinoids, 20 and 21 respectively. In previous years (2012–2014), the vast majority of first time reports were for synthetic cannabinoids.

Bath salts are sold under a variety of brand names such as, Bloom, Blue Silk, Ivory Wave, Purple Wave and Vanilla Sky. They are purchased locally at head or smart shops or readily accessible and technically legal over the Internet [Coppola and Mondola, 2012]. Most of these allegedly legal substances are actually composed by previously banned compounds like MDPV, methylone and mepherdone [Brandt *et al*, 2010a]. These cathinones are commonly sold in the form of white or yellowish powder or in capsules [Karila and Reynaud, 2011]. MDPV is commonly available as white light tan powder and reported to have a slight odor (potato-like odor) upon exposure to air [Gorun *et al*, 2010].

The main routes for administration of these substances include ingestion either by swallowing capsules or swallowing powder wrapped in cigarette paper [Deluca *et al*, 2009] and nasal insufflation [Lindsay and White, 2012]. Other routes such as inhalation, intravenous injection and sublingual delivery have been also reported [Mas-Morey *et al*, 2012].

Even though statistics on the prevalence of synthetic cathinones use in the U. S. are limited. However, recent data from The American Association of Poison Control Centers (AAPCC) reported a significant increase in calls related to bath salts from 2010 (304 calls) to 2011 (6136 calls) [AAPCC, 2013] and these numbers are comparable to the statistics from the UK [Spyker *et al*, 2012].

It is important to note that the legal status of the synthetic cathinones vary greatly from country to country and even among states and this status is always changing based on new findings related to possible risks for public safety. Until the fourth trimester of 2011, the synthetic cathinones were unscheduled in the U. S. However, on October 21, 2011, the Drug Enforcement Administration scheduled MDPV, methylone and mephedrone under the Schedule I of Controlled Substances Act temporarily and later on, these three derivatives were permanently banned in the U. S. [DEA, 2011, 2012; Bretteville-Jensen *et al*, 2013]. Despite this recent scheduling as controlled substances within the U. S. and other countries, these derivatives, which are labeled and sold as bath salt products, are still on the market. This is attributed to the lack of information, reliability and consistency on the chemical composition of these products. Additionally, since the law is always a step behind, several new cathinone derivatives keep emerging in the recreational markets every year to avoid legal detection [Valente *et al*, 2014].

1.4. Chemistry

The synthetic cathinones are phenylalkylamine derivatives which are closley related to amphetamines except the ketone group being introduced at the β-position of the amino group. Therefore, these derivatives are often entitled β-keto amphetamines [Zaitsu *et al*, 2011]. These cathinones are analogues of the natural cathinone and they are synthesized by adding different substituents at different locations of the basic cathinone molecule as illustrated in Scheme 1.

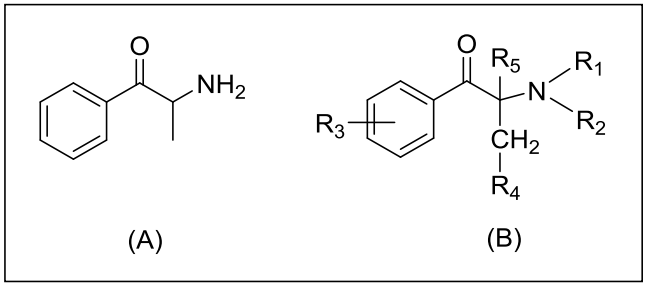

Scheme 1. Chemical structure of natural cathinone (A) and the general structure for the synthetic cathinones (B) [Valente *et al*, 2014].

This group of psychoactive compounds can be chemically separated into four families (see Figure 3). The fisrt analogues were those synthesized for therapeutic purposes including *N*-alkylated derivatives at R_1 and/or R_2 and in some cases alkyl or halogen substituents at R_3. The 3,4-methylenedioxy group [Dal Cason, 1997] can be added to the aromatic ring to make another family of these cathinones which are structurally related to 3,4-methylenedioxymethamphetamines [Zaitsu *et al*, 2011]. Another group of these synthetic cathinones is the derivatives of α-PPP which is characterized by a pyrrolidinyl substitution at the nitrogen atom [Westphal *et al*, 2007]. A combination of 3,4-methylenedioxy group and the pyrrolidinyl group produces the next family of synthetic cathinones which include MDPV, MDPPP (3',4'-methylenedioxy-α-pyrrolidinopropiophenone) and MDPBP (3',4'-methylenedioxy-α-pyrrolidinobutiophenone) [Kelly, 2011]. A unique structural characteristic has been reported in NRG-1 (Neuregulin-1)

products, which contain naphyrone [Brandt *et al*, 2010b] with its two isomeric forms (α-naphyrone and β-naphyrone).

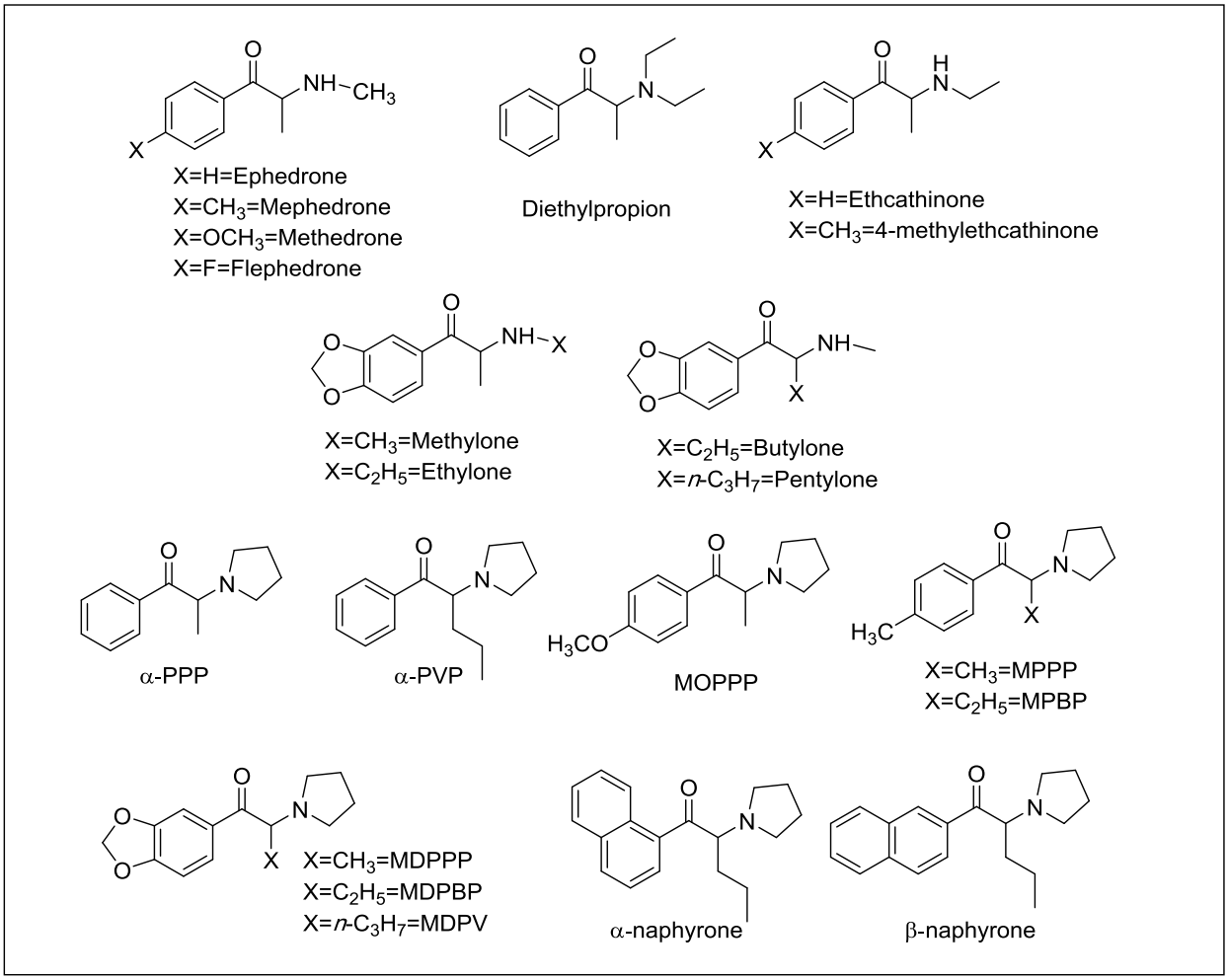

Figure 3. The chemical structures of the various synthetic cathinone derivatives with diverse substituents at R_1–R_4 positions [Valente *et al*, 2014].

1.5.Pharmacokinetics

Cathinone is the main active alkaloid in the khat plant and it was found that 100 g of fresh leaves have 78-343 mg of cathinone [Klein *et al*, 2012; Sakitama *et al*, 1995]. After half an hour of chewing khat leaves, the psychostimulant effects start to appear and last approximately 3 hours [Brenneisen *et al*, 1990]. Around 60 % of cathinone is absorbed from the oral mucosa, and further absorption occurs in the stomach and small intestine [Arunotayanun and Gibson, 2012]. The

ingested dose of cathinone is mainly eliminated as cathine and norephedrine metabolites [Brenneisen *et al*, 1986] with less than 7 % appearing unchanged in the urine.

The doses of synthetic cathinones vary among different derivatives and depend on the potency and route of administration [Prosser and Nelson, 2012]. Furthermore, the variable contents of the purchased bath salts, concentration and purity are also important factors that make the pharmacokinetics and pharmacodynamics unpredictable [Davies *et al*, 2010]. Structurally, the presence of β-keto group in cathinones increases the polarity of these compounds and thus, decreases their ability to cross the blood-brain barrier (BBB) [Schifano *et al*, 2011] and their potency compared to non-keto derivatives for example, methylone and MDMA, respectively [Cozzi *et al*, 1999]. The polarity issue occurs mainly in the *N*-alkylated derivatives and to less of an extent with the pyrrolidine substituted cathinones since the pyrrolidine ring greatly reduces the polarity of these derivatives [Coppola and Mondola, 2012]. This polarity issue is not the only factor that affects the transfer of these cathinones across the BBB, derivatives such as MDPV, methylone, ephedrone and mephedrone were reported to exhibit higher permeability (with MDPV being the highest) across the BBB and evidences show that these derivatives are actively transported into the brain via specific influx carriers [Simmler *et al*, 2013].

Like all synthetic cathinones, the natural cathinone undergoes phase I metabolism, which is the reduction of β-keto group into alcohol by the liver microsomal enzymes [Brenneisen *et al*, 1986] to yield cathine and norephedrine as shown in Scheme 2. It has been reported that the metabolism was determined to be stereoselective with the *S*-(–)-cathinone being primairly

metabolized to norephedrine, while *R*-(+)-cathinone reduced into cathine [Mathys and Brenneisen, 1992].

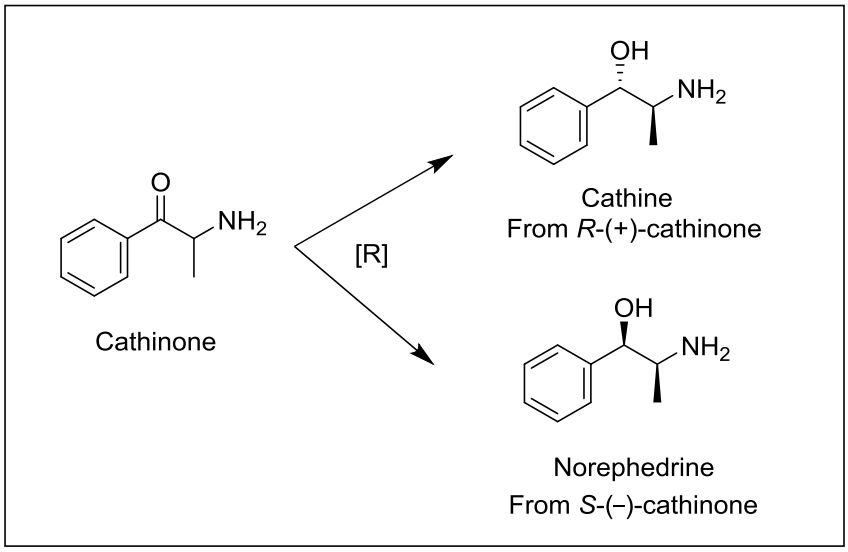

Scheme 2. Cathinone phase I metabolism (reduction) [Brenneisen *et al*, 1986].

This stereoselective reduction was also reported to proceed in synthetic derivatives like ephedrone yielding ephedrine [Sparago *et al*, 1996] which will further undergo *N*-demethylation to yield norephedrine [Paul and Cole, 2001]. Mephedrone can undergo phase I oxidation besides the *N*-demethylation (see Scheme 3). The methyl group on the phenyl ring can be oxidized to yield an alcohol, which upon oxidation yields a carboxylic acid followed by reduction at the β-keto group. It has been found that CYP2D6 is the main enzyme responsible for phase I metabolism of mephedrone [Pedersen *et al*, 2013]. The *N*-demethylation product of mephedrone can be either oxidized at the methyl group or reduced at the β-keto group [Meyer *et al*, 2010b].

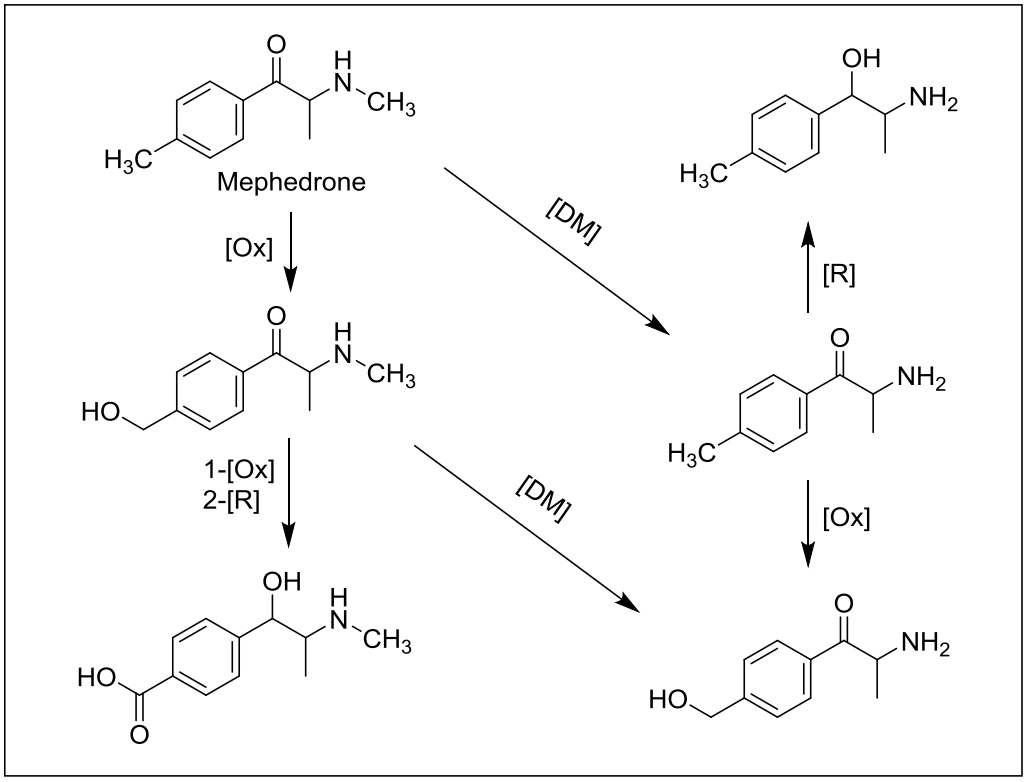

Scheme 3. Mephedrone phase I metabolic pathways determined in rat and human urine [Meyer *et al*, 2010b].

A recent *in vitro* method using LC–MS to identify phase I and II metabolites of mephedrone has been reported [Khreit *et al*, 2013] and it characterized seven phase II metabolites which resulted from the acetylation and/or glucuronidation as shown in Scheme 4.

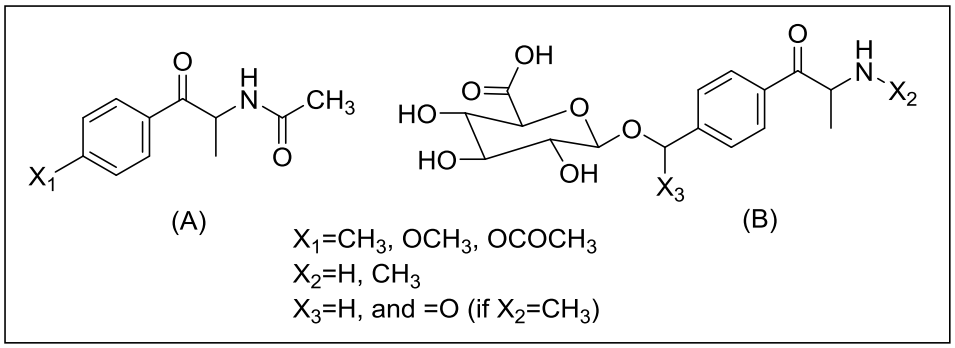

Scheme 4. Phase II metabolites of mephedrone, (A): Acetylation, (B): Glucuronidation [Khreit *et al*, 2013].

The metabolism of the 3,4-methylenedioxy *N*-alkylated cathinones like methylone and ethylone has been characterized [Kamata *et al*, 2006] and they exhibit three pathways shown in Scheme 5. The minor *N*-dealkylation pathway, the reduction of β-keto group and finally, the conversion of methylenedioxy group to the corresponding catechol (demethylenation) followed by *O*-methylation mediated by catechol *O*-methyltransferase (COMT). The phase II metabolism is likely the glucuronidation and sulfonation of the alcohol group [Shima *et al*, 2009].

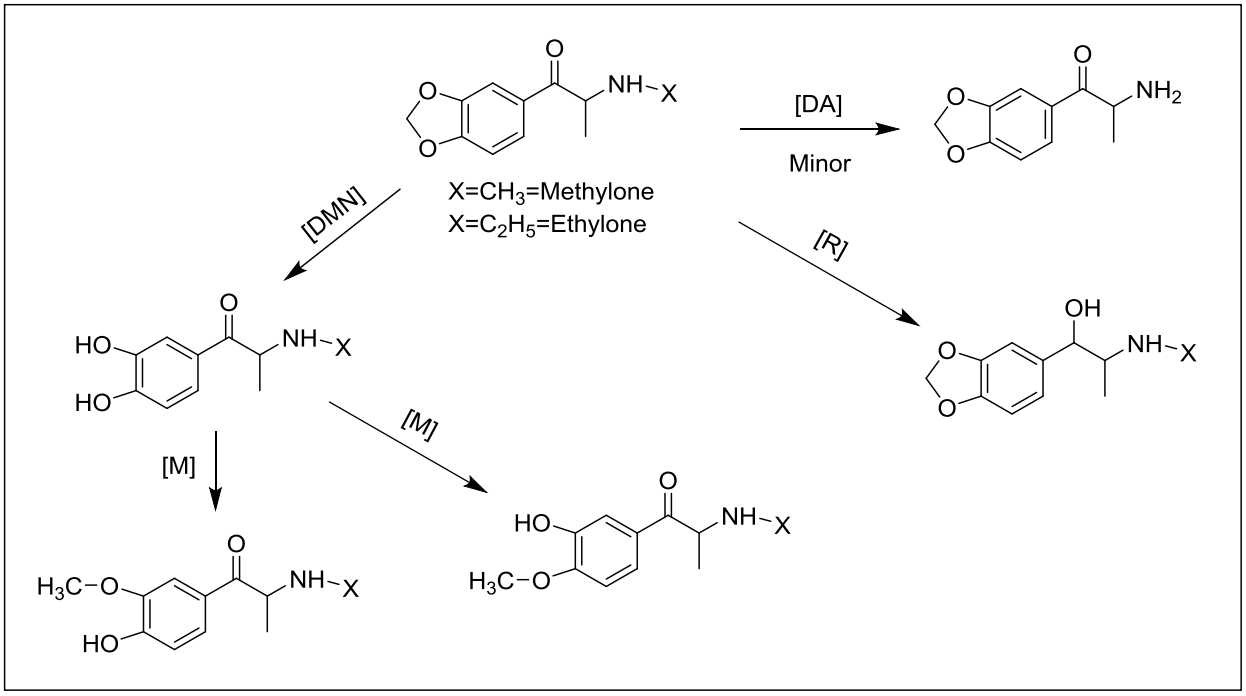

Scheme 5. Phase I metabolism of methylone and ethylone [Kamata *et al*, 2006; Zaitsu *et al*, 2009].

The pyrrolidine derivatives such as MDPV have been reported to undergo reduction of the β-keto group as well as the formation of catechol and methoxy catechol pyrovalerone as the main metabolites [Strano-Rossi *et al*, 2010]. Another study proposed further biotransformation for α-PVP and MDPV [Meyer *et al*, 2010a]. It involves the degradation of the pyrrolidine ring and the formation of the primary amine. It also involves hydroxylation of the side-chain and the 2-position of the pyrrolidine ring followed by dehydrogenation and subsequent ring opening and oxidation

of the aldehyde (see Scheme 6). The phenyl ring of α-PVP can be hydroxylated at 4-position [Sauer *et al*, 2009]. This hydroxylated product along with previous hydroxyl containing metabolites can undergo phase II metabolism. Flephedrone has been reported [Meyer *et al*, 2012; Pawlik *et al*, 2012] to undergo similar phase I metabolic reactions to α-PVP which include hydroxylation of the phenyl ring, β-keto reduction and *N*-demethylation to yield a primary amine. However, a slower metabolic transformation is predicted due to the stability of this compound, which results from fluorination and the resistance of C-F bond to the enzymatic cleavage [Westphal *et al*, 2010].

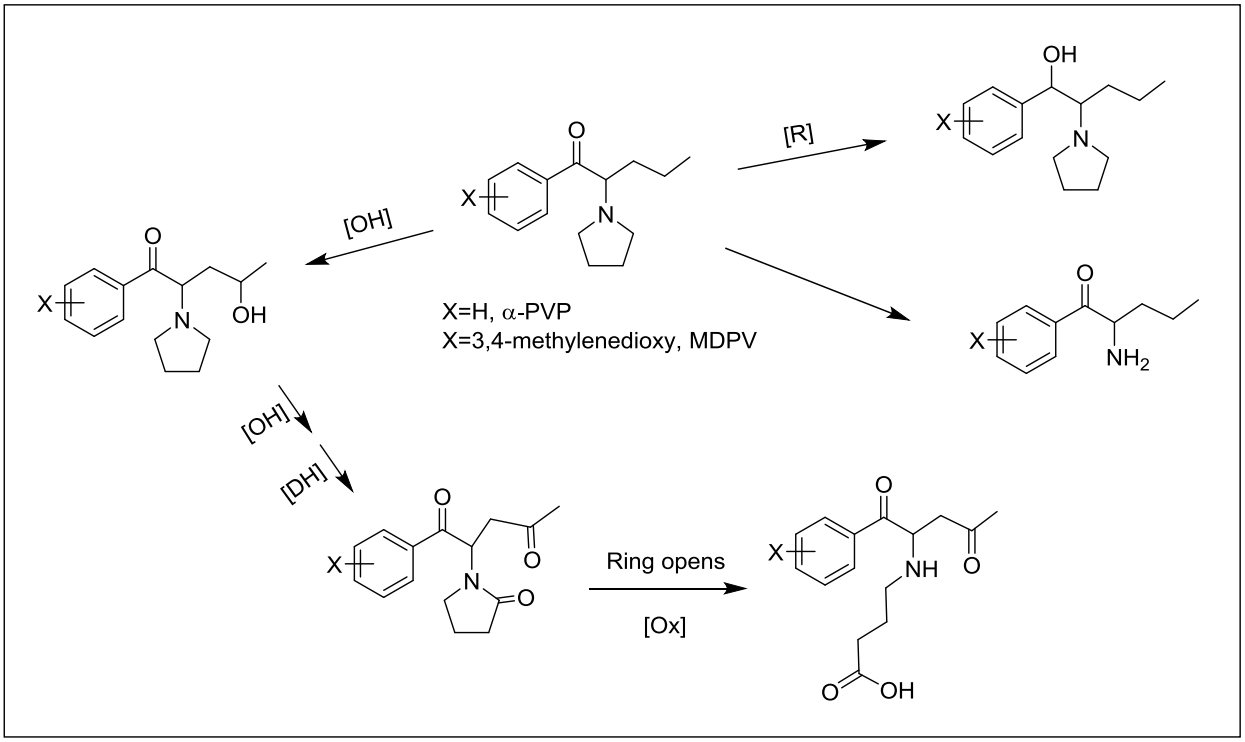

Scheme 6. Proposed phase I metabolism of α-PVP and MDPV [Meyer *et al*, 2010a; Sauer *et al*, 2009].

1.6. Pharmacodynamics

The designation of "natural amphetamine" given to cathinone is attributed to the structural similarity between cathinone and amphetamine, and the amphetamine-like subjective effects of khat [Kalix, 1992]. Cathinone is the β-keto analogue of amphetamine, while its metabolites are structurally related to norepinephrine. Like amphetamine, cathinone has both CNS stimulant and sympathomimetic effects and early pharmacological reports [Kalix 1983; Kalix and Braenden, 1985] on khat leaves demonstrated that cathinone and its metabolites can induce an amphetamine-like dopamine release with cathinone being the most potent. This higher potency is the consequence of the lipophilic character and favorable CNS penetration of cathinone compared to its metabolites [Kalix, 1991]. In regards to the peripheral effects, administration of cathinone or chewing khat results in sympathomimetic syndrome which is characterized by increased heart rate and blood pressure, mydriasis and hyperthermia. These effects suggest that cathinone induces the release of catecholamines at nerve endings in a similar manner to amphetamine [Kalix, 1992].

Similar to amphetamine, the methyl group at the α-position of the amino group prevents the inactivation of cathinone and its metabolites by monoamine oxidase (MAO) [Siegel *et al*, 1999]. Additionally, it has been reported that cathinone displays a greater inhibition of MAO than amphetamine and has a higher selectivity to MAO-B [Nencini *et al*, 1984; Osorio-Olivares *et al*, 2004]. This inhibition results in a decrease in dopamine degradation and consequently, the synaptic accumulation of this catecholamine.

Due to the limited information on the pharmacology of these "legal highs" including synthetic cathinones, research regarding these cathinones usually tend to compare the subjective effects with similar drugs like amphetamine and cocaine. In fact, synthetic cathinones and

amphetamines were reported to induce their effects by interacting with membrane monoamine transporters, which includes the dopamine transporter (DAT), norepinephrine transporter (NET) and serotonin transporter (SERT) leading to a higher concentration of these biogenic amines in the synaptic cleft [Baumann *et al*, 2012; Cameron *et al*, 2013]. The different affinity and selectivity of these cathinones toward the monoamine transporters produce a complex array of adrenergic and serotonergic effects. When interacting with monoamine membrane transporters, drugs can be classified as either substrates (translocated into cells where they disrupt vesicular storage and stimulate non-exocytotic release of neurotransmitters by reversing the normal direction of transporter flux), like amphetamines, or blockers like cocaine (inhibit the reuptake of the neurotransmitters) [Baumann *et al*, 2013a].

Recent studies with different *in vivo* and *in vitro* models showed that synthetic cathinones act as inhibitors for all catecholamine transporters and as monoamine releasers as well. However, the selectivity to these transporters vary among these derivatives. In contrast, MDPV (similarly, α-PVP) was reported to induce powerful cocaine-like effects. It acts as a pure monoamine-selective transporter blocker with higher potency for DAT and NET and lower potency for SERT in comparison to cocaine. Unlike amphetamine, these two derivatives (α-PVP and MDPV) do not promote monoamine release. As mentioned early, these cathinones have demonstrated a high permeability to an *in vitro* blood-brain barrier model with MDPV expressing a very high permeability [Baumann *et al*, 2012; Baumann *et al*, 2013a; Baumann *et al*, 2013b; Simmler *et al*, 2013].

1.7. Physiological and toxicological effects in animal studies

Several animal studies showed that the synthetic cathinones induce a dose-dependent hyperlocomotion (hyperactivity) especially MDPV [Lopez-Arnau *et al*, 2012; Marusich *et al*, 2012]. Some derivatives were implicated in cognitive processes [Wright *et al*, 2012], while others affected thermoregulation [Shortall *et al*, 2013]. Abuse liability and reinforcing properties of synthetic cathinones were supported by animal studies. MDPV was confirmed for its ability to induce self-administration patterns [Aarde *et al*, 2013a; Motbey *et al*, 2013]. Few cardiovascular and neurotoxic studies have been reported, and these are related to mephedrone, which demonstrated significant increase in heart rate, blood pressure and cardiac contractility [Meng *et al*, 2012] and significant toxic effects on dopaminergic nerve endings [Sparago *et al*, 1996].

1.8. Subjective effects and adverse toxic reactions

Chewing khat is characterized by rapid onset of psychostimulant effects [Alem *et al*, 1999; Dhaifalah and Santavy, 2004], which include increased energy, excitements, and sense of euphoria as described by users. Additionally, stimulant effects such as improved sense of alertness, enhanced self-esteem, and increased ability to concentrate, associate ideas and communicate have been also described by users, which contributes to the social character of this tradition. Long-term consumption of khat was reported to be associated with severe conditions like tooth decay, periodontal disease, oral cancer, acute and chronic liver disease, and cirrhosis as well as gastrointestinal disorders. Similar withdrawal symptoms to amphetamine and cocaine were reported. They include insomnia, lack of concentration and depression [Al-Motarreb *et al*, 2002; Fasanmade *et al*, 2007; Roelandt *et al*, 2011]. Severe cardiac, neurological, psychological and gastrointestinal complications are common following chronic use of khat and synthetic cathinones [Chapman *et al*, 2010; Corkery *et al*, 2011]. Subjective effects may vary among synthetic

cathinones and they generally include desired effects [Yohannan and Bozenko Jr, 2010] such as mild euphoria, increased empathy, decrease sense of insecurity and hostility and increased libido. Several unwanted subjective effects have been also reported, which include nausea and vomiting, headaches, vertigo, dizziness, palpitations and tremor, muscle twitching, confusion and impaired short-term memory, tachycardia and hypertension, anhedonia, depression with suicidal ideations, psychosis, tolerance and dependence [Bentur *et al*, 2008; Sammler *et al*, 2010; Coppola and Mondola, 2012].

Bath salts induced intoxication usually involves hallucinations, paranoia, panic attacks, aggressiveness, agitation, chest pain and seizures, hyponatremia and hyperthermia, acute liver failure, kidney injury and symptoms related to serotonin syndrome [AAPCC, 2013; James *et al*, 2011; Wood *et al*, 2010; Warrick *et al*, 2012]. Some of these side effects are associated with particular derivatives for example, hyperthermia is commonly associated with MDPV [Garrett and Sweeney, 2010; Levine *et al*, 2013]. The specific combination of these effects as well as their intensity and severity vary with each cathinone derivative.

1.9. Analytical detection of synthetic cathinones

The structural diversity of synthetic cathinones and the rapid appearance of new analogues of these cathinones present a practical limitation for traditional immunoassays (limitation for immunogen design and ultimately antibody-based screening), suggesting that either chromatographic or mass spectrometry-based screening techniques may be more appropriate. This limitation is attributed to the fact that the detection of synthetic cathinones using amphetamine immunoassays are often negative (Swortwood *et al*, 2014), results are highly variable between manufacturers (Regester *et al*, 2015) and cross reactivity for some synthetic cathinones may occur

with traditional amphetamine, methamphetamine or MDMA immunoassays (Toennes and Kauert, 2002; Truscott *et al*, 2013; de Castro *et al*, 2014). Confirmation of unknown drugs using hyphenated mass spectroscopic techniques such as gas chromatography–mass spectrometry (GC–MS) or liquid chromatography–mass spectrometry (LC–MS) rely upon reproducible chromatographic separation (retention time) and characteristic fragmentation (mass spectra).

1.9.1. Analytical detection of synthetic cathinones using GC–MS and LC–MS

GC–MS is the main tool used for the detection and identification of unknown drugs in forensic and other drug screening laboratories because of its excellent separation and identification abilities. LC–MS is a non-destructive exact mass determination technique. It utilizes chemical ionization to identify the molecular ion of drugs or their metabolites. It has been reported that GC–MS was used as a basic screening method for analysis of synthetic cathinones in human performance and postmortem toxicology, while LC–MS/MS confirmation method was used to analyze cases that had a history indicative of synthetic cathinone use or in which subject behavior suggested synthetic cathinone use [Marinetti and Antonides, 2013]. Furthermore, GC–MS and LC–high-resolution MS (LC–HR-MS) were utilized to identify phase I and II metabolites of MDPV and the human cytochrome- P450 (CYP) isoenzymes responsible for its main metabolic step(s) in rat and human urine and human liver microsomes [Meyer *et al*, 2010a]. Other studies indicated that LC–HR-MS was also utilized for the quantification of synthetic cathinones and metabolites in urine [Concheiro *et al*, 2013].

Although LC–MS and other hyphenated LC techniques are becoming more popular, GC–MS remains, the most widely used technique in routine forensic toxicology laboratories. Figure 4 shows the electron ionization mass spectrum of MDPV reported by Westphal [Westphal *et al*,

2009], which is heavily dominated by the *m/z* 126 base peak. The mass spectrum of MDPV also shows the fragment ions at *m/z* 149, 121, 97, 84 and 69 as well as other ions of low relative abundance.

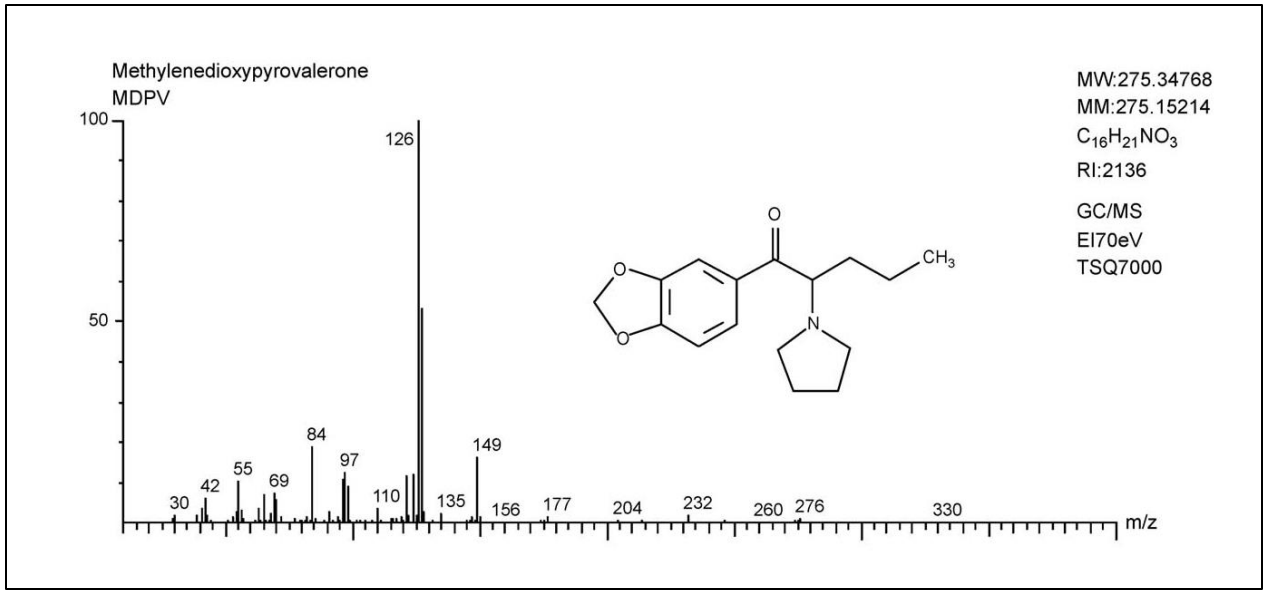

Figure 4. EI spectrum (70 eV) of MDPV [Westphal *et al*, 2009].

Scheme 7 below illustrates the EI mass spectral fragmentation pathway. The radical electron of the nitrogen atom induces a fast alpha-cleavage reaction (α-1) of the benzoyl bond and produces a base peak iminium cation at *m/z* 126. The alternative alpha-cleavage reaction (α-2) produces an iminium cation at *m/z* 232 with low intensity by the loss of an *n*-propyl radical. M-15 and M-29 alpha-cleavage fragments are found with low intensities at *m/z* 260 and *m/z* 246, respectively. Ionization at the carbonyl oxygen atom and alpha-cleavage reaction (α-3) yields a methylenedioxybenzoyl cation at *m/z* 149, and a subsequent (CO) loss is responsible for the ion at *m/z* 121 [Westphal *et al*, 2009]. The extensive fragmentation leaves very few qualifier ions. An additional challenge is that due to the tertiary amine, the pyrrolidine-type cathinones lack the active hydrogen necessary for commonly used or widely accepted approaches to derivatization. The use of multiple and complementary analytical methods such as GC–MS, GC–MS/MS and GC–IR are

often necessary for the specific identification of these cathinone derivatives as will be discussed in the next sections.

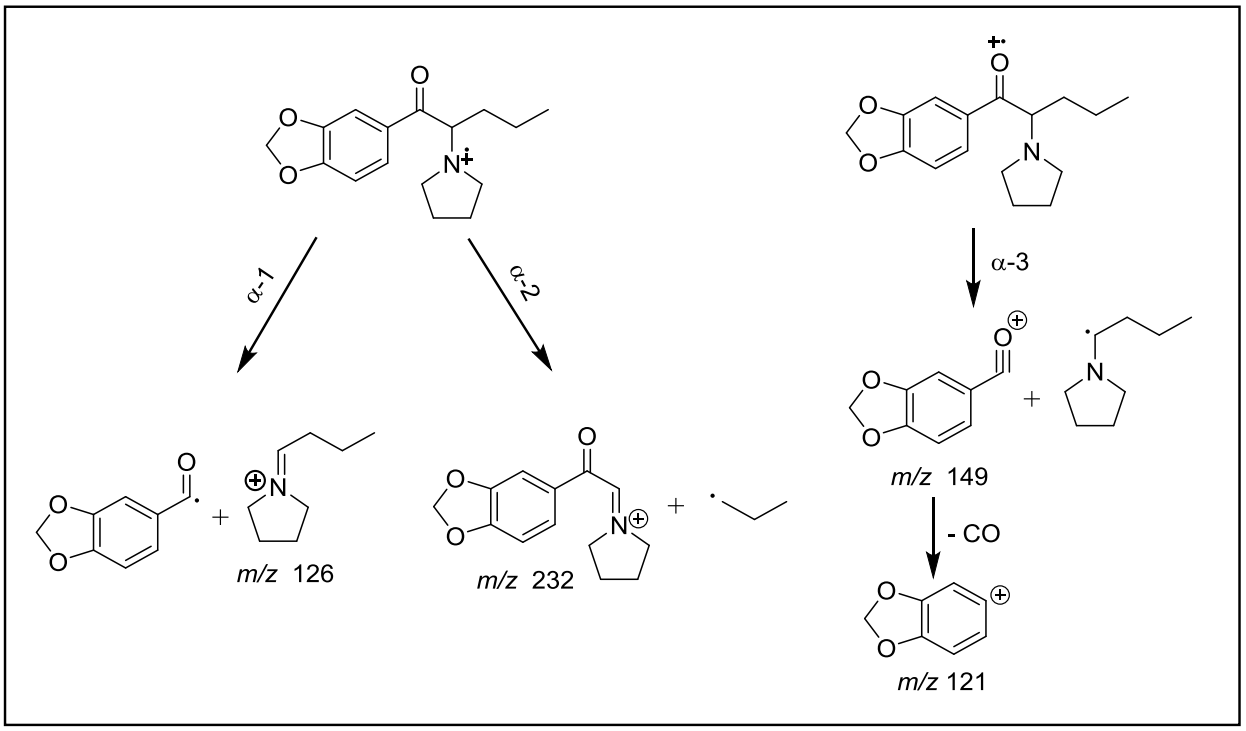

Scheme 7. Proposed EI-MS fragmentation pathway for MDPV [Westphal *et al*, 2009].

1.9.1.1. Thermal degradation of cathinone derivatives in GC–MS

Although GC–MS is considered the first choice for identification of unknown drugs, some alkylamine-type cathinones such as methcathinone and 4-methylmethcathinone are known to undergo thermal decomposition during GC–MS analysis. [Noggle *et al*, 1994; Tsujikawa *et al*, 2013b]. Despite the fact that derivatization has proven to be effective to avoid thermal degradation [Tsujikawa *et al*, 2013b], it is not applicable for pyrrolidine-type cathinones because of its tertiary amine structure as mentioned in the previous section.

Three factors have been evaluated [Tsujikawa *et al*, 2013a] to investigate the thermal decomposition of α-PVP during GC–MS analysis, namely the injection method (splitless or split,

split ratio), injector temperature and the surface activity on the inlet liner. The results showed that the split injection and the use of deactivated liner were effective to prevent the thermal decomposition of α-PVP (deactivated liner also minimized the degradation with splitless). The decomposition product of this derivative was proposed to be an enamine with the double bond located in the side-chain as demonstrated in Figure 5 shown below. The proposed structures of the fragment ions were supported by deuterium labeling experiment.

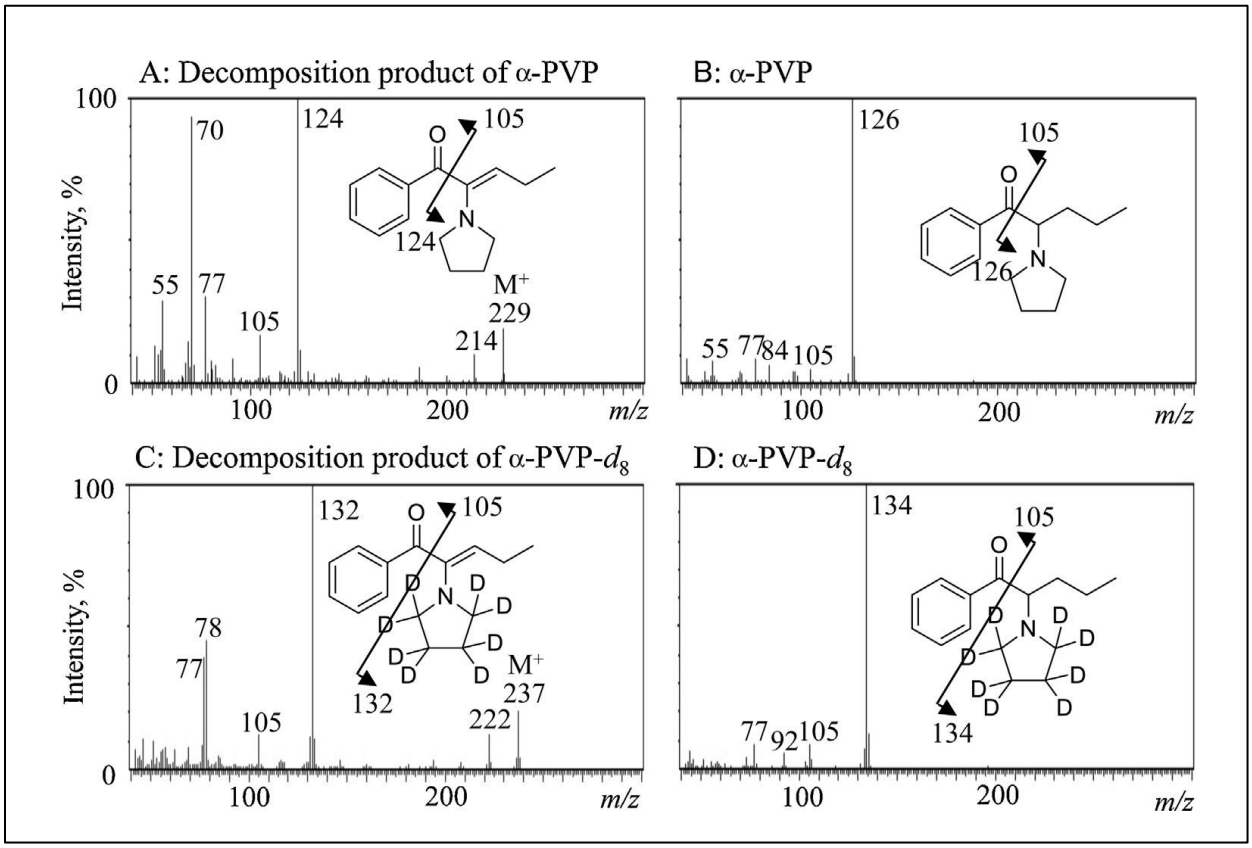

Figure 5. Electron ionization mass spectra of (A) decomposition product of α-PVP, (B) intact α-PVP, (C) decomposition product of α-PVP-D_8 and (D) intact α-PVP-D_8 [Tsujikawa *et al*, 2013a].

1.9.2. Gas chromatography with infrared detection (GC–IR)

The absorption of IR radiation is also considered one of the non-destructive techniques that can be used for the identification of organic molecules. The region from 1250 to 600 cm^{-1} is generally classified as the "fingerprint region" and is usually a result of bending and rotational

energy changes of the molecule as a whole. However since the clandestine samples are usually impure, overlapping absorptions of different molecules present in the sample becomes a possibility. Hence, this region is not useful for identifying functional groups, but can be useful for determining whether samples are chemically identical.

GC–MS detection is perhaps the most common technique used for forensic drug identification. However, regioisomeric molecules yielding regioisomeric fragment ions present a significant challenge for mass-based methods of identification. Infrared spectroscopy is a useful confirmatory method for identification and differentiation of regioisomeric substances having mass-based equivalence. Gas chromatography with vapor phase infrared detection has proven to be a reliable partner to GC–MS for the complete and exact structural determination in a number of designer drug categories [Smith *et al*, 2018; Abdel-Hay *et al*, 2013; Awad *et al*, 2009].

1.9.3. Nuclear magnetic resonance (NMR)

NMR is a nondestructive flexible technique that can be used for the simultaneous identification of pure compounds and even mixtures of compounds in one sample. Its advantages, compared to GC–MS techniques, include stereochemical differentiation and the capability to analyze nonvolatile compounds. However, the lack of use in forensic laboratories can be attributed to the high cost of instrumentation and the poor sensitivity of NMR. Solid state NMR also can be used for analytical purposes in much the same way as solution NMR. The observed chemical shifts however differ in the solution and solid states because of conformational freezing and packing effects. 1H and 13C NMR were utilized to confirm the structure of MDPV in a seized sample in Germany in 2007 [Westphal *et al*, 2009].

1.10. The instability of hydrochloride salts of cathinone derivatives in air

Cathinone derivatives can be classified into two types based on their amino groups, alkylamine-type (secondary amines) like methcathinone and pyrrolidine-type like MDPV. The pyrrolidine-type cathinones contain a tertiary amine group [Tsujikawa *et al*, 2015]. Tertiary amines can be easily oxidized by molecular oxygen into amine oxides [Aleksandrov, 1980]. The salt form of these amines is usually difficult to oxidize due to the protonation of the amine group [Saal, 2010]. However, the salt of MDPV was reported to be extremely unstable in air [Wang *et al*, 2012]. The decomposition of hydrochloride salts of various cathinone derivatives in air has been evaluated [Tsujikawa *et al*, 2015]. The pyrrolidine-type cathinones afforded two types of decomposition products, which were proposed to be a cyclic amide (2-pyrrolidone, lactam) and *N*-oxide derivatives, while secondary amine-type cathinones showed different decomposition products, possibly including dealkylated derivatives.

1.11. Project rational

The rapid proliferation of new psychoactive substances has led to the development of drug analogue laws attempting to control unspecified drug molecules not yet known to exist. Based on a report from the UNODC, approximately 650 new psychoactive substances have been reported by 102 countries and territories since 2008 [UNODC, 2016]. Additionally, by the end of 2017, the EMCDDA was monitoring more than 670 new psychoactive substances that have been identified in Europe [EMCDDA, 2018].

A total of 75 new psychoactive substances appeared for the first time in 2015 according to the 2016 World Drug Report [UNODC, 2016]. A total of 20 of these first time reports in 2015 represented new synthetic cathinone derivatives and for the first time in history, the number of new synthetic cathinones rivaled the number of reported new synthetic cannabinoids, 20 and 21 respectively. The 2018 European Drug Report describes the synthetic cathinones as the second largest group of new substances monitored by the EMCDDA, with a total of 130 different substances identified from 2008–2018 in clandestine drug samples [EMCDDA, 2018].

A number of synthetic cathinones (aminoketones, "bath salts") have appeared on the illicit drug market in recent years including methcathinone, mephedrone, methylone and MDPV (3,4-methylenedioxypyrovalerone). These compounds represent a new emphasis in the development of designer drugs [German *et al*, 2014; Lewin *et al*, 2014; Katz *et al*, 2014] with a variety of aromatic ring substituent, hydrocarbon side-chain and amino group modifications of the basic cathinone molecular skeleton.

The synthetic cathinones produce central nervous system stimulation and other psychoactive effects as a result of elevations in CNS neurotransmitter levels for the various

catecholamines [Coppola and Mondola, 2012; Cozzi *et al*, 1999]. MDPV is a designer drug with stimulant effects similar to those of cocaine and amphetamine [Kriikku *et al*, 2011]. It is an analogue of pyrovalerone, a psychostimulant compound that was the first commercially available drug from the alpha-pyrrolidinophenone class. It came to the market in the 1970's and was removed later due to abuse potential [Meyer *et al*, 2010a; Gardos and Cole, 1971]. MDPV has also been described as a synthetic cathinone derivative since it can be viewed as a structurally modified cathinone [Gibbons and Zloh, 2010].

The designer style molecular modification and synthesis of analogues in a number of drug categories are possible due to the commercial availability of many regioisomeric forms of common precursor substances. A single synthetic pathway utilizing a variety of regioisomeric precursor materials can yield numerous closely related products. These compounds in many cases have identical molecular framework, elemental composition, functional groups and often equivalent or identical mass spectral fragments. Chromatographic co-elution of regioisomeric substances that yield regioisomeric or identical mass spectral fragment ions would require a unique strategy for identification.

Exploration and current clandestine designer drug development concepts in the aminoketone drugs based on substituted amphetamines and related phenethylamines models [Zaitsu *et al*, 2009] are likely to continue for many years. Clandestine production of these drugs can be based on common precursor chemicals. Therefore, legal control of key precursor substances is not likely and might not prevent the further clandestine/designer exploration of this group of compounds. In fact, the legal control of a specific drug of abuse often provides the driving force for the development of new designer substances. Issues of designer aminoketone identification as

well as regioisomer relationships in these designer molecules will continue to be significant in forensic drug analysis.

Perhaps the U. S. Controlled Substance Analogue Act would make all these "isomers" controlled substances. Therefore, it could be argued that isomer differentiation is not necessary in forensic drug science. However, the compound must be specifically identified in order to even know if it falls into the category as an analogue of a controlled substance. These circumstances all point to the strong need for a thorough and systematic investigation of the forensic chemistry of these substituted aminoketones. The use of multiple and complementary analytical methods such as GC–MS, GC–MS/MS and GC–IR are often necessary for the specific identification of one compound from a series of closely related structural isomers.

This project will investigate the forensic analytical chemistry of the current and future regioisomeric and homologous designer cathinone derivatives. The resulting analytical data as well as methods for reference standard synthesis represent important advancements in forensic drug chemistry. The goal of this work is to have the data and methods for differentiation among these designer substances available to assist in drug identification.

1.12. Purpose, goals and objectives

The purpose of this project is to develop regioisomer specific methods for the identification of ring substituted aminoketone compounds (cathinone derivatives). This will be accomplished by:

1) The chemical synthesis of all regioisomeric forms of selected aromatic ring substituted aminoketones.
2) Generation of a complete analytical profile for each compound using the following analytical techniques: GC–MS, GC–CI-MS, GC–MS/MS and GC–IR.
3) Chromatographic studies to separate/resolve all regioisomeric aminoketones having overlapping analytical profiles.
4) Design and validation of confirmation level methods to identify each compound to the exclusion of other regioisomeric forms.

Based on the structure of the unsubstituted cathinone molecule, designer modifications are possible in four distinct regions (see Scheme 8) of the molecule: the aromaric ring, the alkyl side-chain, the amino group and the carbonyl functionality. Based on the structures of common synthetic cathinones in Figure 1 (see Section 1.1.), the first three of these areas of possible designer modifications are currently being explored by clandestine chemists. Legal control of a specific molecule often provides the driving force for clandestine development of additional substituted cathinone designer molecules. The proposed designer modifications in the various regions of the basic cathinone structure depicted in Scheme 8 are very likely and can be based on the commonly reported designer manipulations as well as the commercial availability of precursor materials.

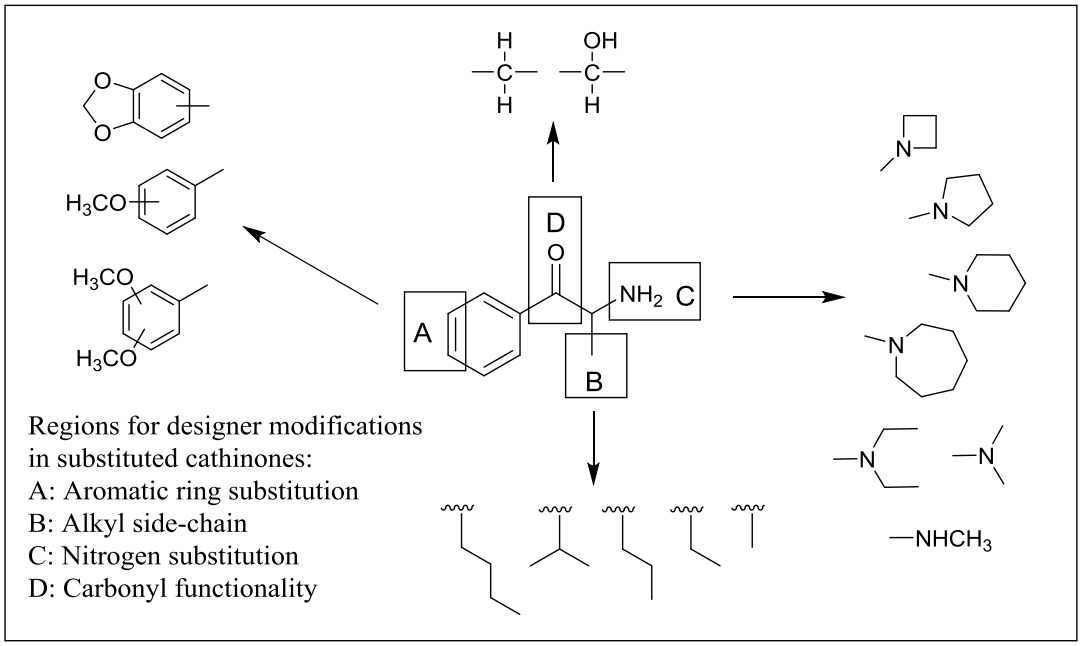

Scheme 8. Molecular regions for designer modification in cathinone bath salts.

Figure 6 shows the general structures for the compounds to be prepared and evaluated in this project. As demonstrated in Scheme 8, in Region A, there are three regioisomeric variants for each monosubstituted aromatic ring with one alkyl side-chain (*ortho*-, *meta*-, *para*- or 2-, 3-, 4-substituted), six regioisomers for equivalent disubstitution (for example dimethoxy). In Region B, *n*-alkyl groups such as methyl, ethyl, *n*-propyl and butyl have been reported in marketed samples of bath salt/cathinone derivatives. Region C is generally a secondary or tertiary amine and *N*-methyl, ethyl, dimethyl and pyrrolidine are commonly encountered in clandestine samples. Region D can be modified to its reduced forms, the hydroxyl and the desoxy moieties.

The appearance of increasingly structurally diverse aminoketone derivatives in clandestine samples highlights several key issues of immediate forensic significance. First, most of these compounds have regioisomeric analogues, which would not be readily differentiated and specifically identified using standard forensic analytic methodology. The second key issue of

forensic importance among the aminoketone compounds involves designer drug development. Many of these compounds contain aromatic substituents known to enhance hallucinogenic or entactogenic activity in the phenylalkylamine (amphetamine and methylenedioxy-amphetamine) drugs of abuse series. As regulatory controls tighten with respect to available aminoketones, designer derivative exploration and synthesis are expected to continue. This is particularly important in these aminoketone compounds since the syntheses are relatively straightforward and many starting materials are readily accessible. Further designer exploration would likely parallel that observed in the phenylalkylamine series of drugs and involve methoxy, dimethoxy, bromo-dimethoxy, methylenedioxy, trifluoromethyl, chloro, and methyl substituents, as well as regiosiomers of these substitution patterns.

In July of 2011, the NDIC [U. S. DOJ-NDIC, 2011] issued a "Situation Report" examining the threat that synthetic cathinone abuse poses to the United States and the difficulty that U. S. law enforcement faces in preventing the manufacture and distribution of synthetic cathinones and synthetic cathinone products. The four major concerns in the NDIC report were as follows:

1) The distribution and abuse of synthetic cathinones in the U. S. will increase in the near term.
2) More synthetic cathinones will be abused in the long term.
3) Different synthetic cathinones will surface as commercial drug testing companies develop drug screens to detect existing synthetic cathinones.
4) The global nature of Internet chemical sales, particularly of synthetic cathinones, will present increasing challenges to U. S. law enforcement in the long term.

These points highlight the need to develop specific, selective and reliable analytical methods to identify existing cathinone products in the clandestine market place, and versatile methods that

can be used to readily identify new designer analogues as they emerge.

The overall goal of this project is a comprehensive and systematic analytical study of the likely structural variations in clandestinely prepared designer bath salt aminoketones. The availability of all the necessary compounds to establish and prove the structure-retention, structure-fragmentation and other structure-property analytical relationships is the first step in this research. The specific project deliverables are:

1) The chemical synthesis of regioisomeric and homologous compounds related to MDPV.

2) Synthesis of selected deuterium and carbon-13 labeled compounds as needed for MS fragmentation confirmation.

3) GC–MS evaluation of the regioisomeric aminoketones.

4) Evaluation of GC methods for the separation of all isomers producing equivalent mass spectra.

5) Evaluation of GC–MS, GC–MS/MS and GC–IR data for specific differentiation of all isomers producing equivalent mass spectra.

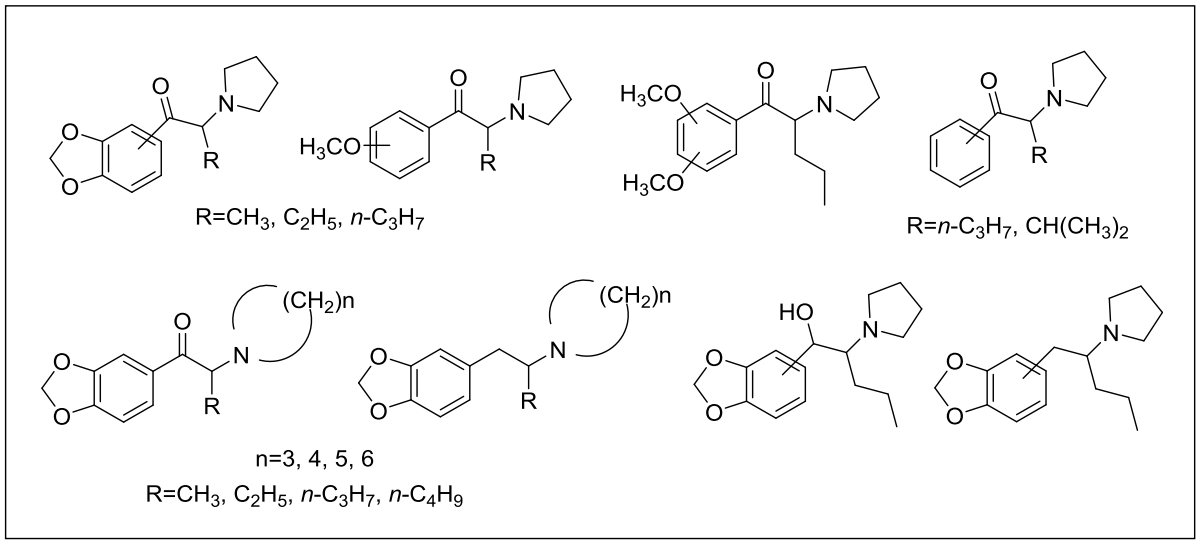

Figure 6. General structures for the bath salt aminoketones in this study.

2. Synthesis, analytical studies and isotope labeling of the regioisomeric and homologous cathinone derivatives

Regioisomeric substances are considered a significant challenge for the analytical techniques used to identify specific molecules. This is considered extremely important when some of these molecules are legally controlled drugs and others may be uncontrolled, non-drug species or imposter molecules. Methylenedioxypyrovalerone has direct regioisomers (of equal molecular weight and fragmentation products of identical mass) as well as homologous substances of homologous molecular weight and fragmentation products of homologous mass. The ability of the analytical method to distinguish between regioisomers directly enhances the specificity of the analysis for the target drugs of abuse. The mass spectrum is often the confirmatory piece of evidence for the identification of drugs of abuse in the forensic laboratory. While the mass spectrum is often considered a specific "fingerprint" for an individual compound, there may be other substances, not necessarily having any known pharmacological activity, capable of producing very similar or almost identical mass spectra. These imposter substances provide the possibility for misidentification as the drug of abuse itself. In the case of the cathinones, there may be many positional isomers, direct or indirect regioisomers, as well as isobaric compounds which yield a similar mass spectrum. A compound co-eluting with the controlled drug and having the same mass spectrum as the drug of abuse would represent a significant analytical challenge. The ultimate concern then is "if the forensic scientist has never analyzed all the non-drug substances, how can she/he be sure that any of these compounds would not co-elute with the drug of abuse?"

The significance of this question is related to many factors, chief among these is the chromatographic system separation efficiency and the number of possible counterfeit substances. Furthermore, the ability to distinguish between these regioisomers directly enhances the specificity of the analysis for the target drugs of abuse.

NMR is a nondestructive flexible technique that can be used for the simultaneous identification of pure compounds and even mixtures of compounds in one sample. Its advantages, compared to GC–MS techniques, include stereochemical differentiation and the capability to analyze nonvolatile compounds. However, the lack of use in forensic laboratories can be attributed to the high cost of instrumentation and the poor sensitivity of NMR. In addition, NMR requires pure samples, which are hard to satisfy in the case of biological samples.

Infrared spectroscopy is considered a confirmation method for the identification of organic compounds due to the uniqueness of infrared spectra for very similar organic molecules. Gas chromatography with infrared detection (GC–IR) is characterized by scanning quickly enough to obtain vapor phase IR spectra of compounds eluting from the capillary GC columns.

All the regioisomers, direct and indirect as well as isobaric compounds have a strong possibility to be misidentified as the controlled drug, by some analytical methods especially mass spectrometry. In this project, all direct ring regioisomers, and side-chain homologous compounds related to 3,4-MDPV drug of abuse are compared by chromatographic and spectroscopic techniques, and methods for their differentiation are explored. Gas chromatography coupled to ion trap (GC–MS/MS) will be utilized to further investigate some less intense product ions and their parent ions. Isotope labeling such as deuterium (D) labeling will be used to confirm mass

spectrometric fragmentation mechanisms that result in the formation of some key fragment ions or to confirm the elemental composition of these fragment ions.

2.1. GC–MS, GC–MS/MS and GC–IR analyses of a series of methylenedioxyphenyl-aminoketones: precursors, ring regioisomers and side-chain homologues of MDPV

The ring substituted cathinone, 3,4-methylenedioxypyrovalerone (3,4-MDPV) and its regioisomer 2,3-methylenedioxypyrovalerone (2,3-MDPV) isomer have almost identical mass spectra with equivalent fragments including the base peak at *m/z* 126 and major product ion fragments at *m/z* 84. Furthermore, the chemical ionization mass spectra for both isomers are also identical with a major peak at *m/z* 276 $[M+H]^+$.

Gas chromatographic separation coupled with infrared detection (GC–IR) provides direct confirmatory data for structural differentiation between the two regioisomers. The mass spectrum in combination with the vapor phase infrared spectrum provides for specific confirmation of each of the regioisomeric and homologous aminoketones. The six aminoketone derivatives were resolved on a 30-meter capillary column containing an Rxi®-35Sil MS stationary phase while their intermediate ketones were resolved on Rtx®-5 stationary phase.

2.1.1. Synthesis of the methylenedioxyphenyl-aminoketones: Ring substituted regioisomers and side-chain homologues of 3,4-methylenedioxypyrovalerone (MDPV)

The synthetic methods needed to prepare the various isomeric and homologous aminoketones in this study are well established in the chemical literature and in our laboratory. The procedures used in this project were those reported by Kavanagh [Kavanagh *et al*, 2012]. These desired compounds were prepared individually from the substituted benzaldehydes via a 4-step synthetic procedure (see Scheme 9). The condensation of alkylmagnesium halides (Grignard reagents) with the individual 2,3- or 3,4-methylenedioxybenzaldehyde yields the corresponding methylenedioxybenzyl alcohols. The oxidation of the alcohols with potassium dichromate (fine powder) gave the precursor ketones. Alpha-bromination of the ketones at the

activated methylene carbon gives the alpha-bromoketones and subsequent displacement of the bromide ion with the pyrrolidine secondary amine yields the desired aminoketone final products. The products are isolated by solvent extraction and purified by preparative thin layer chromatography (TLC) 20:80 ethyl acetate-petroleum ether using Analtech (Newark, DE) glass backed 20 x 20 cm plates with a 1000 µm layer of silica and an inorganic fluorescent 254 nm indicator.

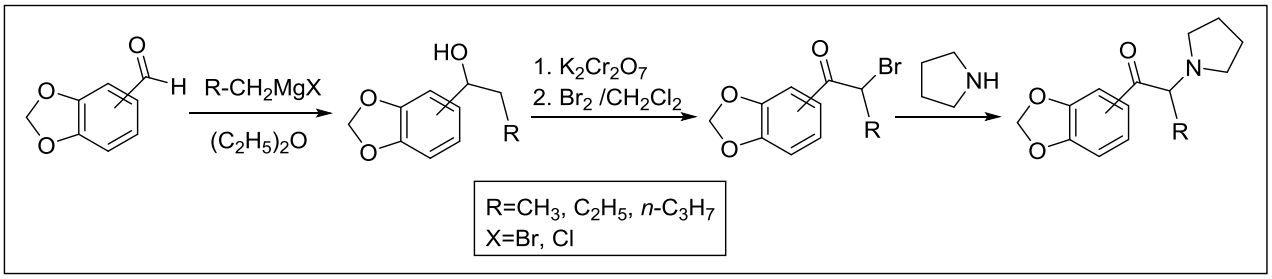

Scheme 9. General synthesis for the six regioisomeric and homologous derivatives of MDPV.

2.1.1.1. Alternative synthesis of the intermediate 3,4-methylenedioxyphenyl-ketones

The 3,4-methylenedioxyphenyl-ketones can be alternatively prepared by two different ways as illustrated in Scheme 10. The first method involves the reaction of 1,3-benzodioxole and the appropriate acyl chloride in the presence of tin (IV) chloride [Aarde *et al*, 2013b]. The second method involves the reaction of 3,4-methylenedioxyphenyl nitile with the appropriate Grignard reagent followed by acidic hydrolysis to afford the ketone [Meltzer et al, 2006; Collins, 2011].

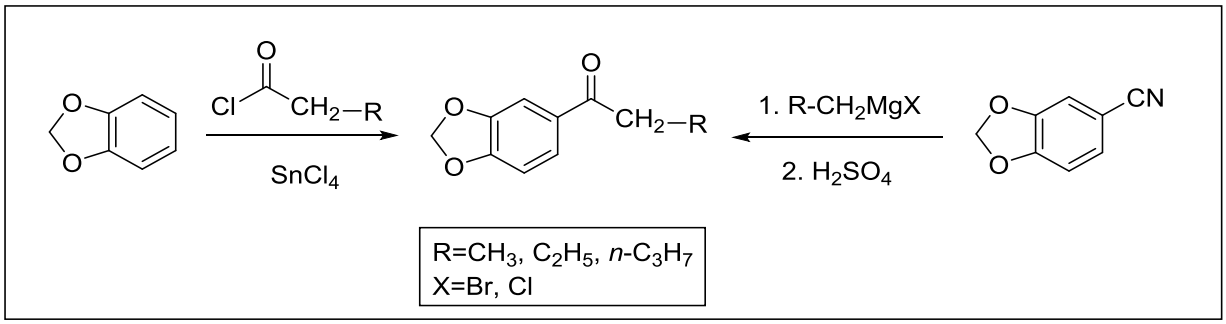

Scheme 10. Alternative synthesis for the intermediate 3,4-methylenedioxyphenyl ketones.

2.1.1.2. Synthesis of the precursor 2,3-methylenedioxybenzaldehyde

Piperonal and 2,3-methylenedioxybenzaldehyde are both commercially available. However, the 2,3-methylenedioxybenzaldehyde was also prepared in our lab. The preparation of 2,3-methylenedioxybenzaldehyde has been reported previously [Soine *et al*, 1983; Casale *et al*, 1995] and is outlined in Scheme 11. 2,3-dihydroxybenzaldehyde was converted to 2,3-methylenedioxybenzaldehyde by adding dibromomethane to a solution of 2,3-dihydroxybenzaldehyde and potassium carbonate in dimethylformamide (DMF), followed by the addition of copper(II)oxide and the resulting mixture was heated at reflux overnight. Solvent extraction followed by Kugelrohr distillation produced the pure 2,3-methylenedioxybenzaldehyde.

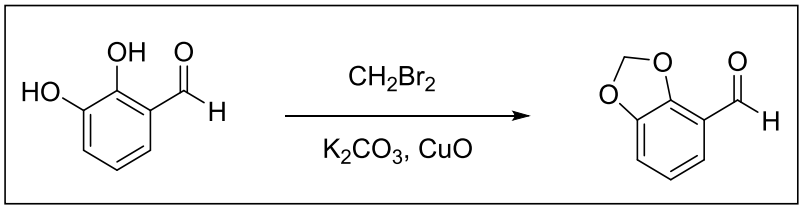

Scheme 11. Synthesis of 2,3-methylenedioxybenzaldehyde.

2.1.2. Gas chromatographic separation

The chromatogram in Figure 7 (Panel A) shows the GC separation of the six regioisomeric and homologous methylenedioxyphenyl-aminoketones in this study. The separation was obtained on a 30-meter capillary column coated with a 0.50 µm film of Rxi®-35Sil MS, a midpolarity phase; similar to 35% phenyl, 65% dimethyl polysiloxane. The temperature program consisted of an initial hold at 70 °C for 1.0 minute, ramped up to 250 °C at a rate of 30 °C/minute followed by a hold at 250 °C for 15.0 minutes. The compounds elute over approximately a 3.0-minute window requiring a total run time of just over 16.0 minutes. The six compounds in this study differ by the position of the methylenedioxy ring substitution and the homologation of the alkyl side-chain. The

elution order in Figure 7A reflects these structure-retention relationships showing increased retention with increasing side-chain length for the homologous series as well as significant retention differences based on the aromatic ring substitution pattern for the methylenedioxy group. For example, the degree of retention of the homologous side-chain series for both 2,3- and 3,4-methylenedioxy ring substitution pattern shows the methyl side-chain eluting before the ethyl and the *n*-propyl group having the highest retention. Furthermore, within each pair of equivalent homologues, the position of the ring methylenedioxy substitution controls the relative retention of the regioisomeric pair. In every case, the 2,3-isomer elutes before the 3,4-isomer, for example MDPV (the 3,4-methylenedioxyphenyl substituted isomer, Compound 6) has much higher retention than its corresponding 2,3-methylenedioxyphenyl substituted isomer, Compound 3, in Figure 7A. The closely eluting critical peak pair in Figure 7A are Compounds 3 and 5 and these closely eluting bands represent the 2,3-methylenedioxy ring substitution pattern with the higher homologue *n*-propyl side-chain group eluting before the 3,4-pattern with the lower side-chain ethyl homologue.

A:

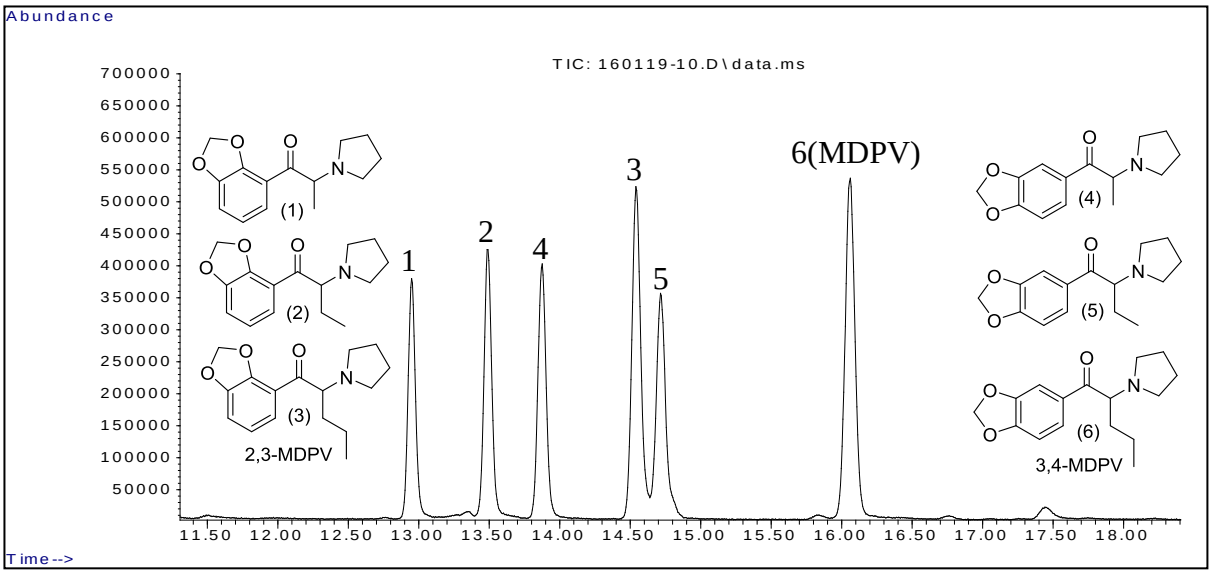

B:

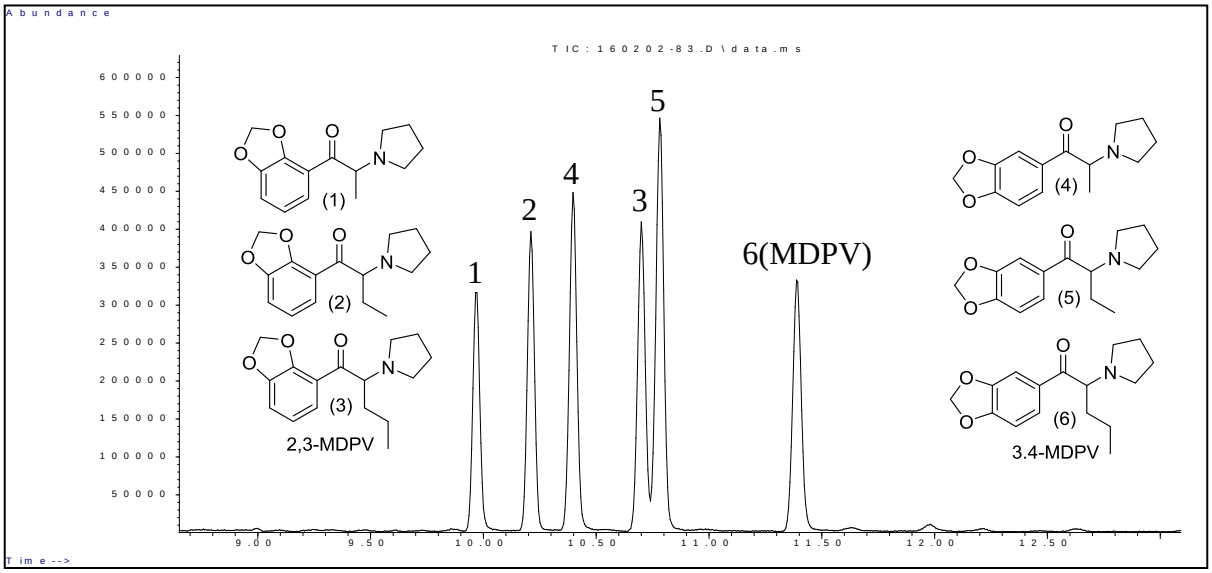

Figure 7. Capillary gas chromatographic separation of the six regioisomeric and homologous methylenedioxyphenyl-aminoketones. GC–MS System 1. A: Rxi®-35Sil MS stationary phase, B: Rxi®-17Sil MS stationary phase.

A similar chromatogram in Figure 7 (Panel B) using the identical temperature program (with the GC injector temperature maintained at 150 °C) was obtained on a column coated with 0.25 µm film of midpolarity Crossbond® silarylene phase; similar to 50% phenyl, 50% dimethyl polysiloxane (Rxi®-17Sil MS) with slightly lower retention and the same elution order. The nonpolar Rtx®-5 column (30 m × 0.25 mm i.d. coated with 0.10 µm film of Crossbond® 5% diphenyl, 95% dimethyl polysiloxane) required a 65.0 minutes run time for adequate resolution of all six compounds (chromatogram not shown). The baseline resolution of a binary mixture of MDPV and its 2,3-MDPV regioisomer (Compounds 3 and 6) was achieved on an Rtx®-5 stationary phase in less than 8.50 minutes using the same temperature program described previously (with the GC injector temperature maintained at 150 °C) and the resulting chromatogram is shown in Figure 8. The separation of the precursor ketones in Figure 9 was accomplished on an Rtx®-5 stationary phase using the exact temperature program and required an analysis time of less than

7.0 minutes. The structure-retention relations observed for these ketones are consistent with the results described for the product aminoketones. However, the elution order is slightly different with each equivalent alkyl side-chain group with the 2,3-methylenedioxy substituted isomer eluting before the 3,4-substituted isomer.

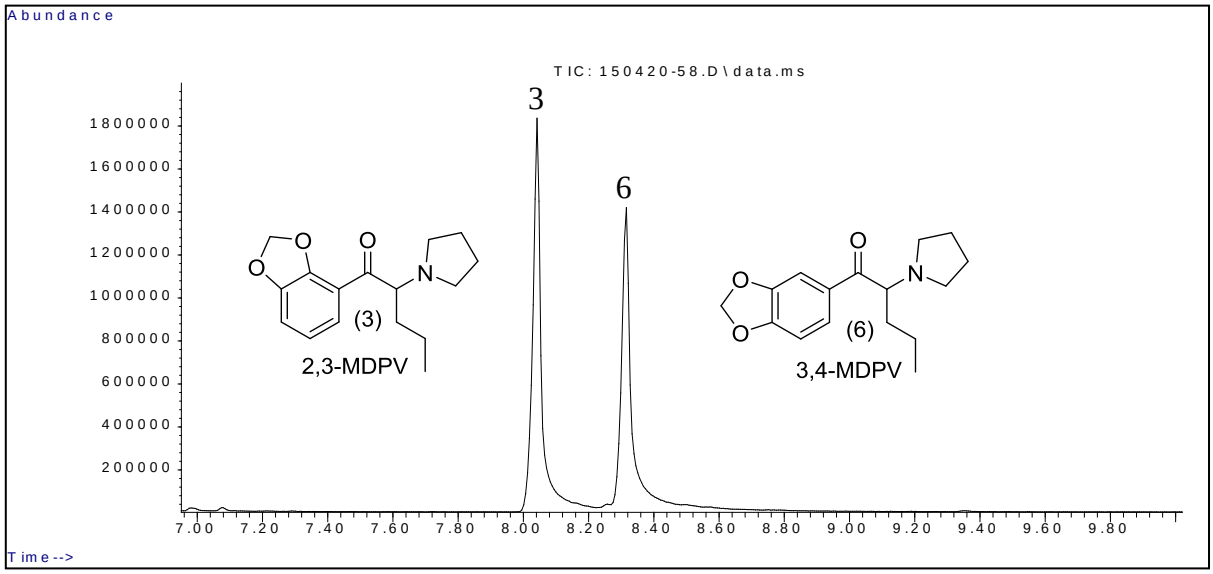

Figure 8. Capillary gas chromatographic separation of the regioisomeric compounds 2,3-MDPV and 3,4-MDPV. GC–MS System 1. Rtx®-5 stationary phas.

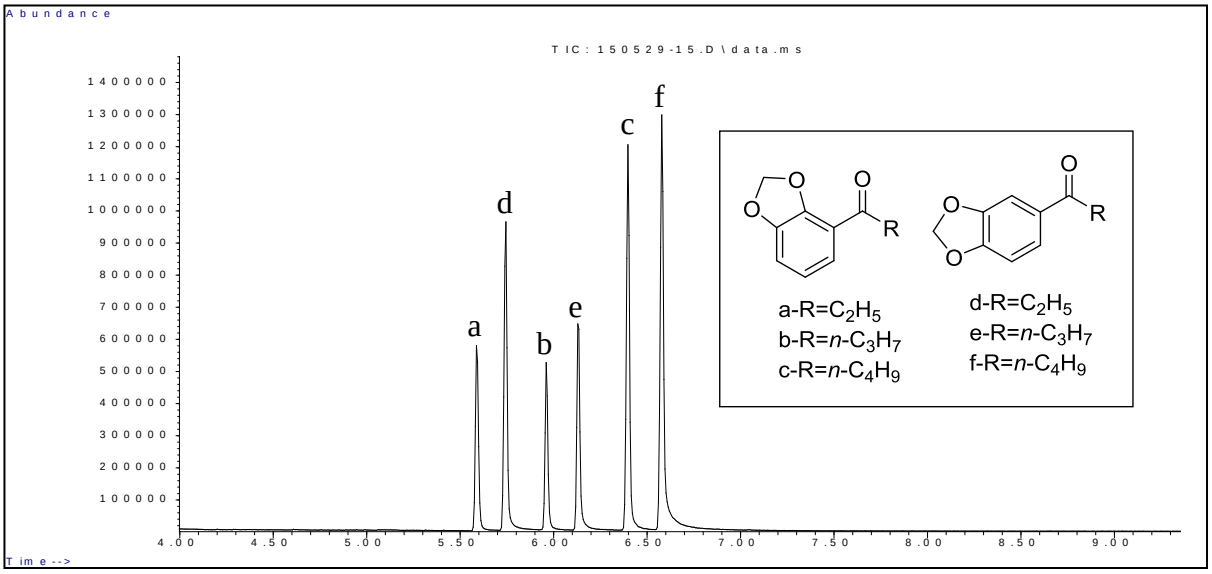

Figure 9. Capillary gas chromatographic separation of the six regioisomeric and homologous methylenedioxyphenyl-ketones. GC–MS System 1. Rtx®-5 stationary phase.

2.1.3. Mass spectral studies (EI-MS, CI-MS and MS/MS)

The EI mass spectra of the six homologous and regioisomeric 2,3- and 3,4-methylenedioxyphenyl-aminoketones (Compounds 1–6) are shown in Figure 10. The base peak in the mass spectra of all these compounds are the result of the amino-group dominated alpha-cleavage process producing the iminium cation fragments. The base peaks in all these spectra occur in a mass range of *m/z* 98 ($C_6H_{12}N^+$), *m/z* 112 ($C_7H_{14}N^+$) and *m/z* 126 ($C_8H_{16}N^+$) and represents the homologous series of iminium cations based on the number of methylene units in the alkyl side-chain. These iminium cations are the result of fragmentation of the bond between the carbonyl carbon and the adjacent side-chain carbon bearing the amine nitrogen of the pyrrolidine ring. The iminium cation is the only fragment of significant relative abundance in these spectra and this fragment provides information about the make-up of the alkyl portion of the molecule. The *m/z* 149 ion seen in all of the spectra is the methylenedioxybenzoyl cation ($ArCO^+$) resulting from initial ionization of the carbonyl oxygen and fragmentation of the same carbon-carbon bond to result in charge retention on the carbonyl portion of the structure. Loss of CO from the *m/z* 149 cation is the likely source of the *m/z* 121 cation observed in most of the spectra. The fragmentation mechanisms for these main ions are explained in Scheme 12 shown below.

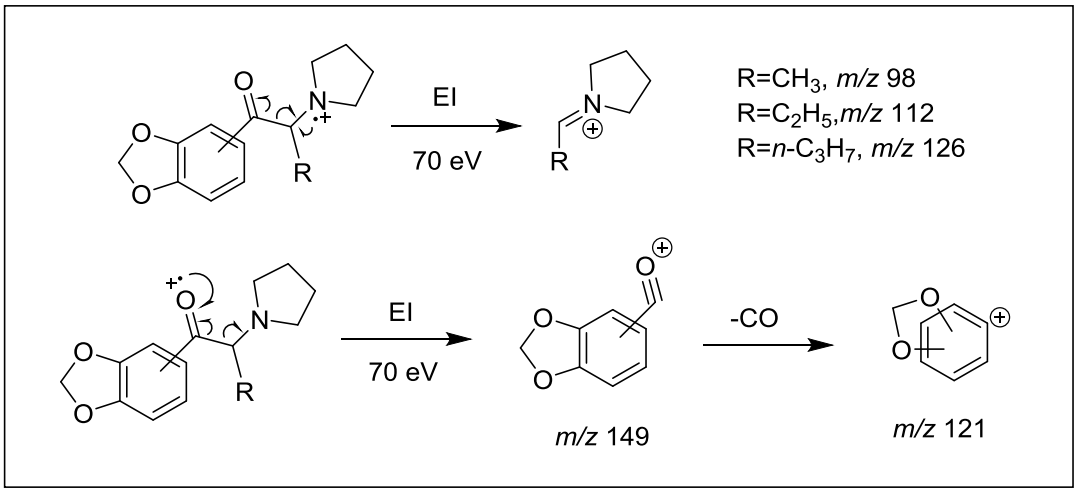

Scheme 12. Structures of the major fragment ions in the mass spectra of the six regioisomeric and homologous methylenedioxyphenyl-aminoketones in this study.

The iminium cation essentially characterizes the nature of the alkylamino-group portion of the molecule attached to the carbonyl carbon. However, these ions as well as the substituted benzoyl cations and resulting fragments, do not provide characterization of the regioisomeric position of substitution of the methylenedioxy-group. The spectra in Figure 10 for the 2,3-series are essentially identical to the 3,4-methylenedioxyphenyl-aminoketones. For example, a comparison of Compound 6 (MDPV) and the corresponding 2,3-regioisomer (Compound 3) shows essentially equivalent mass spectra with little information for isomer differentiation and identification. The mass spectra for the representative intermediate ketones (spectra not shown) show similar overlap of major fragment ions for the regioisomeric pairs.

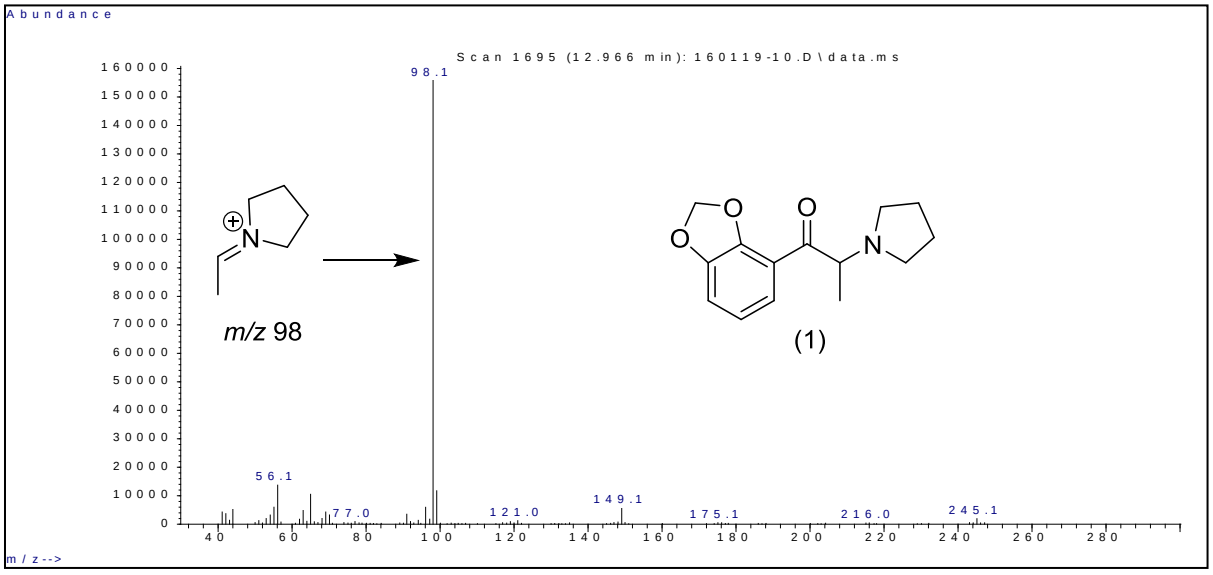
Abundance
Scan 1695 (12.966 min): 160119-10.D\data.ms
98.1
56.1
77.0
121.0
149.1
175.1
216.0
245.1
m/z-->
m/z 98
(1)

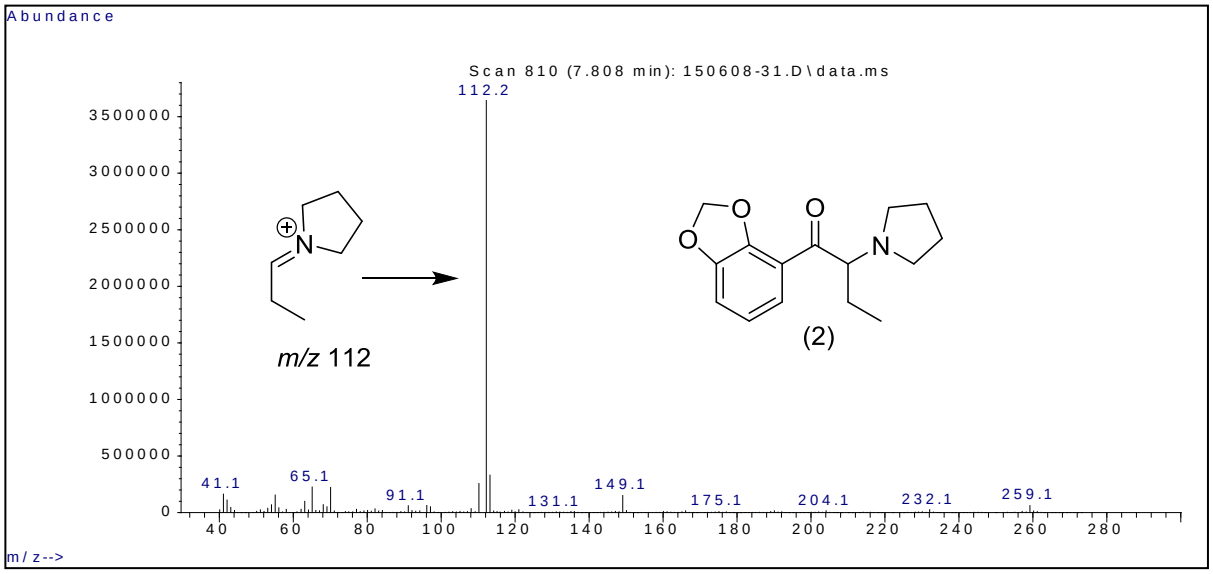
Abundance
Scan 810 (7.808 min): 150608-31.D\data.ms
112.2
41.1
65.1
91.1
131.1
149.1
175.1
204.1
232.1
259.1
m/z-->
m/z 112
(2)

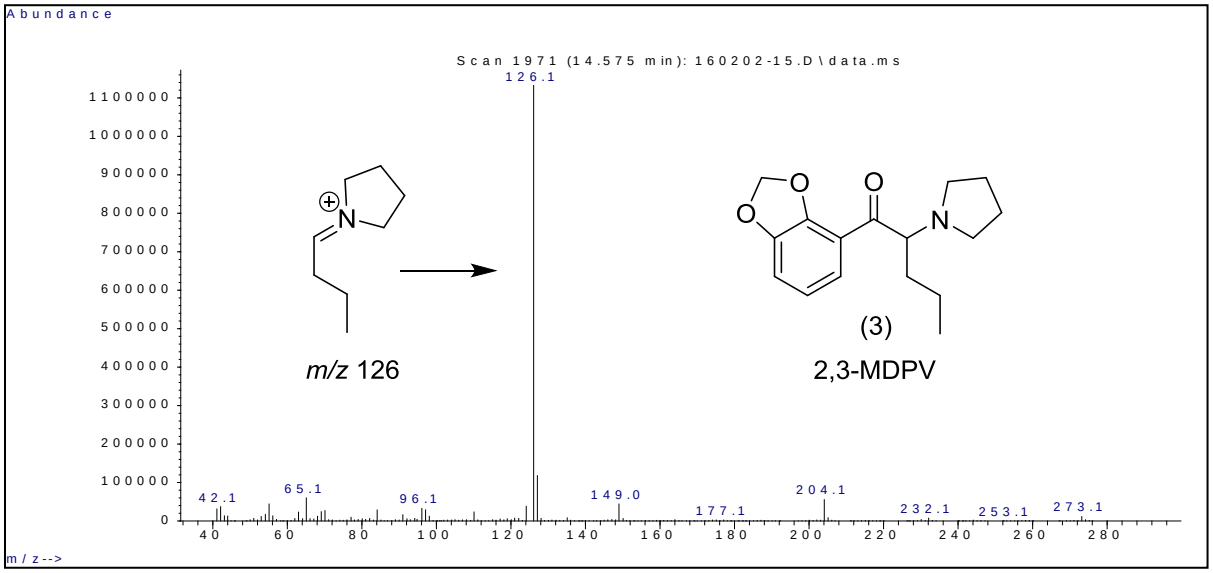
Abundance
Scan 1971 (14.575 min): 160202-15.D\data.ms
126.1
1100000
1000000
900000
800000
700000
600000
500000
400000
300000
200000
100000
0
42.1
65.1
96.1
149.0
177.1
204.1
232.1
253.1
273.1
40
60
80
100
120
140
160
180
200
220
240
260
280
m/z-->
m/z 126
(3)
2,3-MDPV

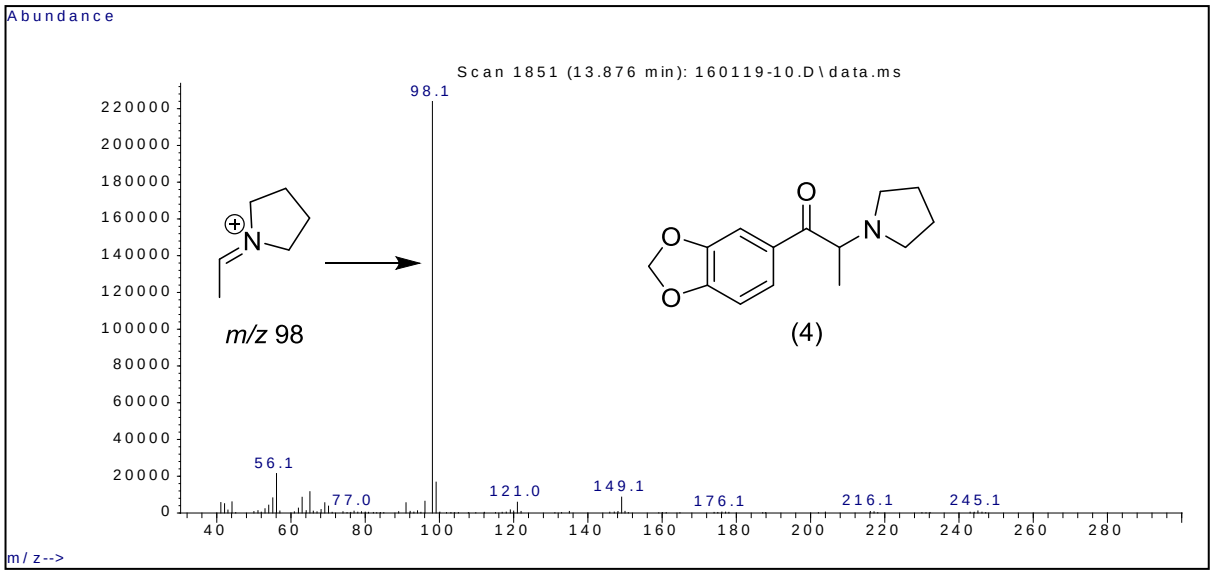
Abundance
Scan 1851 (13.876 min): 160119-10.D\data.ms
98.1
220000
200000
180000
160000
140000
120000
100000
80000
60000
40000
20000
0
56.1
77.0
121.0
149.1
176.1
216.1
245.1
40
60
80
100
120
140
160
180
200
220
240
260
280
m/z-->
m/z 98
(4)

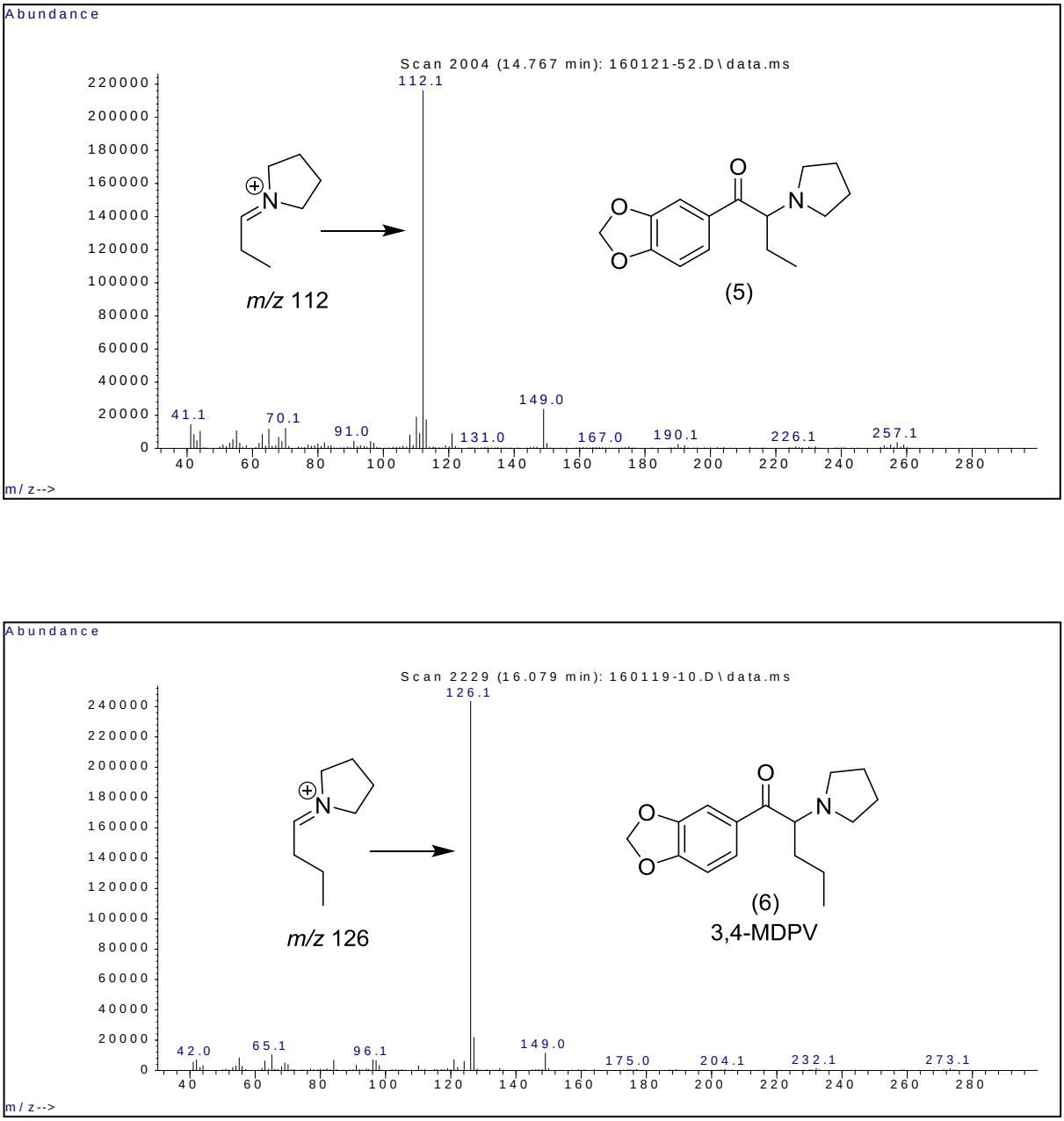

Figure 10. EI mass spectra of the six regioisomeric and homologous methylenedioxyphenyl-aminoketones in this study. GC–MS System 1.

The GC–CI-MS studies for Compounds 3 and 6 were performed on a column (30 m × 0.25 mm i.d.) coated with 0.10 µm film of Crossbond® 100% dimethyl polysiloxane (Rtx®-1). The chemical ionization mass spectra in Figure 11 confirm the molecular weight for the two

regioisomeric aminoketones (Compounds 3 and 6) via the intense $[M+H]^+$ ion. These spectra were generated using methanol as the CI reagent gas. Thus, GC–CI-MS confirms the molecular weight for these compounds and the EI mass spectra provide information about that portion of the molecule bonded to the methylenedioxybenzoyl moiety common to these two compounds. Chromatographic analysis was performed using a temperature program consisting of an initial hold at 70 °C for 1.0 minute, ramped up to 250 °C at a rate of 30 °C/minute followed by a hold at 250 °C for 15.0 minutes.

A:

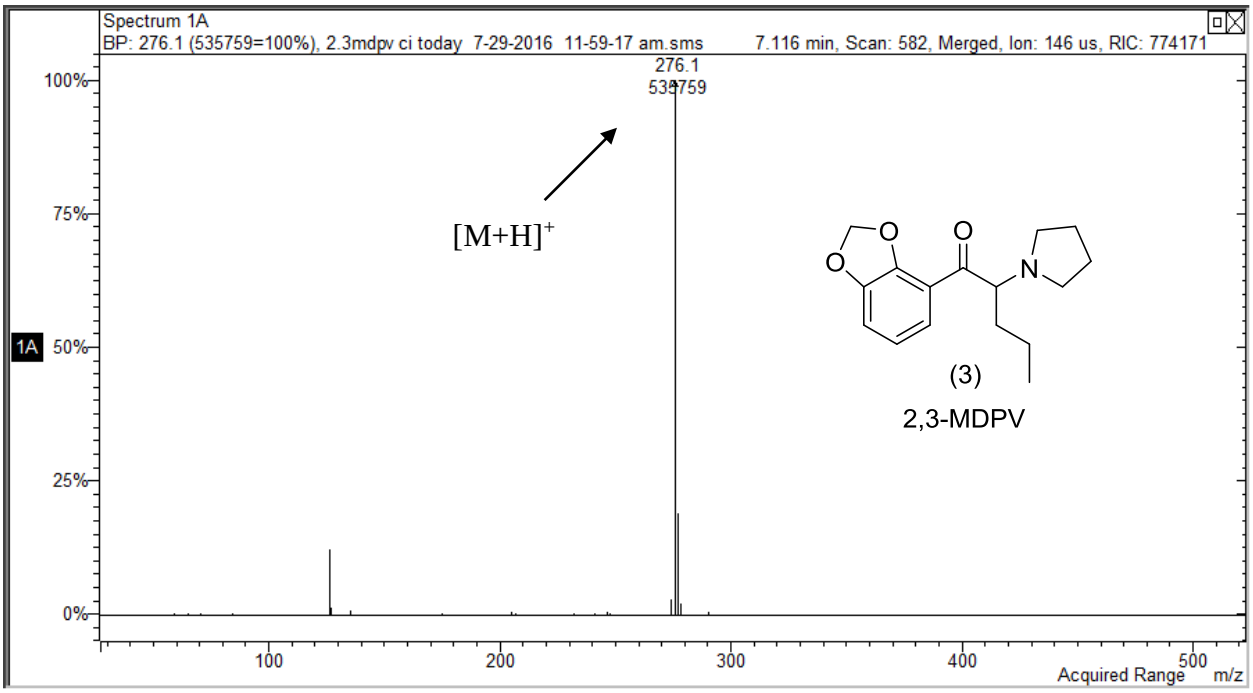

B:

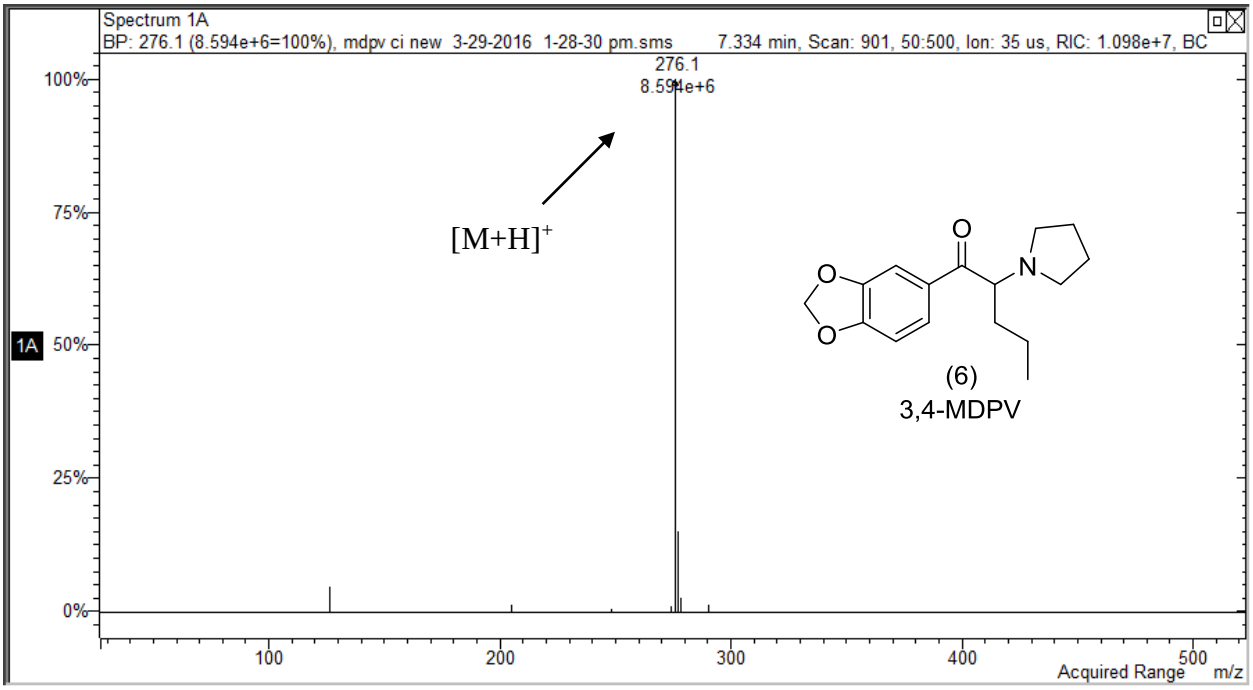

Figure 11. Chemical ionization mass spectra (CI-MS) for Compounds 3 and 6. GC–MS System 2.

A second less obvious homologous series of fragments occurs among the low mass ions and this series provides information concerning the exact structure of the iminium cations. Figure 12 shows the low mass region of the EI-MS for Compounds 4, 5 and 6 displaying only the ions occurring in the portion of the spectrum at masses lower than the mass of the base peak. The low mass EI scans for Compounds 1, 2 and 3 generated an analogous pattern. The homologous sequence of interest in Figure 12 is *m/z* 56, 70 and 84 in Compounds 4, 5 and 6, respectively. Each of the ions in this low mass series represents the loss of 42 Da from the iminium cation base peak for these compounds.

The use of product ion MS/MS experiments for each of the base peaks in Compounds 4, 5 and 6 confirmed the iminium cations as the source for the low mass homologous series of ions. For MS/MS experiments, the scan type used was the Automated Method Development function

(AMD) and the optimum MS/MS excitation amplitude was 1.20 volt. The GC–MS/MS studies were performed on a column (30 m × 0.25 mm i.d.) coated with 0.25 µm film of Crossbond® 100% trifluoropropylmethyl polysiloxane (Rtx®-200). Chromatographic analysis was performed using a temperature program consisting of an initial hold at 70 °C for 1.0 minute, ramped up to 250 °C at a rate of 30 °C/minute followed by a hold at 250 °C for 7.0 minutes.

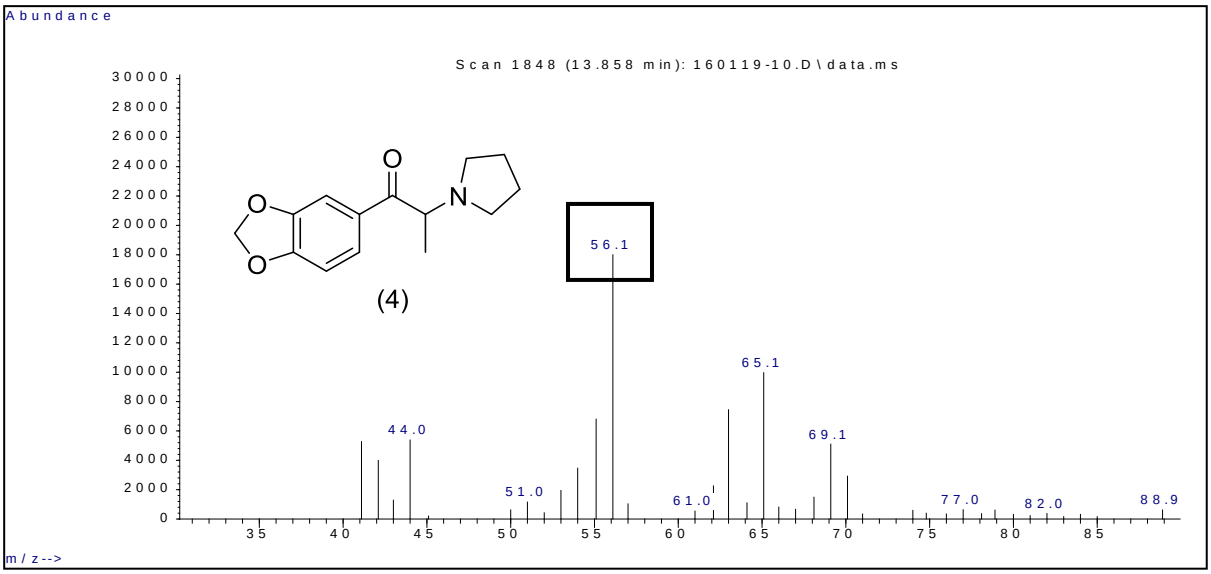

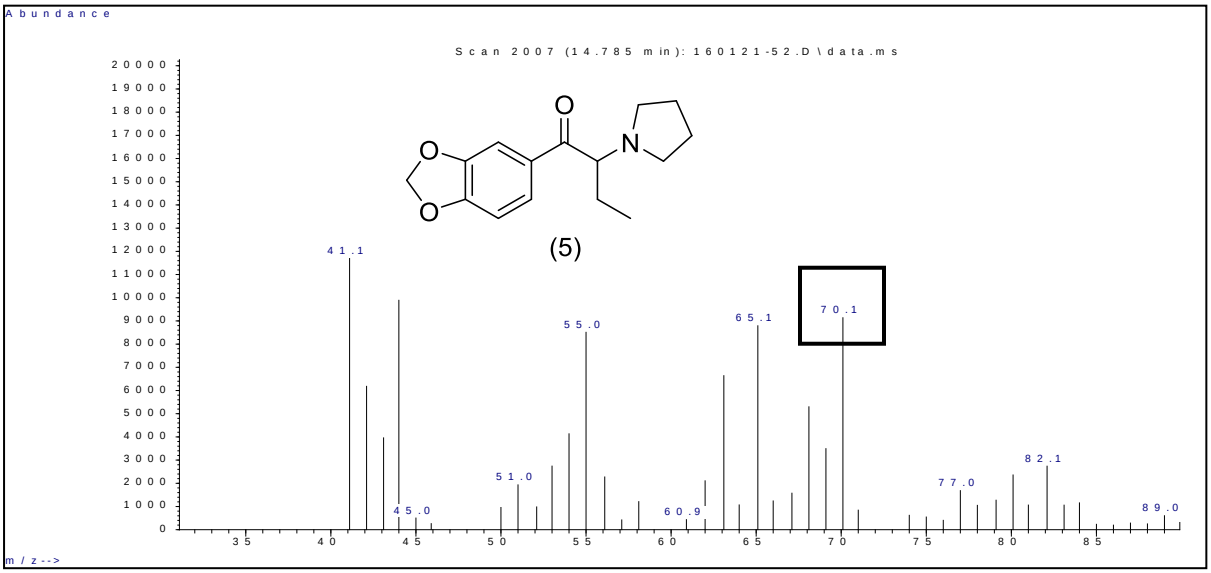

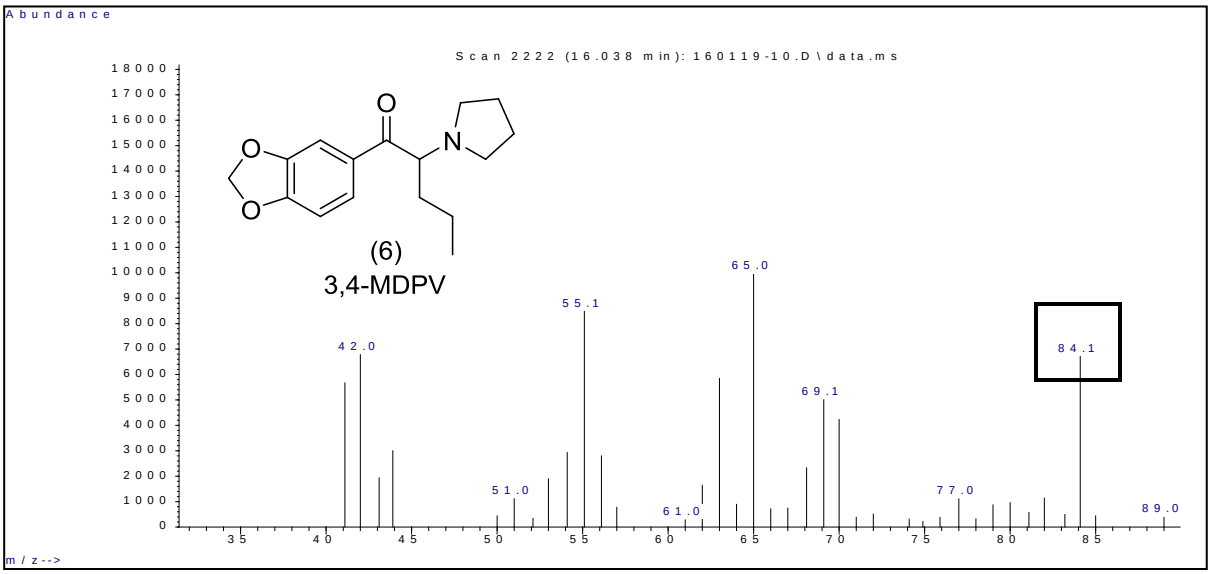

Figure 12. Low mass portion of the EI-MS for Compounds 4, 5 and 6. GC–MS System 1.

The major fragments in the product ion spectra for the iminium cations at *m/z* 98, 112 and 126 appeared at *m/z* 56, 72 and 84 respectively. The loss of a constant 42 Da across this series of homologues could suggest the involvement of both pyrrolidine ring and alkyl side-chain in the formation of these product ions.

The product ion MS/MS spectrum for Compound 3 (2,3-MDPV) in Figure 13 shows the fragments generated from the *m/z* 126 iminium cation indicating the major product ion at *m/z* 84. Thus, the 42 Da (C_3H_6) loss could be from the pyrrolidine ring or the *n*-propyl side-chain. However, the loss of 42 Da in the product ion spectrum for Compound 4 (methyl side-chain) could only come from the pyrrolidine ring portion of this iminium cation.

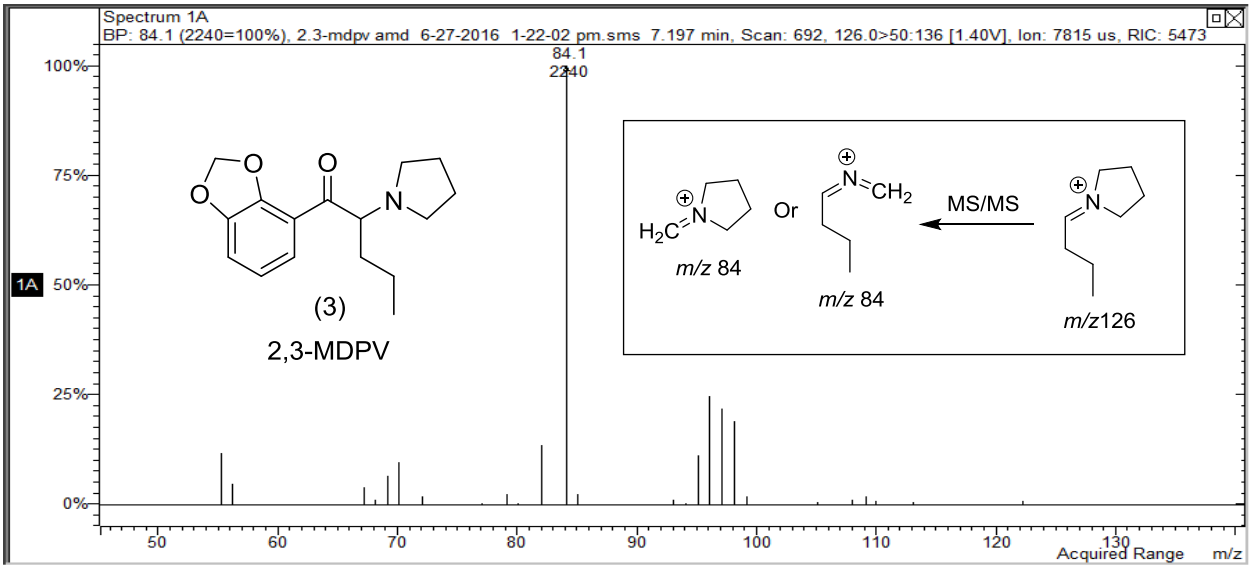

Figure 13. MS/MS scan of the *m/z* 126 base peak for 2,3-MDPV (Compound 3). See Figure 10 for the full scan EI-MS of this compound. GC–MS System 2.

The D_4 analogue of 3,4-MDPV (Compound 6) was synthesized using 2,2,5,5-pyrrolidine-D_4 and this labeled compound subjected to EI-MS as well as product ion MS/MS experiments. The full scan EI-MS in Figure 14A shows the molecular ion and the base peak with a +4 Da increase in mass as expected. Furthermore, the product ion spectrum in Figure 14B also shows a +4 Da mass increase to *m/z* 88 compared to the product ion spectrum for the unlabeled 2,3-substituted analogue in Figure 13. These results confirm the pyrrolidine ring remains a part of the product ion spectrum and this significant product ion is formed from hydrogen migration in the side-chain followed by alkene (propene) elimination (C_3H_6).

14A:

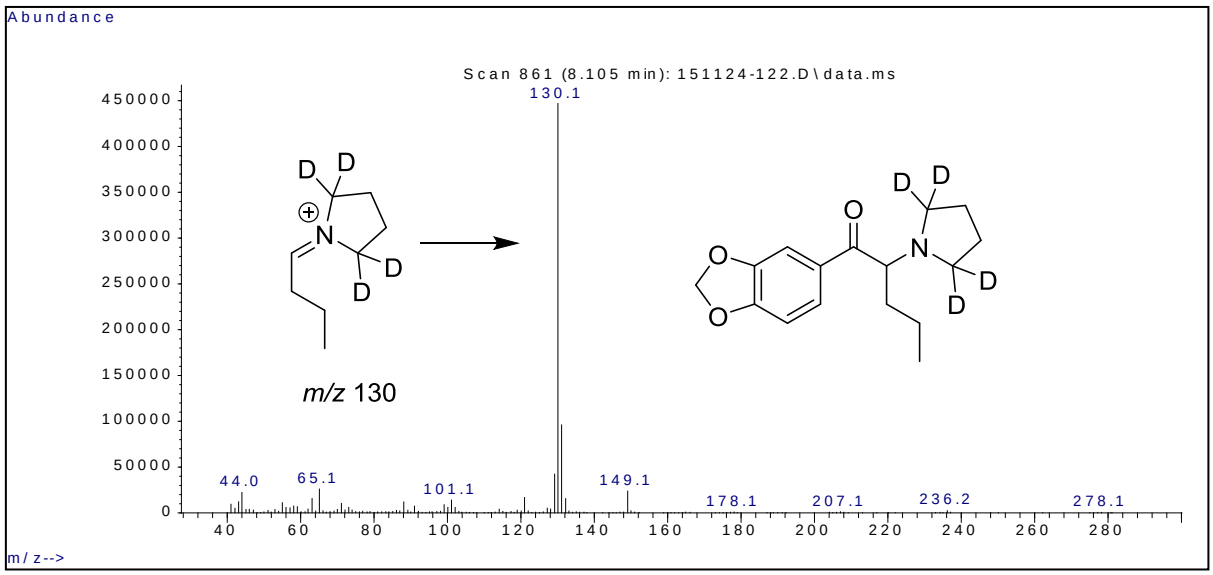

14B:

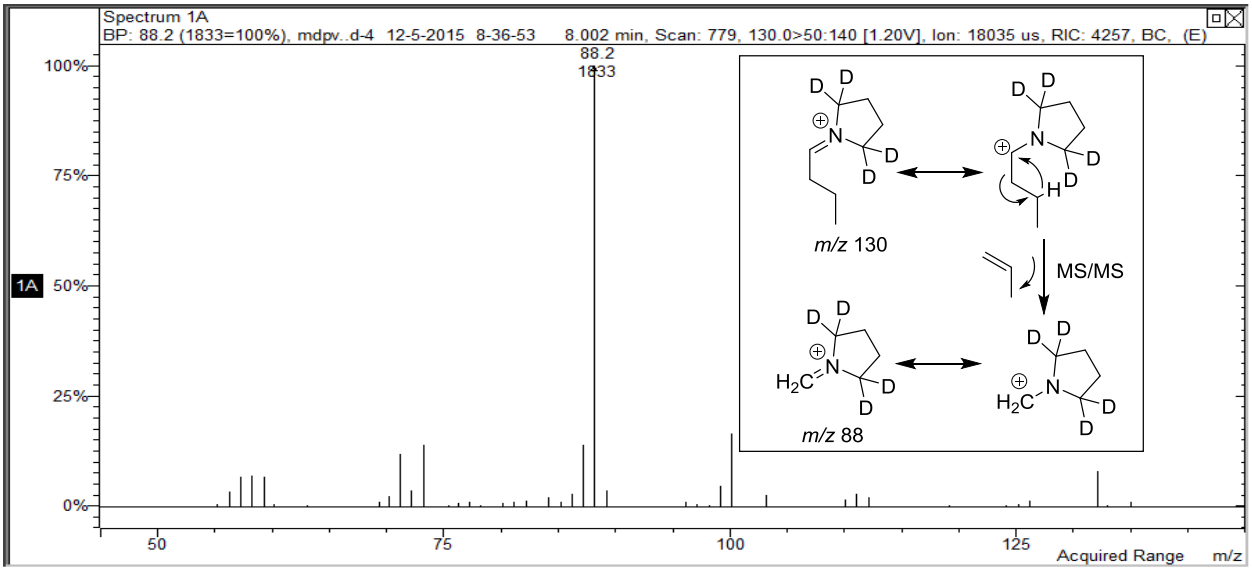

Figure 14. EI-MS and product ion spectra for the pyrrolidine-D_4 analogue of 3,4-MDPV, Compound 6. 14A= GC–MS System 1, 14B= GC–MS System 2.

The pyrrolidine-D_8 analogue of Compound 4 was synthesized using 2,2,3,3,4,4,5,5-pyrrolidine-D_8 and this labeled material subjected to EI-MS and product ion MS/MS evaluation. The results of these experiments showed the base peak iminium cation shifted to *m/z* 106 (Figure

15A), +8 Da higher than the *m/z* 98 iminium cation base peak observed in the unlabeled analogue (see Figure 10). However, the product ion in Figure 15B was shifted only +2 Da higher to *m/z* 58 indicating that only one methylene group from the pyrrolidine ring remained a portion of this new fragment. Additionally, the pyrrolidine-D_4 analogue of Compound 4 was synthesized from 2,2,5,5-pyrrolidine-D_4. The EI-MS scan for the 2,2,5,5-tetra-deutero pyrrolidine analogue of Compound 4 showed a base peak at *m/z* 102 (4 Da higher), however the MS/MS product ion remained at *m/z* 58 (spectra not shown).

These experiments confirm the source of the methylene remaining in the low mass product ion as coming from the pyrrolidine ring positions adjacent to the nitrogen (ring positions 2 or 5). Thus, the loss of 42 Da to yield the product ion for the methyl side-chain homologue in Compounds 1 and 4 results from pyrrolidine ring fragmentation while the equivalent 42 Da loss for the *n*-propyl side-chain (Compounds 3 and 6) occurs via side-chain fragmentation.

15A:

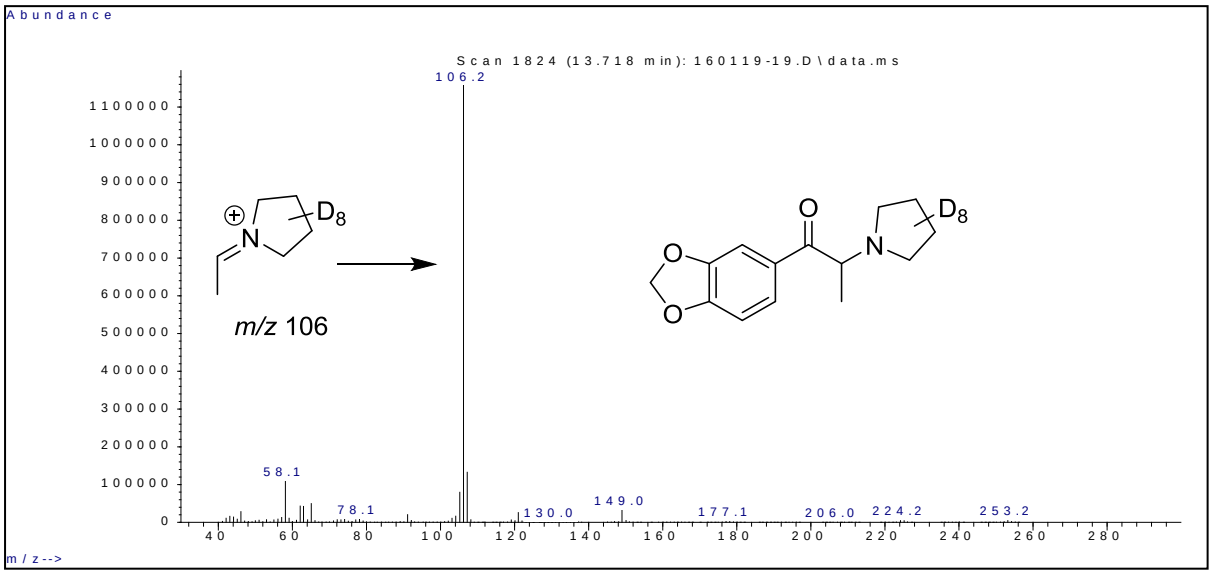

15B:

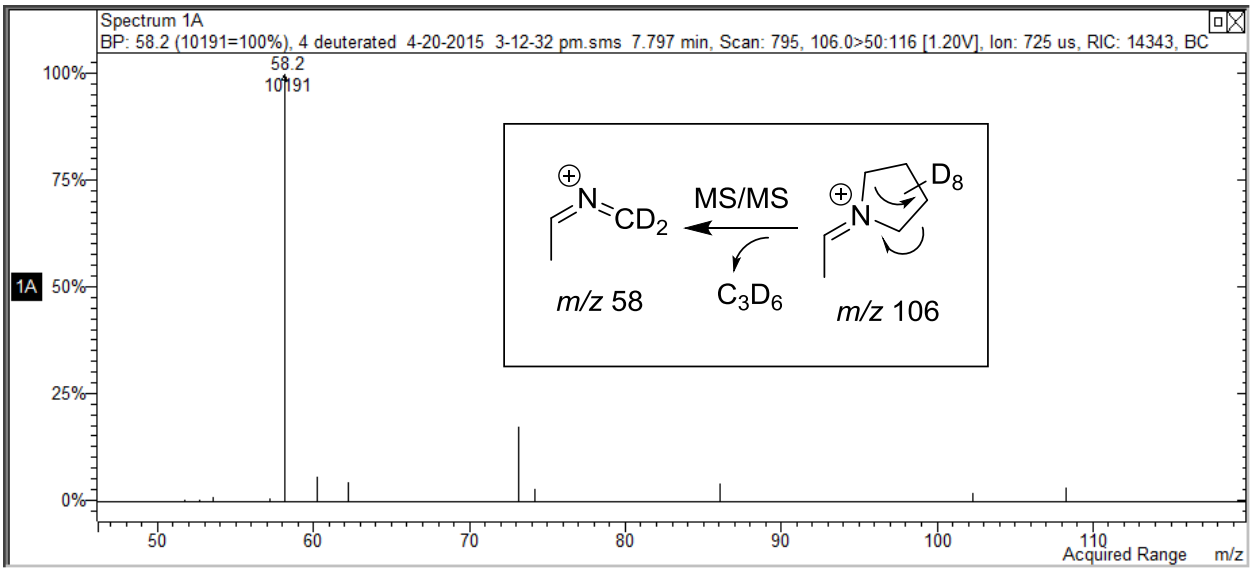

Figure 15. EI-MS and product ion spectra for the pyrrolidine-D_8 analogue of Compound 4. 15A= GC–MS System 1, 15B= GC–MS System 2.

The product ion spectrum for the *m/z* 112 base peak for Compound 5 (the ethyl side-chain homologue) confirms a transition from ring to side-chain fragmentation in the base peak iminium cations as the source for product ion formation. This MS/MS scan is shown in Figure 16 and confirms both ring and side-chain fragmentation to yield a mixture of the two major product ions at *m/z* 70 (ring fragmentation) and *m/z* 84 (side-chain fragmentation).

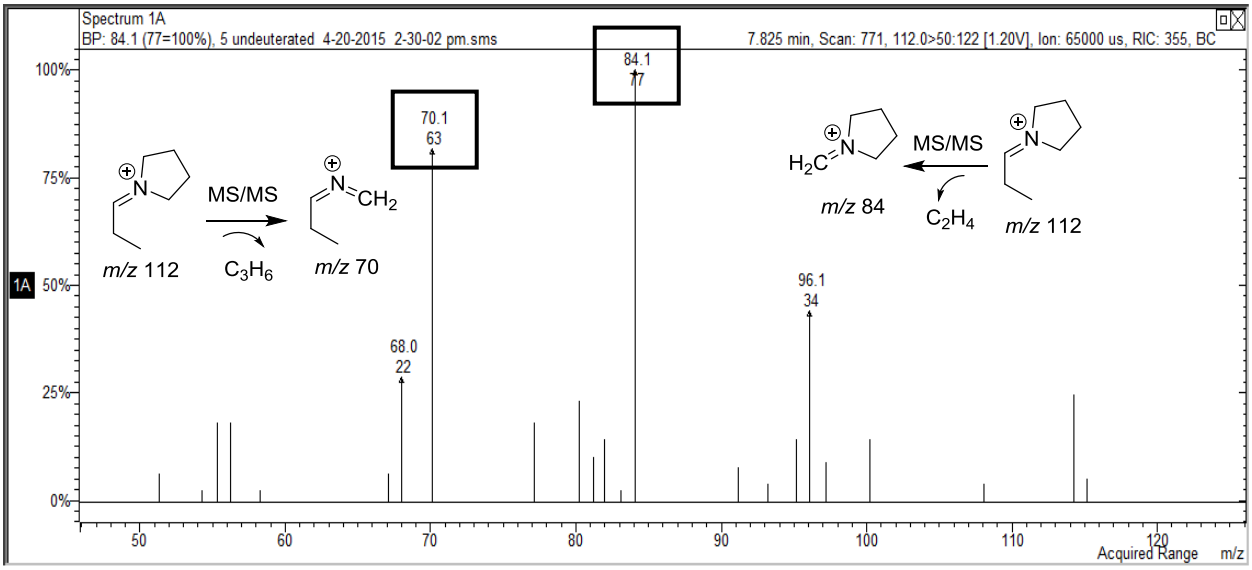

Figure 16. Product ion spectrum of the *m/z* 112 base peak of Compound 5. GC–MS System 2.

The full scan EI-MS spectrum (Figure 17 A) for the pyrrolidine-D_8 analogue of Compound 5 yields the base peak iminium cation at *m/z* 120, a mass shift of 8 Da as expected. The product ion scan (Figure 17 B) of the *m/z* 120 iminium cation yields two major peaks at *m/z* 72 (ring fragmentation, loss of C_3D_6) and *m/z* 92 (side-chain fragmentation, loss of ethylene, C_2H_4). These observed mass shifts are consistent with the assigned structures for these product ion fragments.

17A:

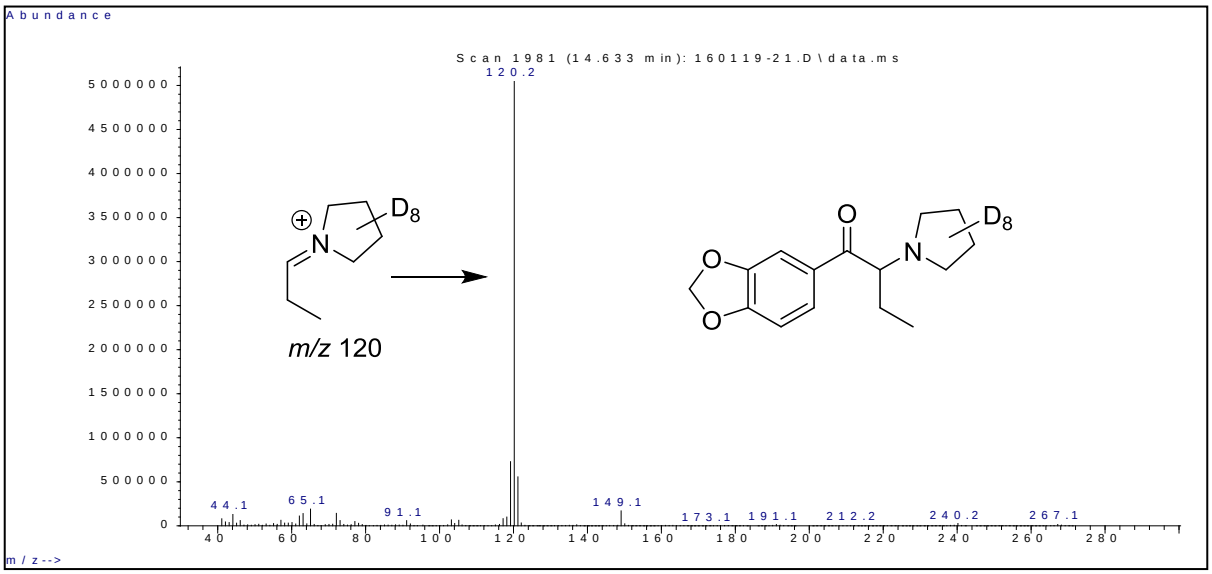

17B:

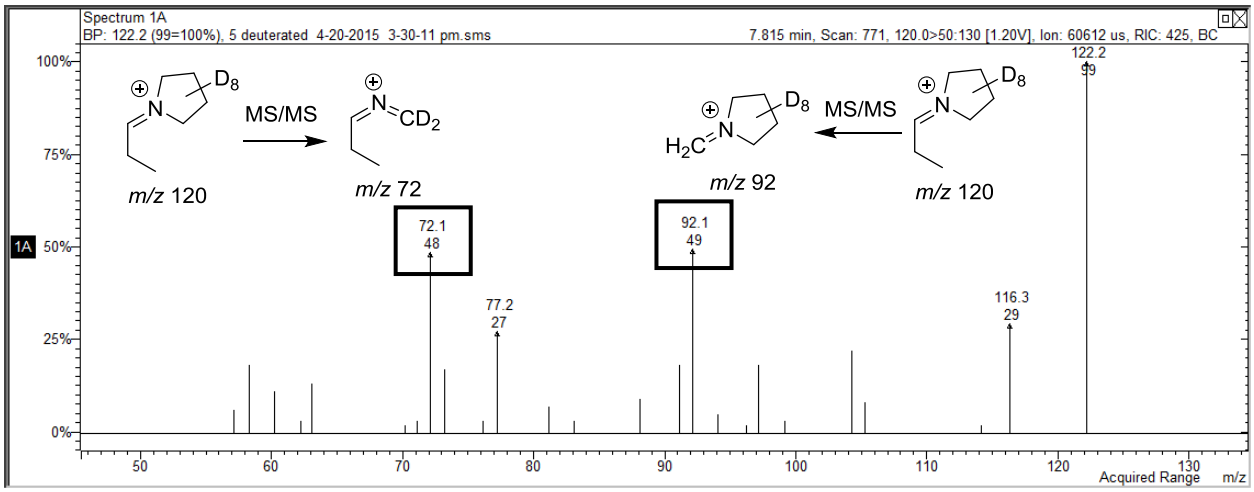

Figure 17. EI-MS and product ion spectra for the pyrrolidine-D_8 analogue of Compound 5. 17A= GC–MS System 1, 17B= GC–MS System 2.

2.1.4. Vapor phase infrared spectrophotometry

Infrared spectrometry is often used as a confirmatory method for drug identification in forensic drug analysis. Gas chromatography with infrared detection (GC–IR) was evaluated for differentiation among the six regioisomeric and homologous compounds. Infrared detection should provide compound specificity without the need for chemical modification of the drug molecule. The vapor phase infrared spectra generated in GC–IR experiments are shown in Figure 18 for an example set of regioisomeric aromatic ring substitution patterns, MDPV and its 2,3-isomer (Compounds 3 and 6). These spectra were generated directly from the chromatography peak as each compound eluted from the capillary GC column. Thus, these infrared spectra have an added level of reliability based on the purity of the chromatography peak generated in the GC–IR experiments following sample injection into the gas chromatograph. The GC–IR vapor phase infrared spectra were recorded in the range of 4000 – 550 cm^{-1} with a resolution of 8 cm^{-1}. Each compound shows a vapor phase IR spectrum with transmittance bands in the regions 1700 – 700

cm^{-1} and 3000 – 2700 cm^{-1}. In general, variations in the position of the methylenedioxy group on the aromatic ring results in variations in the IR transmittance in the region 1700 – 700 cm^{-1} [Awad *et al*, 2009]. All six compounds show a carbonyl band in the 1690 cm^{-1} range and characteristic bands in the 1500 cm^{-1} to 1200 cm^{-1} range. The characteristic bands for aromatic ethers in the 1500 cm^{-1} to 1200 cm^{-1} range provide information concerning the position of the methylenedioxy ring and its relationship to the aminoketone side-chain.

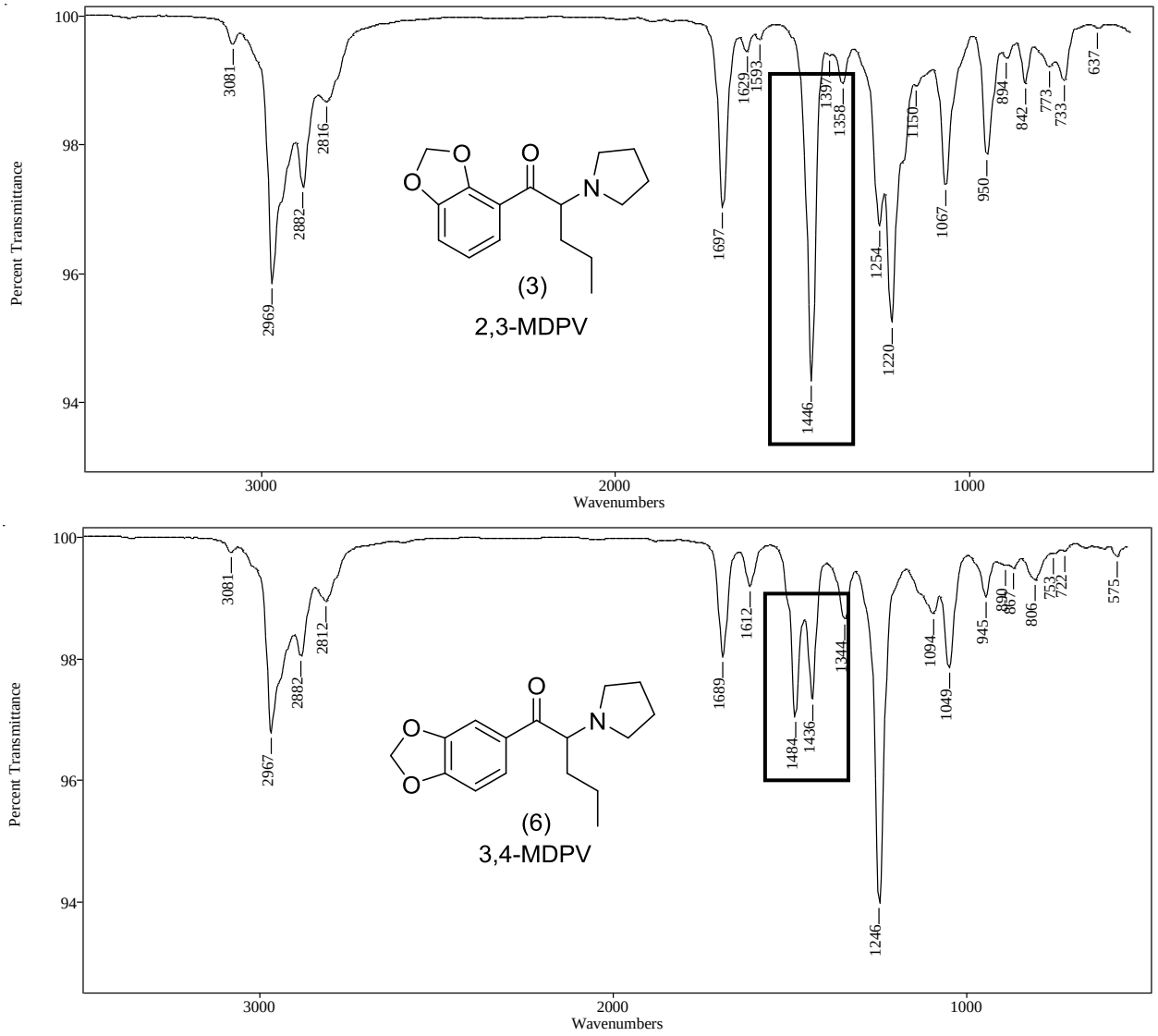

Figure 18. An example set of vapor phase IR spectra for Compound 3 (2,3-MDPV) and Compound 6 (3,4-MDPV).

The 2,3-methylenedioxy substitution pattern in Compound 3 shows a characteristic absorption in the 1500 cm^{-1} to 1200 cm^{-1} range consisting of a strong singlet band centered in the 1446 cm^{-1} range and a less intense doublet peak in the 1254/1220 cm^{-1} range. However, the 3,4-methylenedioxy substitution pattern in Compound 6 shows a doublet absorption pattern with peaks centered at 1484 cm^{-1} and 1436 cm^{-1} and an intense singlet absorption band at 1246 cm^{-1}.

The vapor phase IR spectra for the other four aminoketones (spectra not shown) as well as another example set of intermediate ketones in Figure 19 show the identical strong singlet band in the 1450 cm^{-1} range for the 2,3-substitution pattern and the corresponding doublet absorption in the same region for the 3,4-methylenedioxyphenyl substitution pattern. The structure correlated vapor phase IR absorption bands are consistent across both the precursor aldehyde and intermediate ketones as well as the target aminoketone final products. The precursor aldehydes 2,3-methylenedioxybenzaldehyde and 3,4-methylenedioxybenzaldehyde (piperonal) have identical mass spectra (not shown) but can be easily differentiated by the characteristic absorption bands in the 1500 cm^{-1} to 1200 cm^{-1} range in the vapor phase IR (spectra not shown). The 1500 cm^{-1} to 1200 cm^{-1} range for the 2,3- and 3,4-substituted series of compounds shows the sharp singlet absorption band at approximately 1450 cm^{-1} for the 2,3-isomer and the equal intensity doublet absorption bands in the same region for the 3,4 substitution pattern.

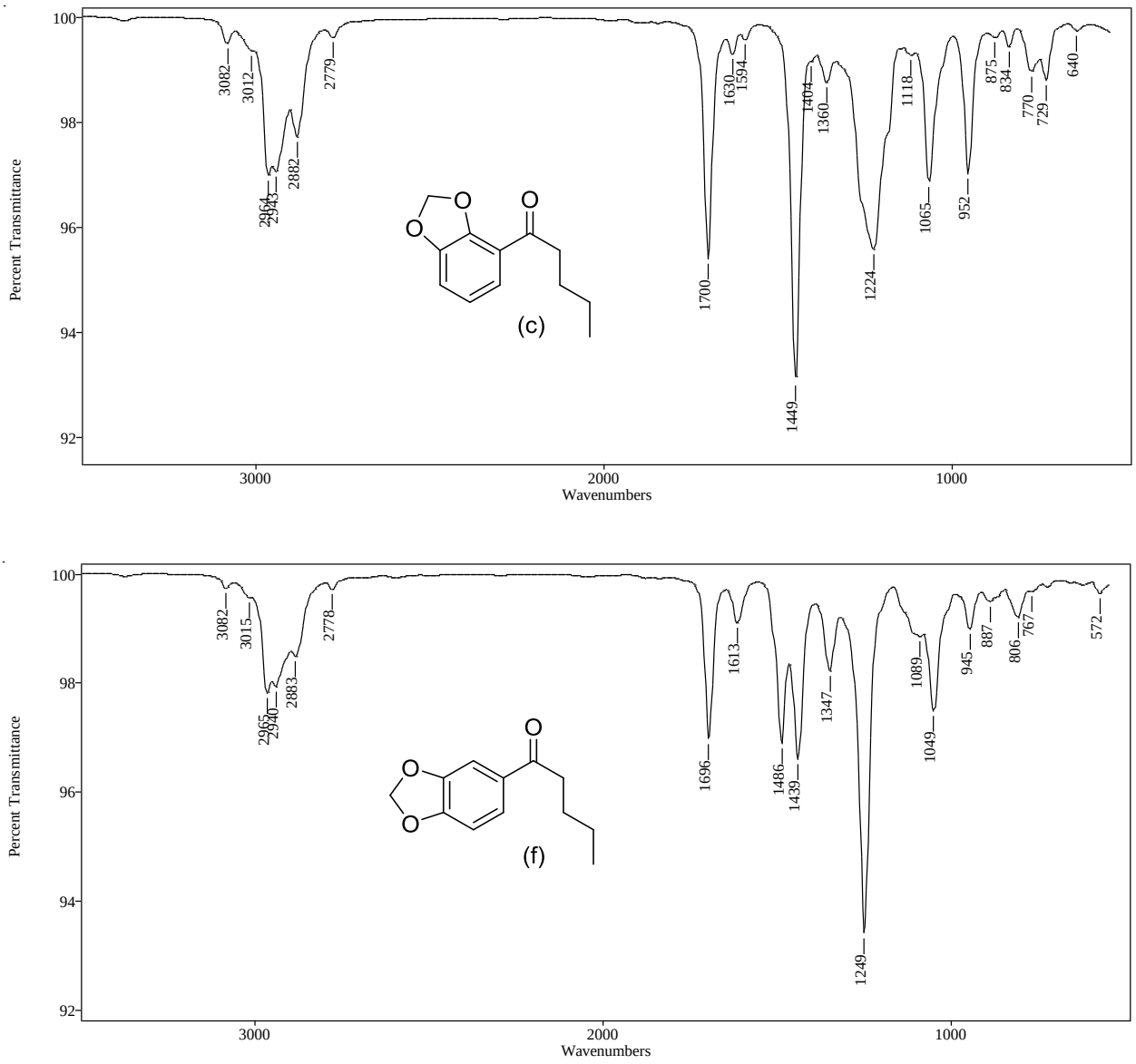

Figure 19. An example set of vapor phase IR spectra for the intermediate ketone c (2,3-methylenedioxyvalerophenone) and intermediate ketone f (3,4-methylenedioxyvalerophenone).

2.1.5. Conclusion

Characterization of the ring substitution pattern, the alkyl side-chain and the cyclic tertiary amine portions of synthetic designer drugs related to 3,4-methylenedioxypyrovalerone **(**MDPV) was accomplished by a combination of GC–MS, GC–MS/MS and GC–IR techniques. Six regioisomeric and homologous methylenedioxyphenyl-aminoketones were separated via capillary gas chromatography using an Rxi®-35Sil MS stationary phase. Chromatographic retention increases with the hydrocarbon content of the alkyl side-chain and the 3,4-methylenedioxy substitution pattern shows higher retention than the corresponding 2,3-methylenedioxy isomer.

The absorption bands in the 1500 cm^{-1} to 1200 cm^{-1} range in the vapor phase infrared spectra readily allows for differentiation of the aromatic ring substitution pattern in the target aminoketones and the related synthetic precursor materials. The full scan EI mass spectra show homologous base peaks and the product ion spectra of these iminium cations characterize the alkyl side-chain portion of the molecule.

2.2. Differentiation of regioisomeric methylenedioxyphenyl-aminoketones and desoxy cathinone derivatives: Cyclic tertiary amines and side-chain regioisomers of MDPV by GC–MS, GC–MS/MS and GC–IR

The aminoketones and the desoxy phenethylamine analogues in this study represent a combination of alkyl side-chain and cyclic amines (azetidine, pyrrolidine, piperidine and azepane) to yield a set of molecules of identical elemental composition as well as major mass spectral fragment ions (base peaks) of identical elemental composition. A series of regioisomeric cyclic tertiary amines were prepared and evaluated in EI-MS, MS/MS product ion and IR experiments. These desoxy phenethylamine analogues of the aminoketone designer drug, 3,4-methylenedioxypyrrovalerone (MDPV) related to the natural product cathinone were prepared from piperonal (3,4-methylenedioxybenzaldehyde) via the intermediate ketones. The aminoketones and the desoxy phenethylamine regioisomers were each separated in capillary gas chromatography experiments using an Rxi®-17Sil MS stationary phase with the aminoketones showing greater retention than the corresponding desoxyamines.

The electron ionization mass spectra for the aminoketones as well as the desoxy phenethylamines yield equivalent *m/z* 126 regioisomeric iminium cation base peaks. Product ion fragmentation provides useful data for differentiation of regioisomeric cyclic tertiary amine iminium cations. Deuterium labeling in both the cyclic amine and alkyl side-chain allowed for the confirmation of the structure for the major product ions formed from the EI-MS iminium cation base peaks. Variations of ring size and hydrocarbon side-chain length yield a series of regioisomeric products having equivalent regioisomeric EI-MS iminium cations. These iminium cation base peaks show characteristic product ion spectra which allow differentiation of the ring and side-chain portions of the structure. The azetidine series yields products exclusively by side-chain fragmentation while the pyrrolidine series undergoes ring fragmentation for the methyl side-

chain and both ring and side-chain fragmentation for the higher homologues. The piperadine containing amines undergo side-chain fragmentation in the ethyl, and *n*-propyl side-chains while the methyl side-chain analogue undergoes ring fragmentation. Both side-chain and ring fragmentation yield a mixture of product ions in the higher side-chain homologues for the seven membered cyclic tertiary amines and ring fragmentation occurs in the methyl side-chain analogue. Ring fragmentation in the pyrrolidine series results in the loss of 42 Da from the iminium cation base peak, 28 Da for the piperadine series and 54 Da for the azepane series.

The vapor phase infrared spectra for these desoxy phenethylamines show doublet absorption bands at 1489 cm^{-1} and 1442 cm^{-1} characteristic for the 3,4-methylenedioxy aromatic ring substitution pattern and the unsymmetrical nature of these doublet absorption bands indicates the lack of a carbonyl group at the benzylic position of the alkyl side-chain.

2.2.1. Synthesis of the cyclic tertiary amines and side-chain regioisomers of MDPV

2.2.1.1. Synthesis of the regioisomeric aminoketones

The desired regioisomeric aminoketones were prepared individually from piperonal using the same procedure prescribed previously in (Section 2.1.1.) with the exception of using three different cyclic amines in addition to pyrrolidine, which include azetidine, piperidine and azepane as shown in Scheme 13. The final products were isolated by solvent extraction and purified by preparative thin layer chromatography (TLC) 20:80 ethyl acetate-petroleum ether using Analtech (Newark, DE) glass backed 20 x 20 cm plates with a 1000 µm layer of silica and an inorganic fluorescent 254 nm indicator.

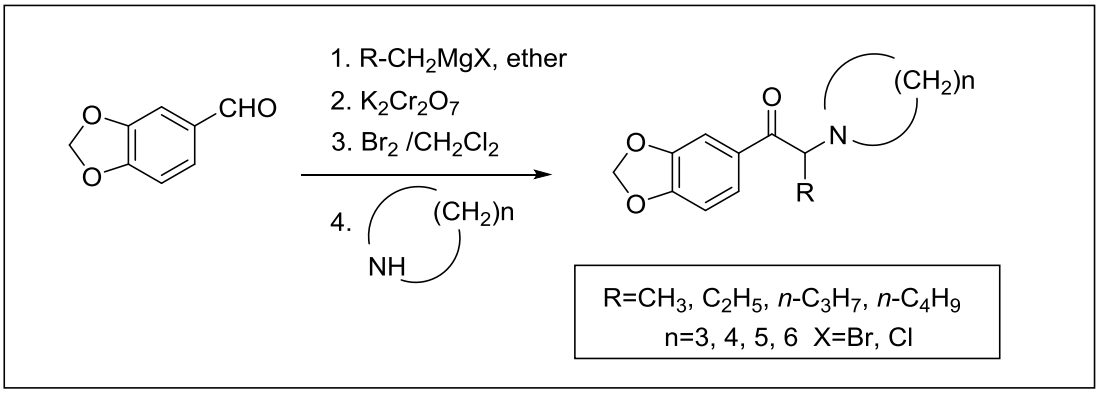

Scheme 13. General synthetic scheme for the four cyclic tertiary amines and side-chain regioisomers of MDPV.

2.2.1.2. Synthesis of the regioisomeric desoxy phenethylamines

The regioisomeric desoxy cathinones were prepared via a 3-step synthetic procedure (see Scheme 14, with desoxy-MDPV as example). Sodium amide was added to a mixture of piperonal and 2-bromoalkanoic acid ethyl esters to yield the corresponding glycidate esters as yellow oils (Darzens reaction). These crude esters were hydrolyzed using aqueous methanol and sodium hydroxide and then acidified to pH 1 with conc. HCl to yield the intermediate ketones as viscous yellow oils. The ketones were then reductively aminated with cyclic amines and subsequently reduced by sodium cyanoborohydride to yield the desired desoxyamine final products. The final products were isolated by solvent extraction and purified by preparative thin layer chromatography (TLC) 20:80 ethyl acetate-petroleum ether using Analtech (Newark, DE) glass backed 20 x 20 cm plates with a 1000 µm layer of silica and an inorganic fluorescent 254 nm indicator.

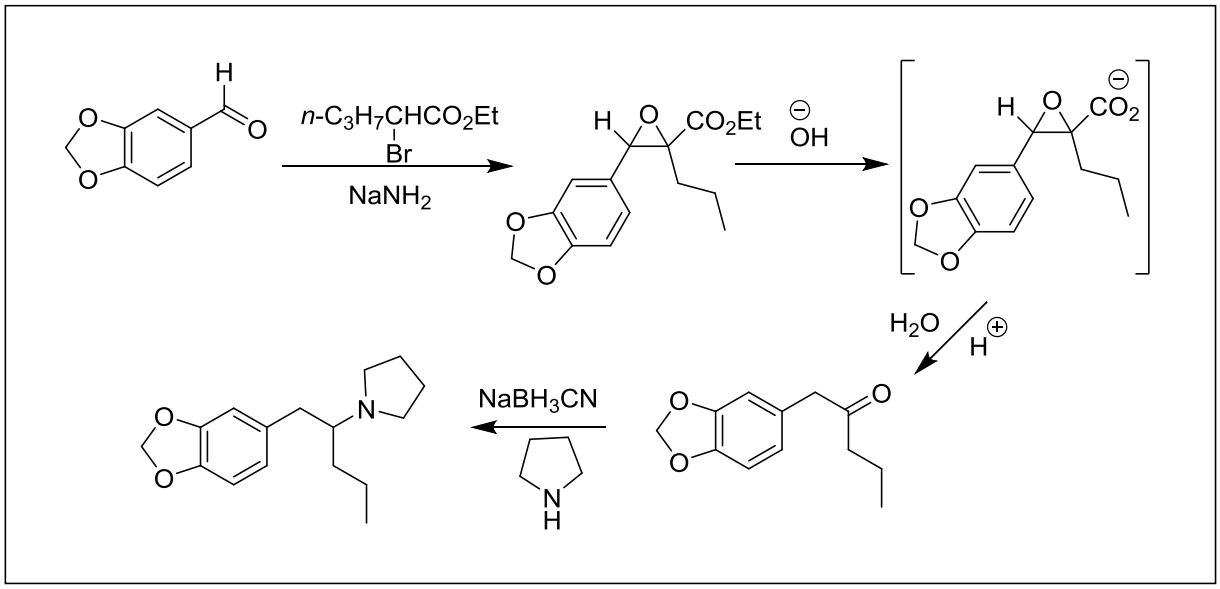

Scheme 14. General synthetic scheme for the desoxy phenethylamines with desoxy-MDPV as example.

2.2.1.2.1. Alternative synthesis of the intermediate ketones for the desoxy phenethylamines

The synthesis of the intermediate ketones was reported in 1986 [Nichols *et al*, 1986]. The ketone was prepared from piperonal by treating with alkyllmagnesium halide. Dehydration of the resulting alcohol yielded 3,4-methylenedioxyphenyl-2-alkene derivative, which was oxidized to the desired ketone (Scheme 15). Another way to prepare the intermediate ketones is the condensation of piperonal with nitroalkane [Clark *et al*, 1995]. The resulting 3,4-methylenedioxyphenyl-2-nitroalkene derivative can be converted to the ketone by treatment with iron, ferric chloride and hydrochloric acid.

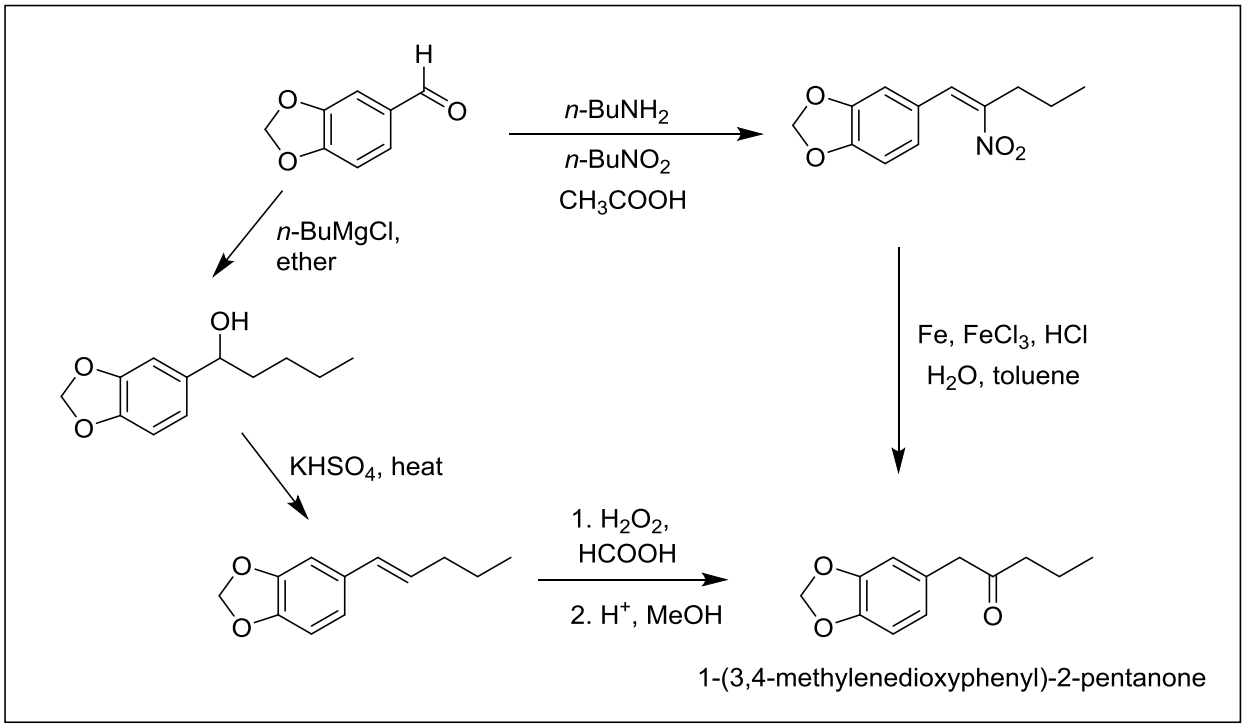

Scheme 15. Alternative synthetic scheme for the intermediate ketones of the desoxy phenethylamines with 3,4-methylenedioxyphenyl-2-pentanone as example.

2.2.2. Gas chromatographic separation

The chromatogram in Figure 20 shows the GC separation for the eight regioisomeric and homologous 3,4-methylenedioxyphenyl-ketones. This capillary gas chromatographic separation was accomplished using a stationary phase of Rxi®-17Sil MS in a 30m x 0.25mm id capillary column. The relative retention for these ketones depends on both the total number of carbons of the side-chain and the position of the carbonyl group. The precursor ketones with the smallest alkyl side-chain (Compounds a and e) elute first and the retention increases with each additional side-chain methylene unit. Within the side-chain regioisomers, the precursor ketone with the carbonyl group at the 2-position of the side-chain elutes before its equivalent isomer with the 1-position carbonyl group (for example, Compound e elutes before Compound a). This relative elution pattern

based on the position of the carbonyl group continues for each alkyl-side chain in this study. The effect of carbonyl position on elution order was further evaluated by a comparison of the retention characteristics for a set of unsubstituted aromatic ring regioisomers. The GC separation (not shown) for 1-phenyl-2-propanone (P-2-P, phenylacetone) and 1-phenyl-1-propanone (P-1-P, propiophenone) using the same column gave a baseline resolution of the two regioisomers in about five minutes with the P-2-P eluting first and P-1-P having the higher retention time. These results are consistent with those described above and in all examples the regioisomers with the carbonyl at the 1-position of the alkyl side-chain gave enhanced retention compared to the regioisomers with the carbonyl at the 2-position. The stationary phase for these separations is the relatively polar Rxi®-17Sil MS containing a 50% phenyl polymer and the enhanced pi-electron conjugated system of the 1-carbonyl isomers shows higher affinity for this material than does the un-conjugated system in the 2-carbonyl isomers.

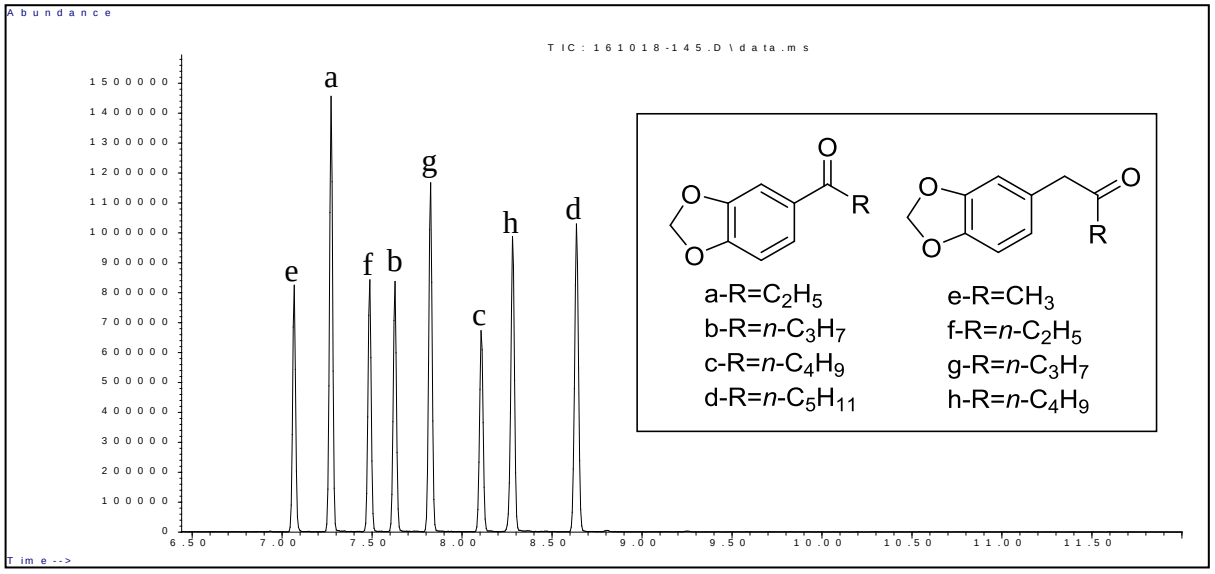

Figure 20. Capillary gas chromatographic separation of the eight precursor regioisomeric and homologous 3,4-methylenedioxyphenyl-ketones on Rxi®-17Sil MS stationary phase. GC–MS System 1.

The chromatograms in Figure 21 show the gas chromatographic separation of the regioisomeric aminoketones and the desoxy phenethylamine analogues. These two sets of compounds each represent a combination of alkyl side-chain length and cyclic tertiary amine ring size to yield molecules of identical elemental composition as well as major mass spectral fragment ions (base peaks) of an identical elemental composition. While the presence of the carbonyl group is unique to Compounds 1–4 yielding two sets of regioisomers (Compounds 1–4 and Compounds 5–8), these eight compounds all yield equivalent EI-MS iminium cation base peaks at *m/z* 126 $(C_8H_{16}N)^+$. The chromatogram in Figure 21A shows the separation of the desoxy phenethylamine series of regioisomers while Figure 21B represents the separation of the corresponding aminoketone cathinone derivatives (Compound 2 is the designer drug of abuse known as MDPV, 3,4-methylenedioxypyrrovalerone).

The desoxy phenethylamine series (Compounds 5–8) each vary in ring size for the cyclic tertiary amino group and the length of the hydrocarbon side-chain. Each methylene unit increase in ring size for the cyclic amino group are offset by a corresponding decrease in one methylene unit in the alkyl side-chain producing this set of regioisomers. For example, Compound 5 consists of a combination of the 4-membered ring cyclic amine azetidine with a four-carbon butyl side-chain (*n*-C_4H_9) while the isomer (Compound 6) with the next higher cyclic amino group (the 5-membered ring pyrrolidine moiety) contains a three carbon *n*-propyl side-chain (*n*-C_3H_7) and this pattern continues for Compounds 7 and 8. The resulting set of four regioisomeric desoxy phenethylamines (Compounds 5–8) has the same elemental composition and mass.

A:

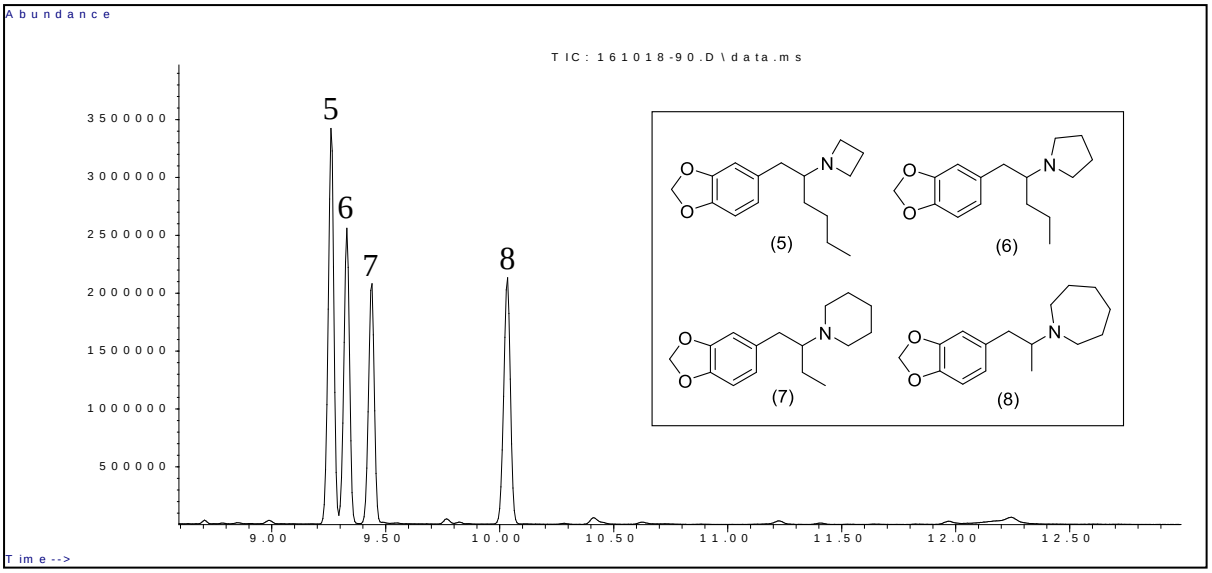

B:

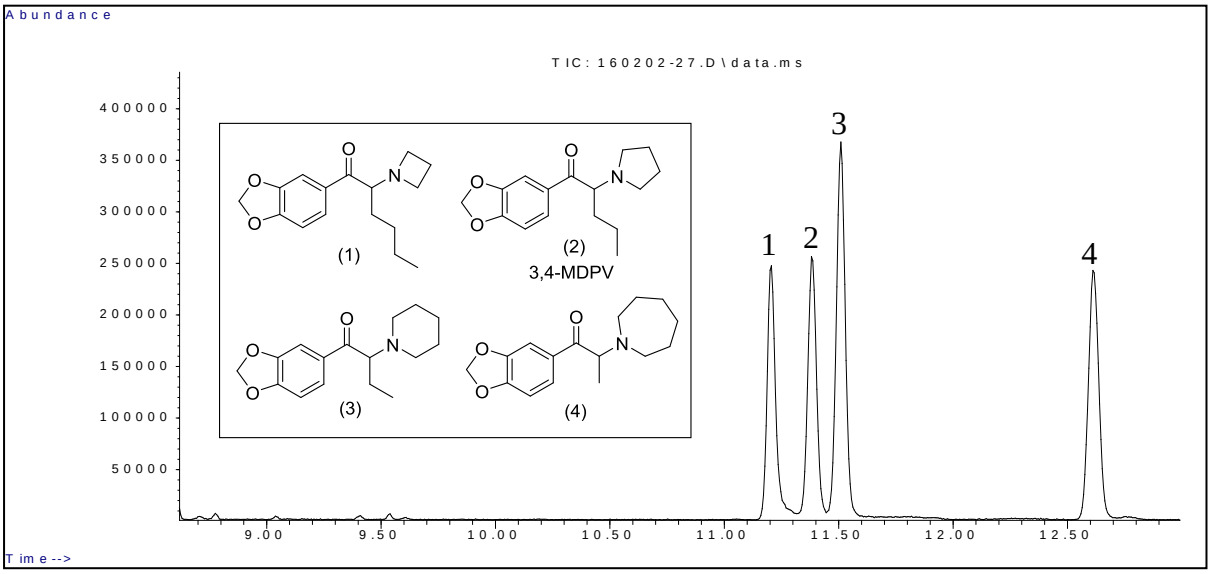

Figure 21. Capillary gas chromatographic separation of the four regioisomeric desoxyamines (A) and the four regioisomeric aminoketones (B) on Rxi®-17Sil MS stationary phase and identical temperature program. GC–MS System 1.

The chromatogram in Figure 21A shows the GC separation of the four regioisomeric desoxy phenethylamine analogues on an Rxi®-17Sil MS stationary phase. This phase is equivalent to a 50% phenyl, 50% dimethyl polysiloxane. The elution order for the regioisomeric amines appears controlled by the size of the cyclic tertiary amine portion of the molecule. The isomer containing the 4-membered ring azetidine (Compound 5) elutes first followed by the pyrrolidine containing isomer then the piperidine containing isomer and finally the 7-membered ring azepane containing isomer displaying the highest degree of retention on this stationary phase.

The chromatogram in Figure 21B was obtained on the same column and stationary phase as well as the identical temperature program as that in Figure 21A. The pattern of molecular modifications in ring size and side-chain length to yield these regioisomers (Compounds 1–4) is identical to that described above. These aminoketone regioisomers show the identical elution order as that observed for the desoxy phenethylamines in Figure 21A. The compounds elute according to cyclic tertiary amine ring size with the azetidine containing isomer eluting first and the azepane containing isomer eluting last. A comparison of the retention properties resulting from side-chain verses ring homologation on the Rxi®-17Sil MS stationary phase revealed significantly greater retention for the ring homologue. The chromatogram illustrating this evaluation is presented in Figure 22 and it shows much greater retention for the expanded ring homologue (pyrrolidine to piperidine) than the side-chain homologue (methyl to ethyl) in a similar series of aminoketone analogues. The selectivity of stationary phase polymers in gas chromatography is a complex mixture of forces including steric and electronic. The relative polar nature of the high phenyl group content of the stationary phase liquid would suggest polar interactions as a central component of the retention of these regioisomeric amines. The larger alkyl side-chain for Compounds 1 and 5 may provide maximum shielding of interactions between the electrons on nitrogen and the phenyl

groups of the stationary phase. These steric effects would be reduced as the alkyl side-chain length decreases allowing more efficient polar association thus increasing retention for the larger ring regioisomers with the smaller alkyl side-chains.

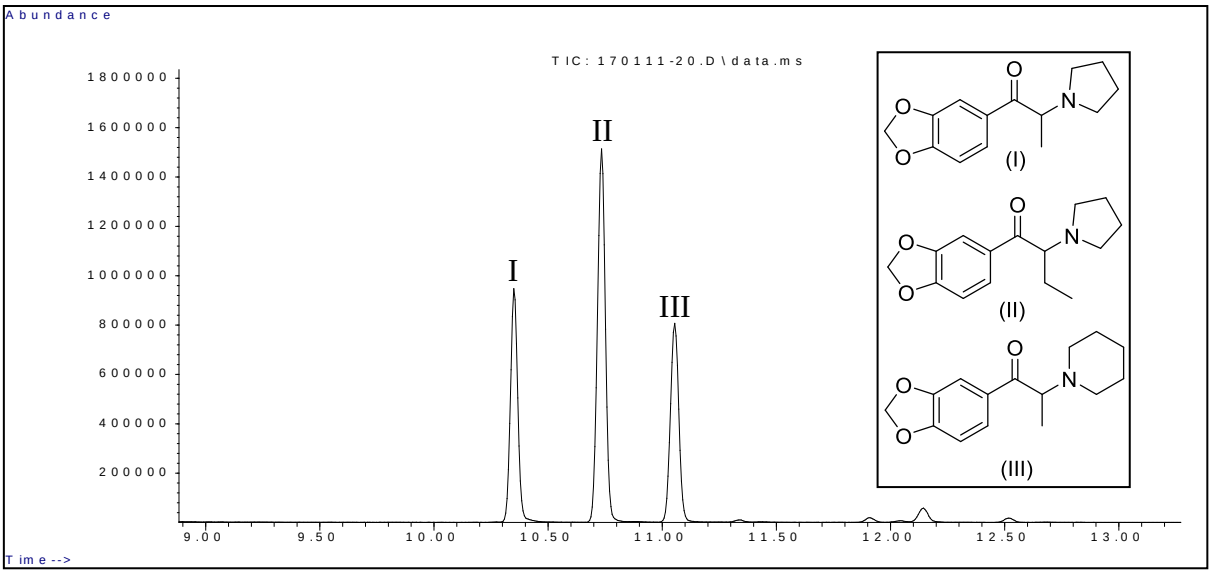

Fgure 22. Capillary gas chromatographic separation of three aminoketone analogues illustrating the effect of side-chain and ring methylene (CH_2) homologation on retention for Compound I.

Since the chromatograms in Figures 21A and 21B were obtained under identical conditions, a comparison of these two elution profiles reveals a role for the carbonyl group in retention for these compounds. This comparison shows a retention increase for the carbonyl containing compounds compared to the corresponding desoxy phenethylamine analogues and suggests enhanced stationary phase affinity based on polar interactions with the carbonyl group. Thus, the fully conjugated and extended pi-electron system of the 1-carbonyl isomers shows higher affinity for the phenyl-group containing stationary phase than does the un-conjugated system of the desoxy phenethylamine analogues. This observation appears consistent with the elution order observed for the regioisomeric ketones in Figure 20.

Compounds 2 and 3 in Figure 21B represent a closely eluting critical peak pair in this analysis. The chromatogram in Figure 23 shows the results of injecting a mixture of Compounds 1–4 using an Rxi®-5Sil MS stationary phase (low polarity Crossbond® silarylene phase; similar to 5% phenyl, 95% dimethyl polysiloxane). One of the components of this essentially co-eluting pair (Compounds 2 and 3) is the designer drug of abuse, MDPV (Compound 2) and this chromatogram illustrates the potential for co-elution of regioisomeric substances of equivalent electron ionization mass spectra. Chromatographic co-elution of compounds having equivalent mass spectra is a concern in forensic drug analysis especially for totally synthetic designer drugs where compounds may be previously unknown. All the GC–MS chromatographic separations were carried out using a temperature program consisted of an initial hold at 70 °C for 1.0 minute, ramped up to 250 °C at a rate of 30 °C/minute followed by a hold at 250 °C for 15.0 minute.

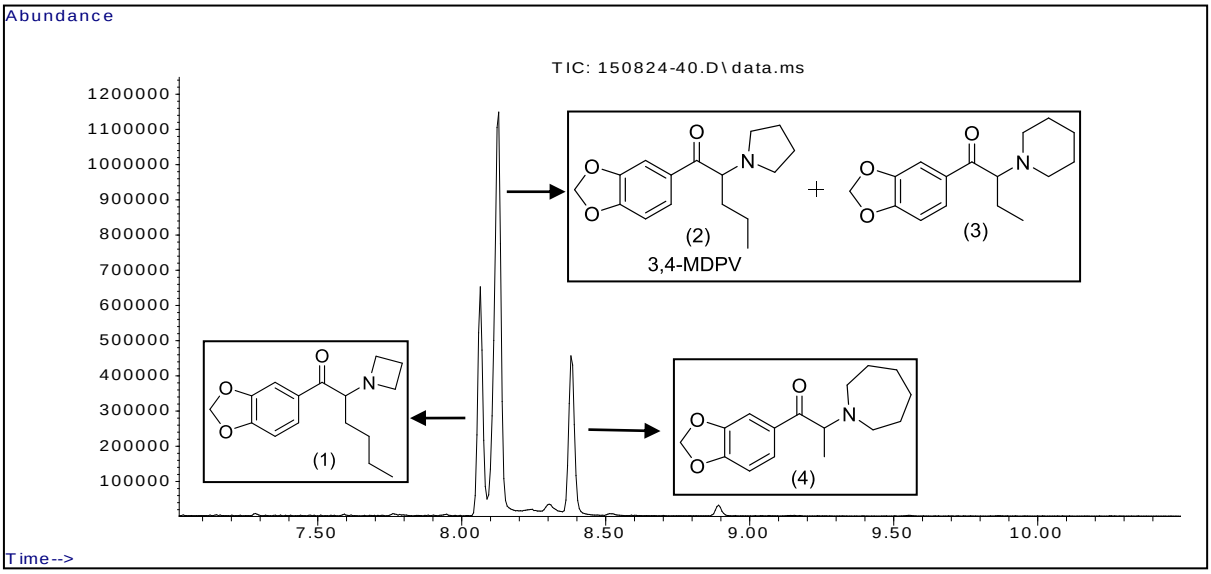

Figure 23. Capillary gas chromatographic separation of Compounds 1–4 with co-elution of Compounds 2 (3,4-MDPV) and 3. GC–MS System 1. Rxi®-5Sil MS stationary phase.

A similar co-elution pattern has been also observed after injecting a sample mixture of Compounds 2 and 3 using CI technique (using methanol as the CI reagent gas) and the identical temperature program described previously. These two isomers each yield an iminium cation base peak at *m/z* 126 and equivalent minor fragment ions including the 3,4-methylenedioxybenzoyl ion at *m/z* 149. The chromatogram in Figure 24 illustrates the co-elution of the two isomers and the chromatography peak was maximized to further emphasize that both isomers are co-eluting under the same peak and no baseline resolution was observed. The GC–CI-MS study was performed on a column (30 m × 0.25 mm i.d.) coated with 0.10 µm film of Crossbond® 100% dimethyl polysiloxane (Rtx®-1), a commonly used stationary phase in forensic analysis. These two examples (shown in Figures 23 and 24) are clear evidences that chromatographic co-elution is a concern among regioisomers despite the different stationary phases that might be available.

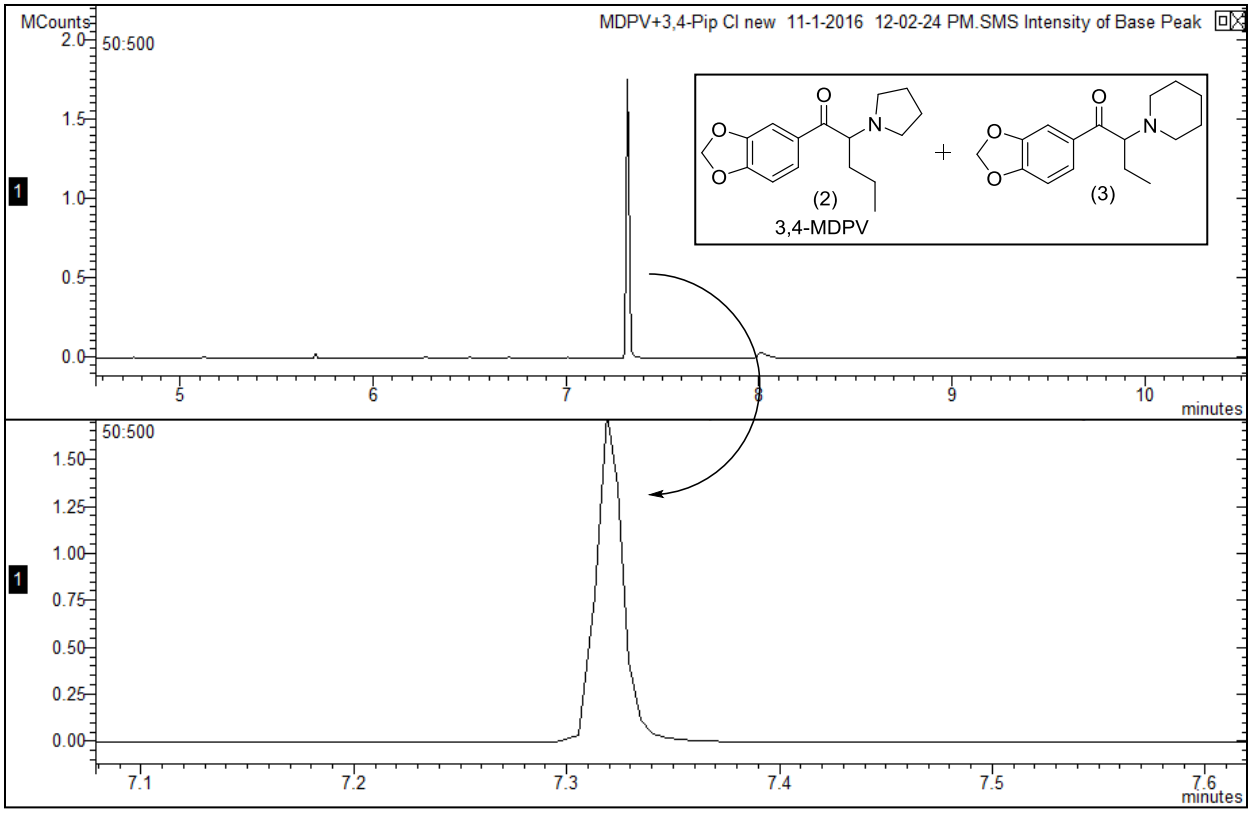

Figure 24. Capillary gas chromatographic co-elution of Compounds 2 (3,4-MDPV) and 3. GC–MS System 2 (CI technique). Rtx®-1 stationary phase.

2.2.3. Mass spectral studies (EI-MS, CI-MS and MS/MS)

The electron ionization mass spectra for the intermediate regioisomeric ketones (Compounds c and g) are shown in Figure 25. While these two examples are for compounds having identical elemental composition ($C_{12}H_{14}O_3$), the position of the carbonyl in the side-chain provides unique and characteristic fragment ions. Compound g with the carbonyl group at the 2-position of the C_5 side-chain generates the 3,4-methylenedioxybenzyl cation (*m/z* 135) as the base peak. While the base peak at *m/z* 149 (3,4-methylenedioxybenzoyl cation) is characteristic for Compound c with the carbonyl group at the 1-position of the side-chain.

A:

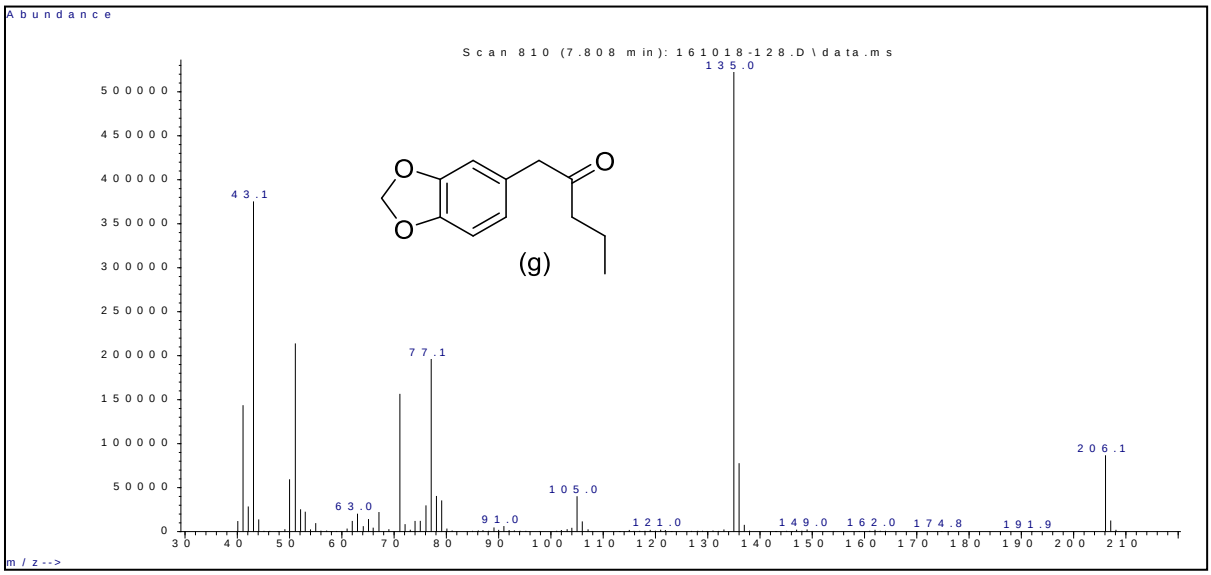

B:

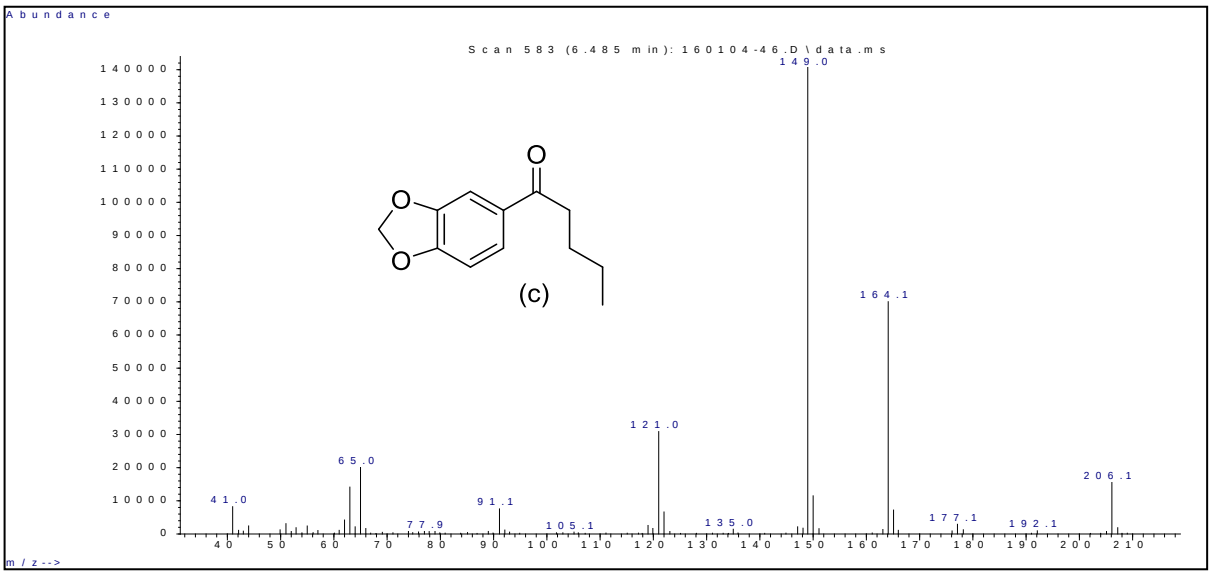

Figure 25. Electron ionization mass spectra (EI-MS) for the intermediate regioisomeric ketones. A: 1-(3,4-methylenedioxyphenyl)-2-pentanone; B: 1-(3,4-methylenedioxyphenyl)-1-pentanone. GC–MS System 1.

The full electron ionization mass spectra (EI-MS) for the four regioisomeric aminoketones are shown in Figure 26. The length of the alkyl side-chain varies in each of the compounds in order to yield the mass equivalent regioisomeric iminium cation species at *m/z* 126, the base peak for the cathinone derivative MDPV. These iminium cations are the base peaks and the only peaks of significant relative abundance in each of the four spectra shown in Figure 26. These fragments are generated by the loss of the 3,4-methylenedioxybenzoyl radical (149 Da) from each of the molecular ions. Each of the four compounds whose spectra are shown in Figure 26 has equivalent molecular ions at *m/z* 275 for the same elemental composition, $C_{16}H_{21}NO_3$. Differentiation of these compounds by GC–MS alone would be based primarily on chromatographic retention characteristics since these four compounds also yield regioisomeric major fragment ions of identical elemental composition. Such a chromatographic identification would require the availability of a number of reference samples for retention time comparisons.

A:

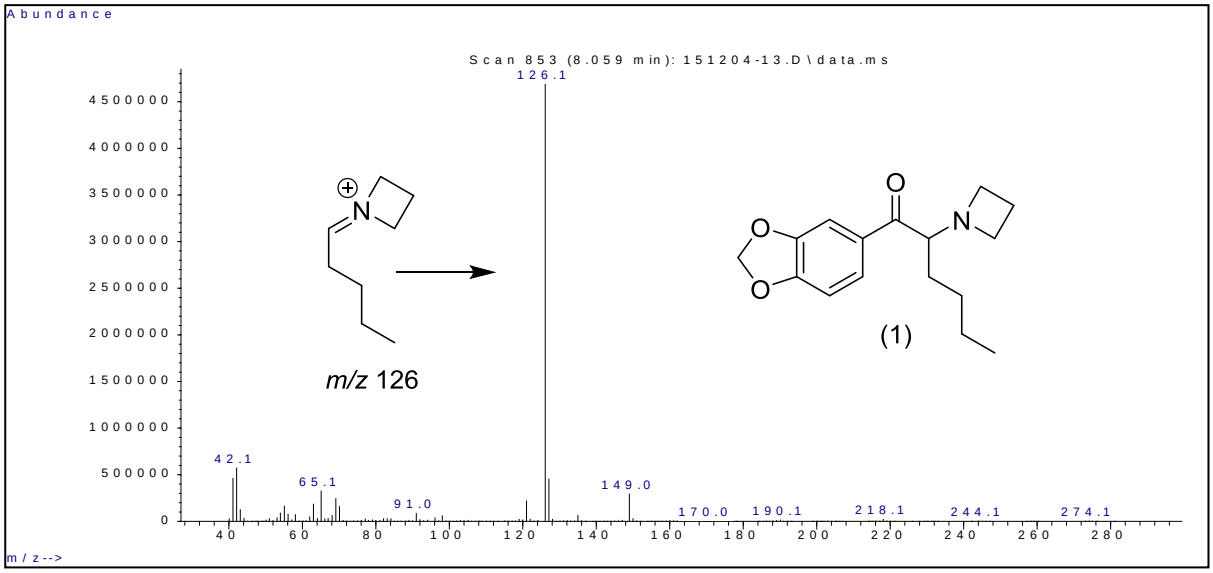
Abundance
Scan 853 (8.059 min): 151204-13.D\data.ms
126.1
4500000
4000000
3500000
3000000
2500000
2000000
1500000
1000000
500000
0
42.1
65.1
91.0
149.0
170.0
190.1
218.1
244.1
274.1
40 60 80 100 120 140 160 180 200 220 240 260 280
m/z-->
m/z 126
(1)

B:

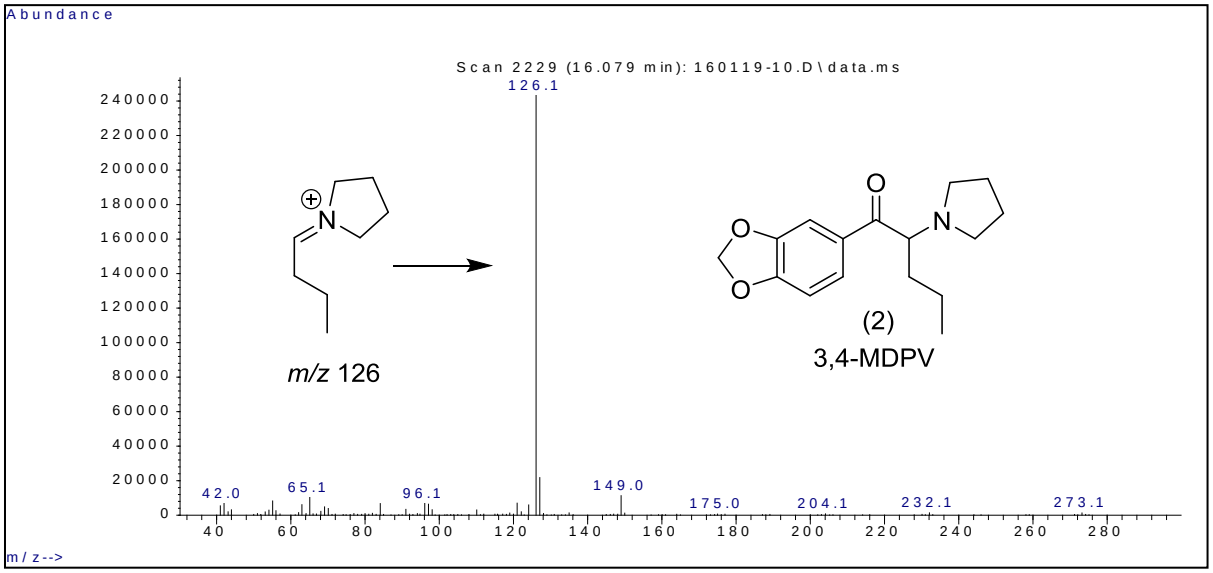
Abundance
Scan 2229 (16.079 min): 160119-10.D\data.ms
126.1
240000
220000
200000
180000
160000
140000
120000
100000
80000
60000
40000
20000
0
42.0
65.1
96.1
149.0
175.0
204.1
232.1
273.1
40 60 80 100 120 140 160 180 200 220 240 260 280
m/z-->
m/z 126
(2)
3,4-MDPV

C:

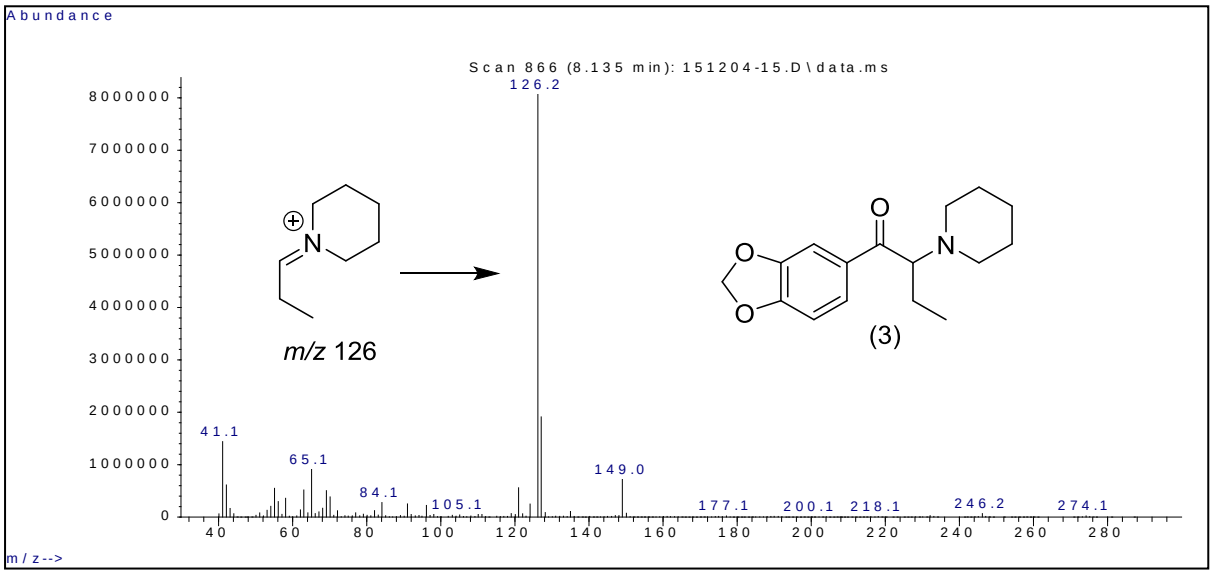

D:

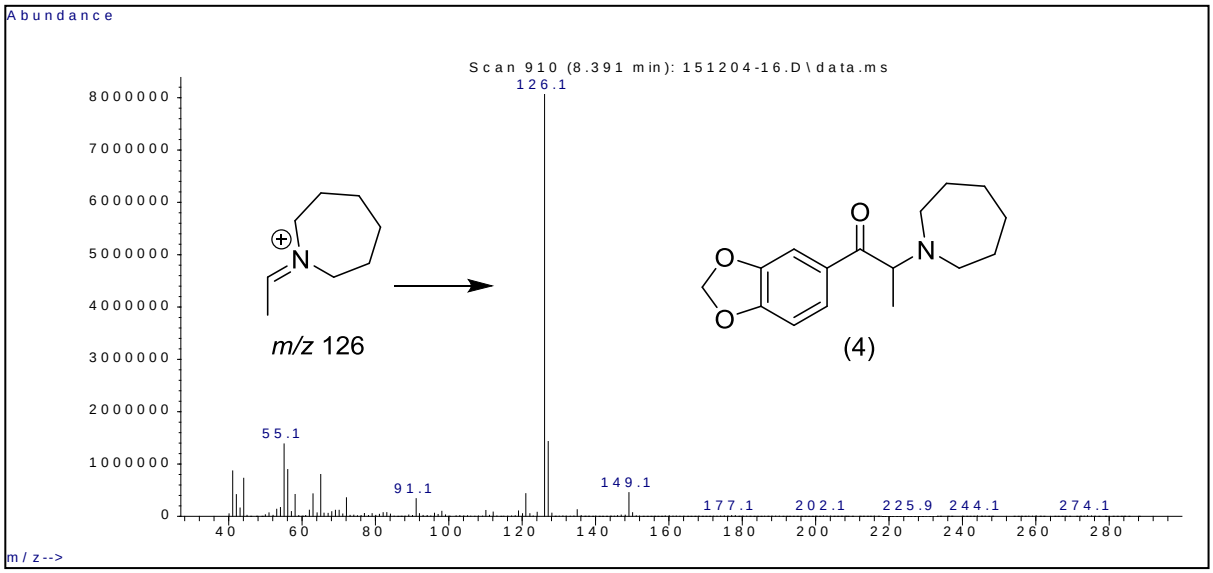

Figure 26. EI-MS for the four regioisomeric aminoketones of MW= 275 and regioisomeric base peak iminium cations at *m/z* 126. GC–MS System 1.

The GC–CI-MS studies for Compounds 1–4 were performed on a column (30 m × 0.25 mm i.d.) coated with 0.25 µm film of Crossbond® 100% trifluoropropylmethyl polysiloxane (Rtx®-200). The chemical ionization mass spectra in Figure 27 confirm the molecular weight for the four regioisomeric aminoketones (Compounds 1–4) via the intense $[M+H]^+$ ion. These spectra were generated using methanol as the CI reagent gas. Thus, GC–CI-MS confirms the molecular weight for these compounds and the EI mass spectra provide information about that portion of the molecule bonded to the 3,4-methylenedioxybenzoyl moiety common to all these compounds. Chromatographic analysis was performed using a temperature program consisting of an initial hold at 70 °C for 1.0 minute, ramped up to 250 °C at a rate of 30 °C/minute followed by a hold at 250 °C for 15.0 minutes.

A:

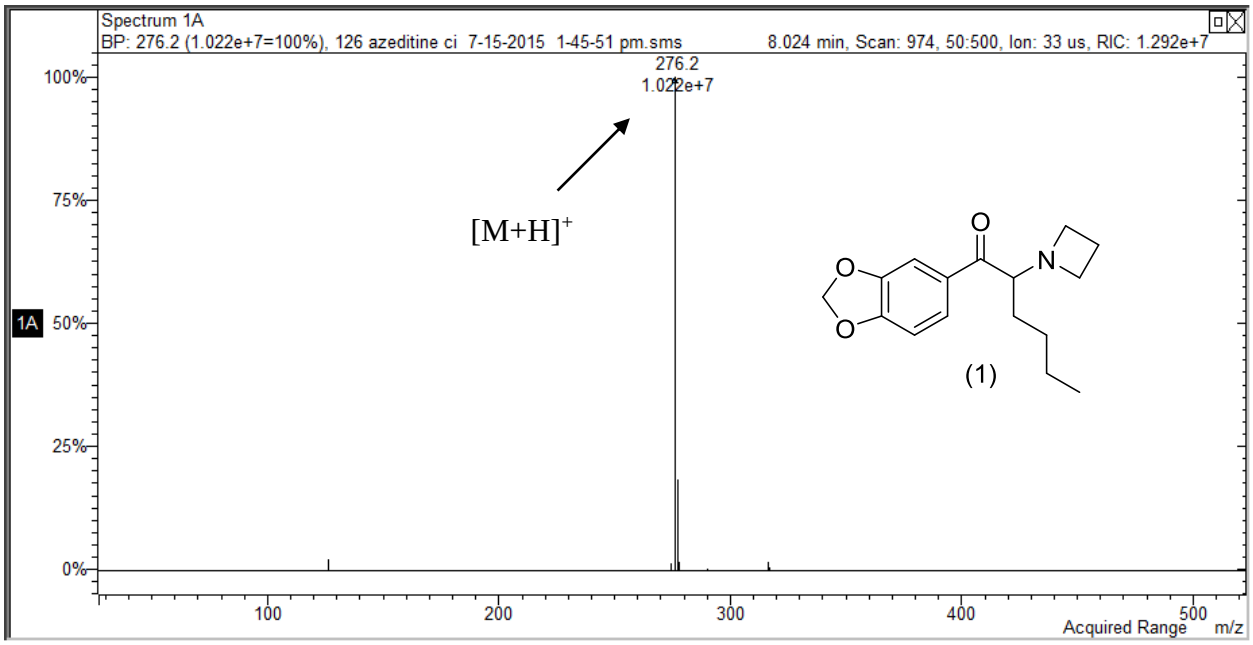

B:

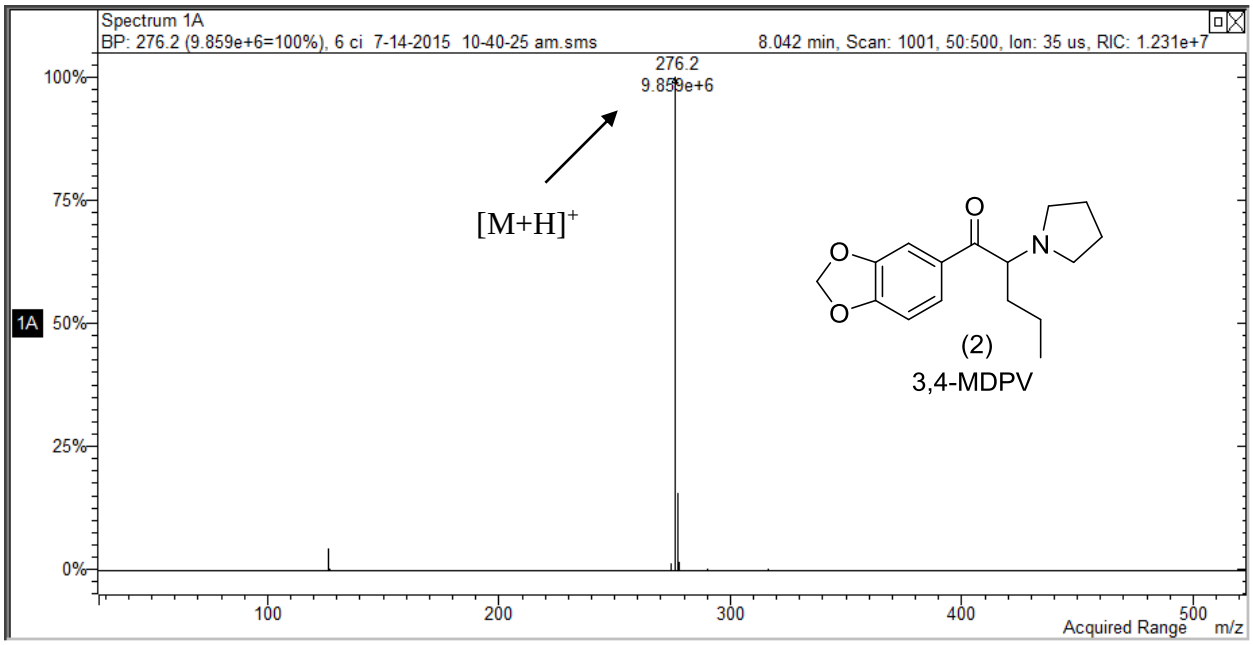
Spectrum 1A
BP: 276.2 (9.859e+6=100%), 6 ci 7-14-2015 10-40-25 am.sms
8.042 min, Scan: 1001, 50:500, Ion: 35 us, RIC: 1.231e+7
276.2
9.859e+6
[M+H]+
1A
100%
75%
50%
25%
0%
100
200
300
400
500
Acquired Range
m/z
O
O
O
N
(2)
3,4-MDPV

C:

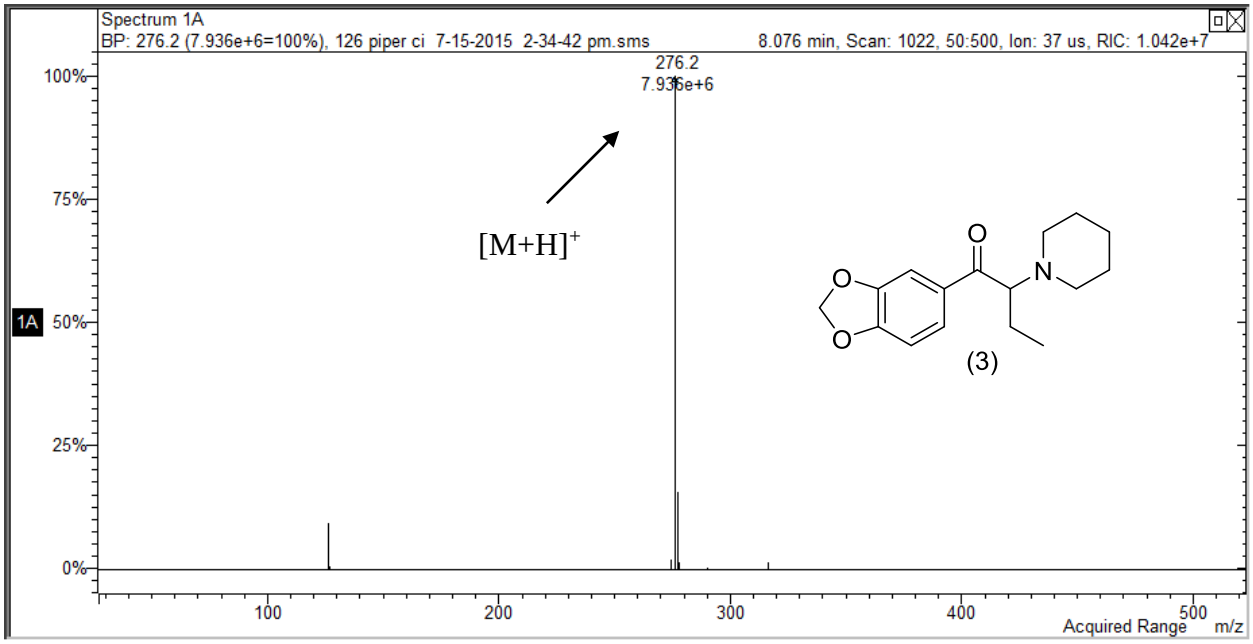
Spectrum 1A
BP: 276.2 (7.936e+6=100%), 126 piper ci 7-15-2015 2-34-42 pm.sms
8.076 min, Scan: 1022, 50:500, Ion: 37 us, RIC: 1.042e+7
276.2
7.936e+6
[M+H]+
1A
100%
75%
50%
25%
0%
100
200
300
400
500
Acquired Range
m/z
O
O
O
N
(3)

D:

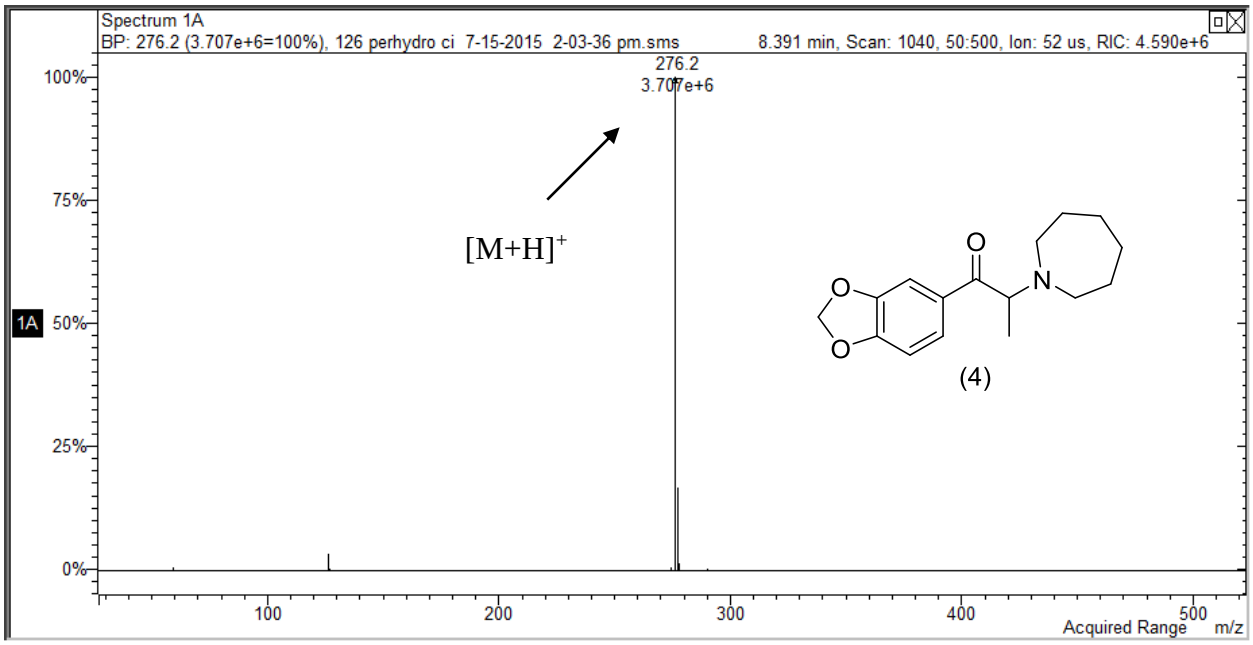

Figure 27. Chemical ionization mass spectra (CI-MS) for Compounds 1–4. GC–MS System 2.

In this study, the MS/MS product ion spectra of the iminium cation base peaks for a variety of tertiary amines were compared in an effort to characterize the structure-fragmentation relationships in these molecules of varying ring size and alkyl side-chains. This project compared the product ion MS/MS spectra of the iminium cations generated from amines containing cyclic fully saturated 4, 5, 6 and 7 membered rings. For MS/MS experiments, the scan type used was the Automated Method Development function (AMD) and the optimum MS/MS excitation amplitudes ranged from 0.20 to 1.60 volts. The GC–MS/MS studies were performed using the same column described for the GC–CI-MS studies (Rtx®-200) with a temperature program consisting of an initial hold at 70 °C for 1.0 minute, ramped up to 250 °C at a rate of 30 °C/minute followed by a hold at 250 °C for 7.0 minutes. The MS/MS spectra for each of the *m/z* 126 iminium cations from Figure 26 are shown in Figure 28 and each of the regioisomeric cations yield a unique product ion. These product ions provide an additional level of mass spectral differentiation for compounds

containing these regioisomeric cyclic tertiary amines. The structures for a number of the cyclic tertiary aminoketones as well as their base peaks and major product ions are shown in Table 1. The full EI-MS scans were done on GC–MS (System 1) in this study and the product ion MS/MS spectra on GC–MS/MS (System 2) in order to have the results confirmed on two different instruments.

A:

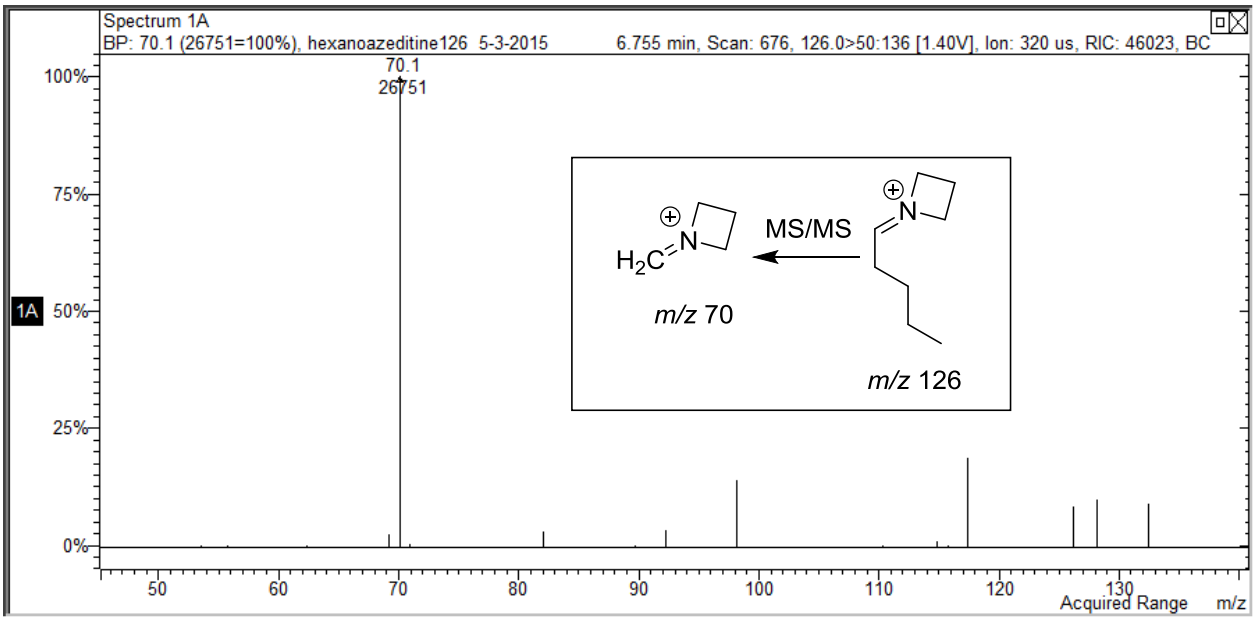

B:

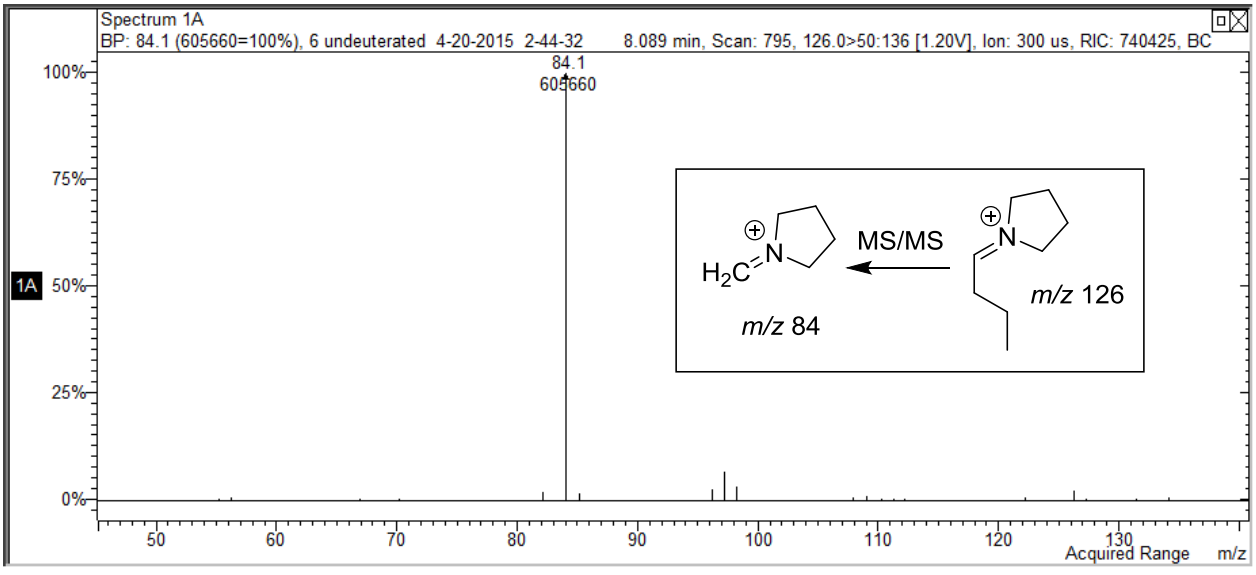

C:

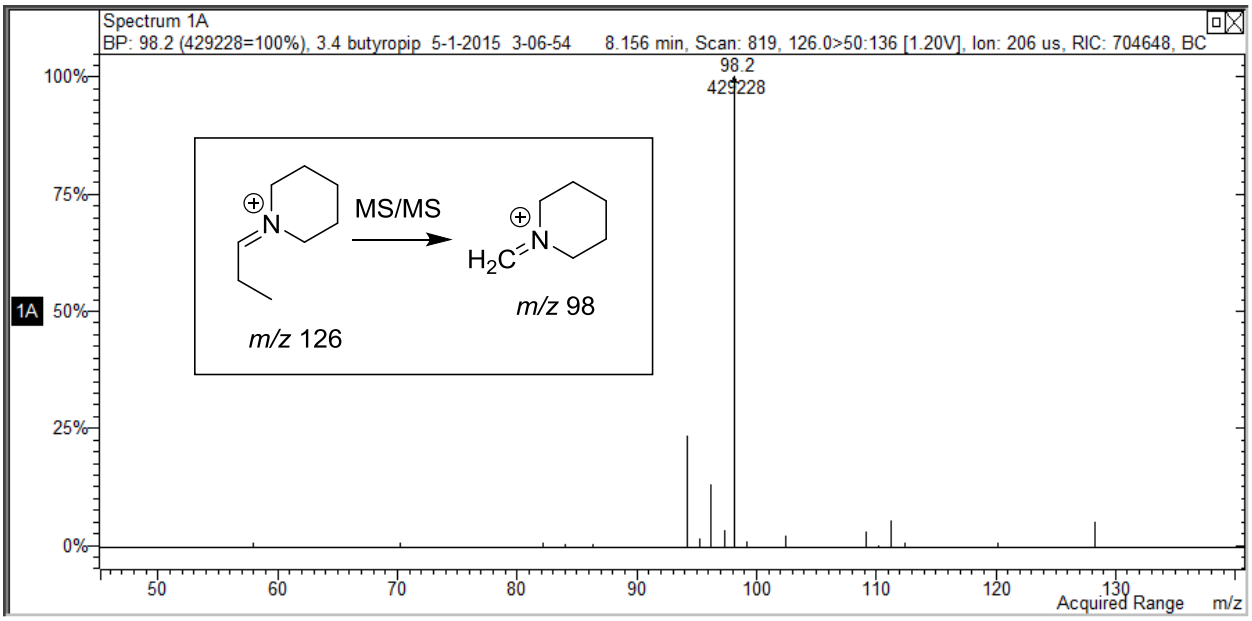

D:

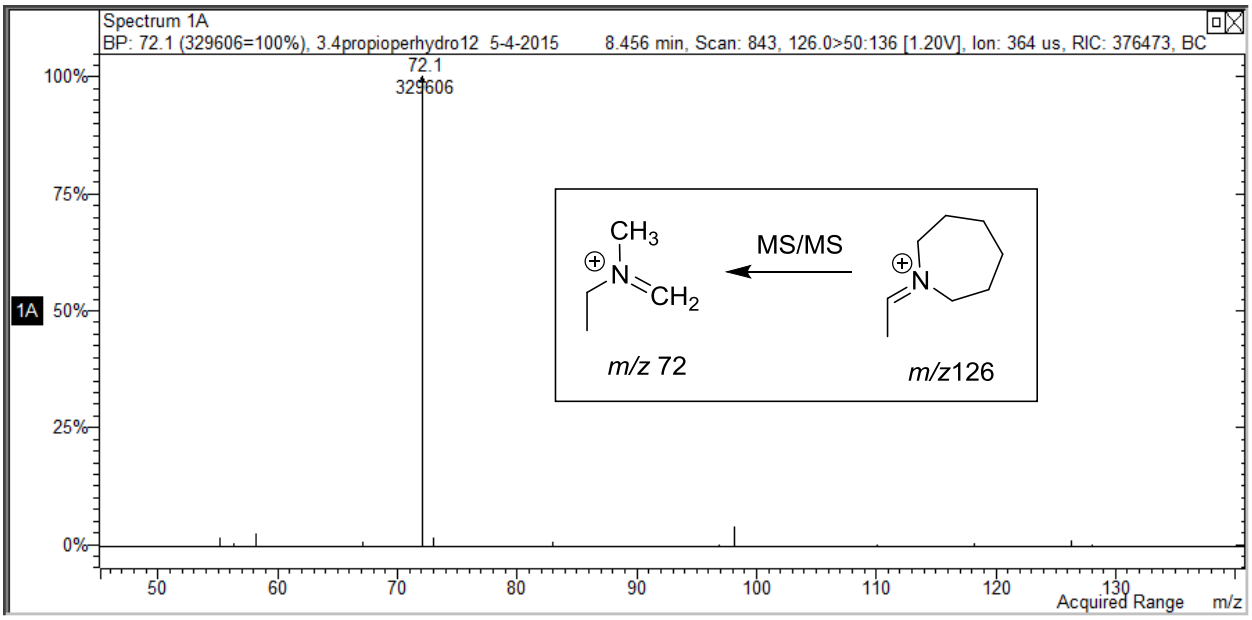

Figure 28. MS/MS product ion spectra for the four regioisomeric *m/z* 126 base peak iminium cations of the aminoketones.

The product ion MS/MS spectrum for the iminium cation formed from the cyclic 4-membered ring (azetidine) containing cathinone derivative is shown in Figure 28A. The *m/z* 126 fragment yields the *m/z* 70 product ion as the only major fragment and this represents the loss of 56 Da from the EI-MS base peak iminium cation. The alkyl side-chain for the azetidine containing iminium cation at *m/z* 126 is composed of a C_4H_9 moiety and the major product ion fragment at *m/z* 70 would suggest a hydrogen rearrangement in the alkyl side-chain with the loss of a butene molecular fragment, C_4H_8. A series of azetidine containing cathinone derivatives of varying alkyl side-chain length were prepared to evaluate the process of product ion formation in this group of compounds. All the alkyl group side-chains yield the *m/z* 70 product ion whenever a four centered H-migration to the carbon atom of the iminium species is possible. The migration of the hydrogen from the side-chain was confirmed via deuterium labeling in the alkyl side-chain. The full EI mass spectral scan of the *n*-propyl side-chain analogue shows a base peak at *m/z* 112 and the major product ion for the *m/z* 112 base peak appears at *m/z* 70. The spectra for the corresponding D_8-labeled *n*-propyl side-chain analogue show the base peak *m/z* 120 and the major product ion occurs at *m/z* 72 (Table 1). The product ion spectrum for the *m/z* 120 ion shows the major fragment at *m/z* 72 indicating the addition of two deuterium atoms into this major MS/MS fragment. The results of these experiments support the proposed structure for the *m/z* 70 product ion shown in Table 1 and the formation of this ion via hydrogen rearrangement from the alkyl side-chain. This *m/z* 70 fragment is the common ion observed for all the azetidine series compounds as long as a four-centered hydrogen rearrangement process is available in the side-chain. In the case of the methyl side-chain, a four centered migration is not possible and no product ion of significance was observed for the iminium cation base peaks for this homologue.

The product ion MS/MS spectrum for the iminium cation (*m/z* 126) formed from the cyclic 5-membered ring amine (pyrrolidine) containing cathinone derivative is shown in Figure 28B. The cathinone derivatives containing a five membered cyclic pyrrolidine ring were compared by evaluating alkyl side-chain homologues as well as some deuterium labeled pyrrolidine ring analogues. The alkyl side-chains including methyl, ethyl and *n*-propyl as well as D_8-pyrrolidine and 2,2,5,5-D_4-pyrrolidine analogues were evaluated in this study. Figure 29 shows a series of mass spectra, which serve to describe the results seen for the methyl side-chain pyrrolidine derivative. The major product ion is formed via fragmentation of the pyrrolidine ring itself to eliminate 42 Da from the EI-MS iminium cation base peak. The full scan EI-MS for the unlabeled compound in Figure 29A shows the base peak for the iminium cation at *m/z* 98 and Figure 29B shows the corresponding product ion scan with the major fragment at *m/z* 56. The 2,2,5,5-D_4-pyrrolidine analogue in Figure 29C indicates the +4 Da mass shift for the base peak at *m/z* 102 as expected and Figure 29D shows the *m/z* 58 product ion occurring from the *m/z* 102 iminium cation. This +2 Da mass shift observed in the *m/z* 58 product ion indicates that one methylene from the pyrrolidine ring remains a part of the structure for this major MS/MS product ion. This spectrum further identifies the one remaining methylene from the pyrrolidine ring as that from the 2 or 5 carbon of the ring, the carbons directly bonded to the nitrogen atom. The proposed mechanism for the formation of the product ion is shown within Figure 29D. The elimination of the side-chain in a four-centered hydrogen rearrangement analogous to the process observed for the azetidine series occurs for the higher side-chain homologues ethyl and *n*-propyl groups.

A:

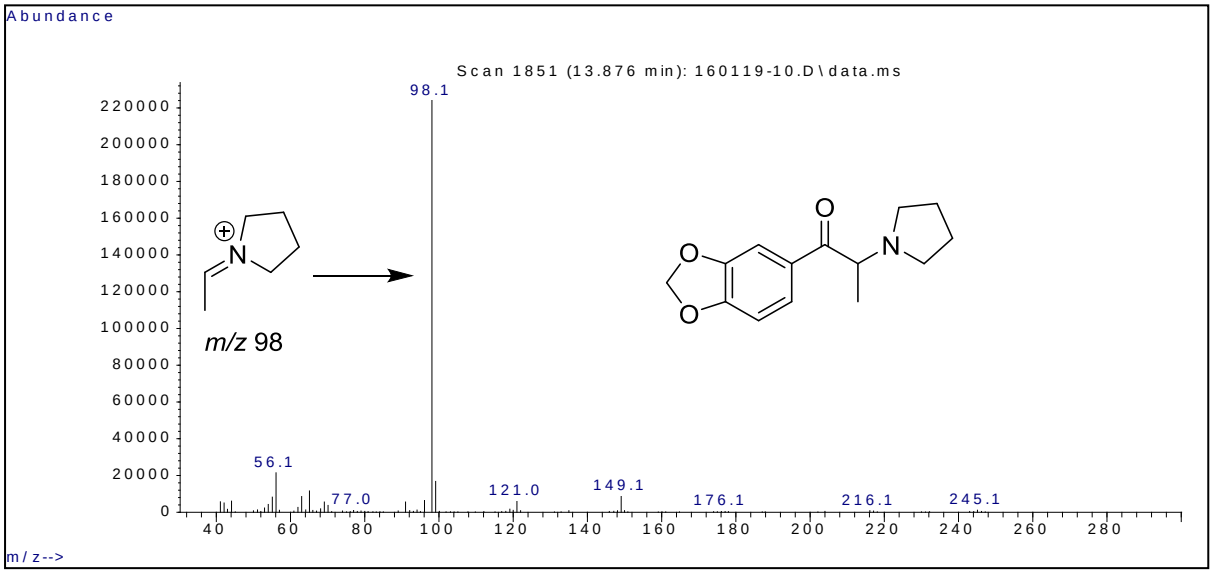
Abundance
Scan 1851 (13.876 min): 160119-10.D\data.ms
98.1
220000
200000
180000
160000
140000
120000
100000
80000
60000
40000
20000
0
56.1
77.0
121.0
149.1
176.1
216.1
245.1
40
60
80
100
120
140
160
180
200
220
240
260
280
m/z-->
m/z 98
O
O
O
N

B:

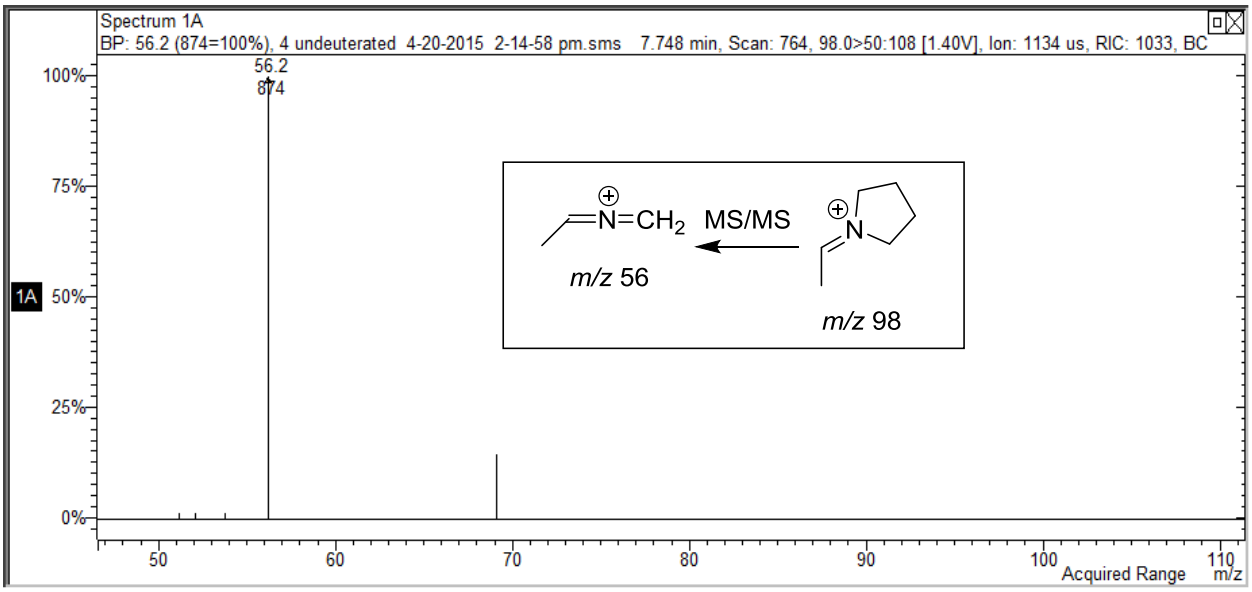
Spectrum 1A
BP: 56.2 (874=100%), 4 undeuterated 4-20-2015 2-14-58 pm.sms 7.748 min, Scan: 764, 98.0>50:108 [1.40V], Ion: 1134 us, RIC: 1033, BC
56.2
874
100%
75%
1A
50%
25%
0%
50
60
70
80
90
100
110
Acquired Range
m/z
N=CH2
MS/MS
m/z 56
m/z 98

C:

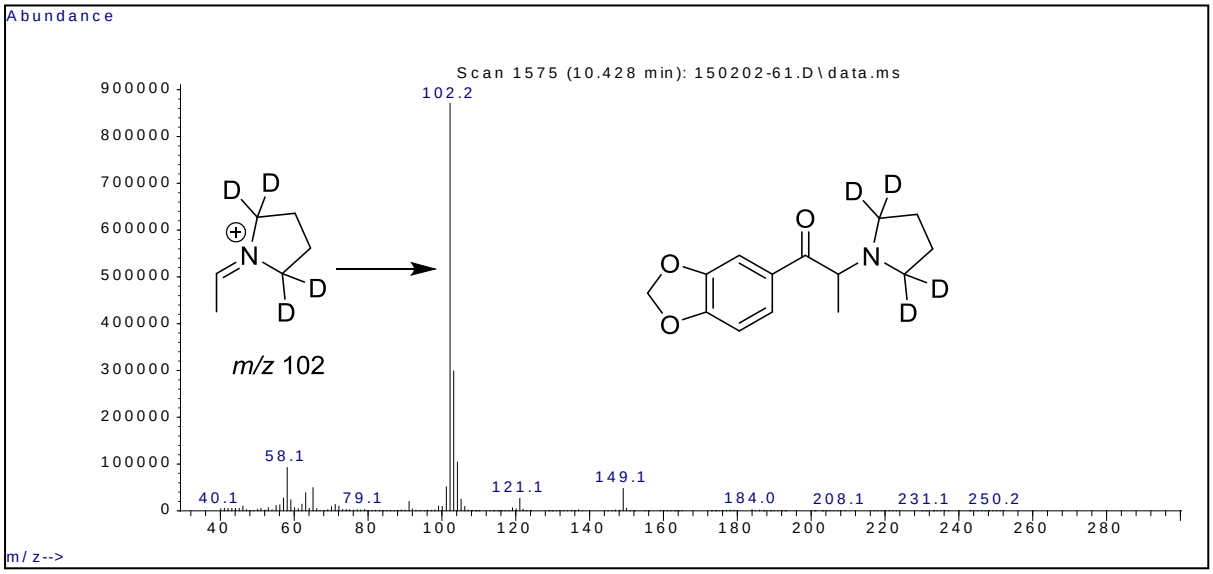

D:

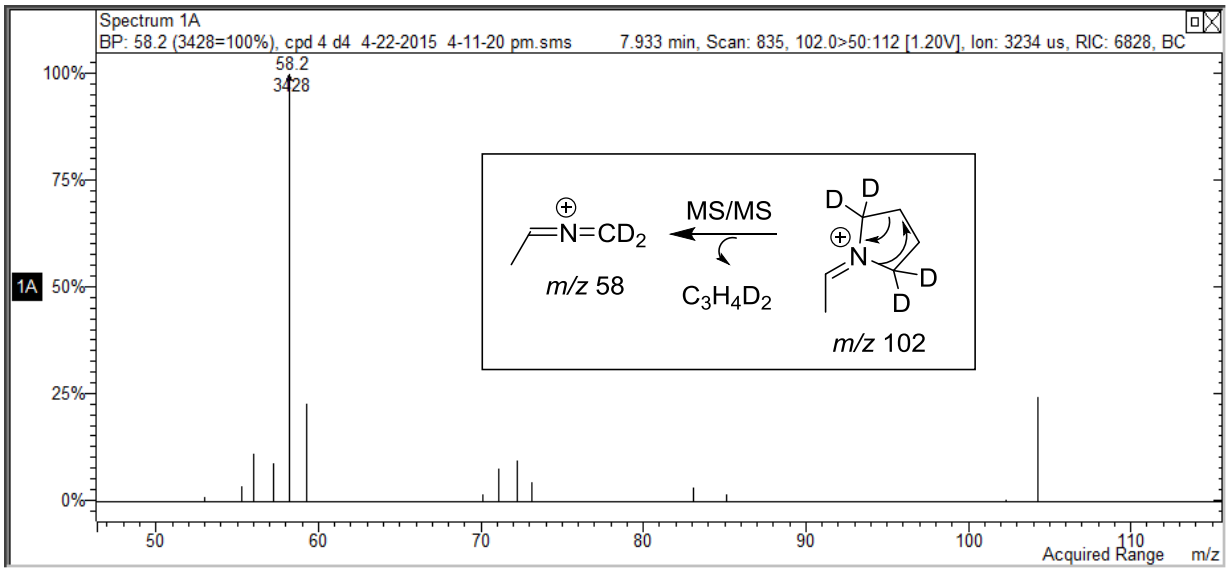

Figure 29. EI-MS and product ion spectra for the methyl side-chain pyrrolidine isomer and the 2,2,5,5-D_4-pyrrolidine analogue.

The structures for the base peak in the EI-MS and product ion spectra for the D_8-pyrrolidine containing aminoketone with the *n*-propyl side chain, D_8-MDPV, are shown in Table 1. The EI-MS and product ion spectra for the unlabeled form of this compound are shown in Figures 26B and 28B, respectively. The full scan EI-MS for D_8-MDPV shows the molecular ion and the base peak (*m/z* 134) with a +8 Da increase in mass as expected. Furthermore, the major product ion (*m/z* 92) shows a +8 Da mass increase compared to the spectrum for the unlabeled analogue (Table 1). These results confirm the pyrrolidine ring remains a part of the major product ion fragment and that no significant ring fragmentation product ion is formed for this compound. The EI-MS and product ion MS/MS spectra for 2,2,5,5-pyrrolidine-D_4 analogue of 3,4-MDPV were discussed in the previous chapter (Section 2.1.3.) and the fragment ions are consistent with the proposed mechanism. In the ethyl side-chain pyrrolidine homologue (spectrum not shown) both ring (*m/z* 70) and side-chain (*m/z* 84) product ions were observed in approximately equal ion intensities.

The product ion MS/MS spectrum for the iminium cation (*m/z* 126) formed from the cyclic 6-membered ring amine (piperidine) containing cathinone derivative is shown in Figure 28C. The piperidine containing compounds were evaluated via the synthesis of a series of alkyl side-chain derivatives as well as D_{10}-piperidine analogues. In this piperidine series, the alkyl side-chain homologues yield a common MS/MS product ion at *m/z* 98 as long as the side-chain based four centered H-migration to the carbon atom of the iminium species is possible. The structures for the full scan EI-MS base peak and major product ion for the piperidine containing *n*-propyl side-chain derivative and the D_{10}-piperidine analogue are shown in Table 1. The major product ion appears at *m/z* 98 and in the D_{10}-piperidine analogue, a mass shift of +10 Da occurs as shown for the *m/z* 108 product ion. This mass shift to *m/z* 108 in the product ion spectrum confirms that the piperidine

ring remains a part of the product ion and the side-chain is the source of the additional fragmentation to form the observed major MS/MS fragment.

While the four centered H-migration of the side-chain yields the common *m/z* 98 product ion for the ethyl and *n*-propyl side-chains in the piperidine series as described above, the methyl side-chain analogue undergoes ring fragmentation. Since the four centered H-migration is not possible in the methyl side-chain, an analogous migration appears to initiate piperidine ring fragmentation for the methyl side-chain analogue. The EI-MS for the methyl side-chain analogue in the piperidine series shows a base peak at *m/z* 112 with the major product ion at *m/z* 84 as illustrated in Figure 30A and 30B, respectively. This *m/z* 84 product ion represents the loss of 28 Da (C_2H_4) from the base peak iminium cation at *m/z* 112.

A:

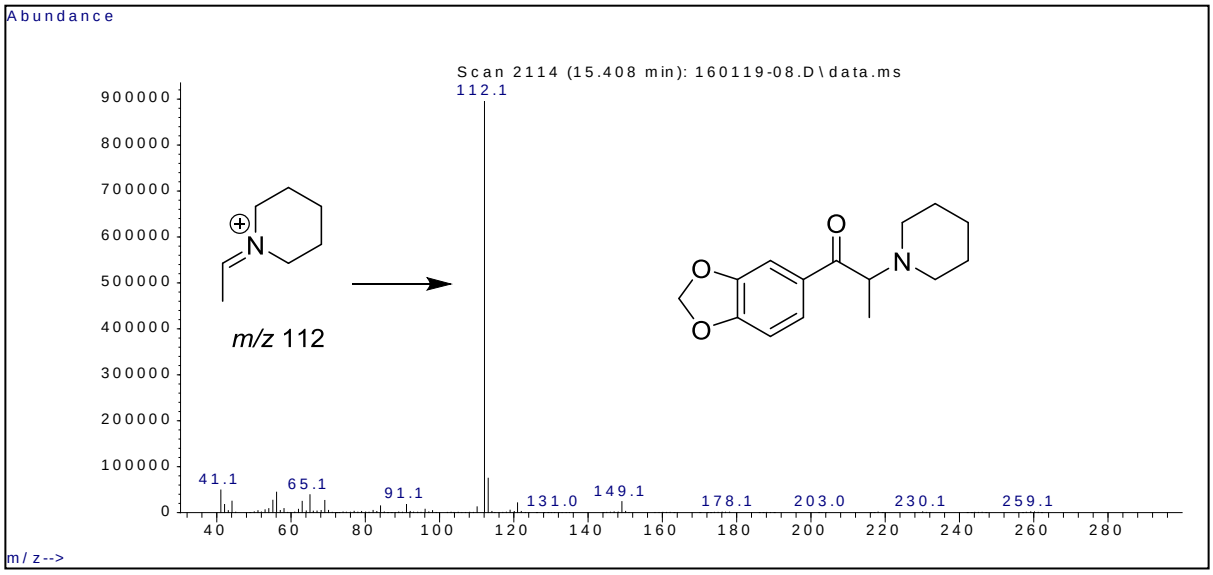

B:

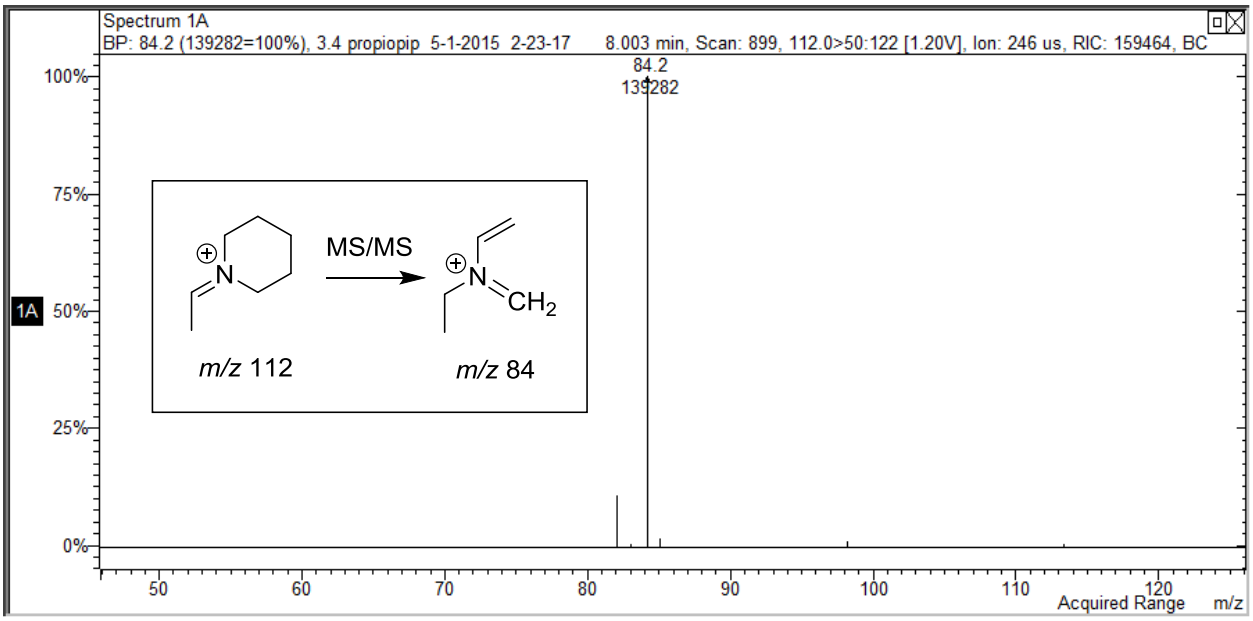

Figure 30. EI-MS and product ion spectra for the methyl side-chain piperidine derivative.

Figure 31A shows the full scan EI-MS for the methyl side-chain D_{10}-piperidine analogue with the base peak at *m/z* 122 while Figure 31B illustrates the product ion spectrum for the *m/z* 122 iminium cation showing a major fragment at *m/z* 90, only a 6 Da mass shift from the equivalent product ion in the unlabeled compound.

A:

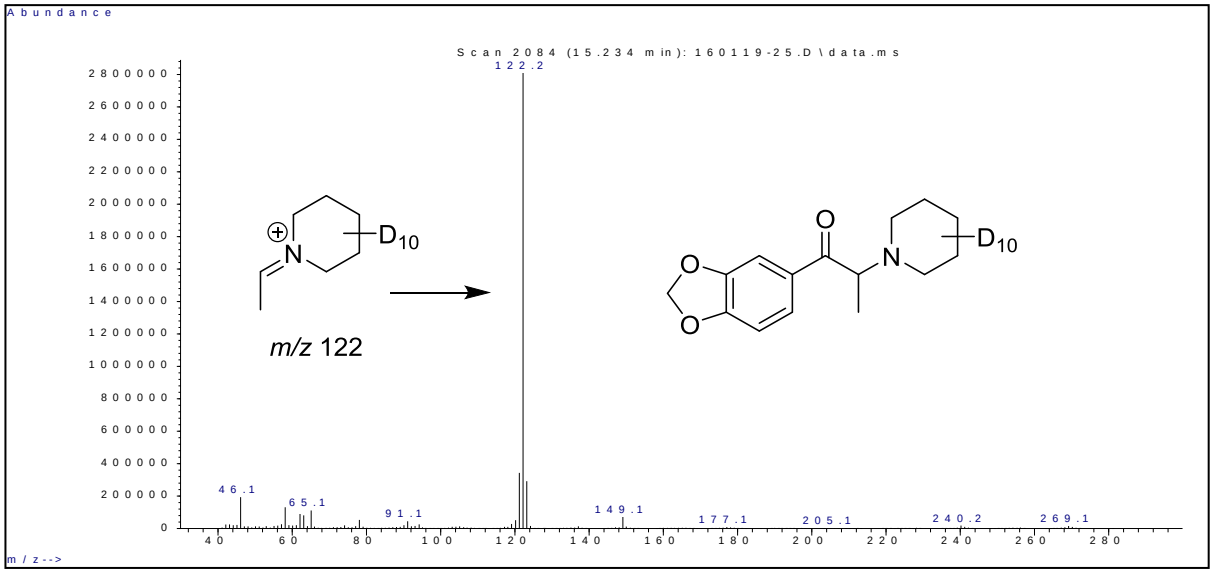

B:

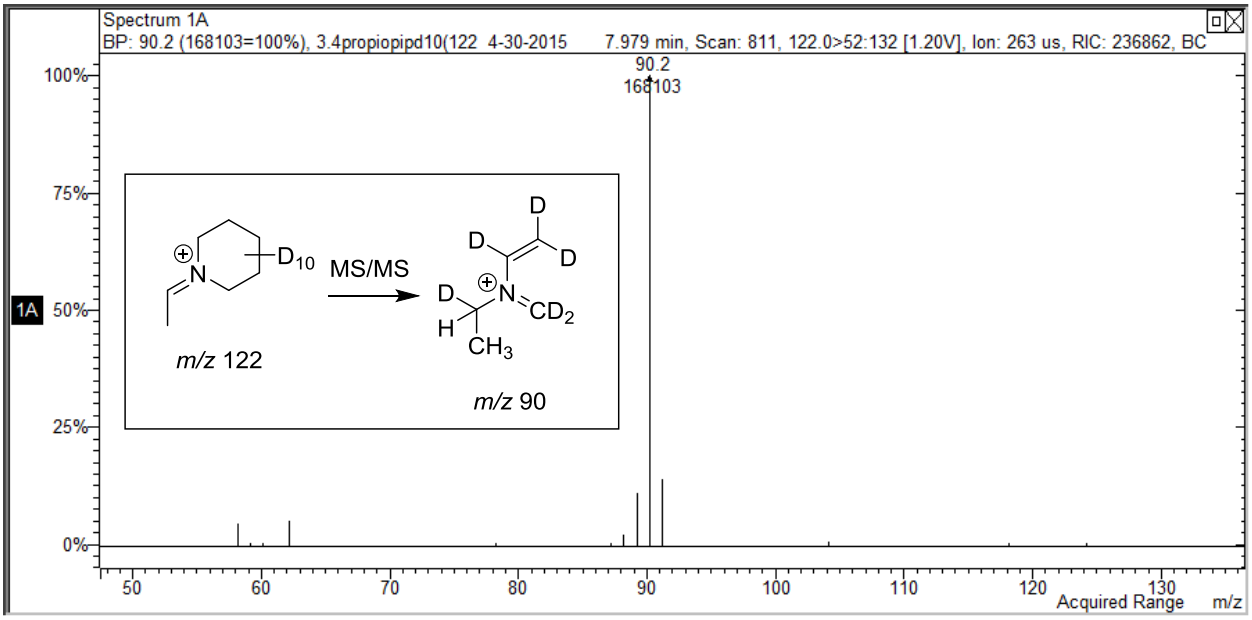

Figure 31. EI-MS and product ion spectra for the methyl group side-chain D_{10}-piperidine derivative.

The fragmentation mechanism shown below (Scheme 16) indicates the alternate four centered H-migration, which appears to operate in this methyl side-chain example. The ethyl and *n*-propyl homologues which allow the four centered H-migration in the alkyl side-chain do not show any appreciable fragments from this potentially competing H-migration from the piperidine ring. However, in the next higher ring homologue series containing the seven membered azepane ring both the ring and side-chain H-migration processes appear to operate perhaps in competition in some compounds.

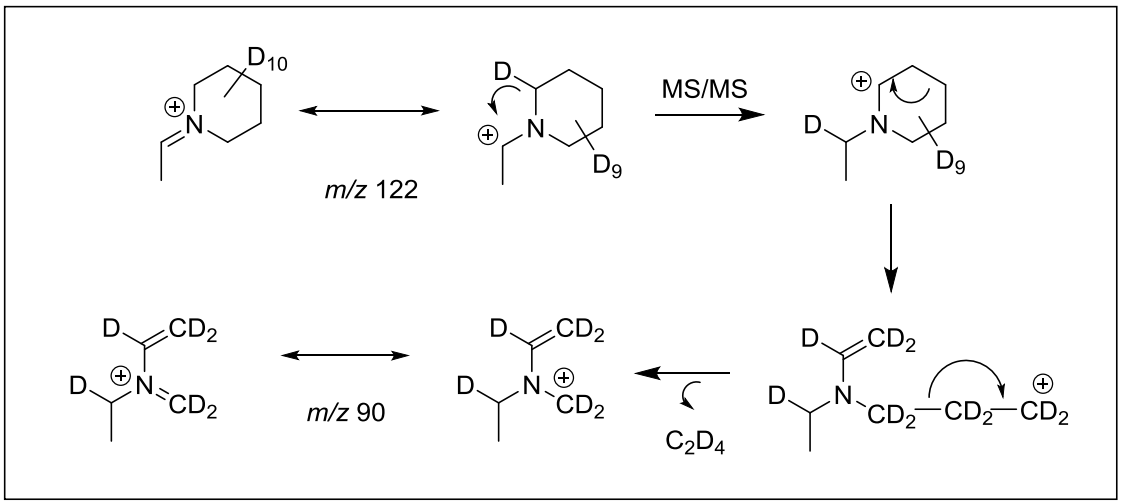

Scheme 16. Fragmentation scheme for MS/MS product ion formation in the methyl side-chain D_{10}-piperidine analogue.

The azepane containing compounds were evaluated via the synthesis of a series of alkyl side-chain derivatives as well as deuterium labeled alkyl side-chain analogues. The product ion MS/MS spectrum for the iminium cation (*m/z* 126) formed from the cyclic 7-membered amine (azepane) containing cathinone derivative is shown in Figure 28D. The *m/z* 72 product ion (Figure 28D) is produced from the *m/z* 126 base peak which consists of the azepane ring with the methyl group side-chain. The homologous ethyl side-chain shows a homologues product ion at *m/z* 86 resulting from the iminium cation base peak at *m/z* 140 (Table 1).These two product ions at *m/z* 72 and 86 represent the loss of a consistent 54 Da from the iminium cation base peaks. The most likely source for this loss would be C_4H_6, butadiene, which could only come from the azepane ring in these small side-chain homologues (methyl and ethyl).

The full scan EI-MS as well as the product ion spectrum for the next higher homologue, the *n*-propyl side-chain, are shown in Figure 32A and 32B. The base peak in the full scan in Figure 32A occurs at *m/z* 154 as expected from the loss of the 3,4-methylenedioxybenzoyl radical from the molecular ion. The product ion spectrum in this example (Figure 32B) shows major fragments at both *m/z* 100 and *m/z* 112. The *m/z* 100 product ion again represents the loss of 54 Da from the base peak while the *m/z* 112 ion represents the loss of 42 Da from the *m/z* 154 base peak. These results suggest that both side-chain and ring fragmentation are involved in the formation of these product ions.

A:

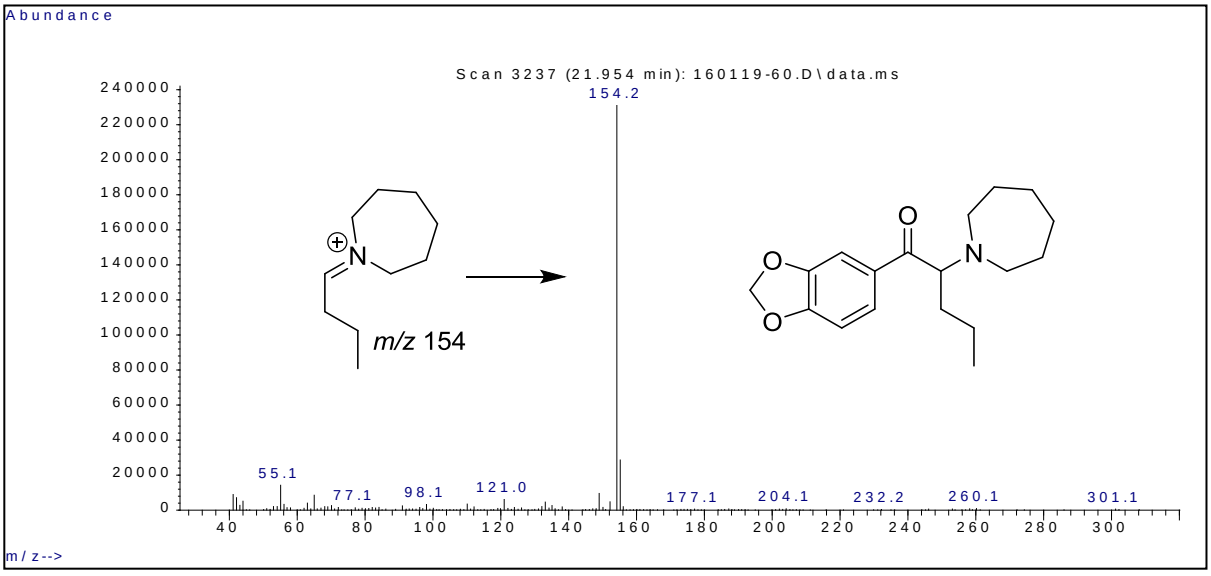

B:

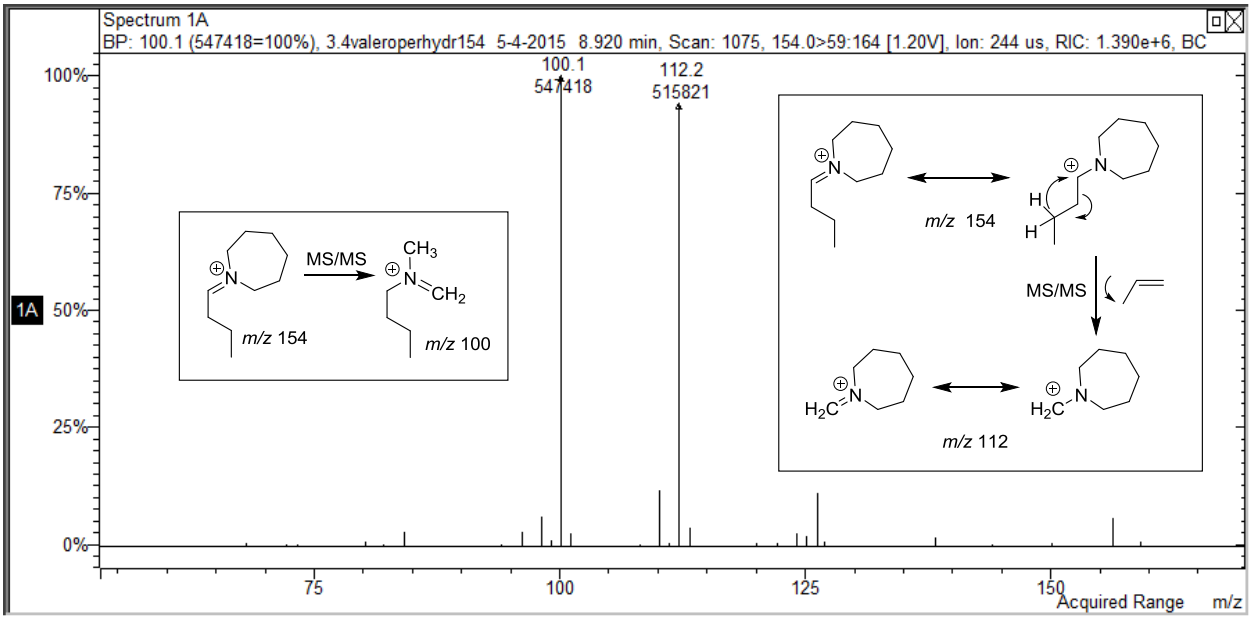

Figure 32. EI-MS and product ion spectra for the *n*-propyl side-chain isomer for the azepane series.

The full scan and product ion spectra for the deuterium labeled *n*-propyl side-chain analogue are shown in Figure 33A and 33B, respectively. The base peak in Figure 33A occurs at *m/z* 162, which represents an 8 Da shift as expected for the major iminium cation. The product ion spectrum in Figure 33B indicates major fragments at *m/z* 108 and *m/z* 114. A direct comparison of the fragment ions in Figures 32B and 32B shows a mass shift of the *m/z* 100 ion to *m/z* 108 in the side-chain labeled analogue indicating the side-chain remains a part of this ion and the fragmentation occurs in the cyclic 7-membered azepane ring system. Furthermore, the +2 Da mass shift for the second major product ion from *m/z* 112 to *m/z* 114 indicates fragmentation of the side-chain to eliminate the propene molecular equivalent. The next higher side-chain homologue (spectra not shown) in this azepane series having the *n*-butyl side-chain shows an analogous set of ions for both side-chain and ring fragmentation of the *m/z* 168 base peak iminium cation. Thus, in the seven membered cyclic tertiary amines both side-chain and ring fragmentation yield a mixture

of product ions in the higher side-chain homologues while only ring fragmentation occurs in the methyl and ethyl side-chains.

A:

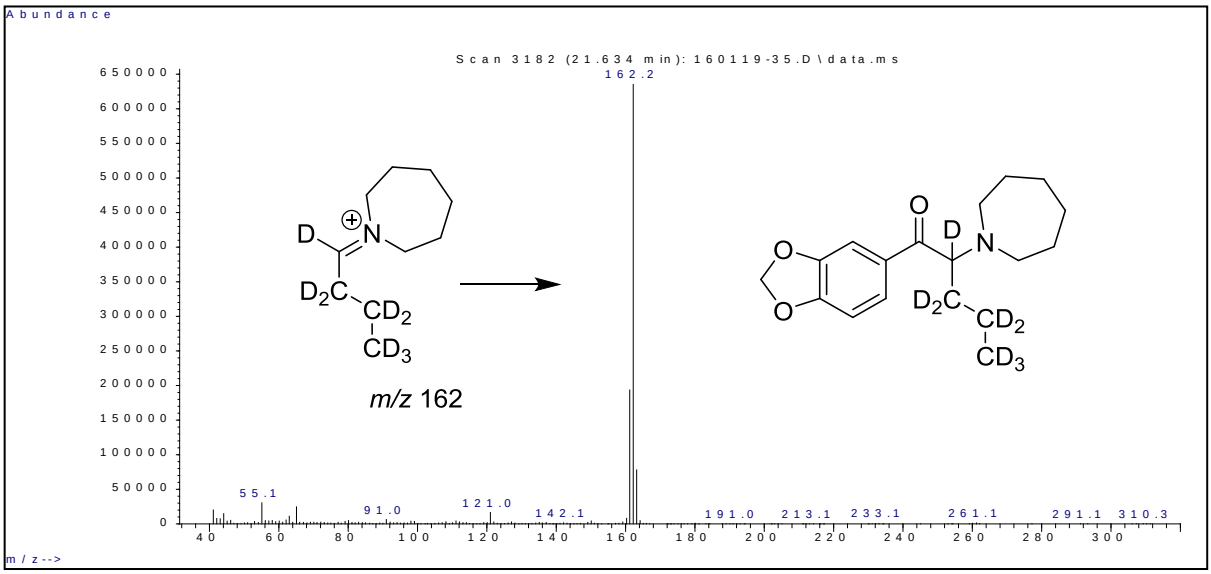

B:

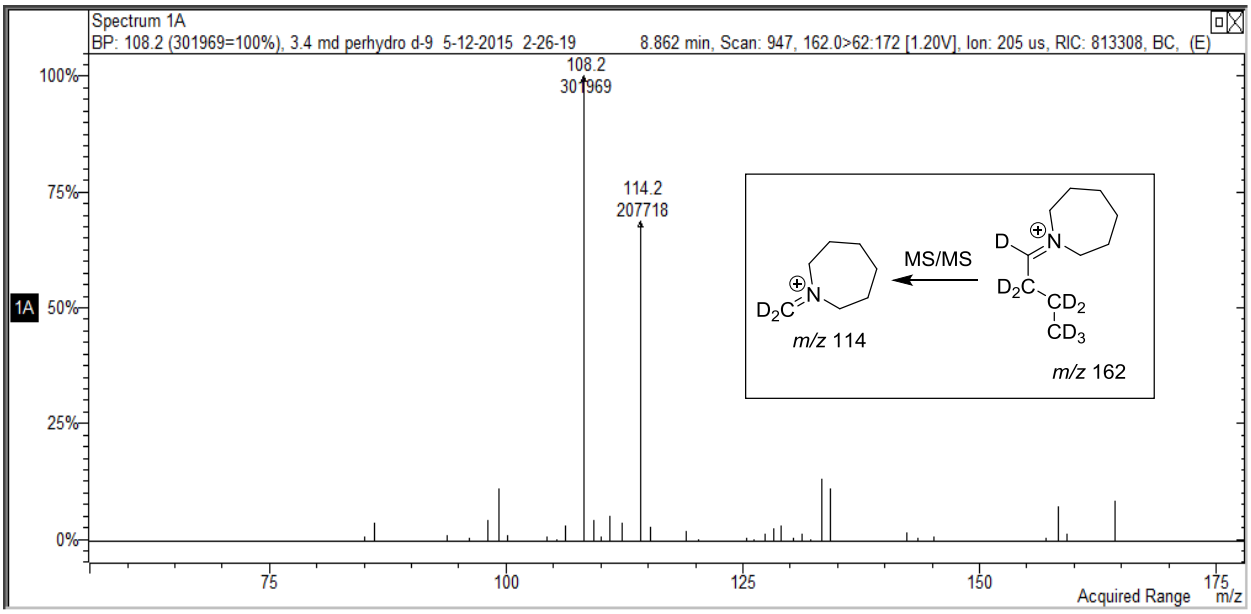

Figure 33. EI-MS and product ion spectra for the D_8-labeled *n*-propyl side-chain analogue of the azepane series.

The fragmentation mechanism shown below (Scheme 17) illustrates the ring fragmentation process for the D_8-labeled *n*-propyl side-chain analogue of the azepane series. This process operates predominantly in the analogues with methyl and ethyl side-chains and it involves two consecutive six centered H-migrarions, which ultimately results in the loss of 54 Da (C_4H_6, butadiene).

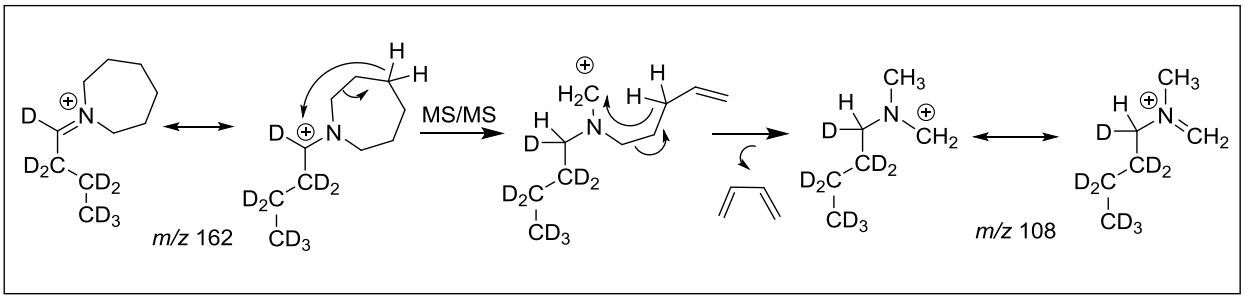

Scheme 17. Fragmentation scheme for MS/MS product ion formation in the *n*-propyl side-chain D_8-azepane analogue.

In summary, many of the more popular cathinone derivative drugs of abuse contain cyclic tertiary amine moieties. In most cases, the cyclic amine is the five-membered pyrrolidine ring. However, other cyclic amines may appear as additional designer modifications. Product ion spectra provide useful structural information in these cyclic tertiary amines that do not form stable acylated derivatives. The table shown below illustrates the structures for a number of the cyclic tertiary aminoketones as well as their base peaks and major product ions.

Table 1. Structures for a series of cyclic tertiary aminoketones and their major EI-MS fragment ions as well as MS/MS product ions.

Parent structure	Iminum cation	Product ion
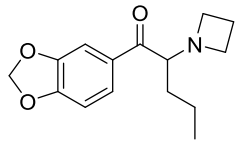	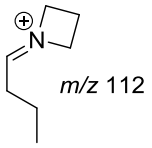 *m/z* 112	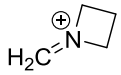 *m/z* 70
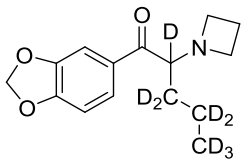	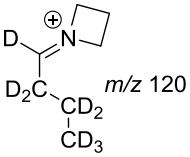 *m/z* 120	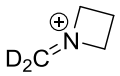 *m/z* 72
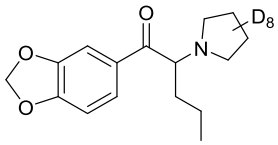	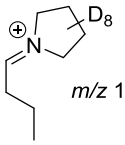 *m/z* 134	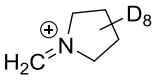 *m/z* 92
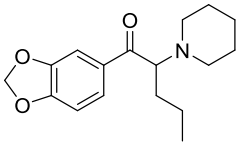	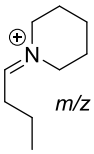 *m/z* 140	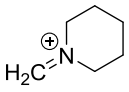 *m/z* 98
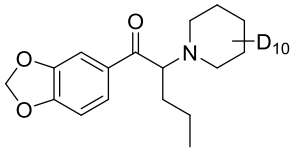	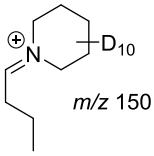 *m/z* 150	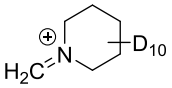 *m/z* 108
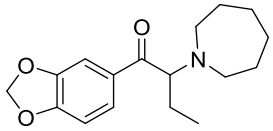	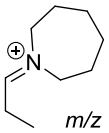 *m/z* 140	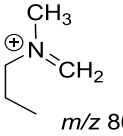 *m/z* 86

The electron ionization mass spectra for Compounds 5–8 also yield the *m/z* 126 iminium cation base peaks identical to the base peaks observed for Compounds 1–4. These regioisomeric iminium cations are the dominant fragments in the spectra and the extensive fragmentation of these molecules yields very little ion current for the molecular ion. The *m/z* 135 fragment for the 3,4-methylenedioxybenzyl cation is the only other high mass ion of significance in these spectra. The chemical ionization mass spectra confirm the molecular weight for these regioisomers via the

intense $[M+H]^+$ ion and the EI mass spectra provide information about that portion of the molecule bonded to the 3,4-methylenedioxybenzyl moiety common to all these compounds. The GC–CI-MS studies were performed on a column (30 m ×0.25 mm i.d.) coated with 0.10 µm film of Crossbond® 100% dimethyl polysiloxane (Rtx®-1). Chromatographic analysis was performed using a temperature program consisting of an initial hold at 70 °C for 1.0 minute, ramped up to 250 °C at a rate of 30 °C/minute followed by a hold at 250 °C for 15.0 minutes. Figures 34A and 34B below show a representative EI-MS and CI-MS spectra for the desoxy-MDPV analogue, Compound 6.

A:

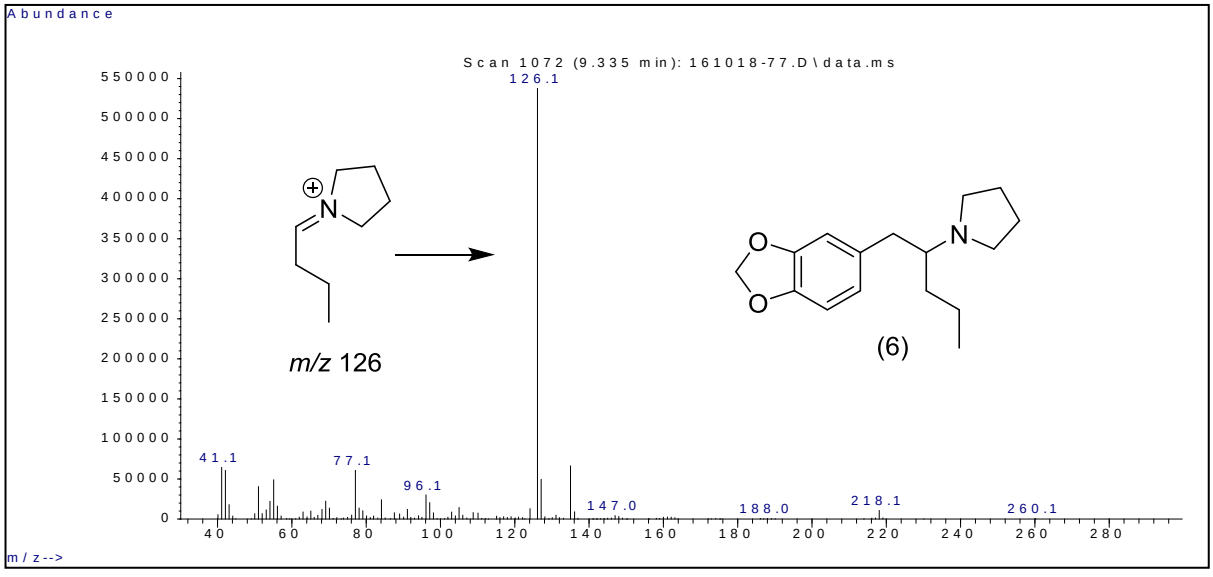

B:

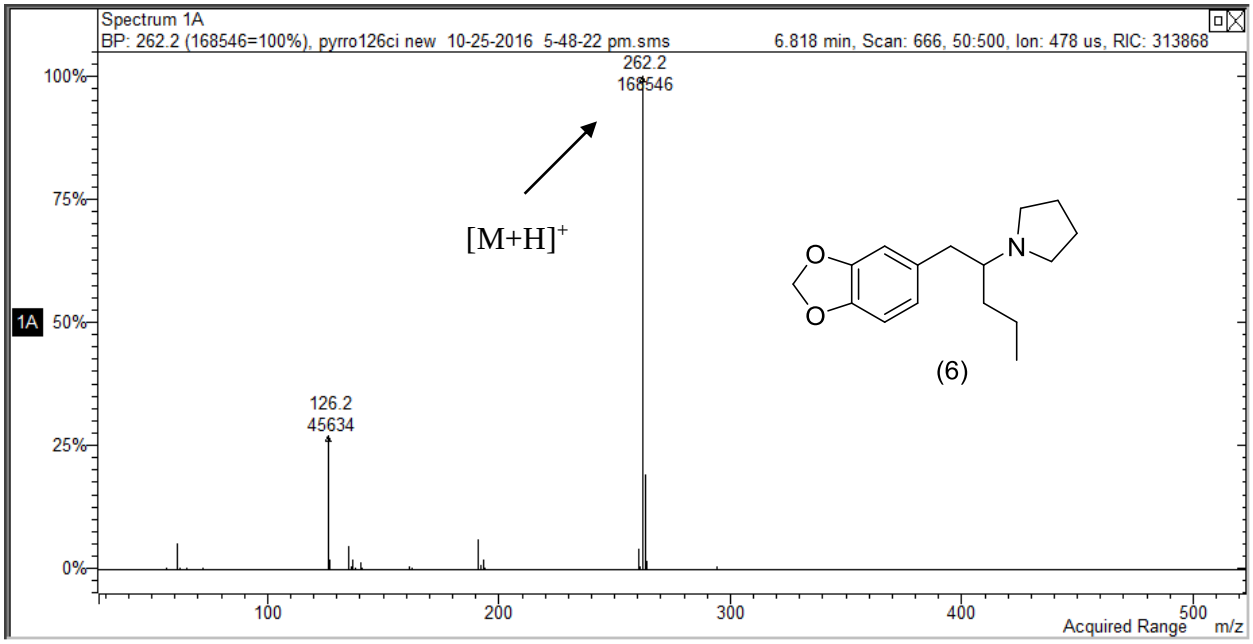

Figure 34. Representative EI-MS (GC–MS System 1) and CI-MS (GC–MS System 2) spectra for Compound 6.

The product ion MS/MS spectra for each of the regioisomeric iminium cations generated by Compounds 5–8 are presented in Figure 35. For MS/MS experiments, the scan type used was the Automated Method Development function (AMD) and the optimum MS/MS excitation amplitudes were 1.00 and 1.20 volts. While the EI-MS gave the equivalent iminium cation base peak for each compound, the corresponding product ion spectra allow differentiation based on the nature of the cyclic tertiary amine portion and the length of the alkyl side-chain of the iminium cation. The product ion spectrum for the *m/z* 126 iminium cation from the azetidine containing isomer (Figure 35A) indicates the *m/z* 70 cation as the major fragment. This product ion occurs via elimination of the C_4H_8 alkene from the side-chain portion of the *m/z* 126 iminium cation. This can be compared to the major product ion at *m/z* 84 (Figure 35B) observed for the pyrrolidine containing iminium cation species and this ion results from the loss of the C_3H_6 alkene from the

side-chain. The major product ion from the piperidine containing iminium cation (Figure 35C) occurs at *m/z* 98 from the analogous loss of C_2H_4 alkene from the side-chain with some less abundant product ions at *m/z* 84 and 70. Thus, the major product ions in Figures 35A–35C represent a homologous series resulting from the loss of butene, propene and ethylene respectively from the side-chain. The product ion from the azepane containing iminium cation whose spectrum is shown in Figure 35D occurs at *m/z* 72 and is the result of fragmentation of the ring portion of the *m/z* 126 iminium cation base peak for Compound 8. The structures for the product ions described in Figure 35 were confirmed for the analogous aminoketones (Compounds 1–4) using deuterium labeling of the cyclic tertiary amine and the alkyl side-chain. Thus, these product ion spectra allow for the differentiation of the *m/z* 126 iminium cations containing the various ring size cyclic tertiary amines. The GC–MS/MS studies were performed using the same column described for the GC–CI-MS studies (Rtx®-1) with a temperature program consisting of an initial hold at 70 °C for 1.0 minute, ramped up to 250 °C at a rate of 30 °C/minute followed by a hold at 250 °C for 7.0 minutes. It is important to note that the source of the iminium cation is a different molecule (Compounds 1–4 and Compounds 5–8) however, once formed; the iminium cation yields product ions consistent with its regioisomeric structure.

A:

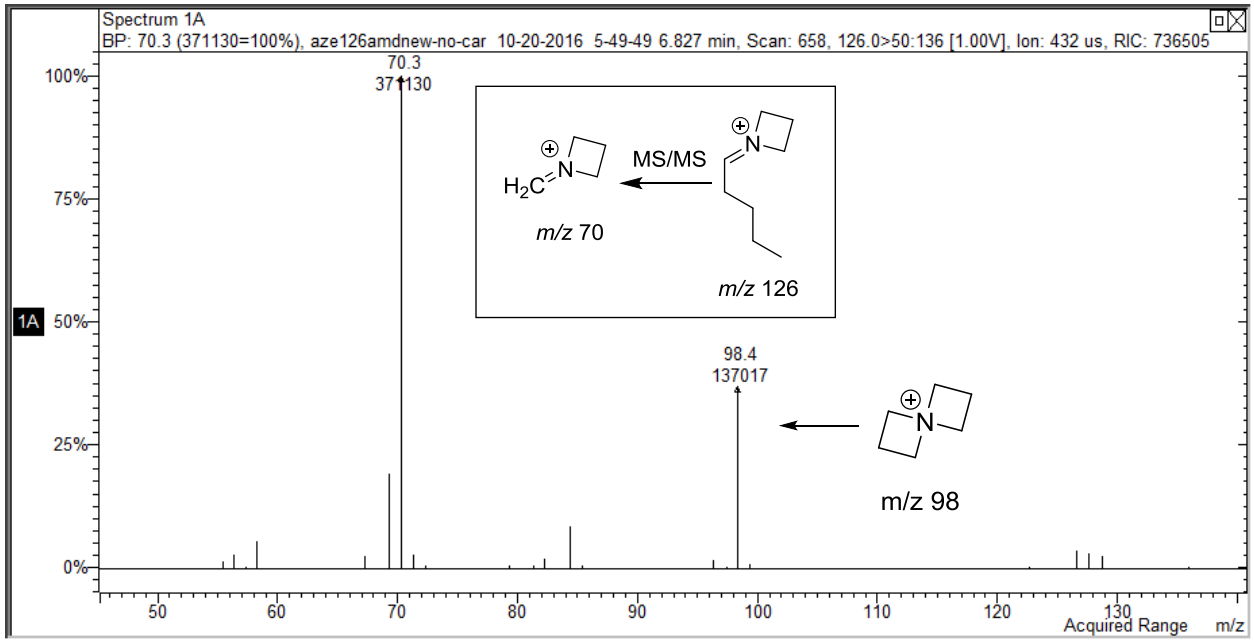
Spectrum 1A
BP: 70.3 (371130=100%), aze126amdnew-no-car 10-20-2016 5-49-49 6.827 min, Scan: 658, 126.0>50:136 [1.00V], Ion: 432 us, RIC: 736505
70.3
371130
98.4
137017
MS/MS
m/z 70
m/z 126
m/z 98
1A
100%
75%
50%
25%
0%
50
60
70
80
90
100
110
120
130
Acquired Range
m/z

B:

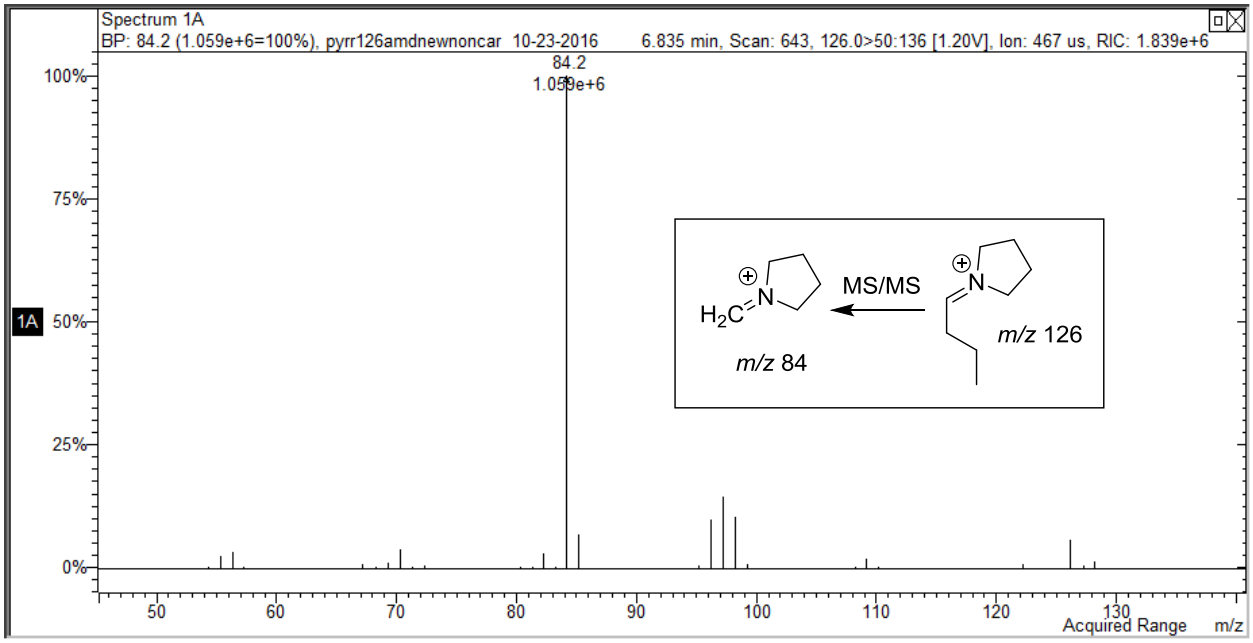
Spectrum 1A
BP: 84.2 (1.059e+6=100%), pyrr126amdnewnoncar 10-23-2016 6.835 min, Scan: 643, 126.0>50:136 [1.20V], Ion: 467 us, RIC: 1.839e+6
84.2
1.059e+6
MS/MS
m/z 84
m/z 126
1A
100%
75%
50%
25%
0%
50
60
70
80
90
100
110
120
130
Acquired Range
m/z

C:

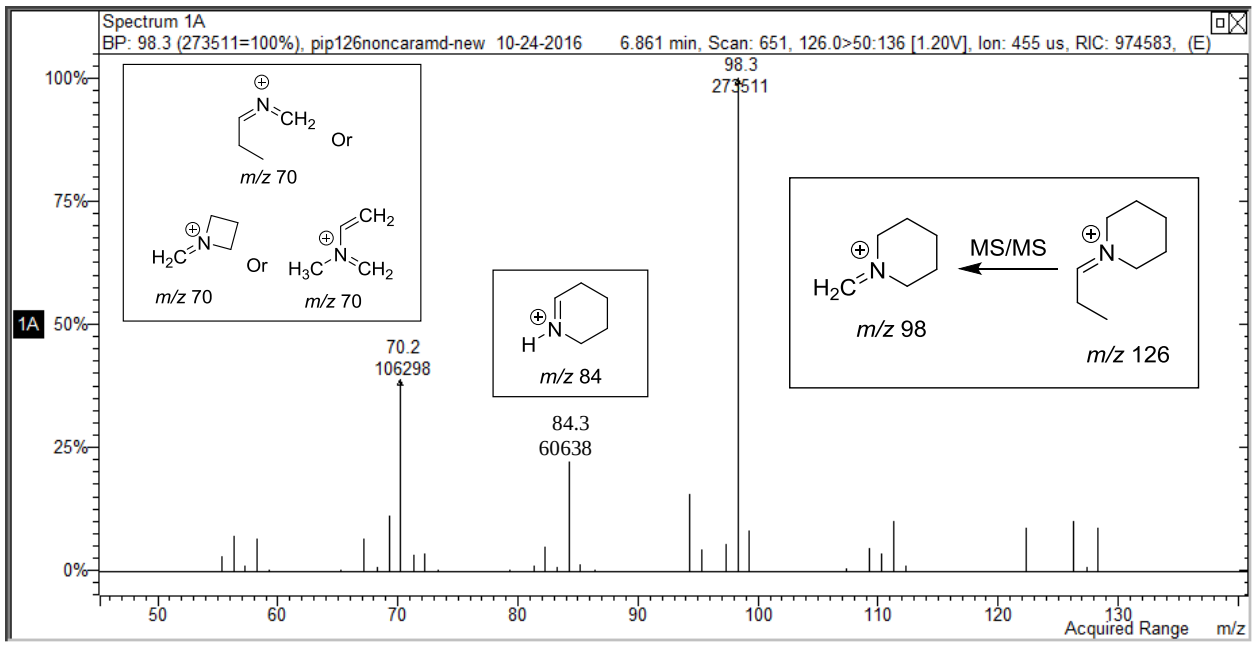

D:

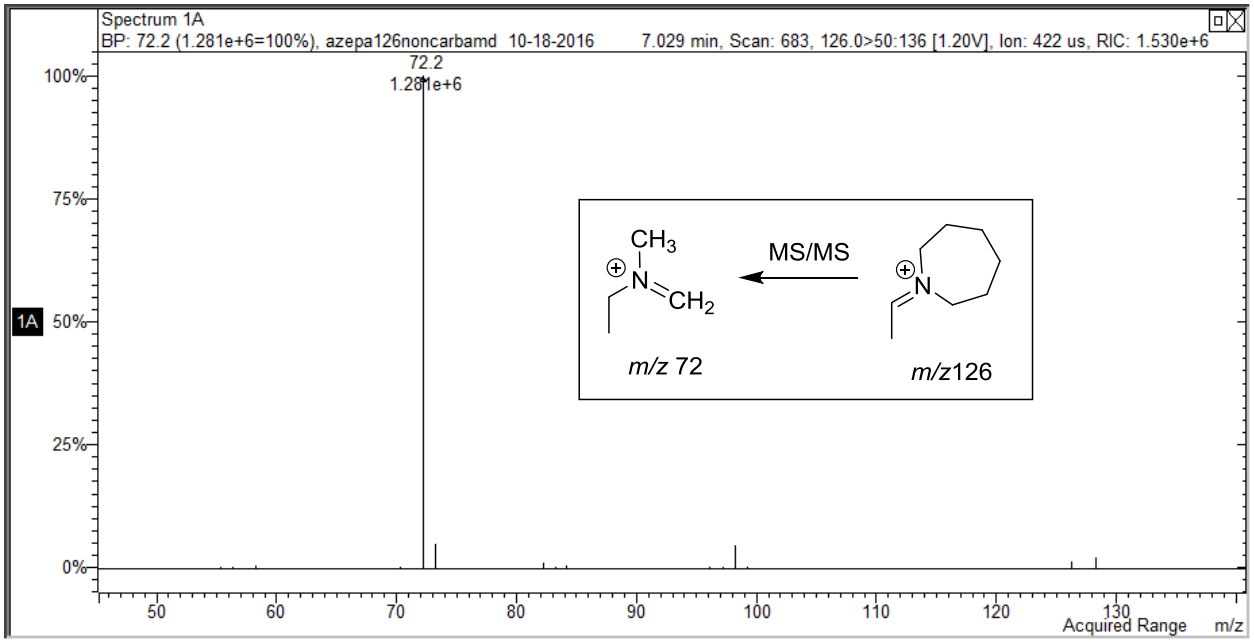

Figure 35. MS/MS product ion spectra for the four regioisomeric *m/z* 126 base peak iminium cations of the desoxy phenethylamines. GC–MS System 2.

2.2.4. Vapor phase infrared spectrophotometry

The vapor phase infrared spectra for the four desoxy phenethylamines and the four regioisomeric aminoketones are shown in Figure 36. The overall absorption band shape as well as individual band position and intensity in the 3000 cm^{-1} to 2700 cm^{-1} provide information for differentiation among the regioisomeric aminoketones as well as the regioisomeric desoxy phenethylamines. The doublet absorption bands at 1489 cm^{-1} and 1442 cm^{-1} are characteristic for the 3,4-methylenedioxy aromatic ring substitution pattern and the unsymmetrical nature of these doublet absorption bands indicates the lack of a carbonyl at the benzylic position of the alkyl side-chain for the desoxy phenethylamines. The analogous aminoketones are characterized by symmetrical doublet absorption bands centered at this wavelength range and these have been previuosly discussed in detail in Section 2.1.4.

The four regioisomeric aminoketones are displaying a slight difference related to the carbonyl absorption band from 1685 cm^{-1} to 1692 cm^{-1} for Compounds 1 to 4, respectively. This may be attributed to the size of the tertiary amine ring for these regioisomers, with azetidine ring (Compound 1) having a smaller influence on the coplanar structure between the aromatic ring and the carbonyl functionality (less double bond character) and a greater influence with the isomer having the azepane ring (Compound 4) which may force the carbonyl group out of the plane (more double bond character).

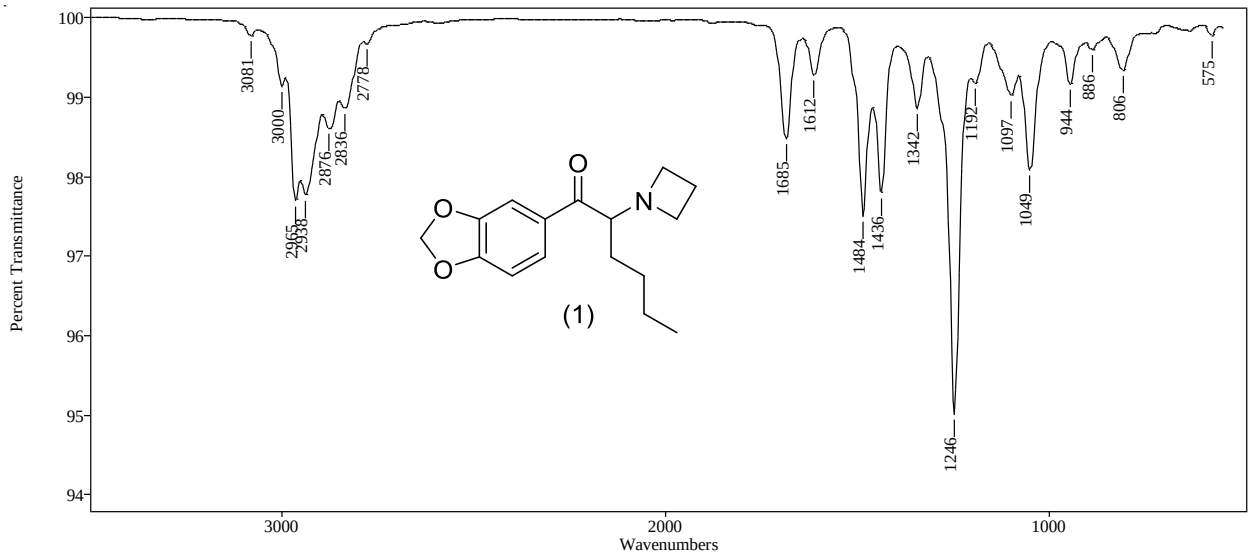
Percent Transmittance
100
99
98
97
96
95
94
3081
3000
2965
2938
2876
2836
2778
1685
1612
1484
1436
1342
1246
1192
1097
1049
944
886
806
575
O
O
O
N
(1)
3000
2000
1000
Wavenumbers

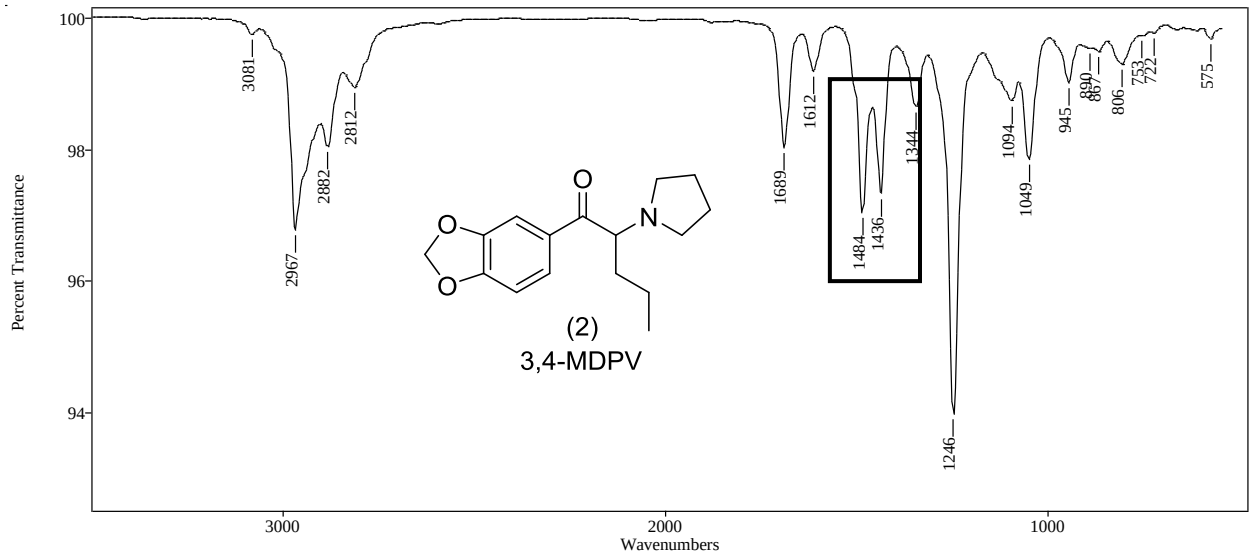
Percent Transmittance
100
98
96
94
3081
2967
2882
2812
1689
1612
1484
1436
1344
1246
1094
1049
945
890
887
806
753
722
575
O
O
O
N
(2)
3,4-MDPV
3000
2000
1000
Wavenumbers

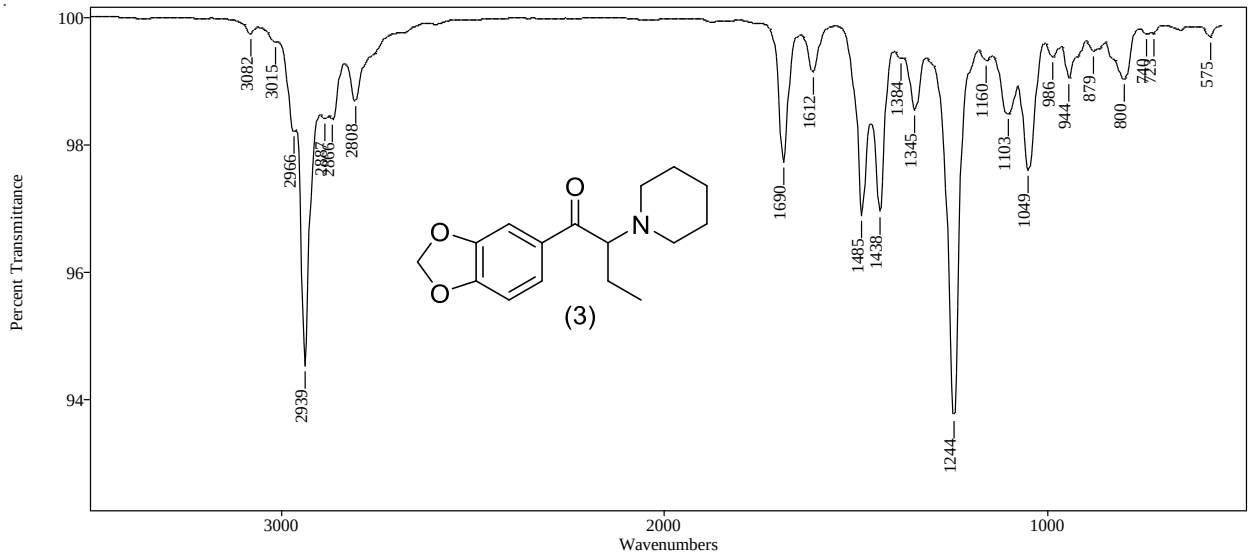
Percent Transmittance
100
98
96
94
3082
3015
2966
2939
2887
2866
2808
1690
1612
1485
1438
1384
1345
1244
1160
1103
1049
986
944
879
800
749
723
575
O
O
O
N
(3)
3000
2000
1000
Wavenumbers

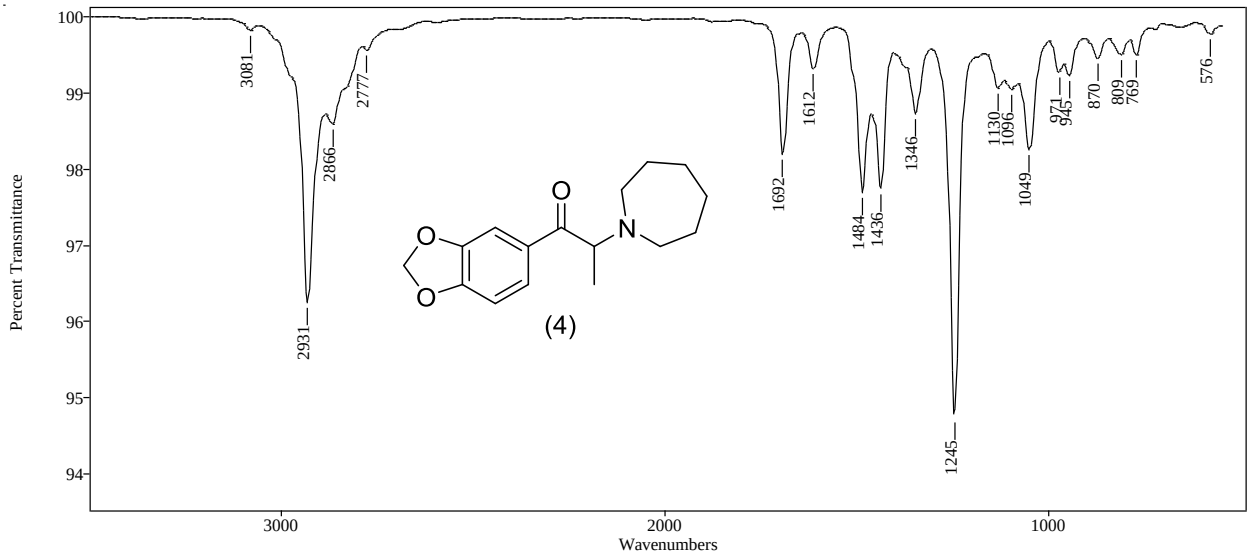
Percent Transmittance
100
99
98
97
96
95
94
3081
2931
2866
2777
1692
1612
1484
1436
1346
1245
1130
1096
1049
971
945
870
809
769
576
O
O
O
N
(4)
3000
2000
1000
Wavenumbers

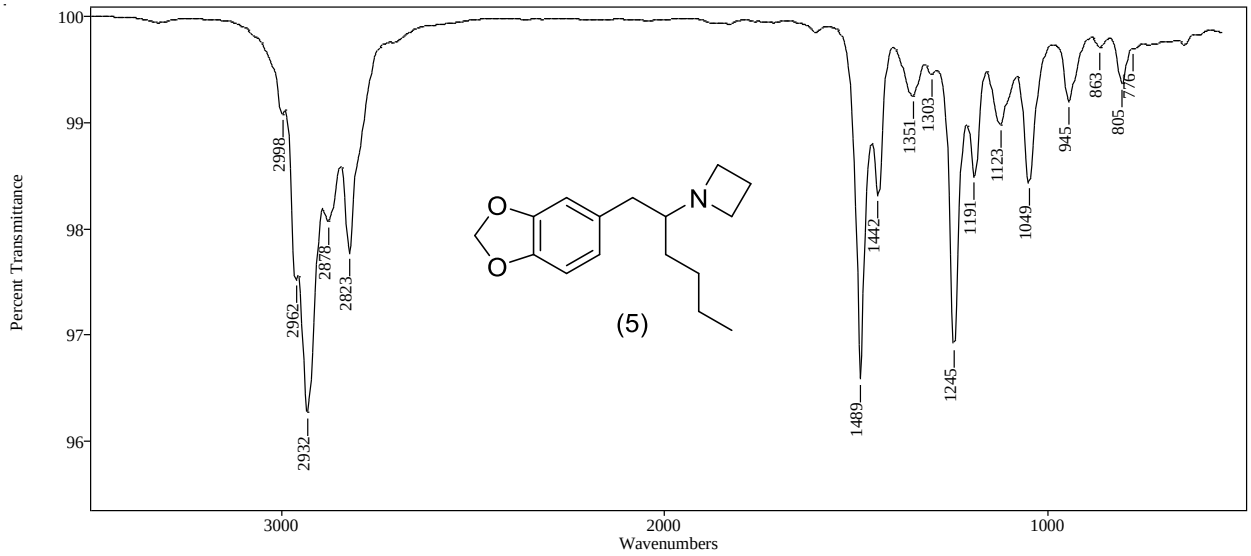
Percent Transmittance
100
99
98
97
96
2998
2962
2932
2878
2823
1489
1442
1351
1303
1245
1191
1123
1049
945
863
805
776
O
O
N
(5)
3000
2000
1000
Wavenumbers

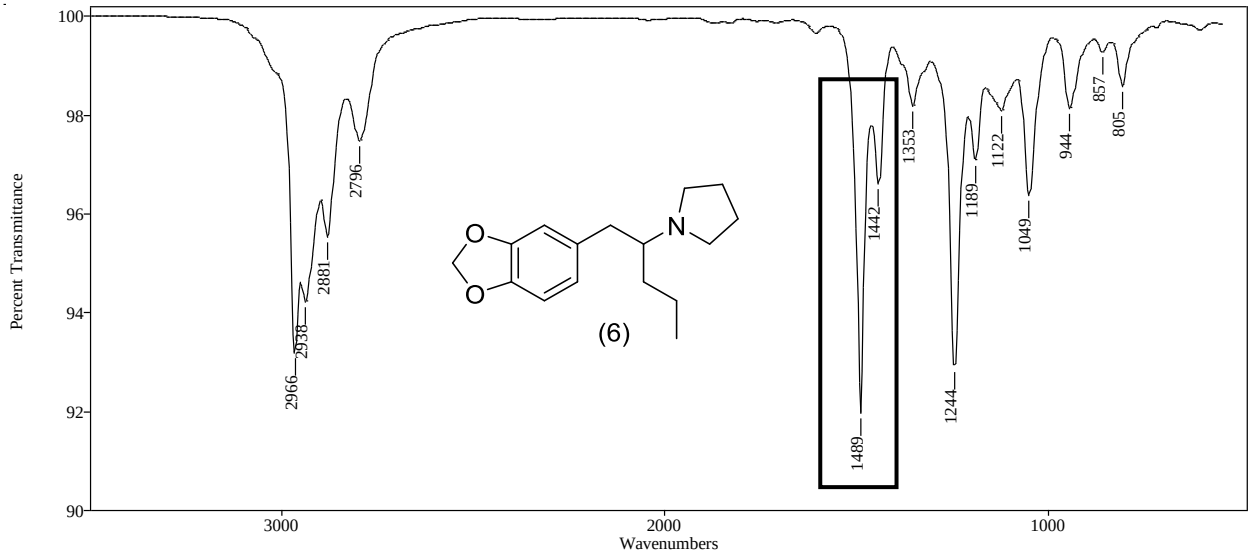
Percent Transmittance
100
98
96
94
92
90
2966
2938
2881
2796
1489
1442
1353
1244
1189
1122
1049
944
857
805
O
O
N
(6)
3000
2000
1000
Wavenumbers

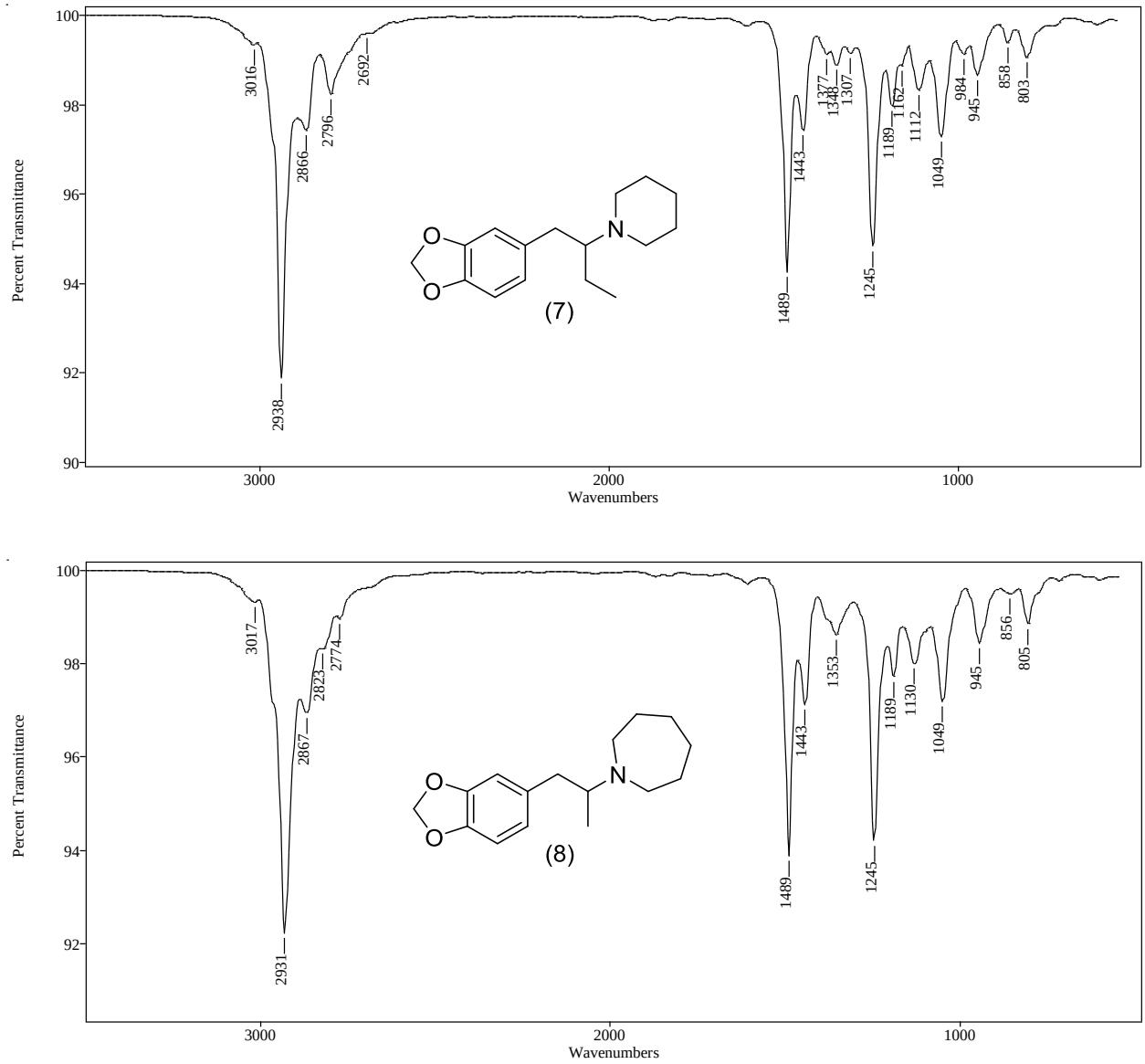

Figure 36. Vapor phase IR spectra (GC–IR) for the four regioisomeric aminoketones (Compounds 1–4) and the four regioisomeric desoxyamines (Compounds 5–8).

The vapor phase infrared spectra (GC–IR) for the two example intermediate ketones (Compounds c and g) are shown in Figure 37. The carbonyl absorption band for Compound c occurs at 1696 cm^{-1} compared to 1724 cm^{-1} for the unconjugated carbonyl in Compound g. The symmetrical doublet absorption bands of equal intensities at 1486 and 1439 cm^{-1} is characteristic for the 3,4-methylenedioxybenzoyl group in which formal conjugation exists between the aromatic

ring and the carbonyl group. Several structure correlated GC–IR studies in our laboratory have demonstrated that this doublet shifts to an unsymmetrical pattern without the conjugated carbonyl as illustrated by the vapor phase infrared spectrum for Compound g.

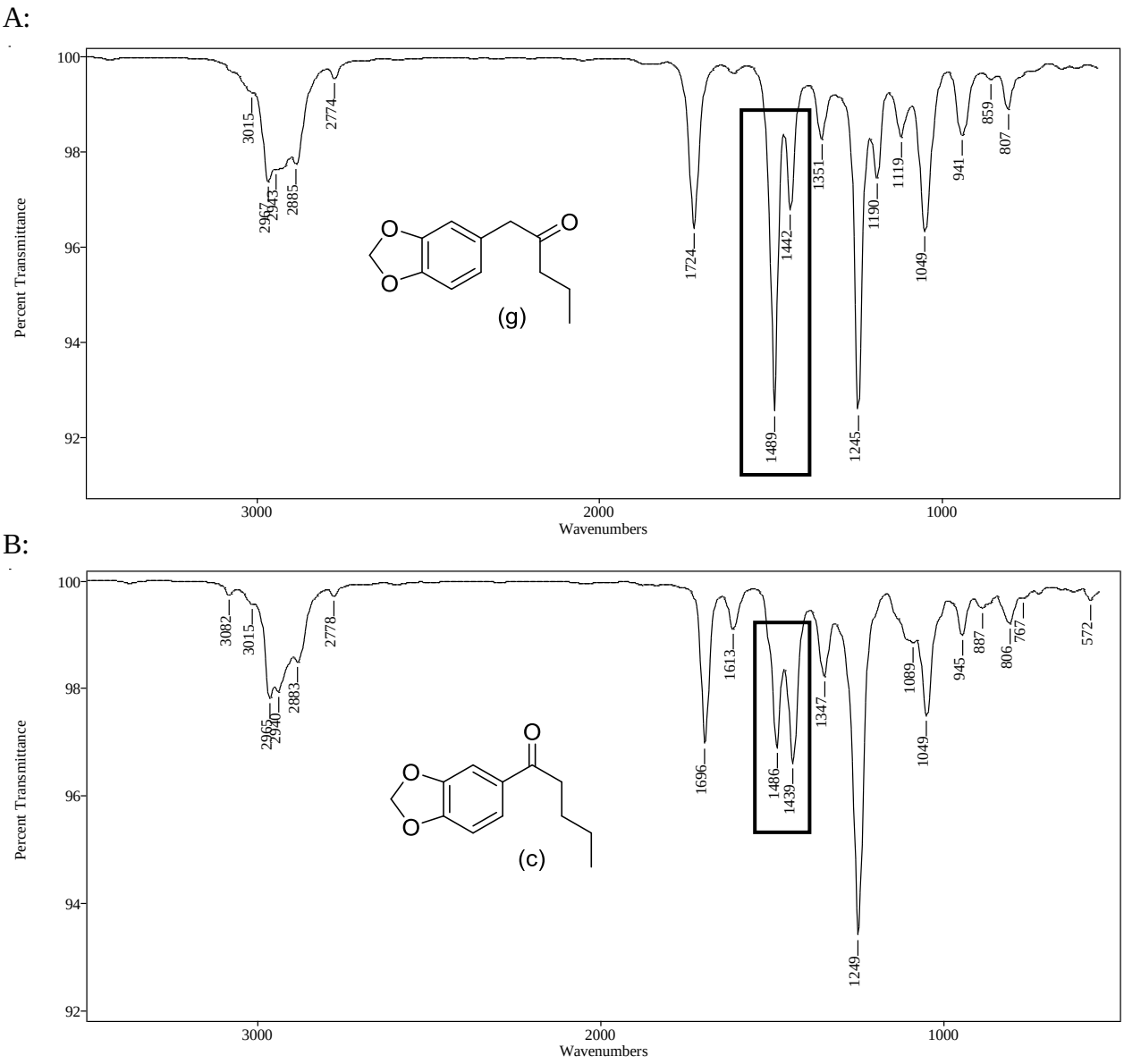

Figure 37. Representative example of vapor phase IR spectra (GC–IR) for the intermediate regioisomeric ketones. A: 1-(3,4-methylenedioxyphenyl)-2-pentanone; B: 1-(3,4-methylenedioxyphenyl)-1-pentanone.

2.2.5. Conclusion

Product ion fragmentation of iminium cations provides useful data for differentiation of regioisomeric cyclic tertiary amines. The cyclic amines azetidine, pyrrolidine, piperidine and azepane were incorporated into a series of aminoketones and desoxy phenethylamines related to the cathinone-type drugs of abuse. Variations of ring size and hydrocarbon side-chain length yield two regioisomeric sets of compounds, aminoketones and desoxy phenethylamines having equivalent regioisomeric iminium cations base peaks at *m/z* 126. The CI-MS spectra provide molecular weight information for these desoxy phenethylamine analogues and their corresponding aminoketone analogues. The MS/MS product ion spectra provide data to characterize the side-chain and cyclic tertiary amine portions of the iminium cation base peaks. The product ions from the *m/z* 126 iminium cation produced by the desoxy phenethylamines and the aminoketones containing the azetidine, pyrrolidine, piperidine and azepane cyclic tertiary amines occur at *m/z* 70, 84, 98 and 72, respectively. The azetidine series of compounds all yield a common product ion at *m/z* 70 as long as a four-centered hydrogen rearrangement process is available in the side-chain. No significant product ion was formed for the azetidine containing iminium cation for the methyl side-chain homologue since the analogous four centered hydrogen migration is not possible in this compound. Product ions in the pyrrolidine series are formed via ring and side-chain fragmentation with side-chain fragmentation dominating in the higher side-chain homologues. The piperidine containing amines undergo H-migration in the side-chain to yield a common *m/z* 98 product ion for the ethyl and *n*-propyl side-chains while the methyl side-chain homologue undergoes ring fragmentation. Both side-chain and ring fragmentation yield a mixture of product ions in the higher side chain homologues for the seven membered cyclic azepane tertiary amines and ring fragmentation occurs in the smaller alkyl side-chains. Ring fragmentation in the pyrrolidine series

results in the loss of 42 Da (C_3H_6) from the iminium cation base peak, 28 Da (C_2H_4) for the piperidine series and 54 Da (C_4H_6) for the azepane series.

The vapor phase infrared spectra for the regioisomeric desoxy phenethylamines are characterized by unsymmetrical doublet absorption bands at 1489 cm^{-1} and 1442 cm^{-1} that indicates the lack of a carbonyl group at the benzylic position of the alkyl side-chain. However, the corresponding regioisomeric aminoketones show a doublet absorption pattern with peaks centered at 1484 cm^{-1} and 1436 cm^{-1}. The aminoketones and the desoxy phenethylamine regioisomers were separated in capillary gas chromatography experiments using an Rxi®-17Sil MS stationary phase and the aminoketones showing greater retention than the desoxy phenethylamines. In both series of compounds chromatographic retention was related to the ring size of the cyclic tertiary amines with the azetidine containing analogue eluting first and the azepane containing derivative eluting last.

2.3. Product ion MS/MS differentiation of regioisomeric side-chain groups in cathinone derivatives

Precursor materials are available to prepare aminoketone drugs containing regioisomeric *n*-propyl and isopropyl side-chain groups related to the drug alpha-pyrrovalerone (Flakka) and MDPV (3,4-methylenedioxypyrrovalerone). The regioisomeric compounds related to Flakka and MDPV were prepared and evaluated in EI-MS and MS/MS product ion experiments. These compounds yield equivalent regioisomeric iminium cation base peaks at *m/z* 126 in EI-MS spectra.

This study describes the use of product ion spectra with deuterium labeling in the analysis of regioisomeric iminium cations generated by the EI-MS for a series of *n*-propyl and isopropyl side-chain cathinone-type tertiary amines (MDPV, iso-MDPV, Flakka and iso-Flakka). These iminium cation base peaks show characteristic product ion spectra, which allow differentiation of the side-chain *n*-propyl and isopropyl groups in the structure. The *n*-propyl side-chain containing iminium cation base peak (*m/z* 126) in the EI-MS yields a major product ion at *m/z* 84 while the regioisomeric *m/z* 126 base peak for the isopropyl side-chain yields a characteristic product ion at *m/z* 70. Deuterium labeling in both the pyrrolidine ring and the alkyl side-chain confirmed the process for the formation of these major product ions.

These regioisomeric compounds yield equivalent EI-MS, CI-MS and IR spectra. However, MS/MS product ion fragmentation provides useful data for differentiation of *n*-propyl and isopropyl side-chain iminium cations from these cathinone derivative drugs of abuse.

2.3.1. Synthesis of the aminoketone derivatives containing regioisomeric *n*-propyl and isopropyl side-chain groups

The precursor ketone valerophenone needed for the synthesis of the current popular drug of abuse alpha-pyrrovalerone (alpha-PVP, Flakka) is available from a variety of commercial sources. The regioisomeric precursor ketone having the isopropyl side-chain, isovalerophenone, is also a commercially available material. The bromination and subsequent substitution with pyrrolidine of these phenones yields Compounds 1 and 2. MDPV and iso-MDPV (Compounds 3 and 4) can be prepared from the starting material piperonal using the same procedure prescribed previously in Section 2.1.1. The deuterated bromoalkanes were used along with magnesium metal to prepare the appropriate labeled Grignard reagents. These deuterated reagents were used to prepare the desired deuterium labeled analogues. The compounds were purified using preparative TLC.

2.3.2. Gas chromatographic separation

The chromatograms in Figure 38 shows the GC separation of the regioisomeric side-chain compounds for both the aromatic ring unsubstituted compounds and the 3,4-methylenedioxy substituted aromatic ring. The separations were obtained on a column (30 m × 0.25 mm i.d.) coated with 0.10 μm film of Crossbond® 5% diphenyl, 95% dimethyl polysiloxane (Rtx®-5). The temperature program consisted of an initial hold at 70 °C for 1.0 minute, ramped up to 250 °C at a rate of 30 °C/minute followed by a hold at 250 °C for 15.0 minutes (with an injector temperature of 150 °C). In both chromatograms, the branched chain regioisomer elutes before the linear *n*-propyl side-chain isomer. This elution order was also observed in the intermediate ketone materials in Figure 39.

A:

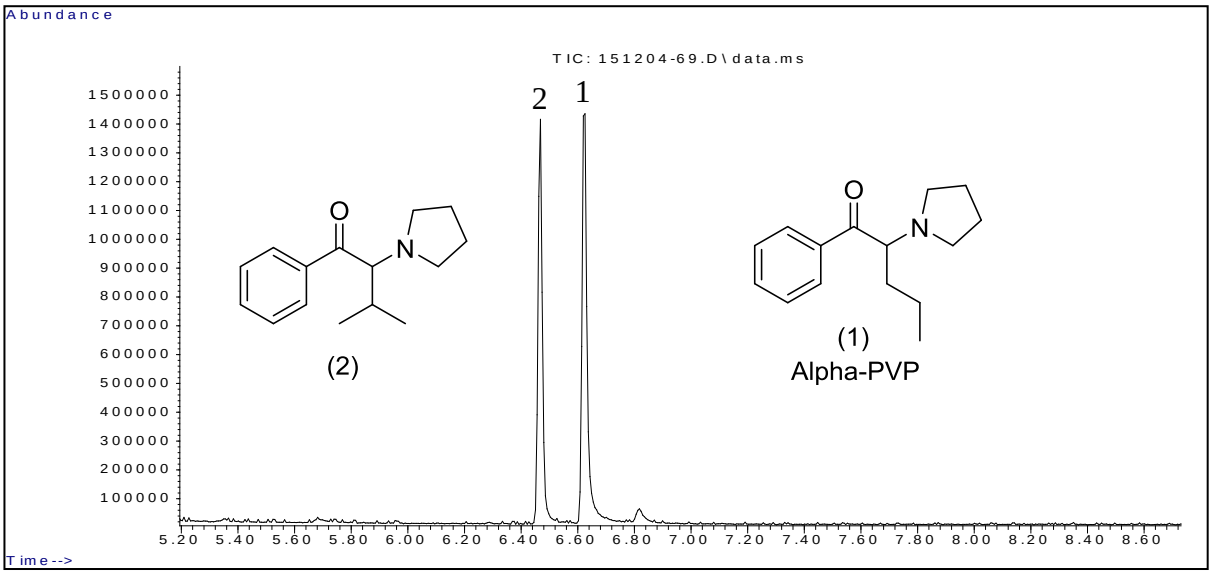

B:

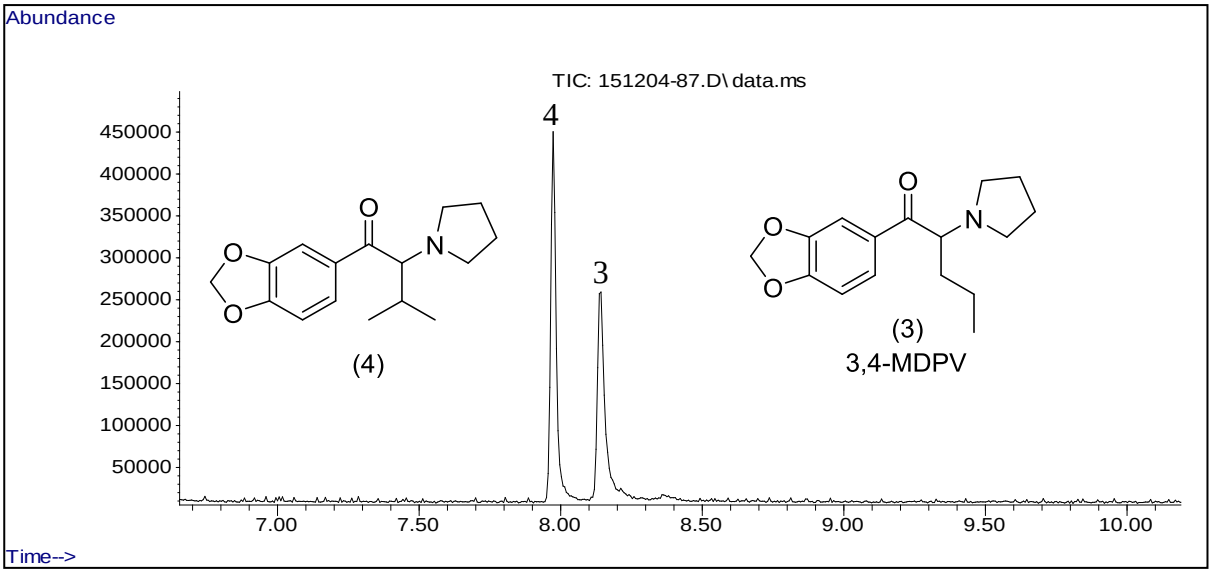

Figure 38. GC separation of the compounds in this study. A: Compounds 1 and 2; B: Compounds 3 and 4. Rtx®-5 stationary phase.

A:

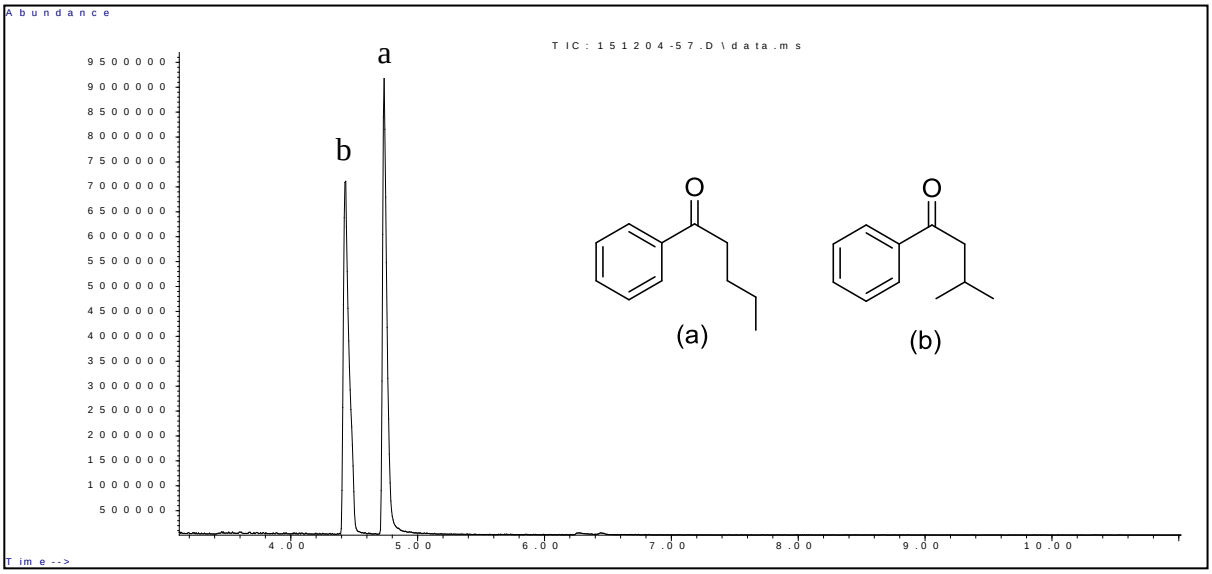

B:

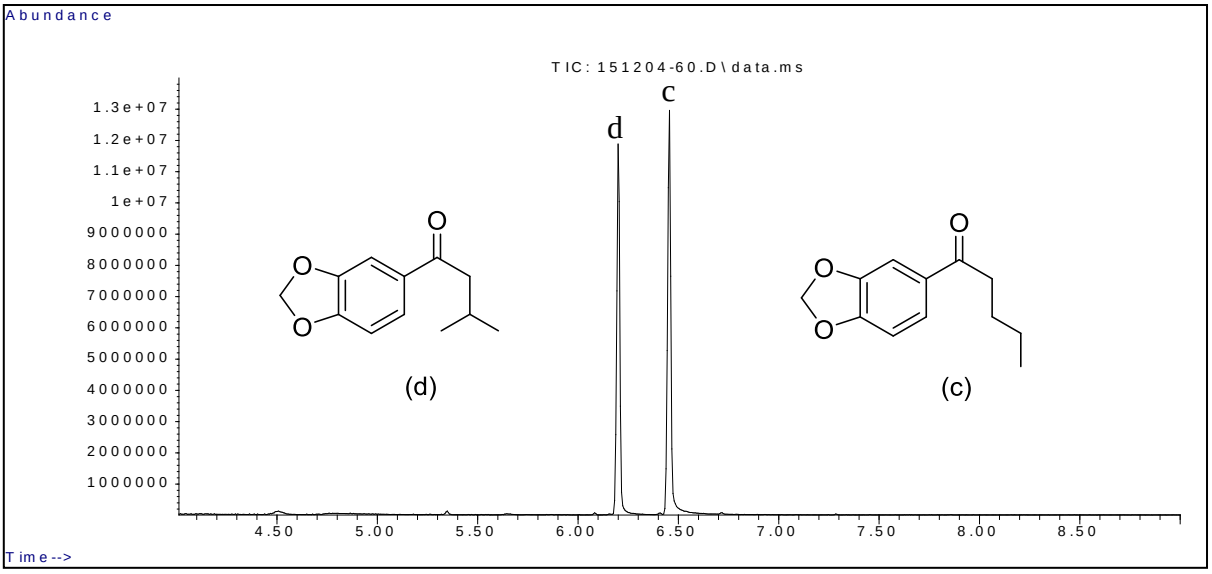

Figure 39. GC separation of the intermediate ketones. A: valerophenone and isovalerophenone; B: 3,4-methylenedioxyvalerophenone and 3,4-methylenedioxyisovalerophenone. Rtx®-5 stationary phase.

2.3.3. Mass spectral studies (EI-MS, CI-MS and MS/MS)

The differentiation between MDPV and iso-MDPV as well as Flakka and iso-Flakka in their pure forms can be easily performed via NMR spectroscopy. The proton NMR splitting patterns for a straight chain *n*-propyl and branched chain isopropyl groups can readily identify these compounds. However, NMR spectroscopy is less applicable to mixture and trace analysis often required for forensic drug identification and biological sample analysis. The present method can be used in the analysis of mixtures or trace amounts of the studied compounds.

The unsubstituted aromatic ring and the 3,4-methylenedioxy substituted ring subdivide these four compounds based on their molecular weight. However, the regioisomeric *n*-propyl and isopropyl side-chains yield equivalent iminium cation base peaks for all four of these compounds. The mass spectra in Figure 40 show the *m/z* 126 iminium cation base peak for the unsubstituted aromatic ring isomers, Compounds 1 and 2 (Flakka and iso-Flakka) and the 3,4-methylenedioxy derivatives, Compounds 3 and 4 (MDPV and iso-MDPV). The mass spectra for these four compounds show the *m/z* 126 iminium cation as the dominant ion in the spectrum and the base peak. Thus, the EI-MS for Compounds 1 and 2 as well as 3 and 4 are essentially identical showing no distinguishing ions to differentiate the straight *n*-propyl and the branched isopropyl chain iminium cations.

A:

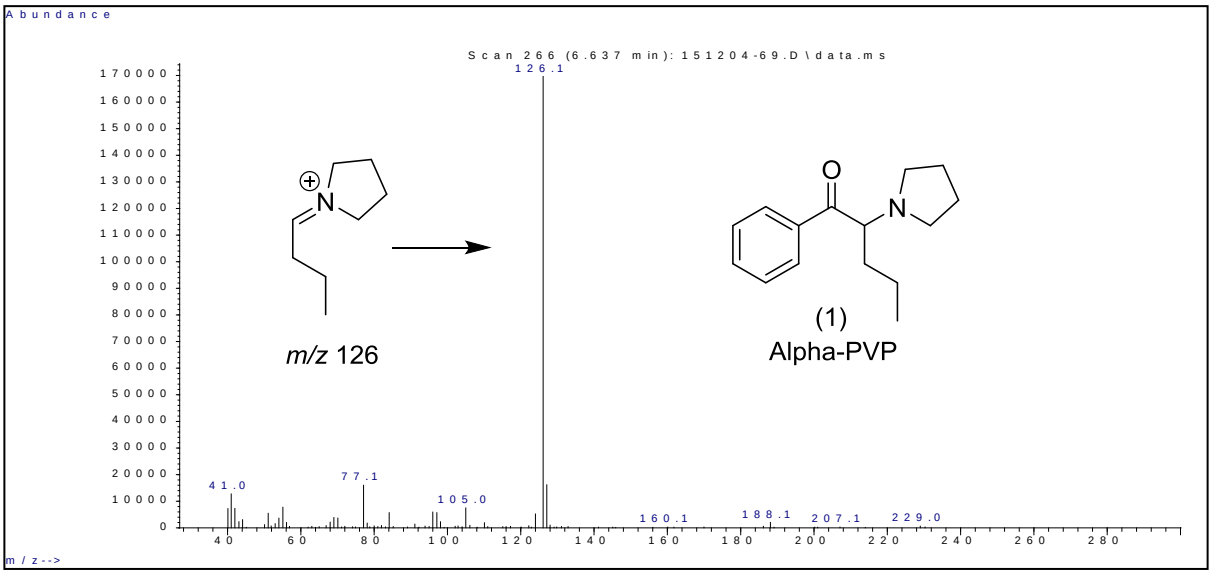
Abundance
Scan 266 (6.637 min): 151204-69.D\data.ms
126.1
41.0
77.1
105.0
160.1
188.1
207.1
229.0
m/z-->
m/z 126
(1)
Alpha-PVP

B:

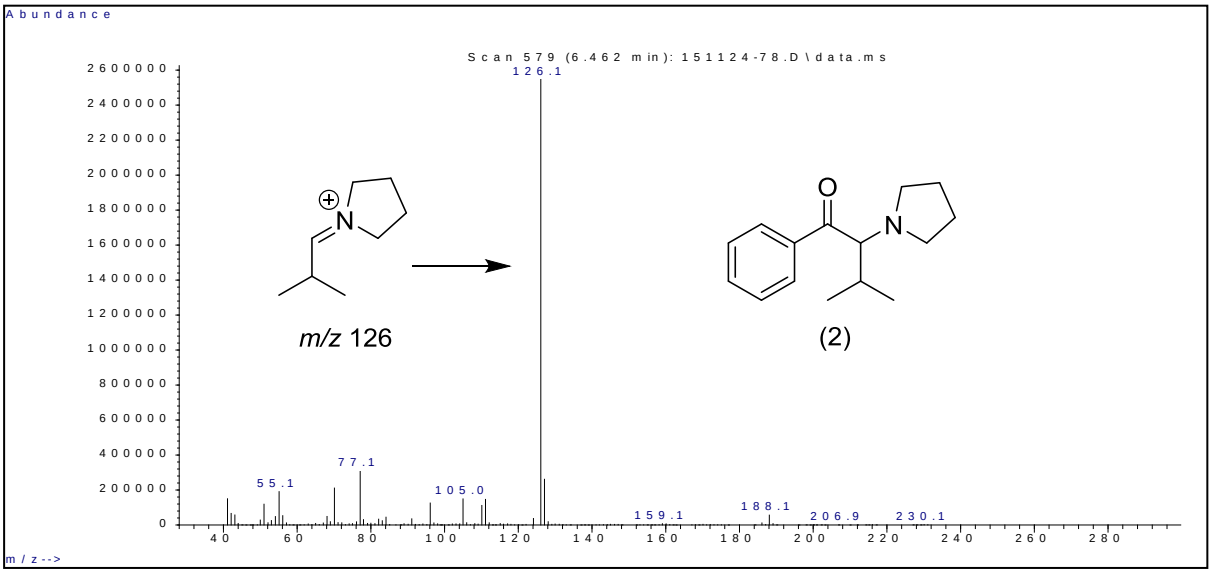
Abundance
Scan 579 (6.462 min): 151124-78.D\data.ms
126.1
55.1
77.1
105.0
159.1
188.1
206.9
230.1
m/z-->
m/z 126
(2)

C:

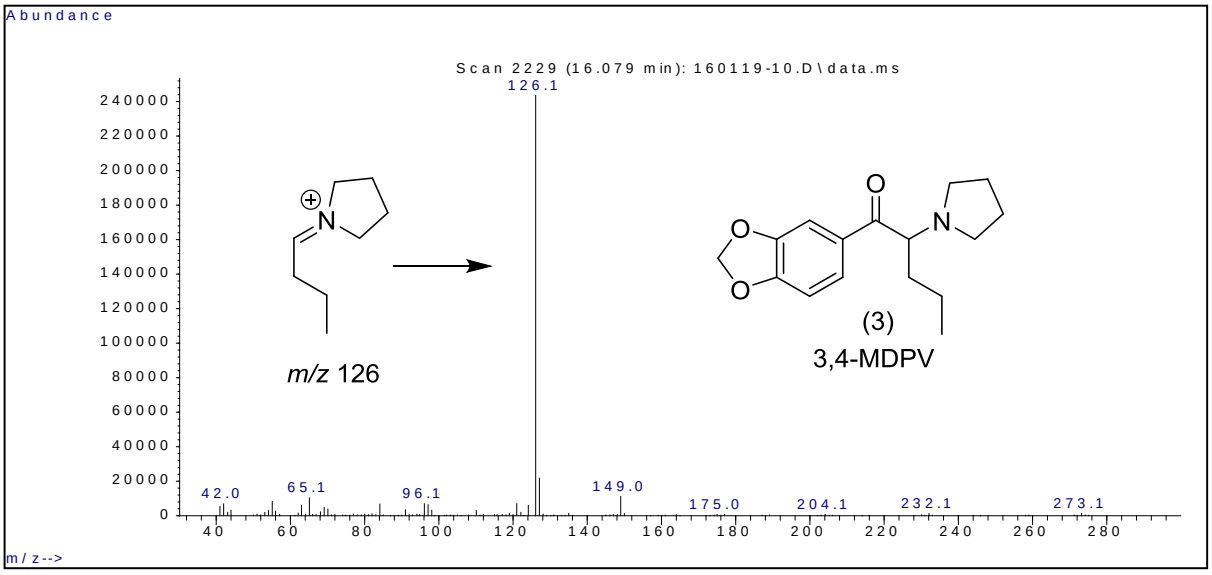

D:

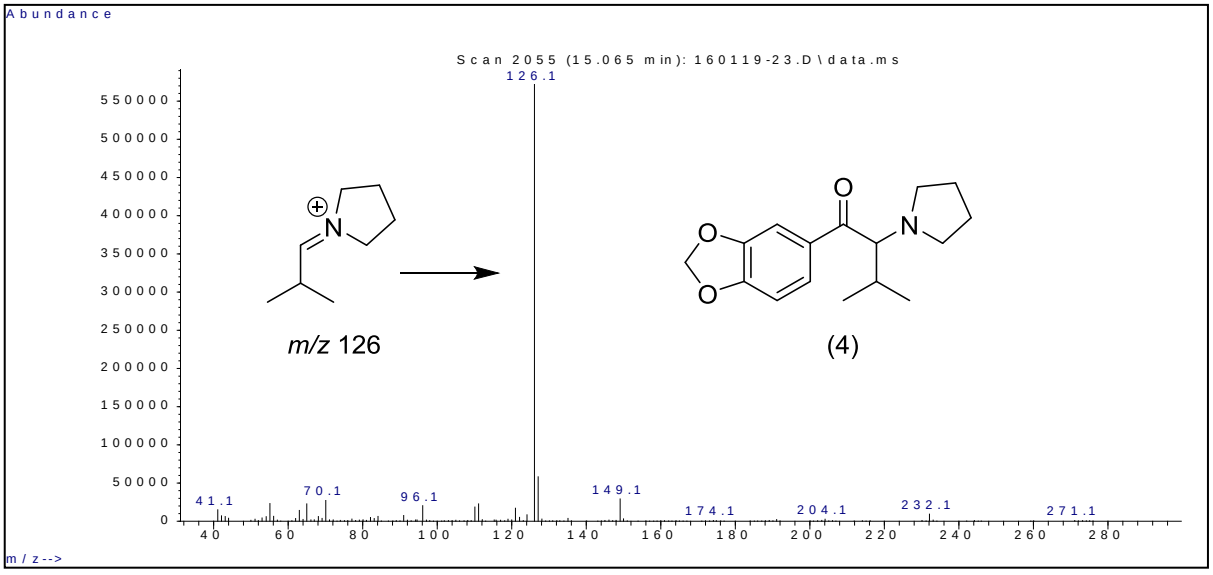

Figure 40. Full scan EI-MS spectra for Compounds1–4 (Flakka, iso-Flakka, MDPV and iso-MDPV). GC–MS System 1.

The GC–CI-MS studies were performed on a column (30 m × 0.25 mm i.d.) coated with 0.25 µm film of Crossbond® 100% trifluoropropylmethyl polysiloxane (Rtx®-200). The chemical ionization mass spectra in Figure 41 confirm the molecular weight for the two sets of the regioisomeric aminoketones, Flakka and iso-Flakka as well as MDPV and iso-MDPV via the intense $[M+H]^+$ ion. These spectra were generated using methanol as the CI reagent gas. Thus, GC–CI-MS confirms the molecular weight for these compounds and the EI mass spectra provide information about that portion of the molecule bonded to the benzoyl moiety or the 3,4-methylenedioxybenzoyl moiety common to all these compounds. Chromatographic analysis was performed using a temperature program consisting of an initial hold at 70 °C for 1.0 minute, ramped up to 250 °C at a rate of 30 °C/minute followed by a hold at 250 °C for 15.0 minutes.

A:

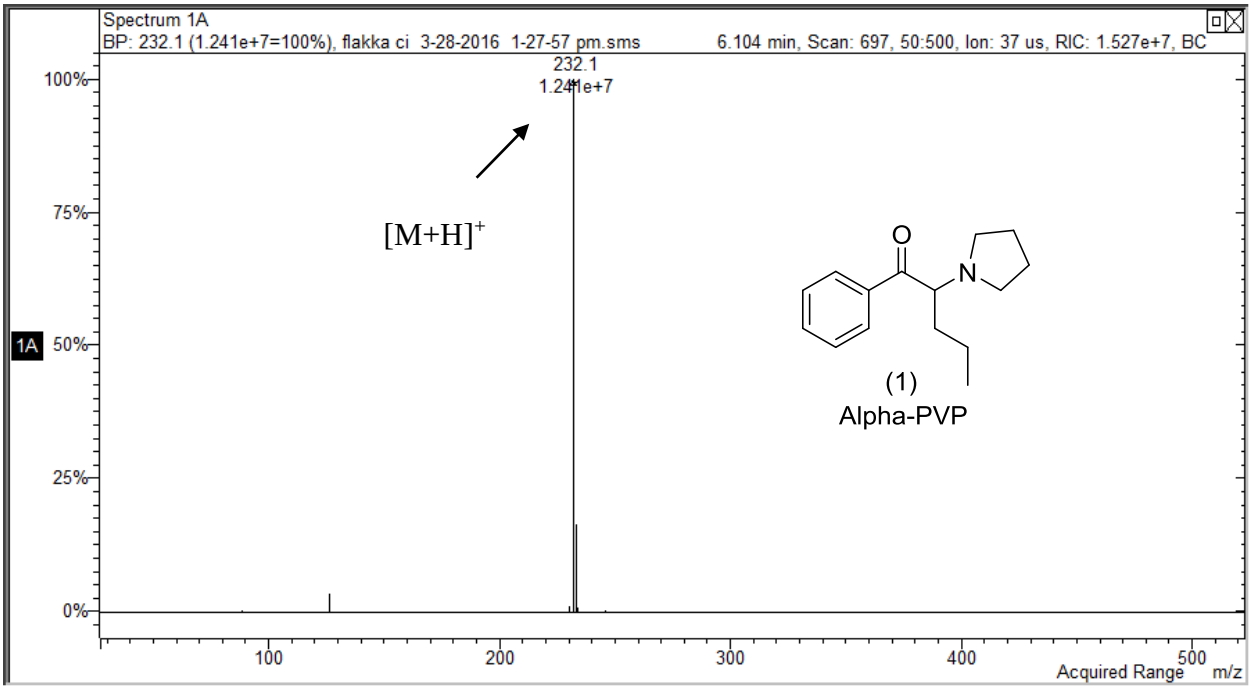

B:

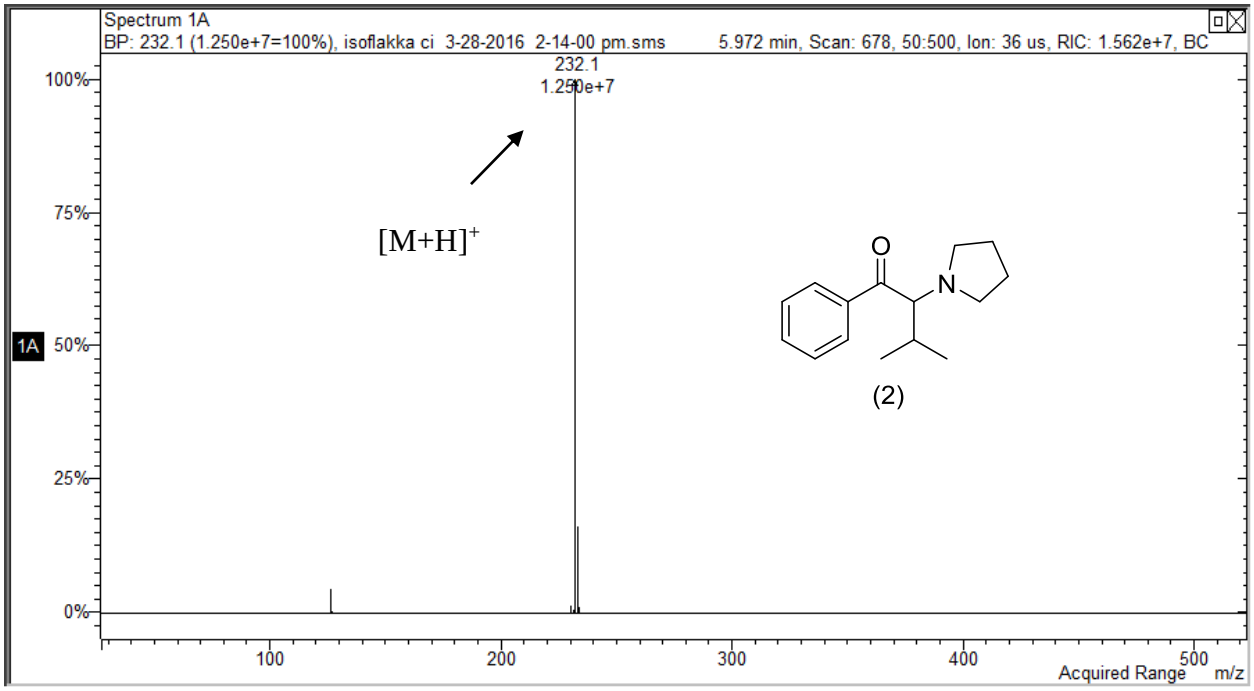
Spectrum 1A
BP: 232.1 (1.250e+7=100%), isoflakka ci 3-28-2016 2-14-00 pm.sms
5.972 min, Scan: 678, 50:500, Ion: 36 us, RIC: 1.562e+7, BC
232.1
1.250e+7
100%
75%
50%
25%
0%
1A
[M+H]+
O
N
(2)
100
200
300
400
500
Acquired Range
m/z

C:

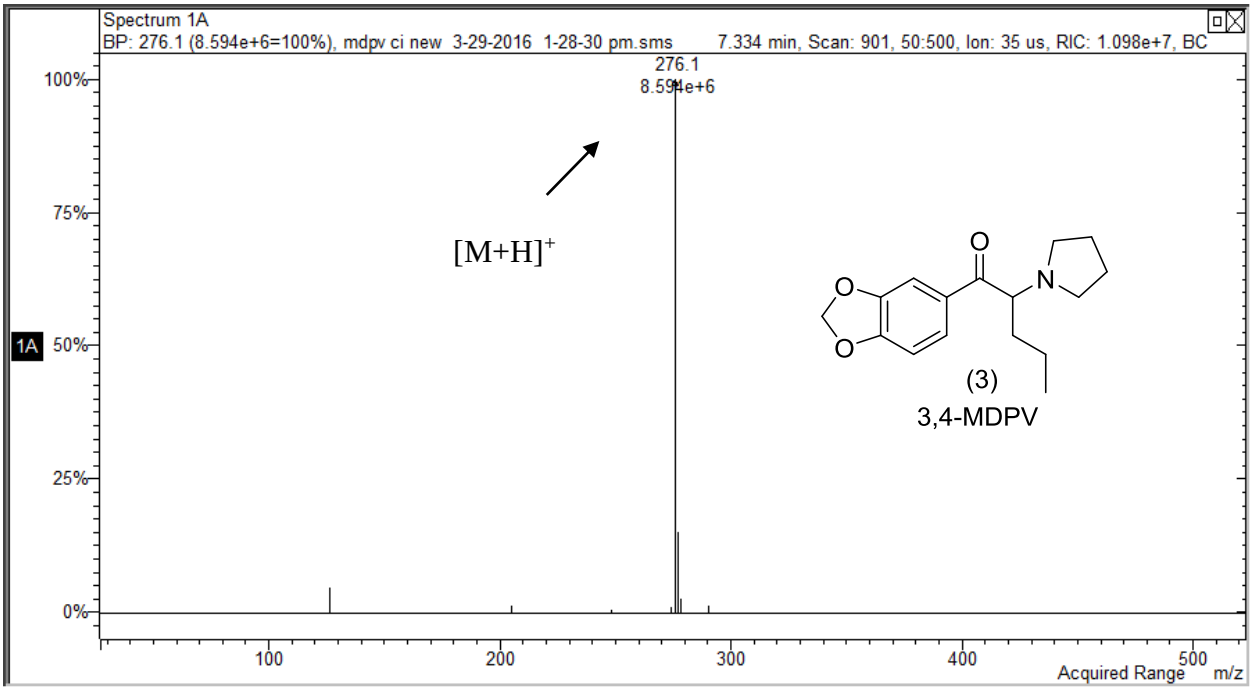
Spectrum 1A
BP: 276.1 (8.594e+6=100%), mdpv ci new 3-29-2016 1-28-30 pm.sms
7.334 min, Scan: 901, 50:500, Ion: 35 us, RIC: 1.098e+7, BC
276.1
8.594e+6
100%
75%
50%
25%
0%
1A
[M+H]+
O
O
O
N
(3)
3,4-MDPV
100
200
300
400
500
Acquired Range
m/z

D:

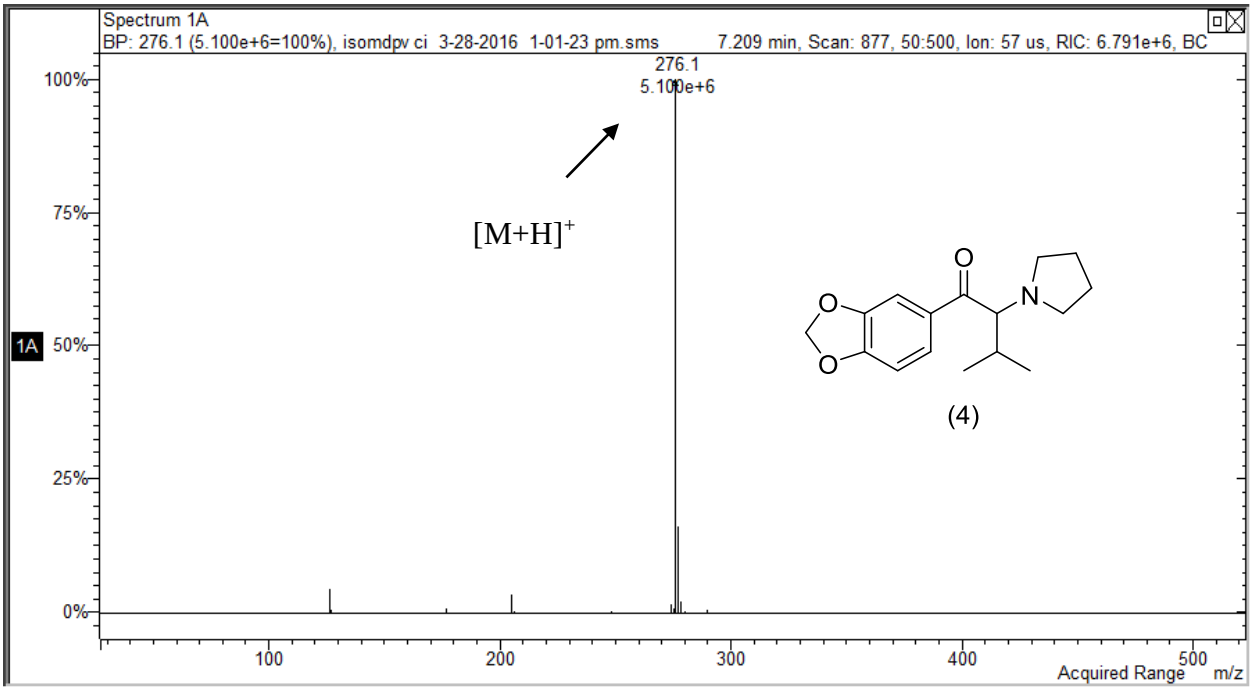

Figure 41. Chemical ionization mass spectra (CI-MS) for Compounds 1–4. GC–MS System 2.

The product ion spectra (MS/MS) for the straight *n*-propyl chain and branched isopropyl chain substituted iminium cations show unique and characteristic product ions which allow differentiation of these regioisomeric side-chains. For MS/MS experiments, the scan type used was the Automated Method Development function (AMD) and the optimum MS/MS excitation amplitudes ranged from 0.20 to 1.60 volts. The GC–MS/MS studies were performed using the same column described for the GC–CI-MS studies (Rtx®-200) with a temperature program consisting of an initial hold at 70 °C for 1.0 minute, ramped up to 250 °C at a rate of 30 °C/minute followed by a hold at 250 °C for 7.0 minutes.

Figure 42 shows the MS/MS product ion spectra for the *n*-propyl side-chain *m/z* 126 iminium cation and the isopropyl side-chain cation generated from Compounds 1 and 2, Flakka and iso-Flakka, respectively. The base peak iminium cation (*m/z* 126) for the *n*-propyl side chain

in Compound 1 yields a major product ion at *m/z* 84 while the isopropyl side-chain shows the major product ion at *m/z* 70. Thus, the regioisomeric side-chains yielding equivalent EI-MS base peaks at *m/*z 126 for Compounds 1 and 2 can be easily differentiated by their unique major product ions.

A:

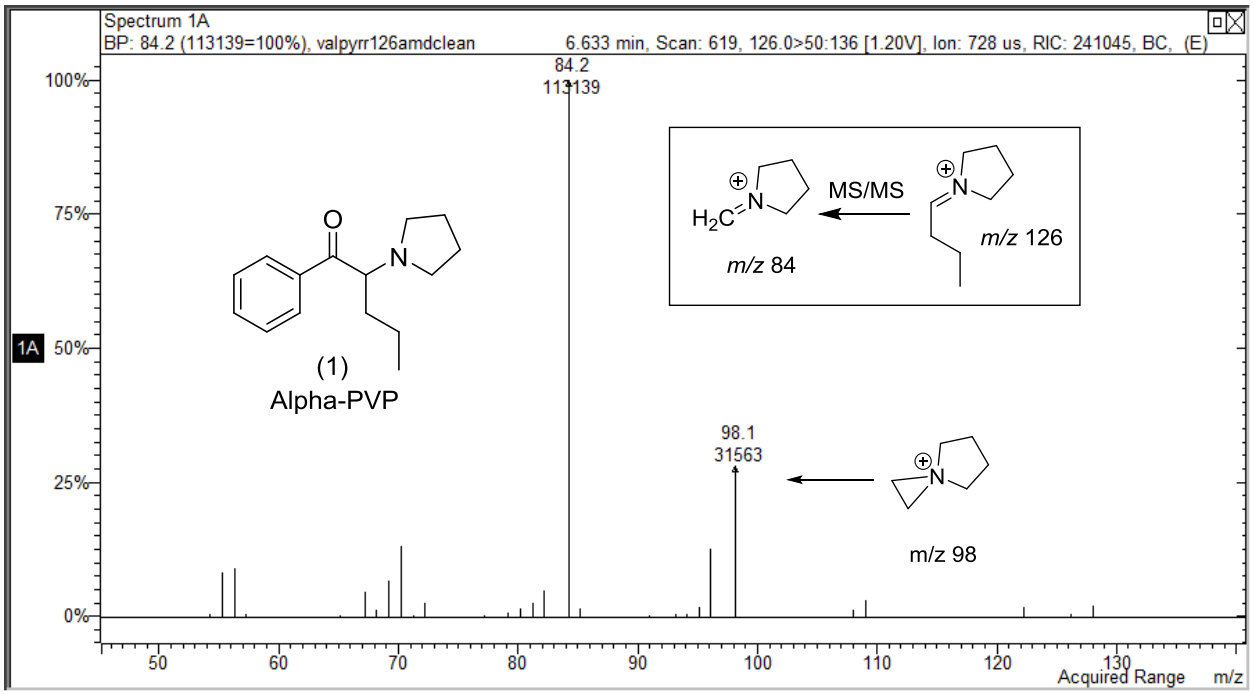

B:

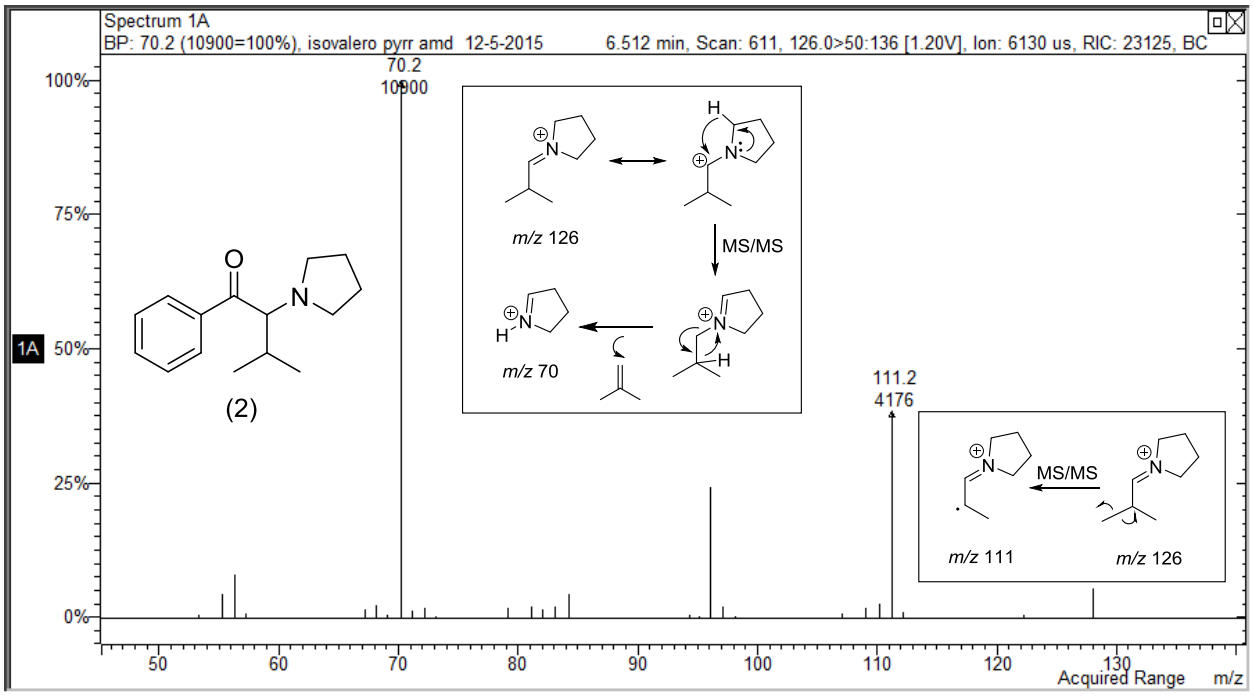

Figure 42. MS/MS product ion spectra for the *m/z* 126 iminium cation base peak for A: alpha-PVP (Compound 1); B: iso-alpha-PVP (Compound 2).

Figure 43 illustrates the equivalent product ion spectral results for the *m/z* 126 iminium cations generated from Compounds 3 and 4, MDPV and iso-MDPV, respectively. The source of the iminium cation is a different molecule however, once formed; the iminium cation yields product ions consistent with its regioisomeric structure.

A:

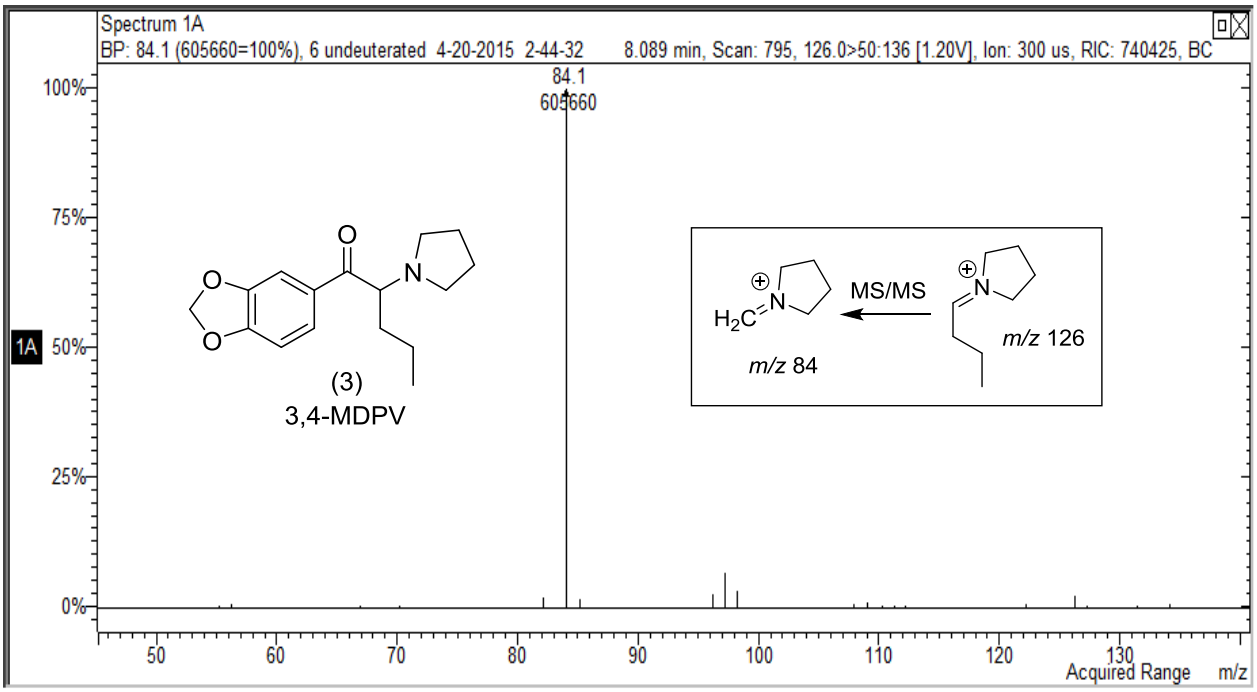

B:

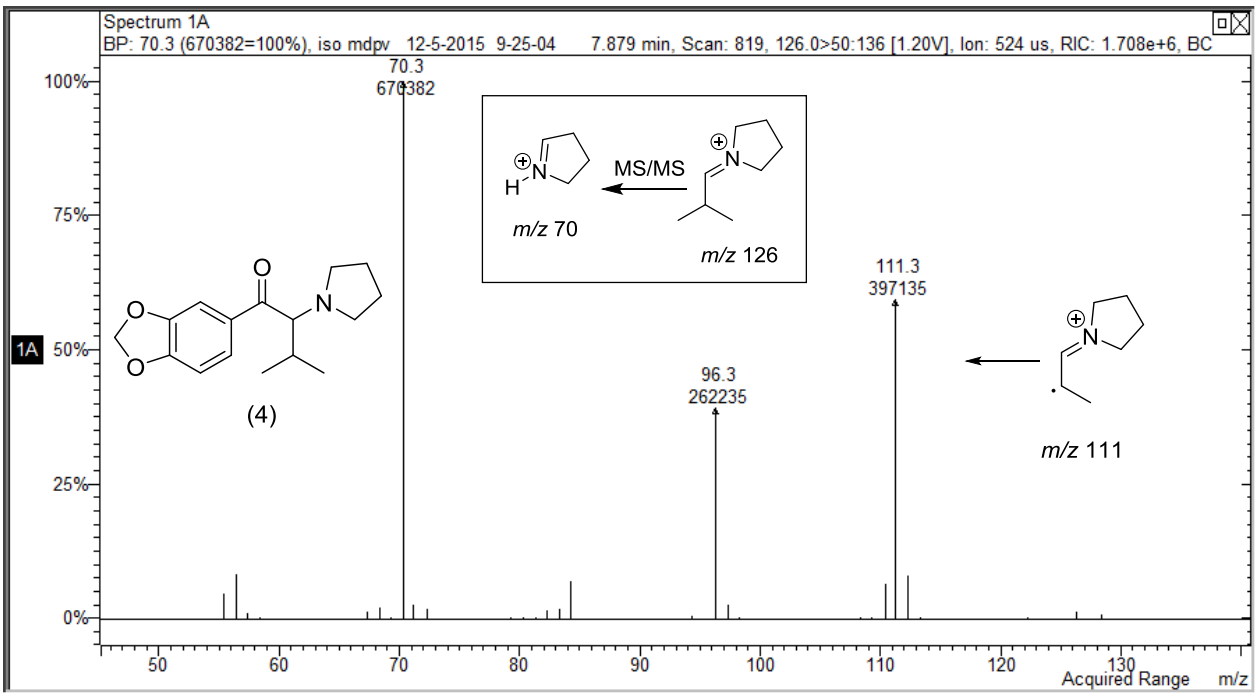

Figure 43. MS/MS product ion spectra for the *m/z* 126 iminium cation base peak for A: MDPV (Compound 3); B: iso-MDPV (Compound 4).

The mechanistic details for the formation of these diagnostic product ions at *m/z* 84 and *m/z* 70 were examined via deuterium labeling experiments. The spectra in Figure 44 show the EI-MS and product ion spectrum for the iminium cation generated from the D_4-analogue of Compound 1. This D_4-analogue of Compound 1 was prepared using 2,2,5,5-D_4-pyrrolidine as the amine component in the synthetic process. Figure 44A confirms the incorporation of the four deuterium atoms into the iminium cation at *m/z* 130 for the full EI-MS for this labeled molecule. Figure 44B further shows the mass shift of +4 Da to *m/z* 88 for the product ion spectrum confirming that all four deuterium labels remain in the product ion and the hydrogen, which migrates, must come from the *n*-propyl side-chain. This fragmentation process has been previously discussed for the D_4-analogue of MDPV (in Section 2.1.3.) and D_8-analogue of MDPV (in Section 2.2.3.) confirming the *n*-propyl side-chain as the source of the migrating hydrogen.

A:

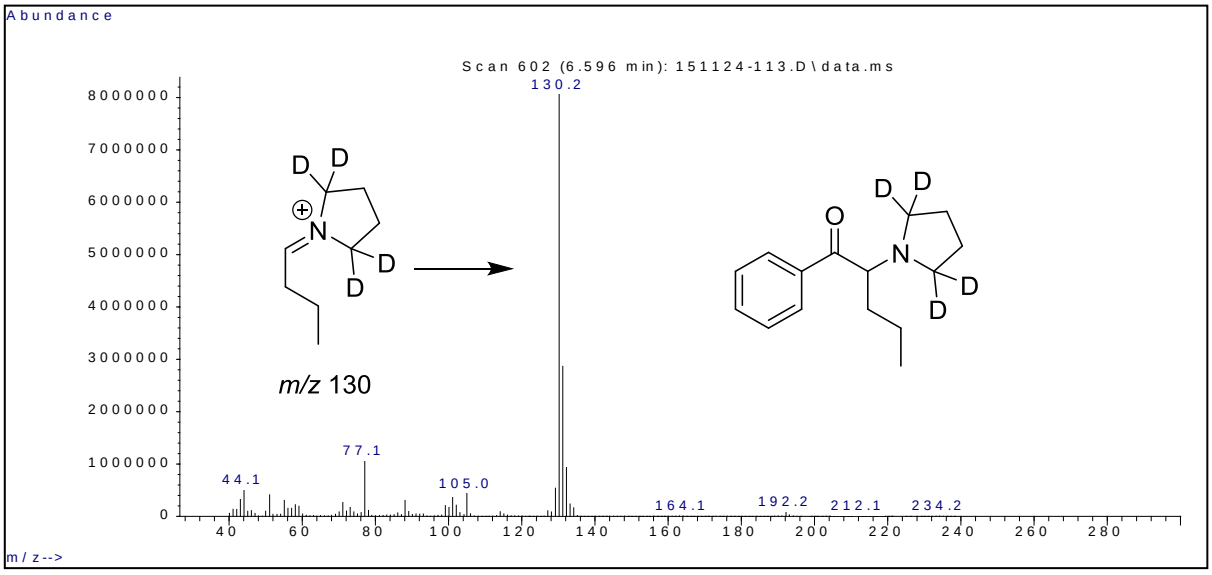

B:

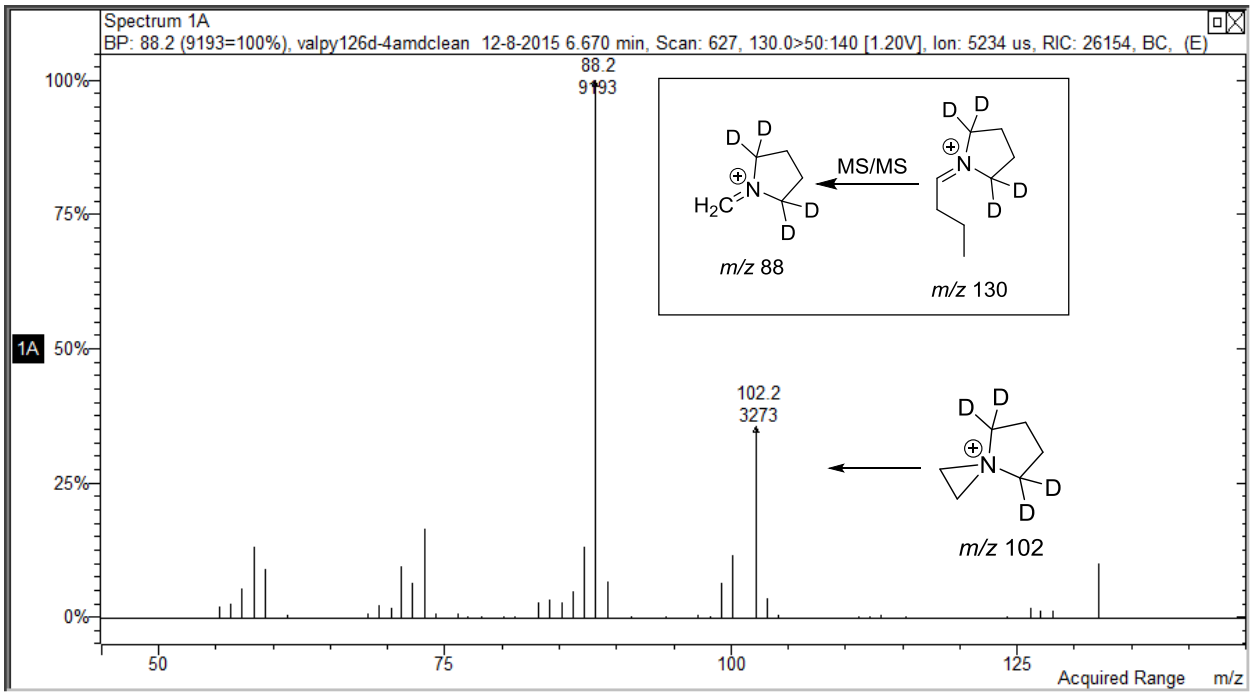

Figure 44. Mass spectra for the 2,2,5,5-D_4-pyrrolidine ring analogue of Compound 1. A: EI-MS full scan; B: product ion spectrum for the *m/z* 130 iminium cation.

The proposed mechanism for the formation of the *m/z* 70 product ion for the isopropyl side-chain containing iminium cation is shown within Figure 42B. The formation of the *m/z* 70 product ion would involve the loss of the entire four carbon fragment (C_4H_8) attached to the pyrrolidine nitrogen or perhaps the four carbons of the pyrrolidine ring. The mechanism shown within Figure 33B suggests the loss of isobutene (C_4H_8) from the side-chain to account for the formation of the *m/z* 70 major product ion. Deuterium labeling of both the pyrrolidine ring and the isopropyl side-chain was used to gather support for the proposed mechanism. The D_4-analogue of Compound 2 was prepared from 2,2,5,5-D_4-pyrrolidine and the product ion spectrum as well as the full EI-MS scan are presented in Figure 45. The mechanism described for the product ion formation in the case of the isopropyl side-chain would suggest conserving three of the four deuterium labels in the resulting product ion. The spectrum in Figure 45A confirms the incorporation of the four deuterium

labels into the molecule and the resulting iminium cation base peak occurs at *m/z* 130 in the full EI-MS scan. The major product ion in Figure 45B confirms the +3 Da mass shift for the dominant product ion at *m/z* 73. This *m/z* 73 product ion also supports the loss of one deuterium in the formation of the product ion from the *m/z* 130 D_4-iminium cation base peak for the D_4-analogue of Compound 2.

A:

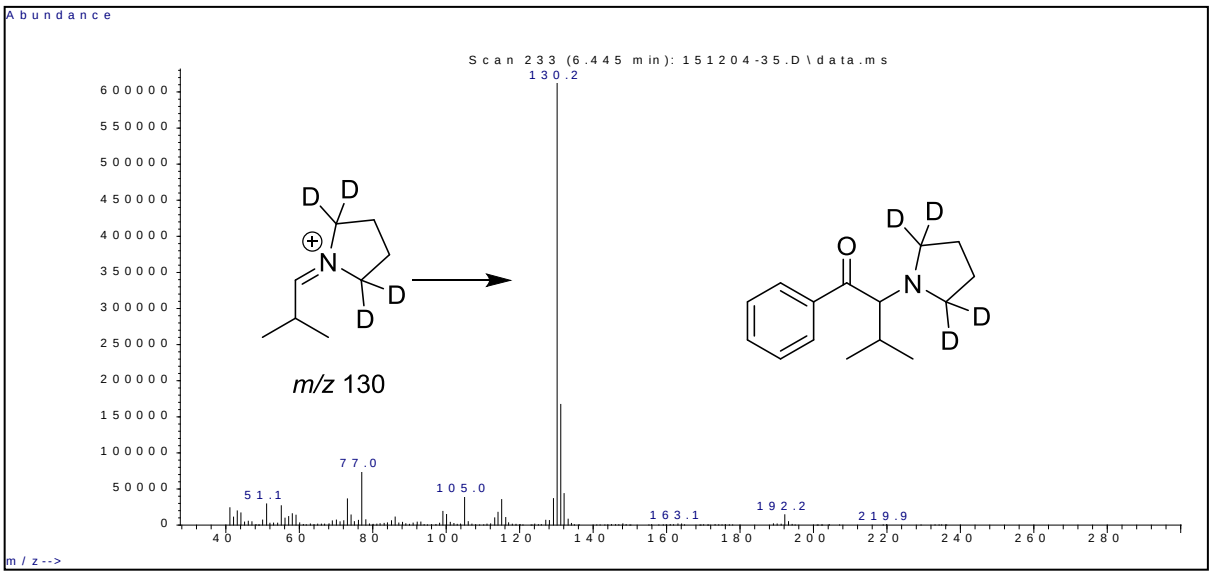

B:

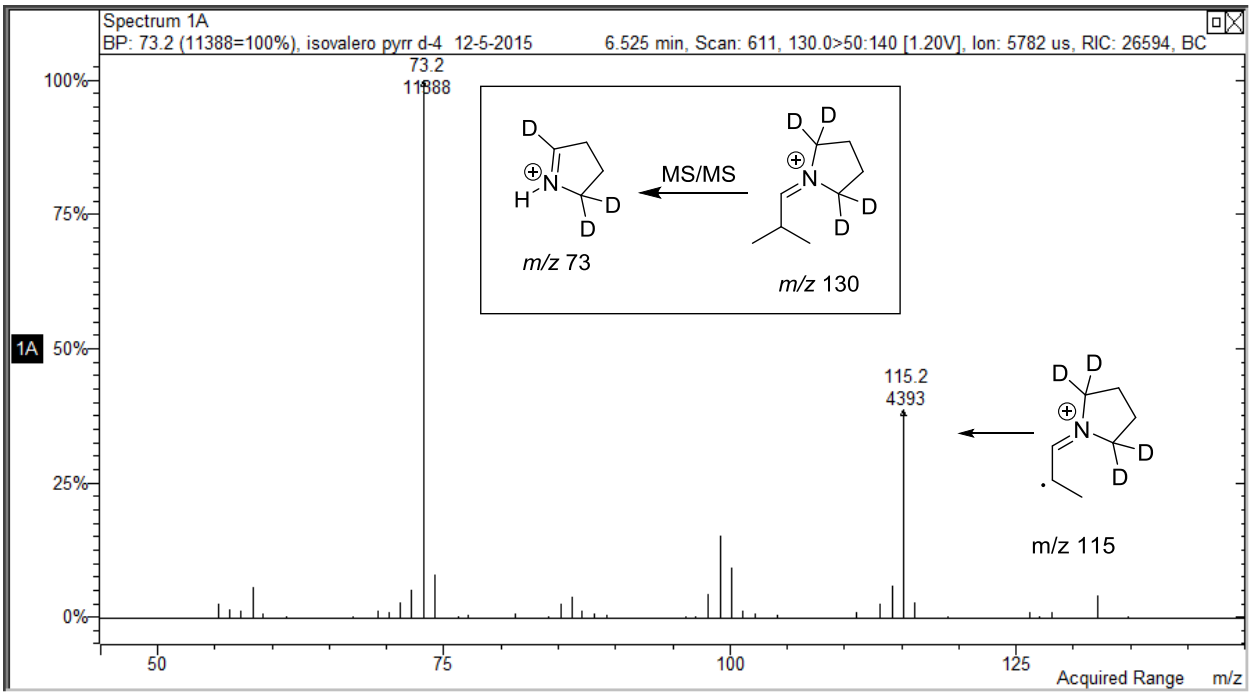

Figure 45. Mass spectra for the 2,2,5,5-D_4-pyrrolidine ring analogue of Compound 2. A: EI-MS full scan; B: product ion spectrum for the *m/z* 130 iminium cation.

Additional support for the mechanism of formation of the product ion from the iminium cation base peak in Compound 2 comes from the spectra in Figure 46. These results show the EI-MS as well as the product ion spectrum for the D_7-isopropyl side-chain analogue of Compound 2. The EI-MS of this compound shows the iminium cation base peak at *m/z* 133, a +7 Da mass shift compared to the *m/z* 126 fragment in the unlabeled compound (Figure 46A). The product ion spectrum for the *m/z* 133 iminium cation (Figure 46B) shows a +1 Da mass shift to *m/z* 71 indicating one deuterium from the D_7-isopropyl group remaining in the product ion fragment. Thus, one deuterium migrated from the isopropyl portion of the side-chain to form the *m/z* 71 major product ion in the spectrum for the D_7-isopropyl side-chain compounds with both the unsubstituted and 3,4-methylenedioxy substituted aromatic ring. The identical EI and product ion

fragments were confirmed by equivalent deuterium labeling experiments in iso-MDPV, Compound 4 (spectra not shown).

A:

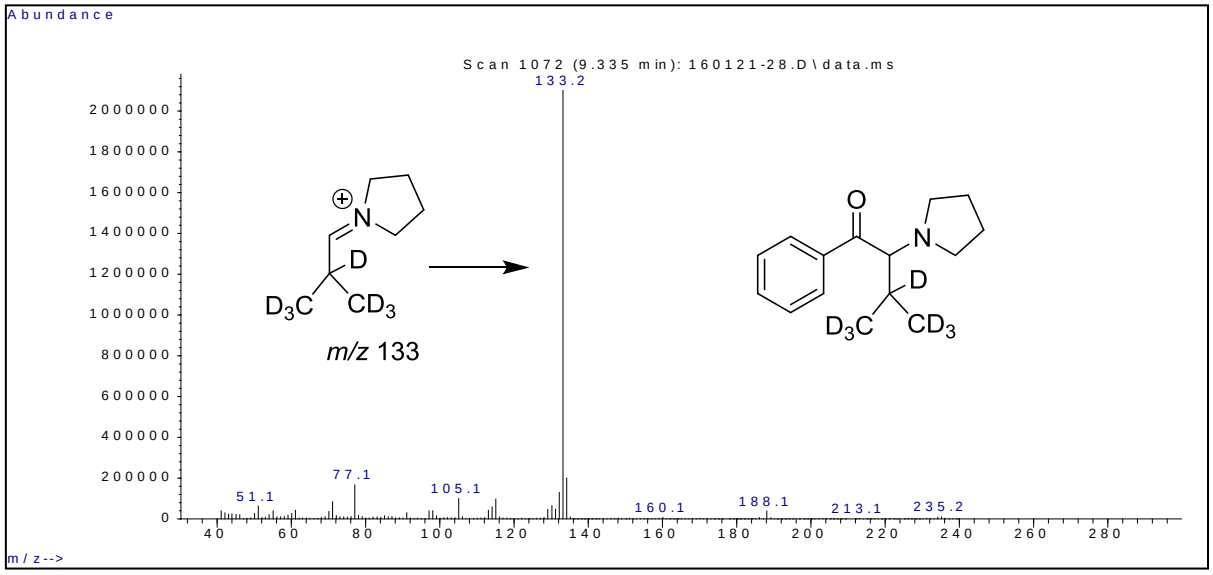

B:

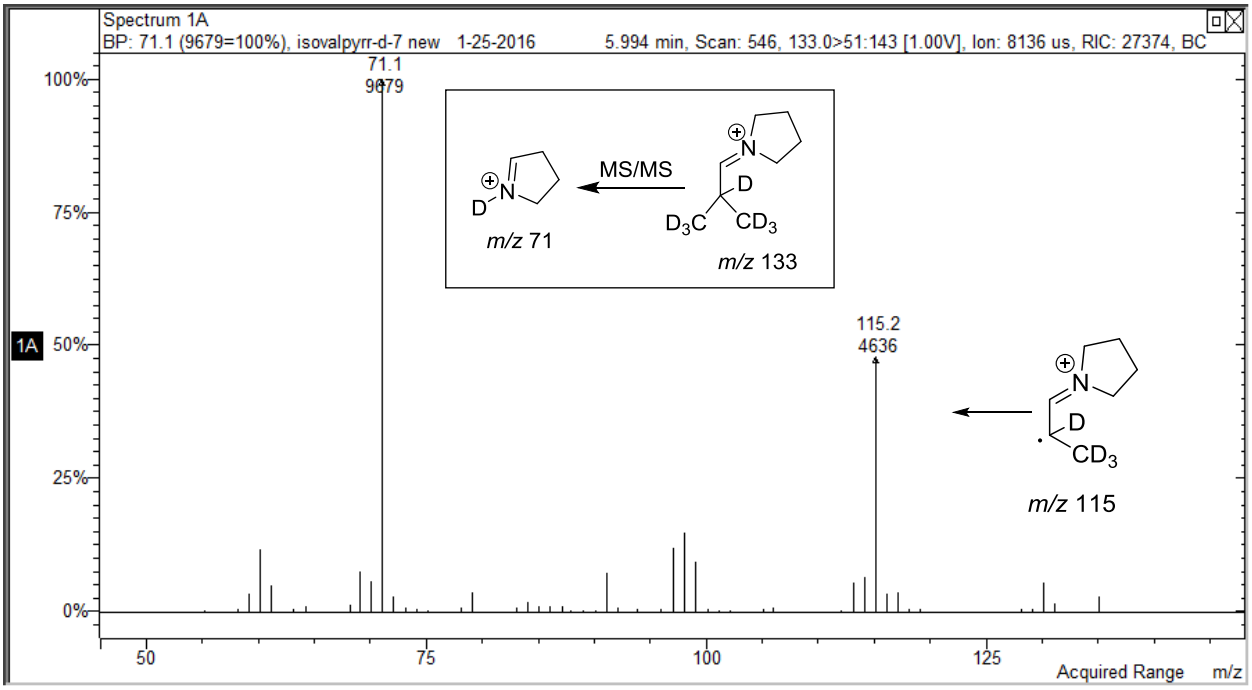

Figure 46. Mass spectra for the D_7-isopropyl side-chain analogue of Compound 2. A: EI-MS full scan; B: product ion spectrum for the *m/z* 133 iminium cation.

2.3.4. Vapor phase infrared spectrophotometry

The vapor phase infrared spectra for the two aromatic ring unsubstituted compounds and the two 3,4-methylenedioxy aromatic ring substituted compounds are shown in Figure 47. Each set of regioisomers displays very similar spectral information. However, the isopropyl side-chain substituted regioisomer has a carbonyl absorption band lower than the *n*-propyl side-chain substituted regioisomer, which could be attributed to the steric effect of the alkyl side-chain on the coplanarity and the resonance between the aromatic ring and the carbonyl functionality. The 3,4-methylenedioxy aromatic ring substituted compounds are characterized by symmetrical doublet absorption bands centered at 1484 cm^{-1} and 1436 cm^{-1} and these have been previuosly discussed in detail in Section 2.1.4.

A:

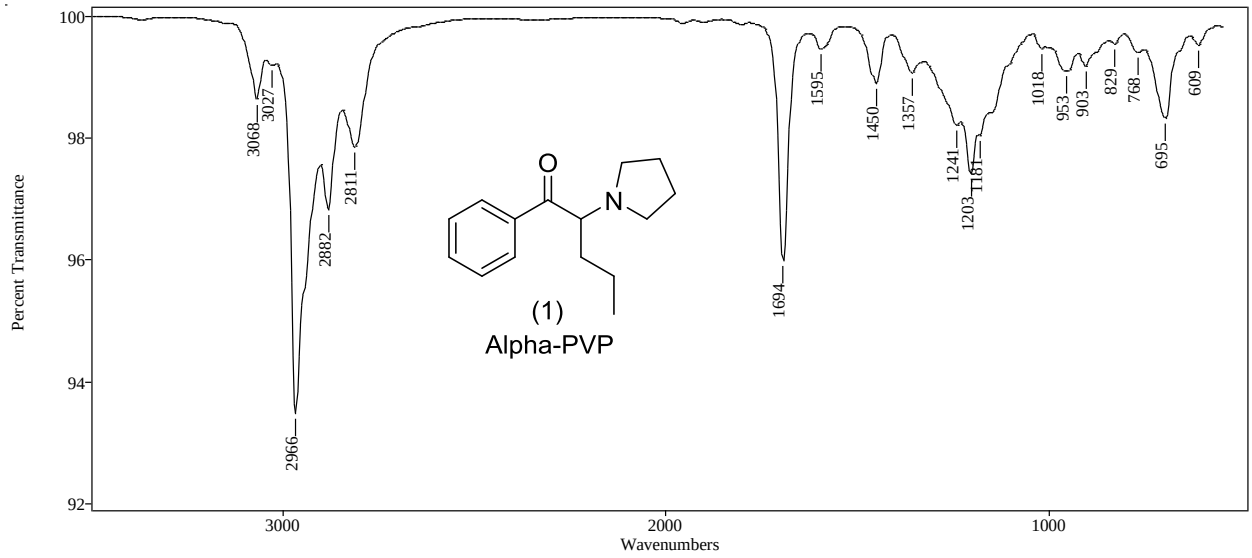
Percent Transmittance
100
98
96
94
92
3068
3027
2966
2882
2811
1694
1595
1450
1357
1241
1203
1181
1018
953
903
829
768
695
609
3000
2000
1000
Wavenumbers
O
N
(1)
Alpha-PVP

B:

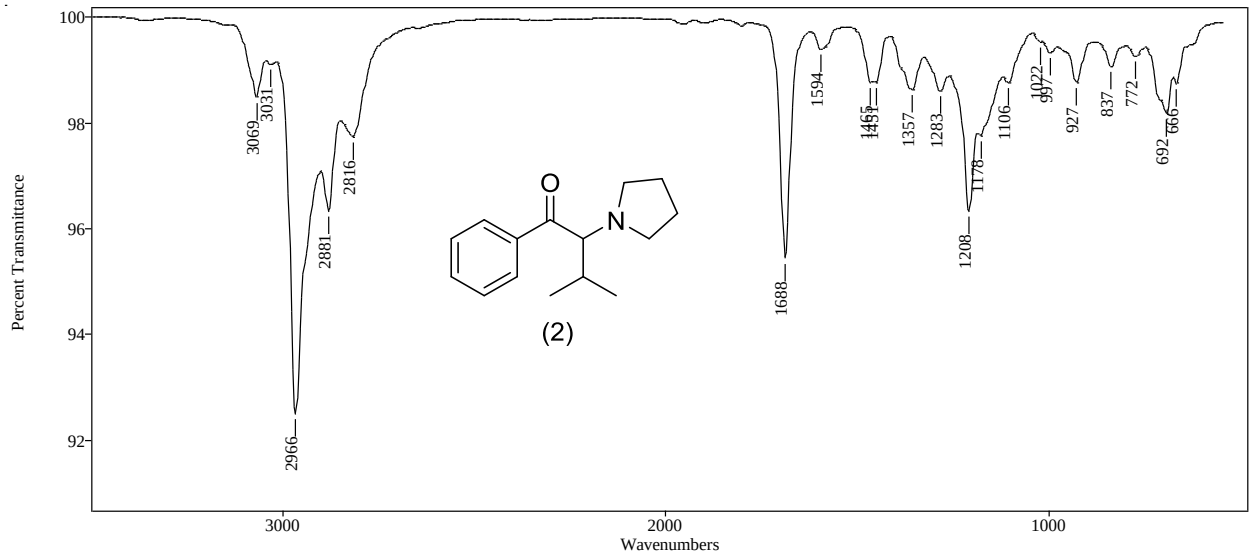
Percent Transmittance
100
98
96
94
92
3069
3031
2966
2881
2816
1688
1594
1455
1431
1357
1283
1208
1178
1106
1022
997
927
837
772
692
666
3000
2000
1000
Wavenumbers
O
N
(2)

C:

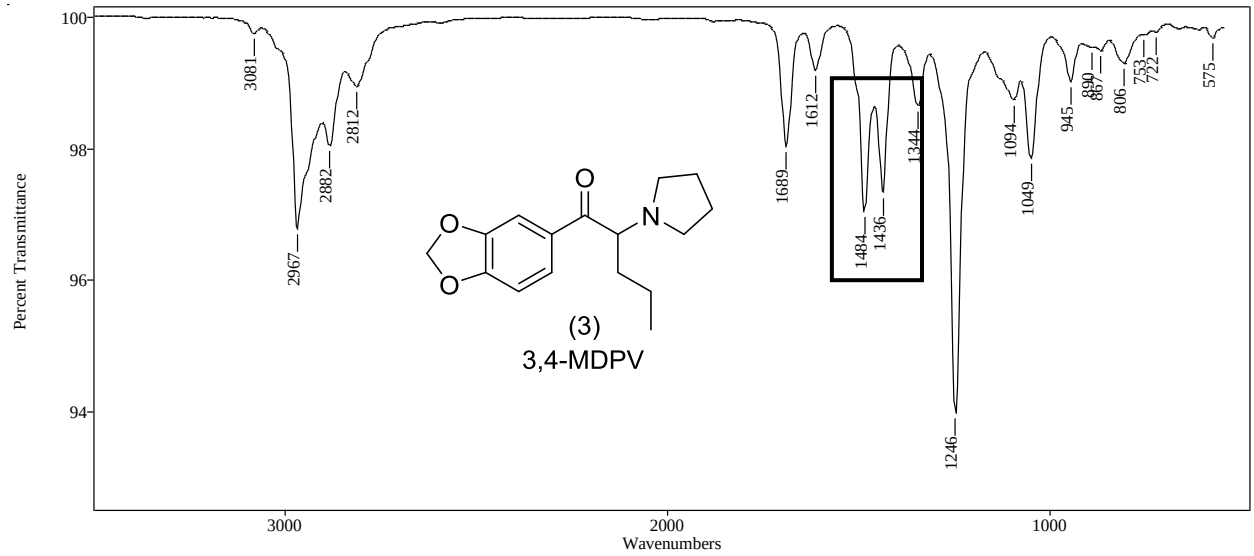

D:

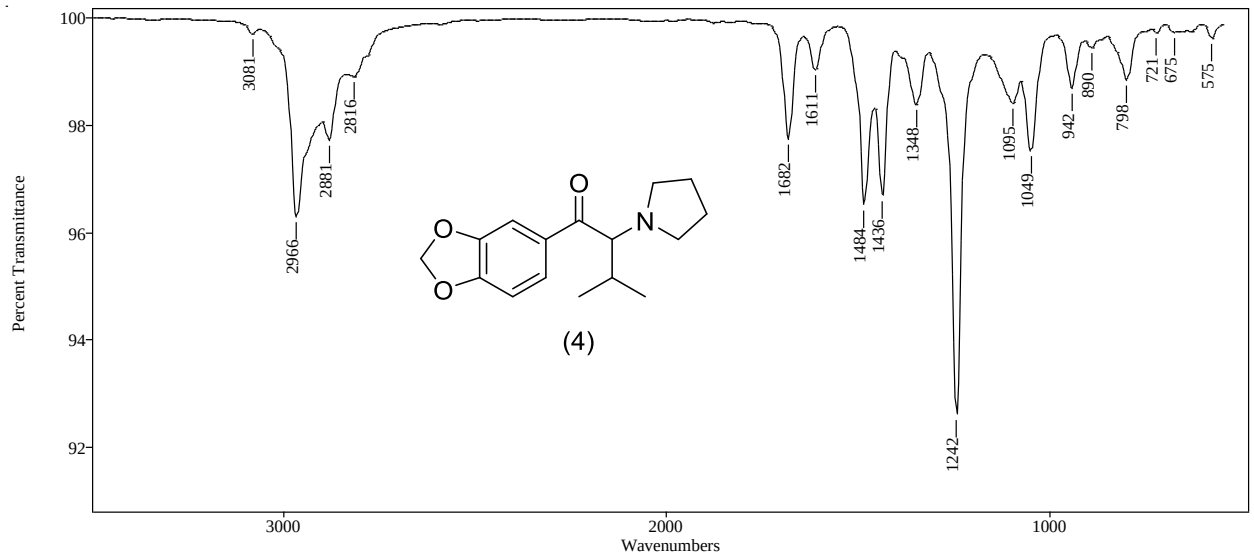

Figure 47. Vapor phase infrared spectra for Compounds 1–4 (Flakka, iso-Flakka, MDPV and iso-MDPV).

2.3.5. Conclusion

Regioisomeric *n*-propyl and isopropyl side-chains in aminoketone cathinone derivatives such as alpha-PVP and MDPV can be differentiated by MS/MS product ion fragmentation. The precursor materials are commercially available for the production of both regioisomeric side-chains. The full EI-MS scan for these compounds yields regioisomeric iminium cations of the same mass at *m/z* 126 for alpha-PVP and MDPV. The major product ion formed from the base peak iminium cation at *m/z* 126 for the *n*-propyl side-chain occurs at *m/z* 84. However, the major product ion for the *m/z* 126 having the isopropyl side-chain occurs at *m/z* 70. Thus, the product ion MS/MS spectrum clearly differentiates these two regioisomeric *m/z* 126 iminium cations. Deuterium labeling of these molecules in the pyrrolidine ring as well as the alkyl side-chain confirmed the mechanistic process for the formation of these major product ions.

The vapor phase infrared spectra for these regioisomeric compounds show very similar bands that cannot distinguish each set of regioisomers. However, the isopropyl side-chain regioisomers have a lower carbonyl absorption bands than the *n*-propyl substituted regioisomers.

2.4. GC–MS, GC–MS/MS and GC–IR differentiations of carbonyl modified analogues of MDPV

A combination of GC–MS, GC–MS/MS and GC–IR techniques can be used to differentiate 2,3- and 3,4-MDPV from the carbonyl modified analogues, aminoalcohols and the corresponding desoxy substituted phenethylamines. These six compounds all yield the identical base peak iminium cation at *m/z* 126 in their electron ionization mass spectrum. The MS/MS evaluation of the iminium cation fragment yields identical major product ions at *m/z* 84. Soft ionization via methanol CI-MS confirms the molecular weight for all these compounds. The only peak in the CI-MS for the aminoketones and the desoxy substituted phenethylamines occurs at $[M+H]^+$. The aminoalcohols show a characteristic fragment ion in CI-MS corresponding to the loss of H_2O from the $[M+H]^+$. Vapor phase infrared spectra (GC–IR) confirm the aromatic ring substitution pattern via unique absorption in the 1450 cm^{-1} range. In all GC separations the 2,3-methylenedioxy substituted isomer elutes before the analogous 3,4-isomer.

2.4.1. Synthesis of the carbonyl modified analogues of MDPV

2.4.1.1. Synthesis of the aminoketones and aminoalcohol derivatives

The desired regioisomeric aminoketones were prepared individually from piperonal and 2,3-methylenedioxybenzaldehyde using the same procedure prescribed previously in Section 2.1.1. The two isomeric aminoalcohol analogues (2,3- and 3,4- substituted isomers) were prepared individually by LAH (lithium aluminum hydride) reduction of 2,3- and 3,4-MDPV, respectively.

2.4.1.2. Synthesis of the desoxy phenethylamine derivatives

The desired regioisomeric desoxy phenethylamines were also prepared individually from piperonal and 2,3-methylenedioxybenzaldehyde using the procedure described in Section 2.2.1.2. The six final products were isolated by solvent extraction and purified by preparative thin layer chromatography (TLC) 20:80 ethyl acetate-petroleum ether using Analtech (Newark, DE) glass backed 20 x 20 cm plates with a 1000 µm layer of silica and an inorganic fluorescent 254 nm indicator. Scheme 18 shown below briefly describes the synthesis of the six target compounds.

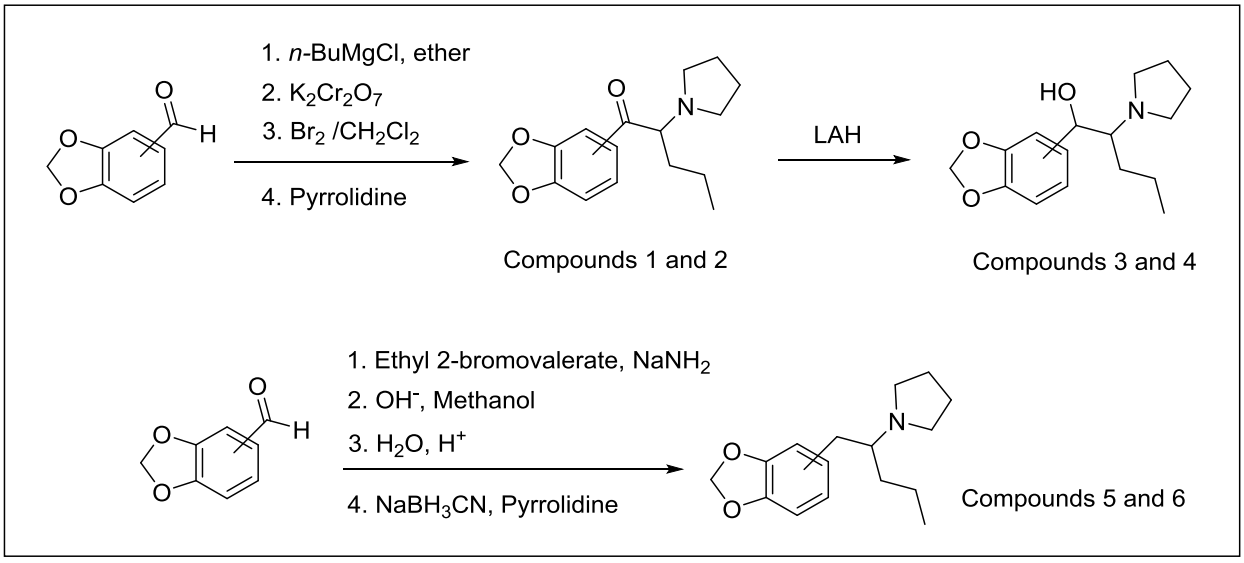

Scheme 18. General synthetic scheme for the six target compounds in this study.

2.4.2. Gas chromatographic separation

The structures for the regioisomeric intermediate ketones and the GC separation of these compounds are shown in Figure 48. These compounds were separated in less than 8.0 minutes using a column (30 m × 0.25 mm i.d.) coated with 0.25 µm film of midpolarity Crossbond® silarylene phase; similar to 50% phenyl, 50% dimethyl polysiloxane (Rxi®-17Sil MS). Both of the 2-pentanone isomers elute before the 1-pentanones and the 2,3-methylenedioxy substituted isomer elutes before the 3,4-isomer for each of the pairs of regioisomeric ketones. The critical peak pair in Figure 48 (Compounds d and a) represent the 3,4-methylenedioxyphenyl-2-pentanone and the 2,3-methylenedioxyphenyl-1-pentanone isomers. These regioisomeric intermediate ketones were separated using a temperature program consisting of an initial hold at 70 °C for 1.0 minute, ramped up to 250 °C at a rate of 30 °C/minute followed by a hold at 250 °C for 15.0 minutes.

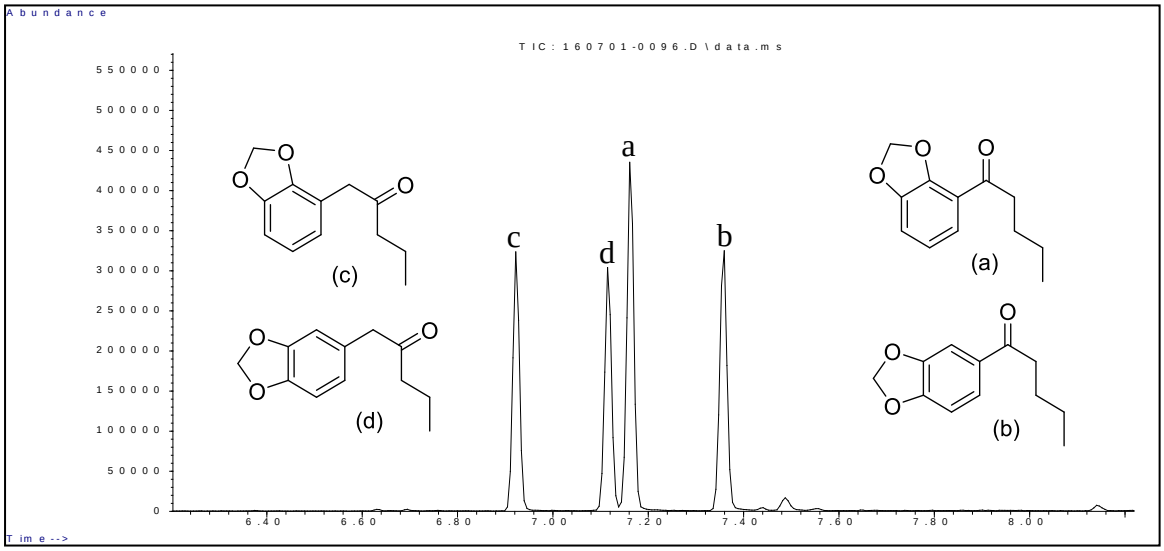

Figure 48. Capillary gas chromatographic separation of the four regioisomeric intermediate ketones on Rxi®-17Sil MS stationary phase. GC–MS System 1.

The GC separation in Figure 49 was obtained on a column (30 m × 0.25 mm i.d.) coated with 0.10 µm film of Crossbond® 100% dimethyl polysiloxane (Rtx®-1) and it shows the resolution of the keto and desoxy analogues in this study (Compounds 1, 2, 5 and 6). The regioisomeric desoxy analogues, Compounds 5 and 6, elute before either of the carbonyl containing 2,3- and 3,4-MDPV isomers (Compounds 1 and 2) on this nonpolar stationary phase. In each case, the 2,3-methylenedioxy substituted isomer eluted well before the 3,4-isomer for each of the equivalent regioisomeric side-chains. The separation of the keto and desoxy analogues was carried out using CI technique (using methanol as the reagent gas). The temperature program applied for CI analysis consisted of an initial hold at 70 °C for 1.0 minute, ramped up to 250 °C at a rate of 30 °C/minute followed by a hold at 250 °C for 15.0 minutes.

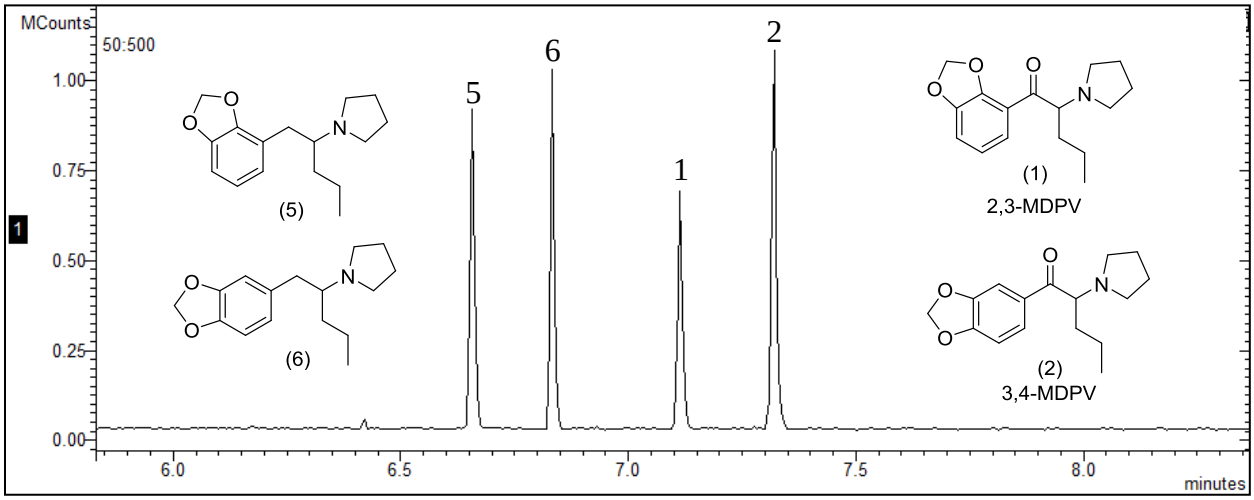

Figure 49. Capillary gas chromatographic separation of the aminoketones and their desoxy analogues on Rtx®-1 stationary phase. GC–MS System 2 (CI technique).

The chromatogram for the separation of the aminoalcohols, Compounds 3 and 4, is shown in Figure 50. This chromatogram shows two major peaks and suggests the possibility of some secondary products of lower relative concentration. These secondary products or broad peaks/baseline in the chromatogram are likely the result of diastereomeric products. These

diastereoisomeric forms of the aminoalcohols are the result of the formation of the second chiral center in these compounds upon reduction of the ketone functionality to the alcohol. The elution order of these aminoalcohols with the methylenedioxy substitution patterns again shows the 2,3-substituted regioisomer eluting before the analogous 3,4-regioisomer. The aminoalcohol regioisomers were separated by using the same column and temperature program applied for the intermediate ketones in Figure 48.

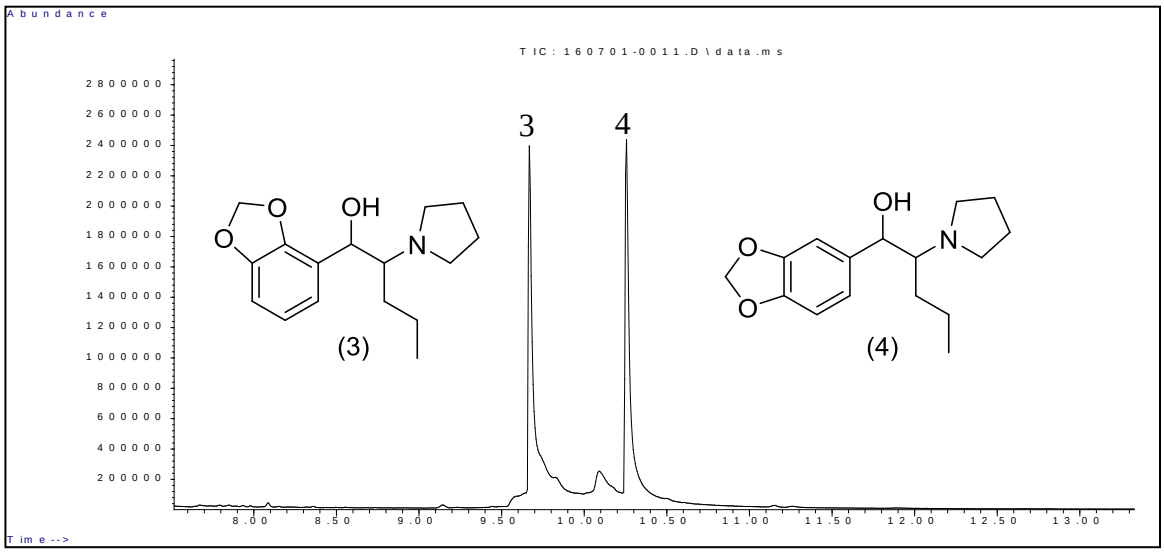

Figure 50. Capillary gas chromatographic separation of the aminoalcohol analogues on Rxi®-17Sil MS stationary phase. GC–MS System 1.

2.4.3. Mass spectral studies (EI-MS, CI-MS and MS/MS)

The GC–CI-MS (using methanol as the reagent gas) and the GC–MS/MS studies for the aminoalcohol derivatives as well as the desoxy phenethylamine derivatives were performed on a column (30 m × 0.25 mm i.d.) coated with 0.10 μm film of Crossbond® 100% dimethyl polysiloxane (Rtx®-1). For MS/MS experiments, the scan type used was the Automated Method Development function (AMD) and the optimum MS/MS excitation amplitude was 1.20 volts. MS/MS analysis was performed using a temperature program consisting of an initial hold at 70 °C

for 1.0 minute, ramped up to 250 °C at a rate of 30 °C/minute followed by a hold at 250 °C for 7.0 minutes. The mass spectral characterization of the 2,3- and 3,4- methylenedioxyphenyl-aminoalcohols is shown in Figures 51 and 52, respectively. Panel A in each figure shows the chemical ionization mass spectra (CI-MS) using methanol vapor as the reagent gas/proton source. This soft ionization technique is a useful method for molecular weight determination for compounds that undergo extensive fragmentation in electron ionization mass spectrometry (EI-MS). The methanol CI spectrum shown in panel A in Figures 51 and 52 indicates significant protonated molecular ion $[M+H]^+$ at *m/z* 278. However, a significant fragment at *m/z* 260 resulting from the loss of 18 Da, water (H_2O), from the $[M+H]^+$ ion is also present in these regioisomeric aminoalcohols. This loss of H_2O in these compounds confirms the presence of the alcohol functionality in Compounds 3 and 4. The fragmentation schemes shown within Figures 51A and 52A indicate the $[M+H]^+$ fragment as the protonated OH group, however the protonated amine is also a reasonable structure for the $[M+H]^+$ ion. The loss of water from the $[M+H]^+$ would follow OH protonation and this elimination process could be assisted by the nitrogen to yield the aziridinium species as well as the benzylic carbocation as shown in the fragment schemes. The spectrum in Figure 52A indicates the fragment resulting from the loss of H_2O is more significant in the 3,4- isomer than in the 2,3 isomer. This could be attributed to the additional stabilization of the protonated hydroxyl group supported by the oxygen at the 2-position of the 2,3-methylenedioxy group in Compound 3. Moreover, the resonance stabilization of the benzylic carbocation by the oxygen at the 4-position of the 3,4-methylenedioxy group in Compound 4.

Panel B in Figures 51 and 52 represents the EI mass spectra for Compounds 3 and 4 illustrating the dominance of the iminium cation fragment and the lack of significant molecular radical cation and molecular weight information. This *m/z* 126 iminium cation is the same base peak as that observed for the aminoketones 2,3- and 3,4-MDPV, Compounds 1 and 2. The EI mass spectra for Compounds 1 and 2 have been described in Section 2.1.3. Thus, these aminoalcohols yield the identical base peak as that observed for the corresponding aminoketone analogues.

The product ion spectra for the *m/z* 126 iminium cation fragments are shown in panel C in Figures 51 and 52 for Compounds 3 and 4, respectively. These identical spectra indicate the major product ion from the iminium cation occurs at *m/z* 84. This loss of 42 Da corresponds to the elimination of a C_3H_6 alkene as expected. Previous studies (described in Sections 2.1.3., 2.2.3. and 2.3.3.) using deuterium labeling experiments identified the *n*-propyl side-chain as the moiety eliminated in the hydrogen rearrangement product ion formation. Other combinations of hydrocarbon side-chain and cyclic tertiary amine rings (described in Section 2.2.3.) can yield regioisomeric forms of the *m/z* 126 iminium cation. However, these other *m/z* 126 base peaks yield unique product ions at other characteristic masses. It is only the *m/z* 126 iminium cation resulting from the combination of the *n*-propyl side-chain and the pyrrolidine ring, which yields the major *m/z* 84 product ion. The *m/z* 126 iminium cations generated from a combination of the appropriate *n*-alkyl side-chain and the 4-membered ring azetidine, 6-membered ring piperidine and 7-membered ring azepane yield major MS/MS product ions at *m/z* 70, 98 and 72, respectively. Thus, a combination of CI-MS, EI-MS and MS/MS spectra provides information to characterize a significant portion of the structural details of the analogues in this study. The CI-MS provides molecular weight information for this series of analogues, which undergo extensive EI

fragmentation. The EI-MS data yield primarily the iminium cation fragment and the MS/MS spectra differentiate the cyclic amine and side-chain portions of the iminium cation.

A:

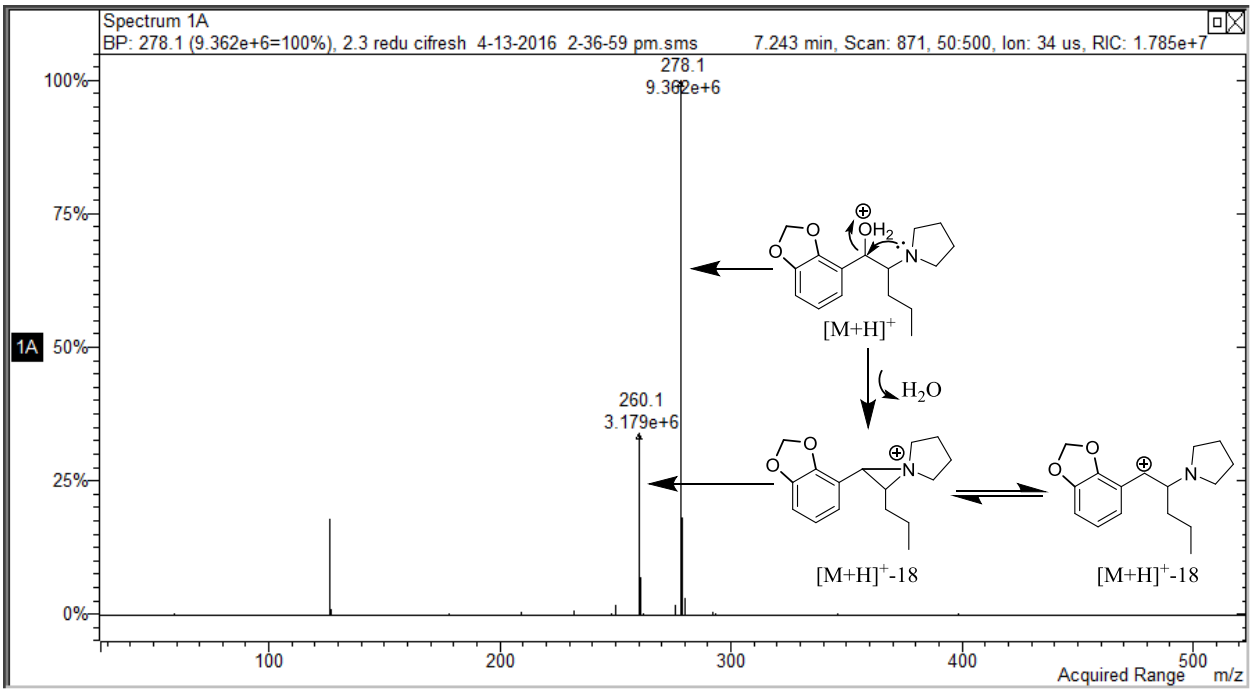

B:

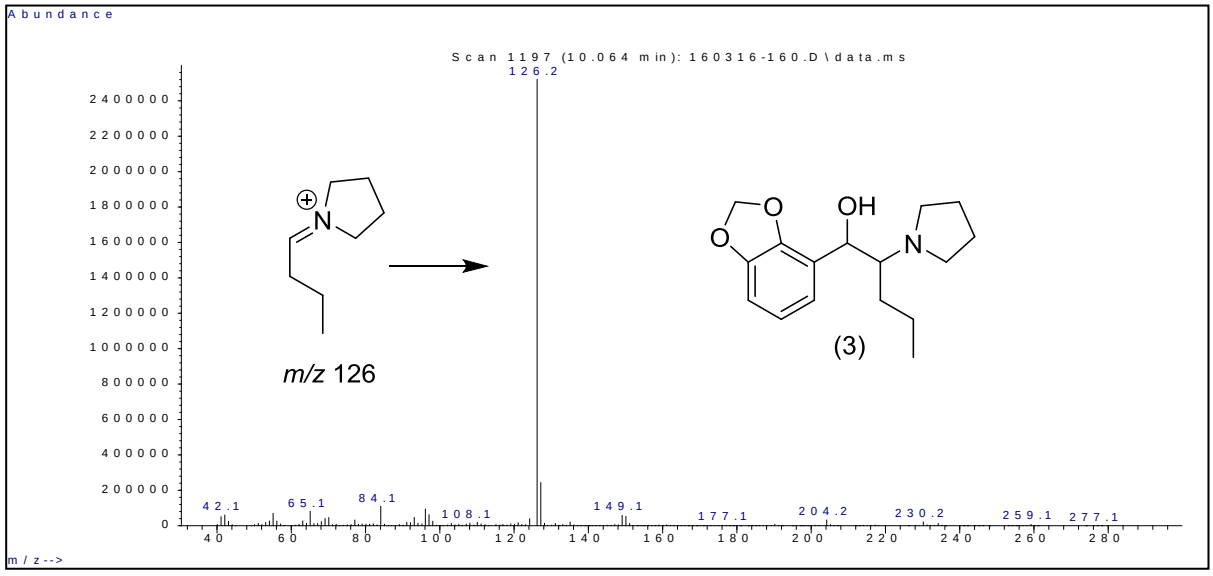

C:

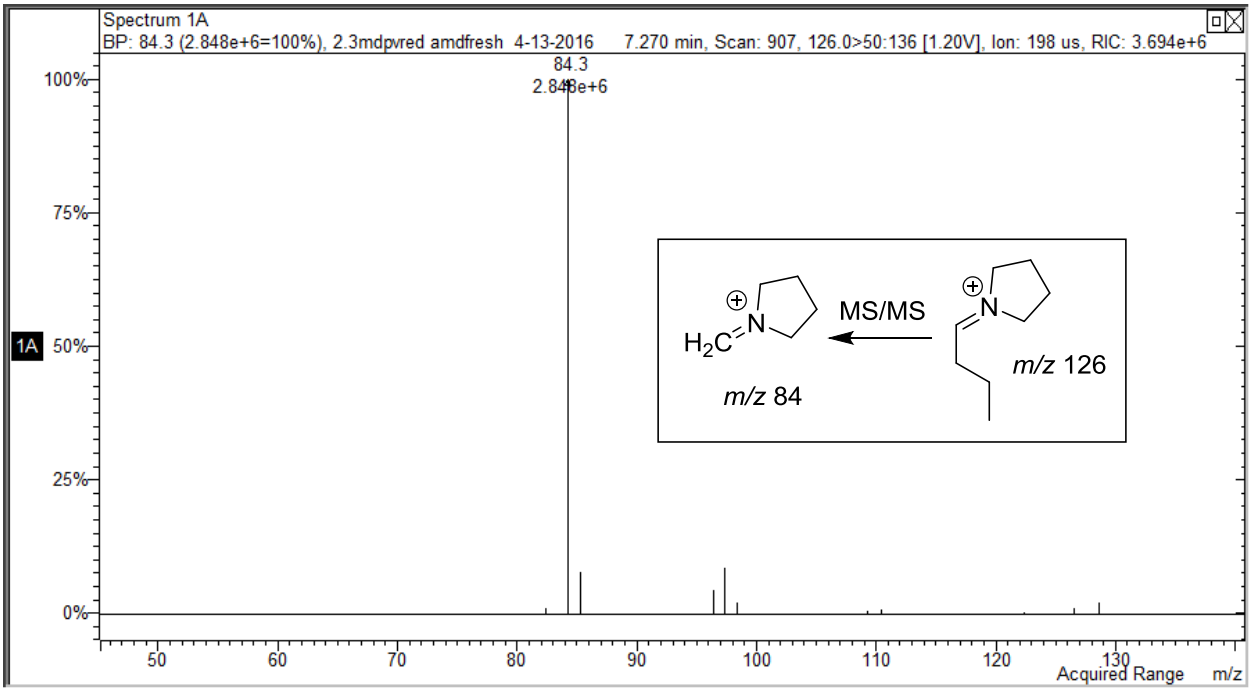

Figure 51. A: CI-MS, B: EI-MS and C: MS/MS spectra for the aminoalcohol analogue of the 2,3-methylenedioxy substituted isomer.

A:

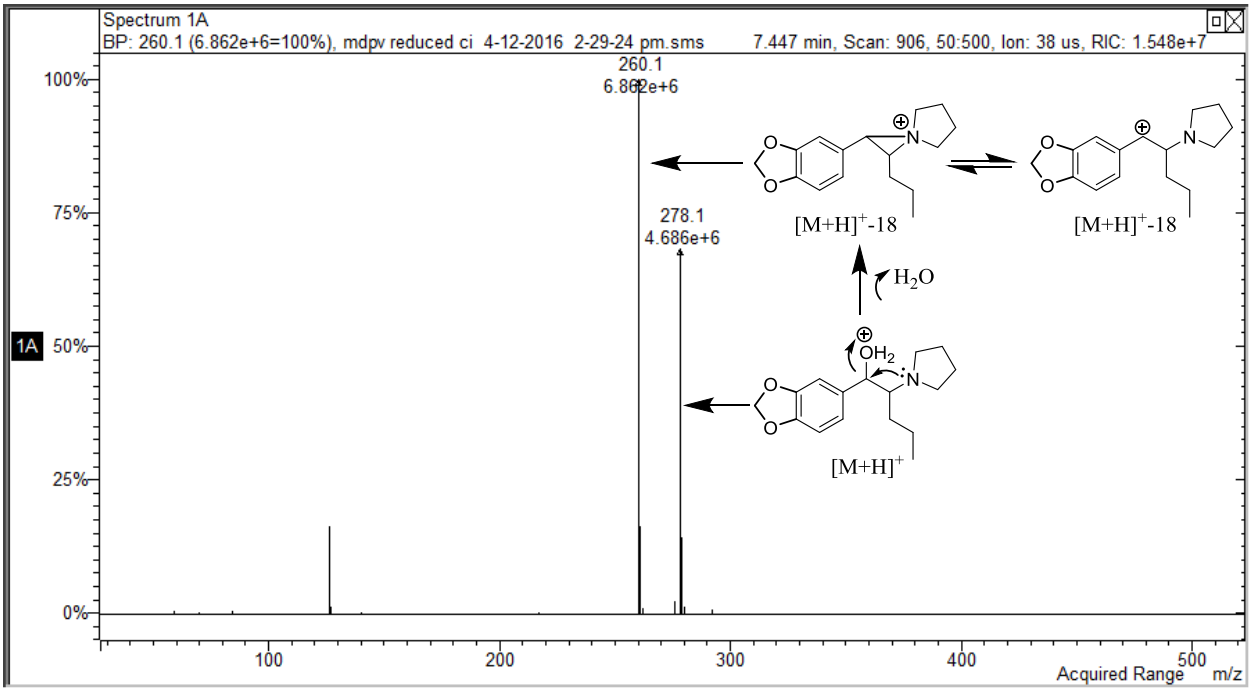

B:

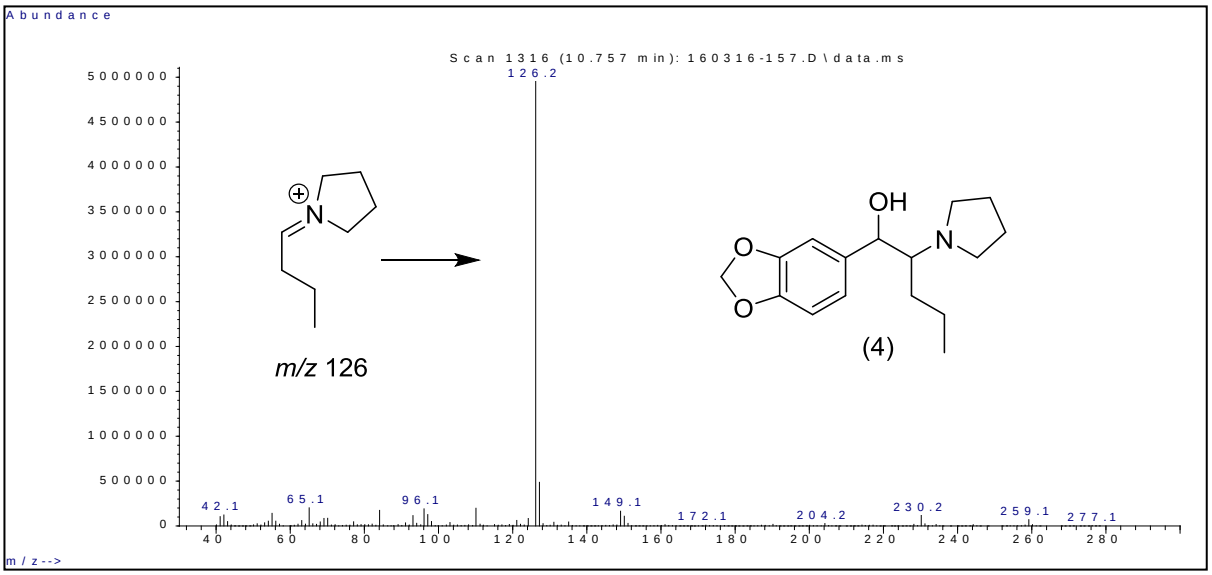

C:

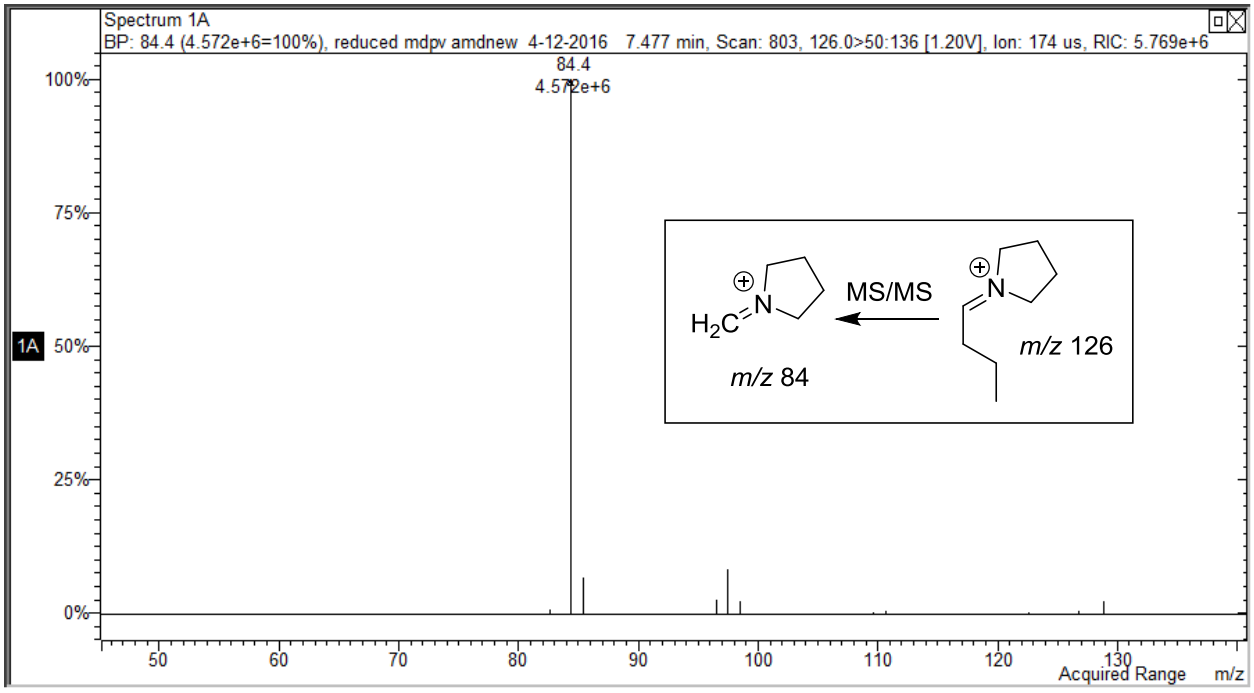

Figure 52. A: CI-MS, B: EI-MS and C: MS/MS spectra for the aminoalcohol analogue of the 3,4-methylenedioxy substituted isomer.

The mass spectral evaluation of the desoxy regioisomers produced the spectra in Figures 53 and 54. Panels A, B and C in these figures display the methanol CI-MS, EI-MS and MS/MS product ion spectra, respectively. The methanol CI data in Figures 53A and 54A allow for the molecular weight confirmation via the $[M+H]^+$ ion of these phenethylamine-type compounds. However, no other structural information can be obtained from these CI spectra. The remaining spectra in panels B and C in Figures 53 and 54 also reveal identical analytical results for these regioisomeric desoxy phenethylamines. The EI spectra in panel B show the identical iminium cations at *m/z* 126 and panel C indicates equivalent MS/MS product ions at *m/z* 84. The mass spectral data for the desoxy analogue of MDPV (Compound 6) have been described in detail in Section 2.2.3.

A:

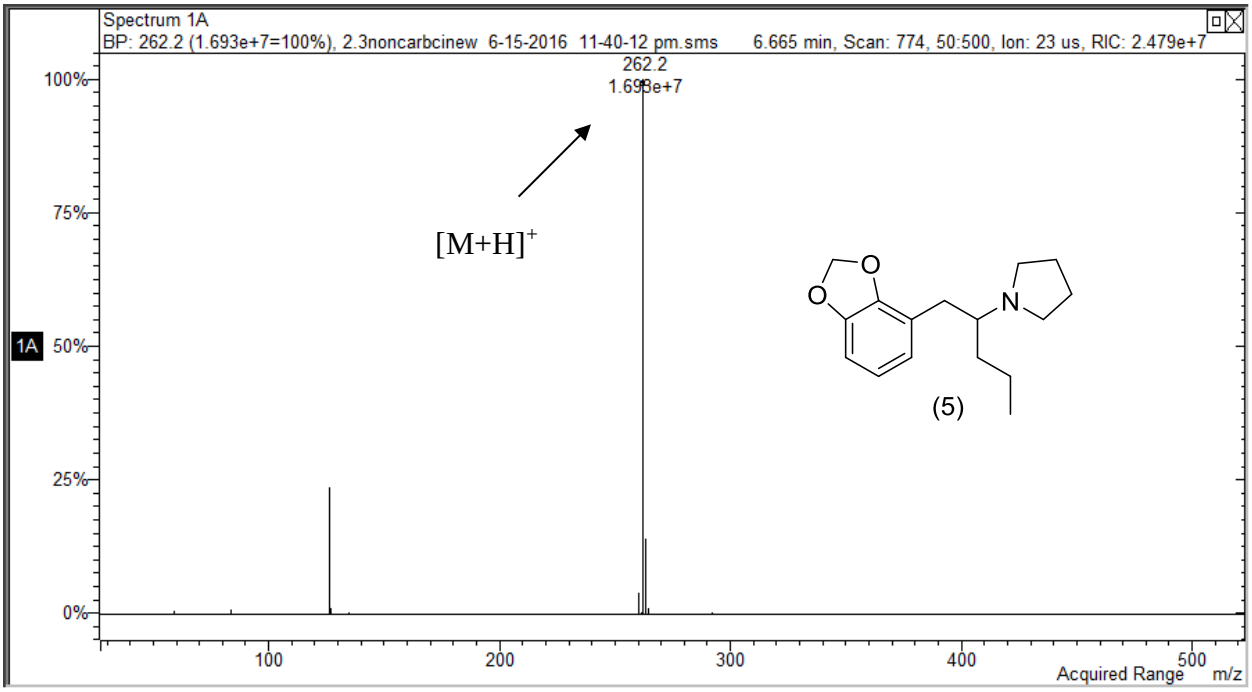

B:

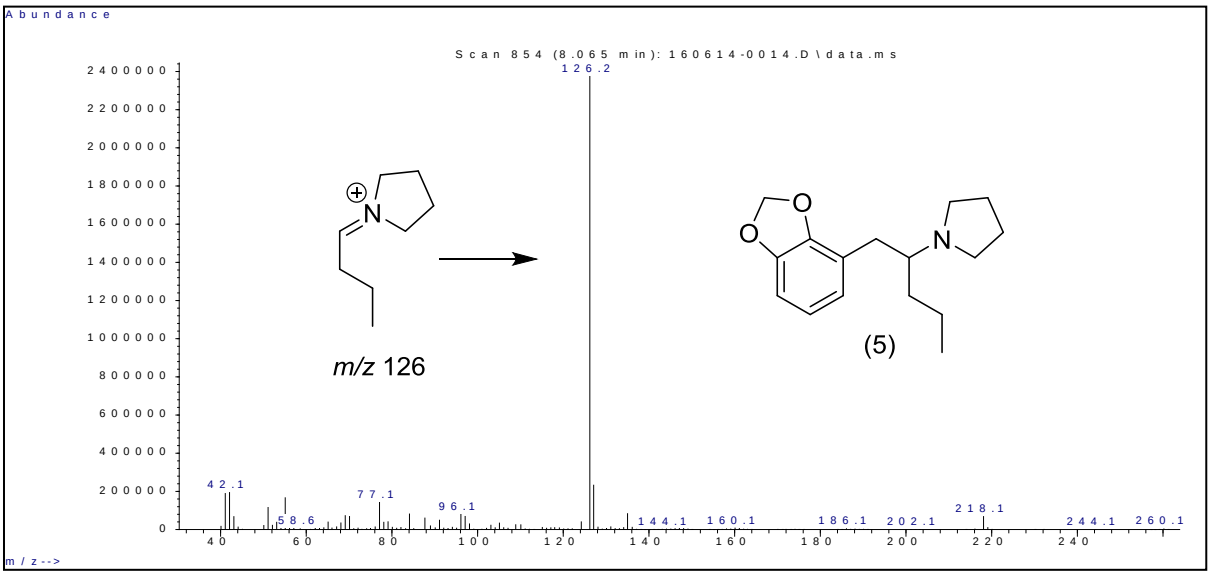

C:

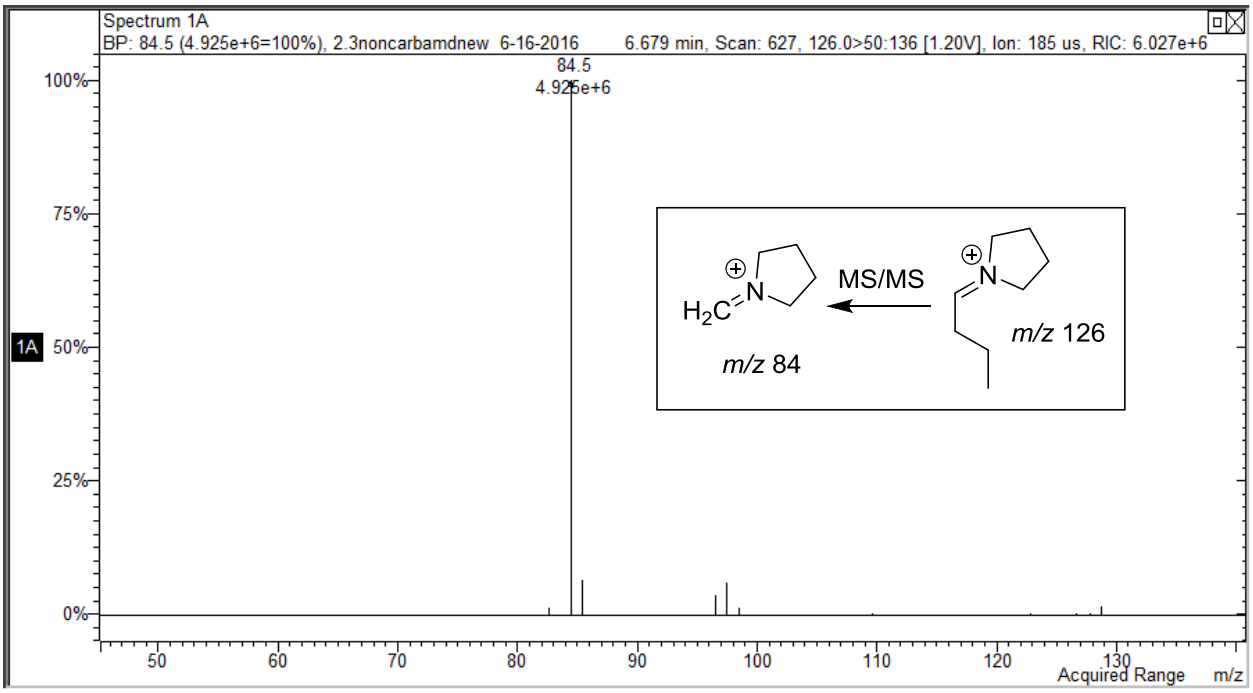

Figure 53. CI-MS, B: EI-MS and C: MS/MS spectra for the desoxy analogue of the 2,3-methylenedioxy substituted isomer.

A:

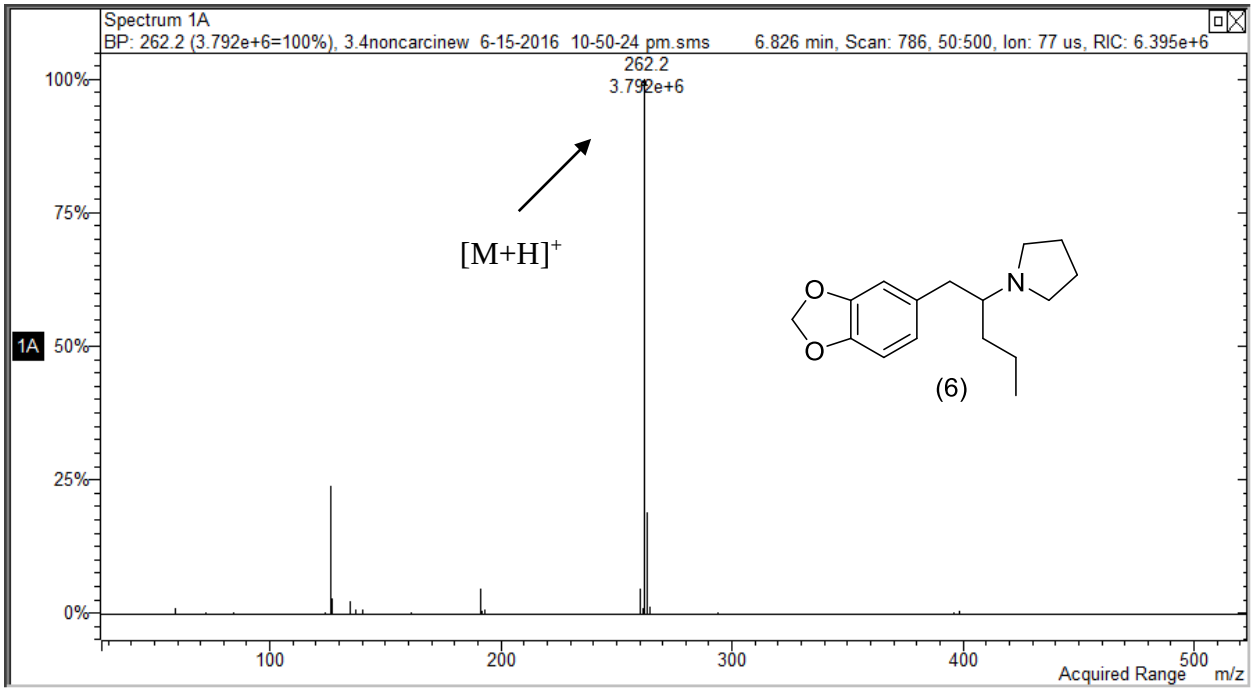
Spectrum 1A
BP: 262.2 (3.792e+6=100%), 3.4noncarcinew 6-15-2016 10-50-24 pm.sms
6.826 min, Scan: 786, 50:500, Ion: 77 us, RIC: 6.395e+6
262.2
3.792e+6
100%
75%
50%
25%
0%
1A
[M+H]+
(6)
100
200
300
400
500
Acquired Range
m/z

B:

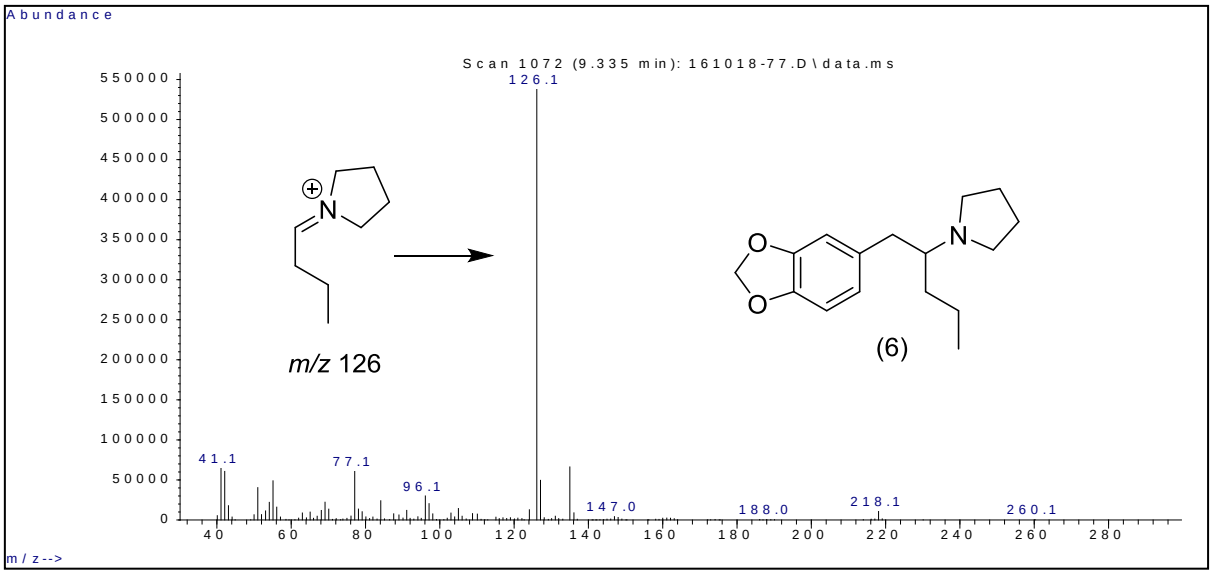
Abundance
Scan 1072 (9.335 min): 161018-77.D\data.ms
126.1
550000
500000
450000
400000
350000
300000
250000
200000
150000
100000
50000
0
41.1
77.1
96.1
147.0
188.0
218.1
260.1
40
60
80
100
120
140
160
180
200
220
240
260
280
m/z-->
m/z 126
(6)

C:

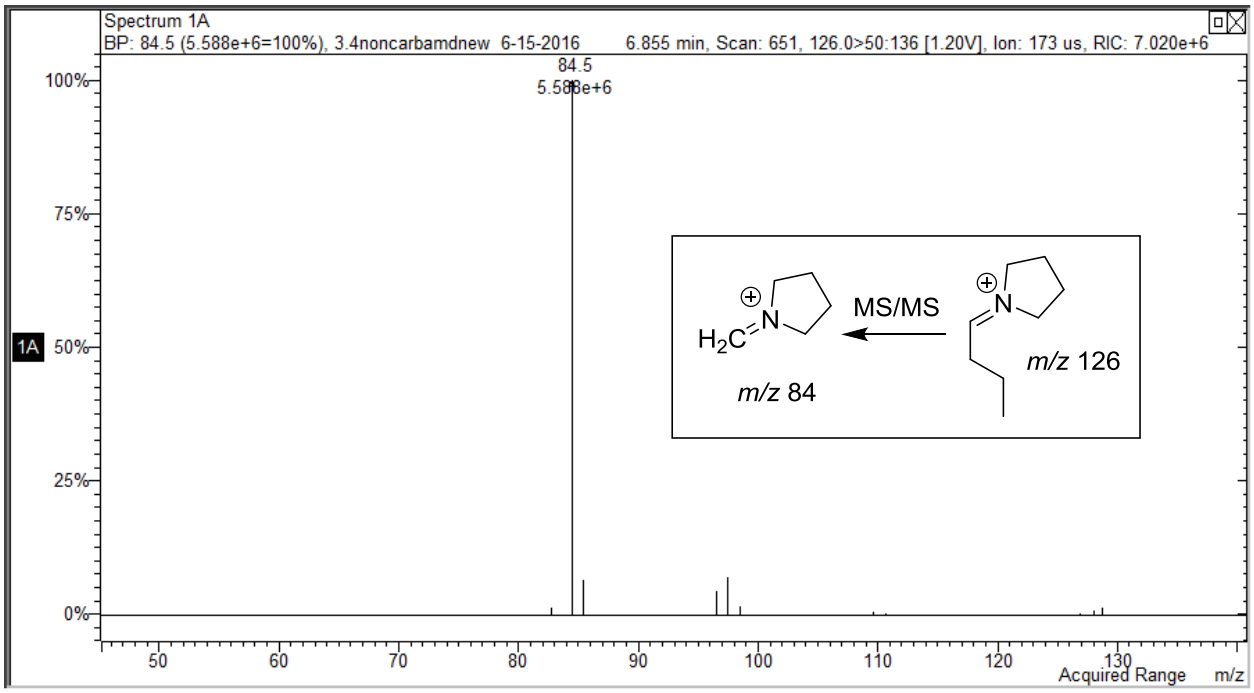

Figure 54. A: CI-MS, B: EI-MS and C: MS/MS spectra for the desoxy analogue of the 3,4-methylenedioxy substituted isomer.

2.4.4. Vapor phase infrared spectrophotometry

The vapor phase infrared spectra in Figure 55 allow for the differentiation of the relative position of substitution of the methylenedioxy group in the aminoalcohols (Compounds 3 and 4). These spectra were generated in GC–IR experiments and the spectra were generated as the chromatography peak eluted from the capillary column. The aromatic ether region of the spectra shows a strong single absorption band for the 2,3-methylenedioxyphenyl substituted isomer at 1456 cm^{-1} in Figure 55A. However, this region of the vapor phase IR spectrum for Compound 4 (the 3,4-methylenedioxyphenyl substituted isomer) shows an unsymmetrical doublet absorption pattern at 1487 cm^{-1} and 1442 cm^{-1} in Figure 55B. This absorption pattern is consistent with the symmetrical doublet absorption pattern observed for the regioisomeric aminoketones, Compounds 1 and 2 (see Section 2.1.4.). The spectra in Figure 55 further indicate a weak and broad absorption

band above 3400 cm^{-1} indicating the presence of the hydroxyl group in these two regioisomeric compounds.

A:

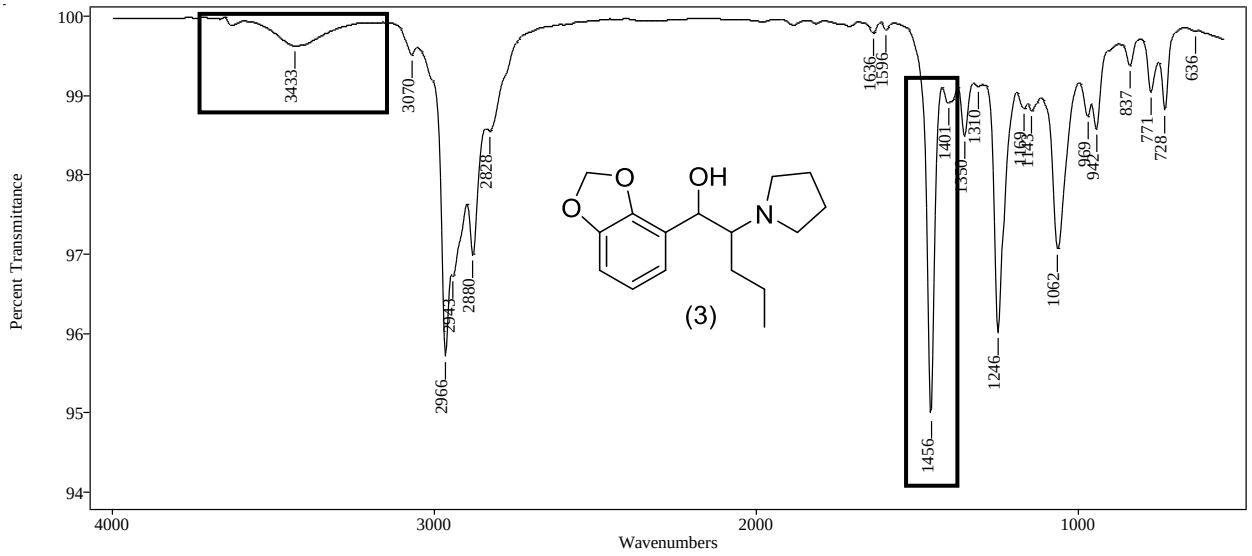

B:

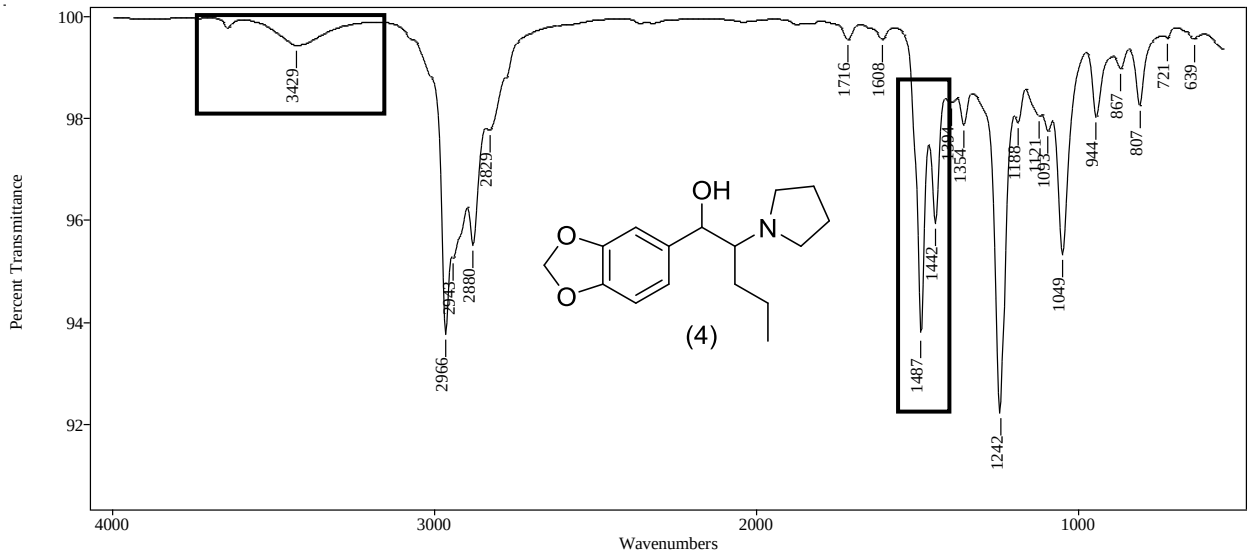

Figure 55. Vapor phase IR spectra for the aminoalcohol analogues (Compounds 3 and 4).

In addition to the chromatographic resolution of Compounds 5 and 6 shown in Figure 49, the vapor phase infrared spectra in Figure 56 differentiate these regioisomeric desoxy substituted phenethylamine analogues. The single strong absorption banad at 1456 cm^{-1} in Figure 56A for

Compound 5 is consistent with the 2,3-methylenedioxy substitution pattern while the unsymmetrical doublet absorption bands at 1489 cm^{-1} and 1442 cm^{-1} in Figure 56B for Compound 6 indicate the 3,4-methylenedioxy substitution pattern. The same absorption patterns (spectra not shown) were also observed for the intermediate ketones, Compounds c and d (see Figure 48 for structures).

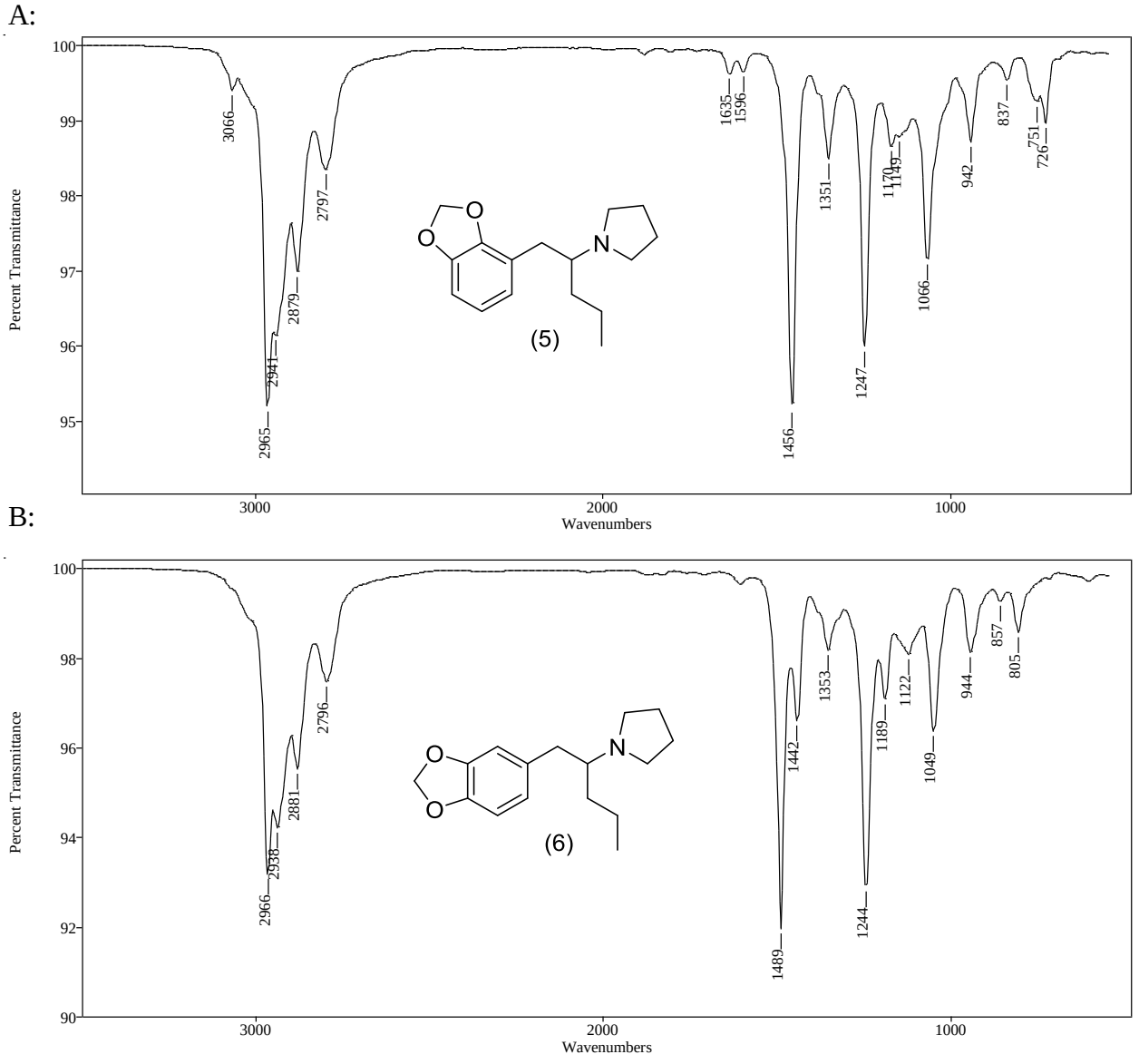

Figure 56. Vapor phase IR spectra for the desoxy phenethylamine analogues (Compounds 5 and 6).

2.4.5. Conclusion

Carbonyl modifications in aminoketones such as MDPV yield the corresponding aminoalcohols and the desoxy substituted phenethylamine analogues. Multiple confirmation methods were necessary for the specific identification of one compound from this set of closely related structural isomers. Extensive fragmentation in the EI-MS yields the identical iminium cation base peak at *m/z* 126 for MDPV as well as the carbonyl modified analogues. The CI-MS provides molecular weight information and one characteristic fragment for the aminoalcohols resulting from loss of water (H_2O) from the protonated molecular ion $[M+H]^+$. The MS/MS product ion spectra provide data to characterize the side-chain and cyclic tertiary amine portions of the iminium cation. The vapor phase infrared spectra differentiate the 2,3- and 3,4-methylenedioxy substitution pattern based on absorption bands in the 1450 cm^{-1} range. The aminoketones and desoxy substituted phenethylamine regioisomers were separated in capillary gas chromatography experiments with the aminoketones showing higher retention times. The two regioisomeric aminoalcohols each likely exist as a set of diastereomers as reflected by the broad chromatography peaks.

2.5. Differentiation of homologous and regioisomeric methoxy-cathinone derivatives by GC–MS, GC–MS/MS and GC–IR

A combination of GC–MS, GC–MS/MS and GC–IR techniques can be used to differentiate the nine methoxy cathinone derivatives related to the designer drug MDPV. Nine homologous and regioisomeric methoxyphenyl-aminoketone cathinone derivatives were prepared from the three commercially available 2-, 3- and 4-methoxybenzaldehydes. The gas chromatographic separation of the nine intermediate methoxyphenones was achieved on a 100% dimethyl polysiloxane (Rtx®-1) stationary phase and the regioisomeric aminoketones were resolved on a 5% diphenyl, 95% dimethyl polysiloxane (Rtx®-5) stationary phase. The chemical ionization mass spectra (CI-MS) show only one major peak occurring at the mass of the protonated molecular ion $[M+1]^+$ while the EI-MS spectra display primarily the iminium cation fragment. The MS/MS product ion spectra for the three homologous iminium cations yield a homologous series of ions representing the loss of 42 Da from the parent species. MS/MS experiments confirmed the loss of 42 Da occurring via pyrrolidine ring fragmentation for iminium cations having the methyl and ethyl side-chains and via side-chain fragmentation for the *n*-propyl side-chain. The vapor phase infrared spectra in the range of 1300 to 1150 cm^{-1} show unique and characteristic absorption pattern for each of the three regioisomeric methoxy-group substitution patterns.

2.5.1. Synthesis of the homologous and regioisomeric methoxy-cathinone derivatives

The desired regioisomeric aminoketones were prepared individually from the three commercially available 2-, 3- and 4-methoxybenzaldehydes using the same procedure (see Scheme 19) prescribed previously in Section 2.1.1. The final nine compounds were purified using acid base extraction to yield the free bases.

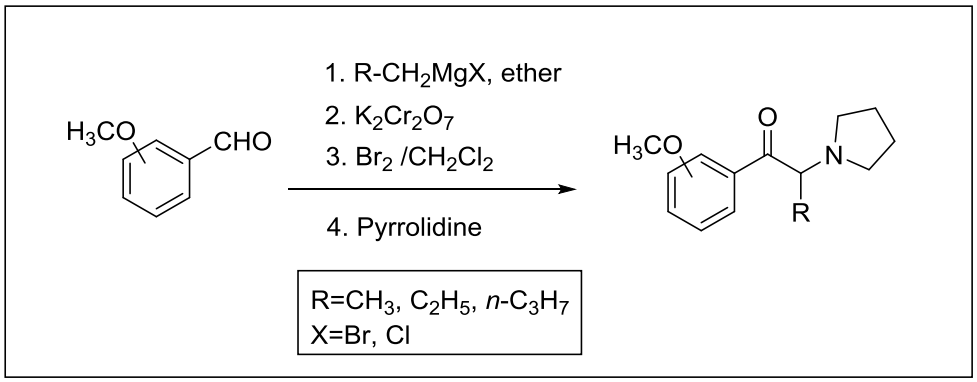

Scheme 19. General synthetic scheme for the nine target compounds in this study.

2.5.2. Gas chromatographic separation

The gas chromatographic separation of the nine intermediate methoxyphenones is shown in Figure 57. The elution order of these regioisomeric and homologous ketones is related to the aromatic ring substitution pattern and the alkyl side-chain group. The two carbon alkyl side-chain regioisomers (a–c) elute first and the 2-methoxy regioisomer elutes before the 3-methoxy isomer followed by the 4-methoxypropiophenone. The elution sequence is repeated for the three carbon alkyl side-chain set of ketones (d–f) and again with the final set of four carbon side-chain methoxyphenones (g–i). These compounds were resolved using a 30-meter capillary column containing a 0.10 µm film of Crossbond® 100% dimethyl polysiloxane, Rtx®-1, a nonpolar stationary phase. The least resolved peak pair in Figure 57 is peaks c and d and these peaks represent the 4-methoxypropiophenone and the 2-methoxybutyrophenone, respectively. The

additional closely eluting peaks (f and g) represent the 4-methoxybutyrophenone and the 2-methoxyvalerophenone side-chain homologue. These regioisomeric intermediate ketones were separated using a temperature program consisting of an initial hold at 70 °C for 1.0 minute, ramped up to 150 °C at a rate of 7.5 °C/minute followed by a hold at 150 °C for 2.0 minutes, then ramped up to 250 °C at a rate of 10 °C/minute followed by a hold at 250 °C for 47.0 minutes.

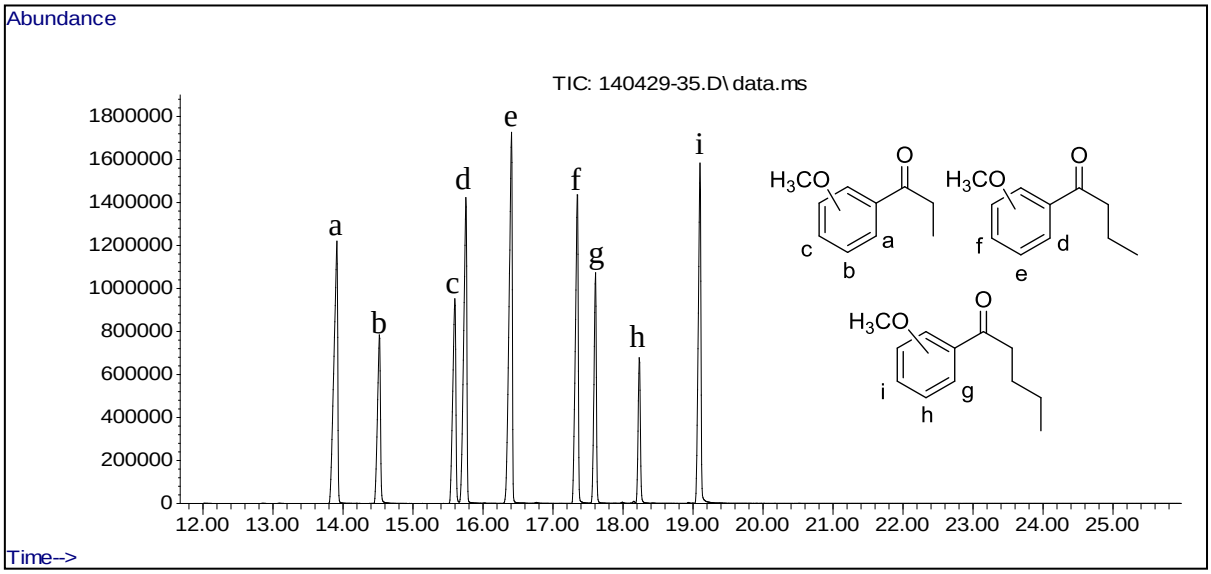

Figure 57. Capillary gas chromatographic separation of the nine regioisomeric and homologous monomethoxyphenyl-ketones on Rtx®-1 stationary phase. GC–MS System 1.

The chromatograms in Figure 58A–C show the GC separation of the regioisomeric aminoketones in this study. The elution order for the regioisomeric methoxy groups is the same as that seen for the intermediate ketones. The 2-methoxy isomers elutes first followed by the 3-isomer with the 4-methoxy isomer displaying the highest degree of retention. Figure 58A shows the methyl side-chain set of regioisomers (1–3); 58B the ethyl (4–6) and 58C the *n*-propyl-side chain regioisomers (7–9). These separations were obtained on a column (30 m × 0.25 mm i.d.) coated with 0.10 µm film of Crossbond® 5% diphenyl, 95% dimethyl polysiloxane (Rtx®-5) and adequate resolution was achieved for each set of regioisomeric compounds having equivalent EI mass

spectra. These regioisomeric sets of compounds were separated using a temperature program consisting of an initial hold at 70 °C for 1.0 minute, ramped up to 250 °C at a rate of 30 °C/minute followed by a hold at 250 °C for 15.0 minutes.

A:

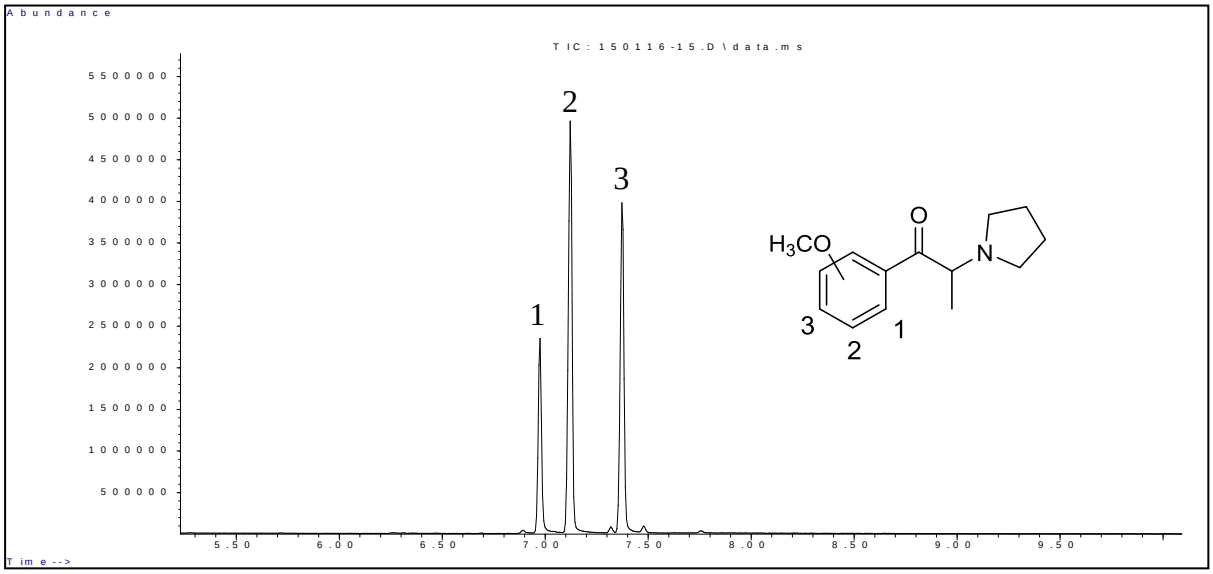

B:

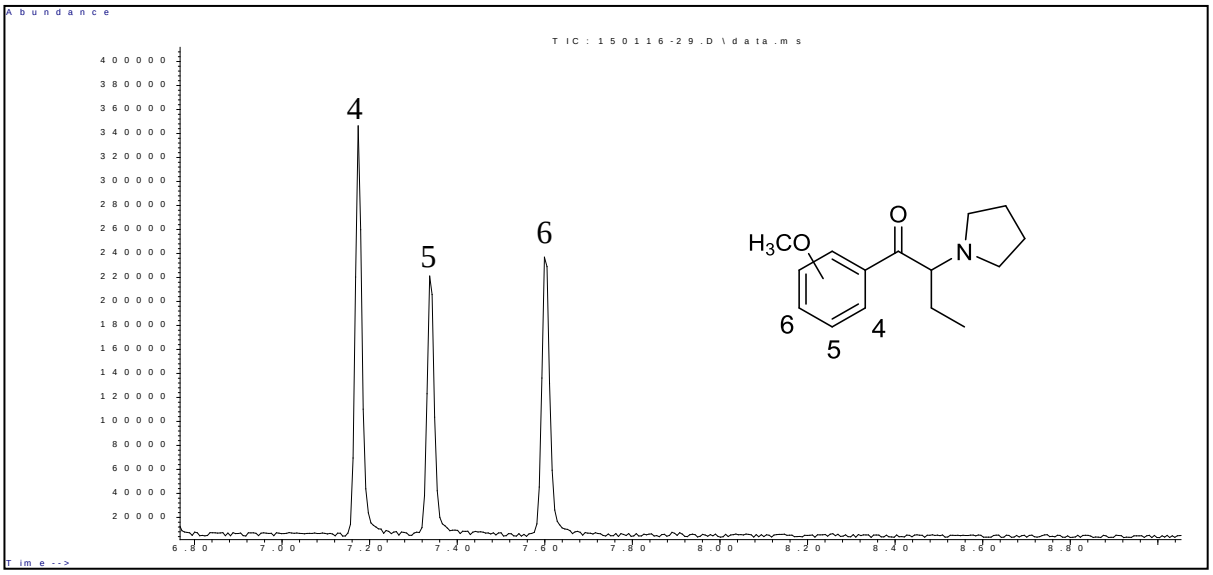

C:

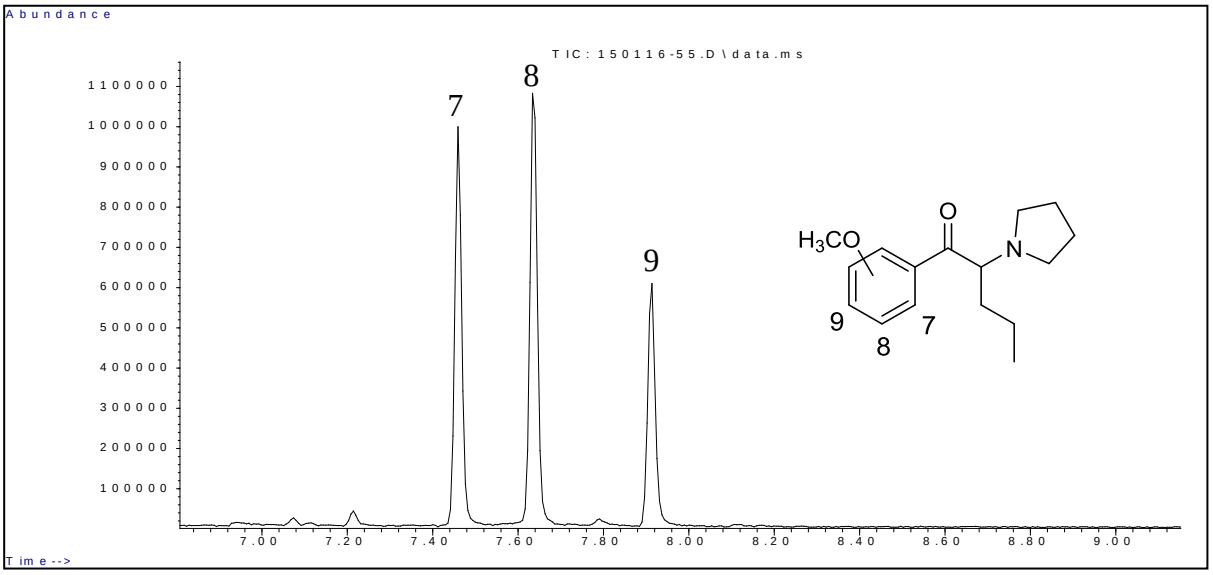

Figure 58. GC separation of the nine compounds in this study. A: Compounds 1, 2 and 3; B: Compounds 4, 5 and 6; C: Compounds 7, 8 and 9. Rtx®-5 stationary phase. GC–MS System 1.

2.5.3. Mass spectral studies (EI-MS, CI-MS and MS/MS)

The electron ionization mass spectra (EI-MS) for a representative selection of three of the intermediate ketones are shown in Figure 59. The base peak in the spectra for these ketones occurs at *m/z* 135 for the methoxybenzoyl $(CH_3OC_6H_4CO)^+$ cation. Additionally, the higher alkyl side-chain homologues show the expected hydrogen rearrangement product at *m/z* 150.

A:

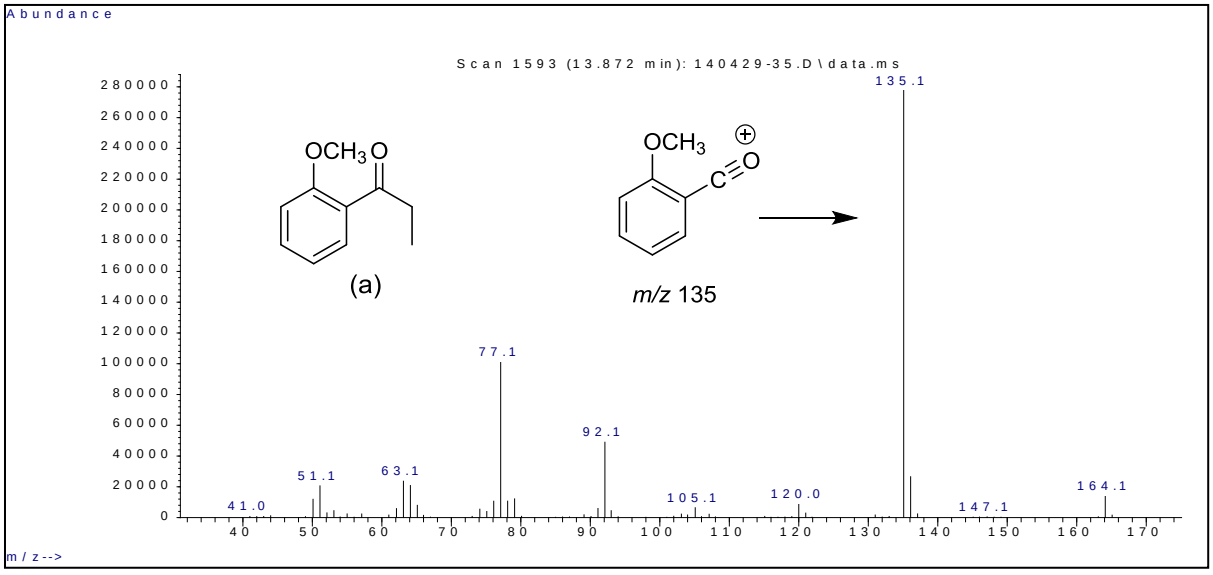
Abundance
Scan 1593 (13.872 min): 140429-35.D\data.ms
OCH3 O
(a)
OCH3
O
m/z 135
135.1
77.1
92.1
51.1
63.1
41.0
105.1
120.0
147.1
164.1
m/z-->

B:

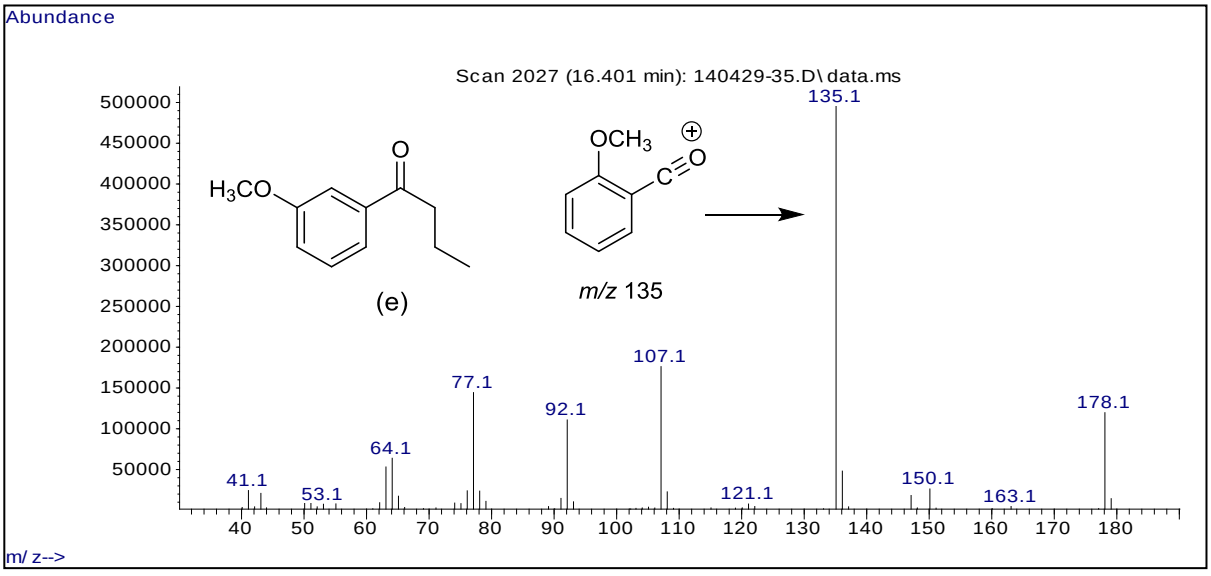
Abundance
Scan 2027 (16.401 min): 140429-35.D\data.ms
H3CO
O
(e)
OCH3
O
m/z 135
135.1
107.1
77.1
92.1
178.1
64.1
41.1
53.1
121.1
150.1
163.1
m/z-->

C:

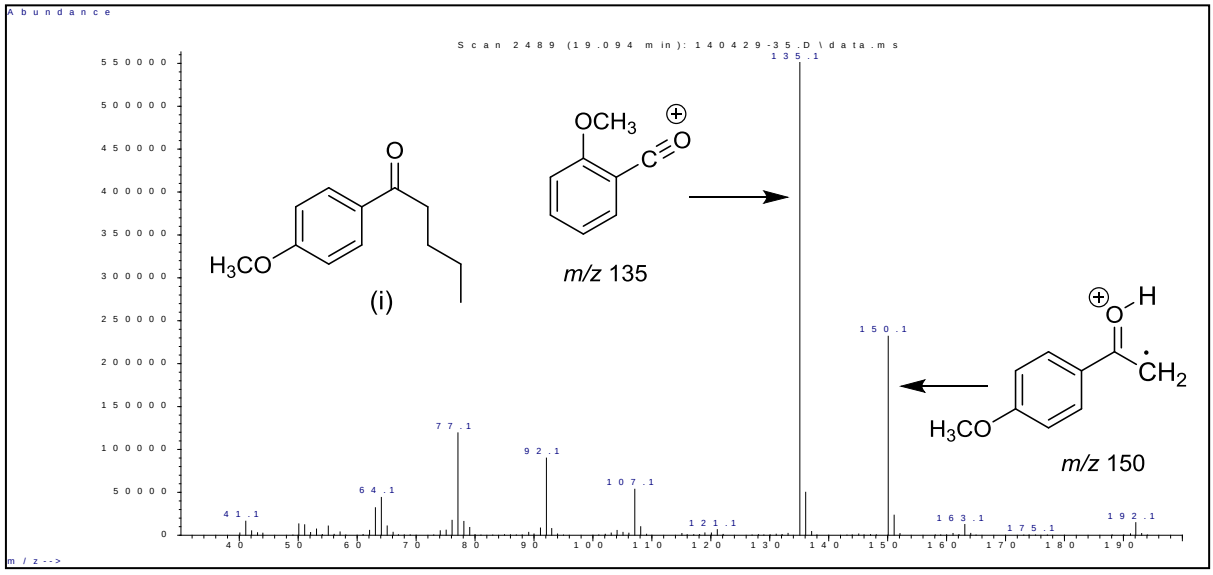

Figure 59. Representative full scan EI-MS spectra for the intermediate ketones: a, e and i. GC–MS System 1.

The GC–CI-MS studies were performed on a column (30 m × 0.25 mm i.d.) coated with 0.10 μm film of Crossbond® 100% dimethyl polysiloxane (Rtx®-1). The GC–CI-MS using methanol as the reagent gas shows only one major peak occurring at the mass of the protonated molecular ion $[M+1]^+$. Sample CI mass spectra for Compounds 1, 5 and 9 are shown in Figure 60. This CI technique confirms the molecular weight for these amines, which show essentially complete fragmentation in the EI mode (displayed in the following section). Chromatographic analysis was performed using a temperature program consisting of an initial hold at 70 °C for 1.0 minute, ramped up to 250 °C at a rate of 30 °C/minute followed by a hold at 250 °C for 15.0 minutes.

A:

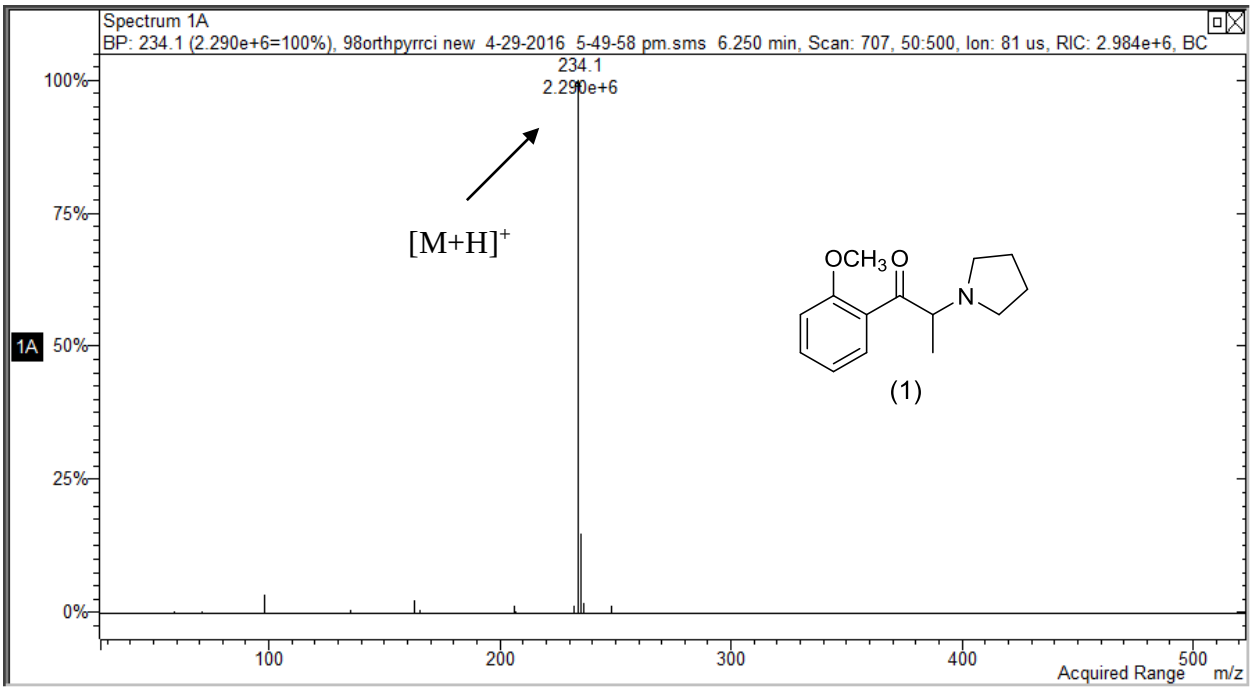
Spectrum 1A
BP: 234.1 (2.290e+6=100%), 98orthpyrrci new 4-29-2016 5-49-58 pm.sms 6.250 min, Scan: 707, 50:500, Ion: 81 us, RIC: 2.984e+6, BC
234.1
2.290e+6
[M+H]+
OCH3 O
N
(1)
1A
100%
75%
50%
25%
0%
100
200
300
400
500
Acquired Range
m/z

B:

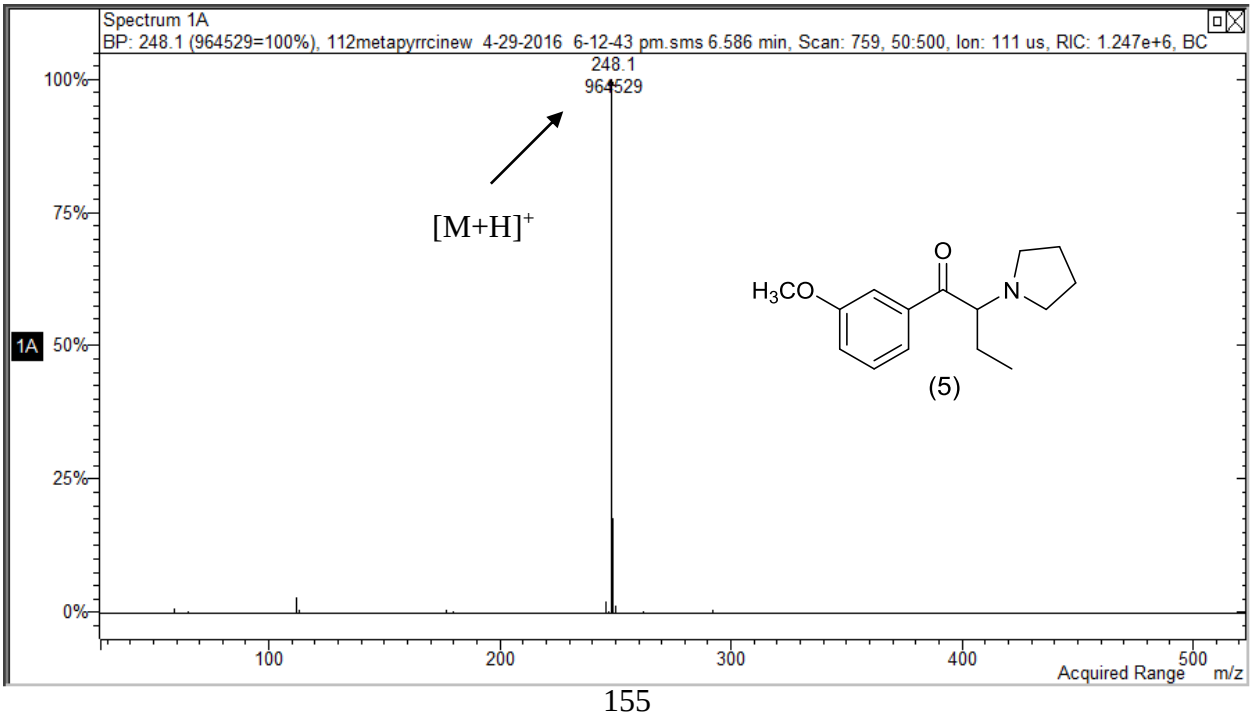
Spectrum 1A
BP: 248.1 (964529=100%), 112metapyrrcinew 4-29-2016 6-12-43 pm.sms 6.586 min, Scan: 759, 50:500, Ion: 111 us, RIC: 1.247e+6, BC
248.1
964529
[M+H]+
O
H3CO
N
(5)
1A
100%
75%
50%
25%
0%
100
200
300
400
500
Acquired Range
m/z

C:

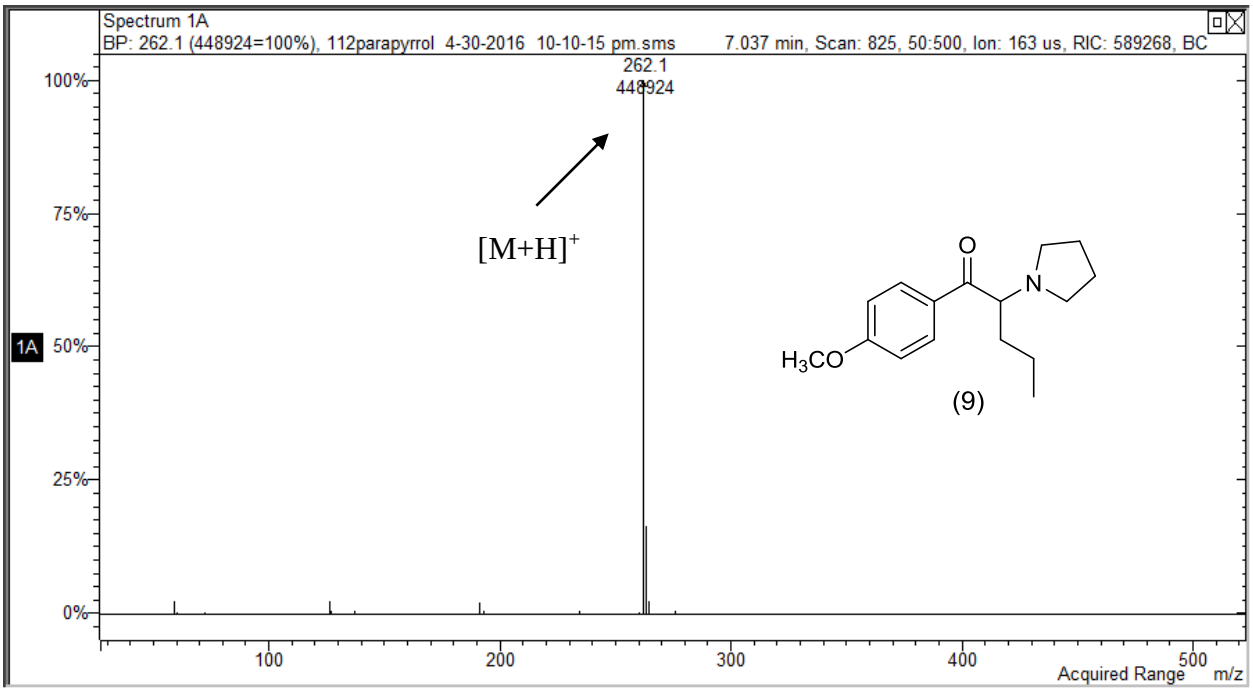

Figure 60. Representative methanol CI mass spectra for Compounds 1, 5 and 9. GC–MS System 2.

The EI-MS spectra for a selection of three of the aminoketone compounds in this study are shown in Figure 61. These three spectra are representative of all nine compounds in this study. The three spectra represent each of the three ring regioisomers and each of the three alkyl side-chain homologues. The iminium cation fragment is the base peak and the dominant feature in all these spectra. The spectra show few ions of significance at masses higher than the iminium cation base peak. Thus, the EI-MS spectrum does not provide clear information on the mass of the molecular radical cation. Compounds 1, 2 and 3 yield identical EI mass spectra and the spectrum for Compound 1 in Figure 61 is representative of all three of these regioisomeric compounds. Each of these compounds (1–3) has the identical elemental composition and molecular weights as well as identical iminium cation base peaks at *m/z* 98. The ethyl side-chain group (Compounds 4–6) for

which Compound 5 is representative (Figure 61) shows iminium cation base peaks at *m/z* 112 along with identical elemental composition. The same relationship exists in Compounds 7–9 and this set of compounds each has the iminium cation base peak at *m/z* 126. Thus, the EI-MS spectrum of Compound 9 in Figure 61 is representative of all three regioisomeric compounds having the *n*-propyl side-chain group.

A:

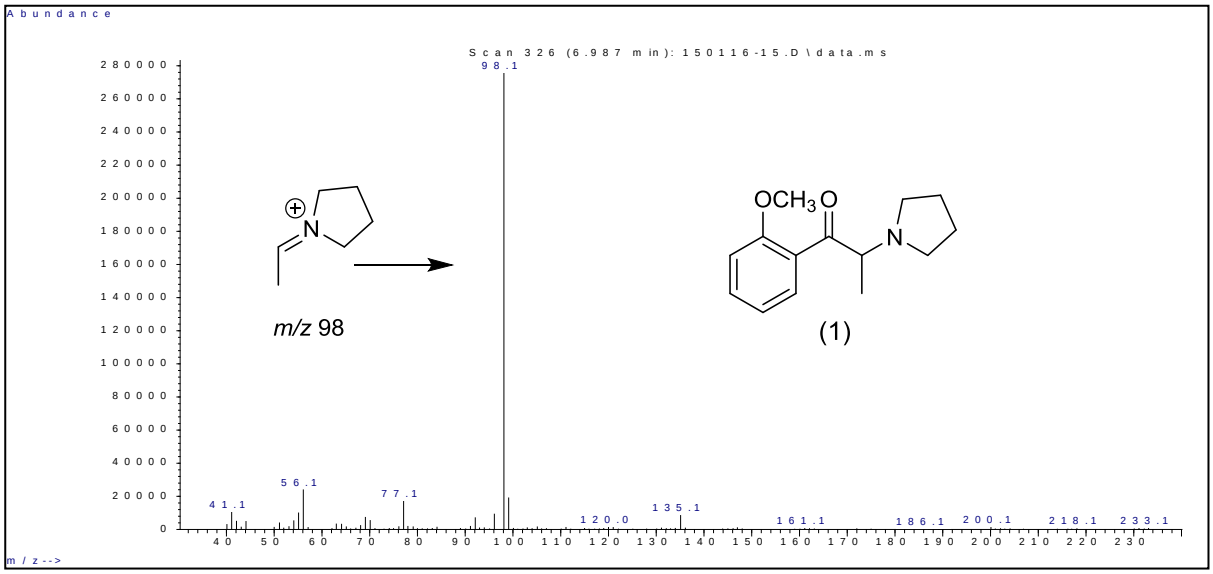

B:

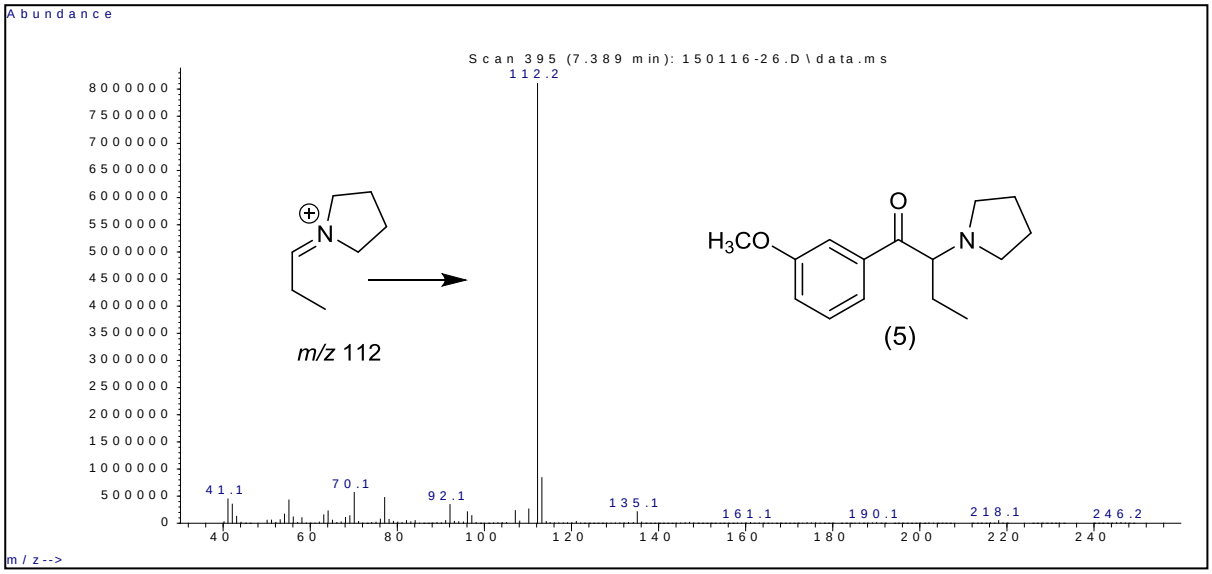

C:

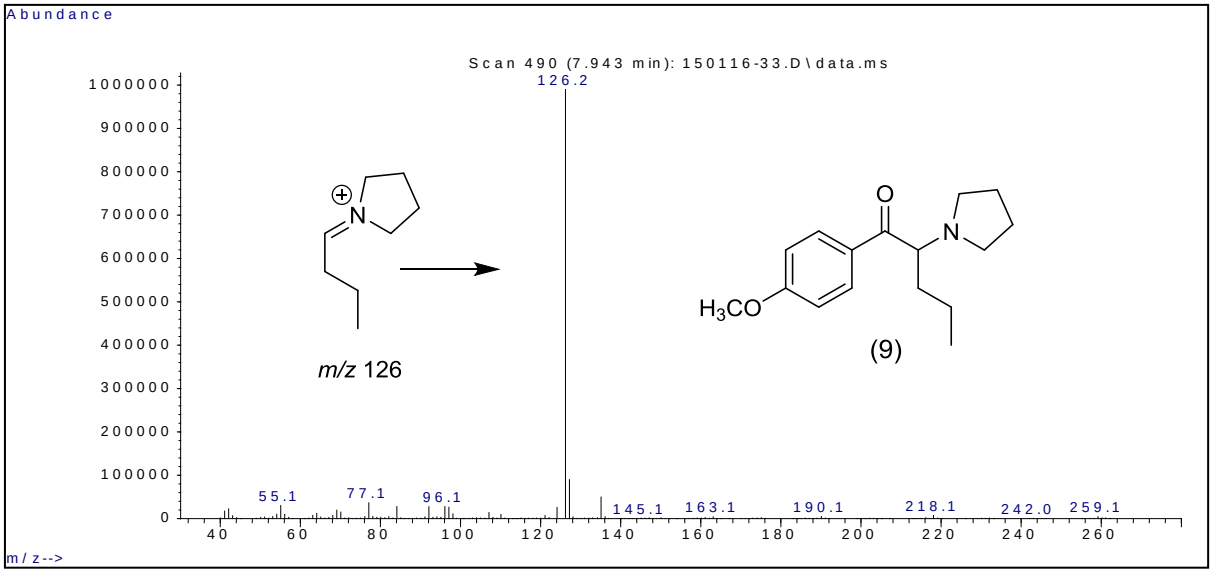

Figure 61. Representative full scan EI-MS spectra for Compounds 1, 5 and 9. GC–MS System 1.

The MS/MS product ion spectra for the three iminium cations are shown in Figure 62. The scan type used was the Automated Method Development function (AMD) and the optimum MS/MS excitation amplitudes were 0.80, 1.00 and 1.20 volts. The GC–MS/MS studies were performed using the same column described for the GC–CI-MS studies (Rtx®-1) with a temperature program consisting of an initial hold at 70 °C for 1.0 minute, ramped up to 250 °C at a rate of 30 °C/minute followed by a hold at 250 °C for 7.0 minutes. Only three homologous iminium cations are generated in the electron ionization mass spectra of these nine compounds. The product ion spectra are shown for the iminium cation base peaks from Compounds 1, 5 and 9 as examples of this entire set of compounds. The structures for the precursor iminium species are provided within the individual MS/MS spectra along with the proposed structures of the major characteristic product ion for each compound. The small side-chain methyl homologue iminium cation (*m/z* 98) shows the major product ion at *m/z* 56 consistent with the loss of 42 Da from the

parent ion species. The highest hydrocarbon side-chain homologue (*m/z* 126) *n*-propyl side-chain whose MS/MS spectrum is shown in Figure 62 yields the *m/z* 84 product ion. This ion also represents the loss of 42 Da from the parent iminium cation species at *m/z* 126. In fact, these three product ion spectra appear to represent another homologous series of ions. The major product ion for Compound 1 occurs at *m/z* 56 and the expected 14 Da increase occurs for Compound 5 (*m/z* 70) and the equivalent product ion for Compound 9 occurs at *m/*z 84. These three product ions each represent the loss of 42 Da from the iminium cation base peak. The loss of 42 Da to yield the *m/z* 56 product ion for Compound 1 must occur via the loss of C_3H_6 from the pyrrolidine ring portion of the iminium cation structure. Likewise, the loss of 42 Da from Compound 5 must occur from the pyrrolidine ring. However, the loss of C_3H_6 for Compound 9 could occur from the pyrrolidine ring or the three carbon alkyl side-chain. Previous studies (in Sections 2.1.3., 2.2.3. and 2.3.3.) using deuterium labels in both the pyrrolidine ring and the alkyl side-chain groups have confirmed the product ion structures shown within Figure 62. These labeling experiments confirmed the loss of 42 Da via pyrrolidine ring fragmentation for iminium cations having the methyl and ethyl side-chains. However, the loss of 42 Da in Compound 9 comes only from side-chain fragmentation and does not involve the pyrrolidine ring based on the previous deuterium labeling studies.

A:

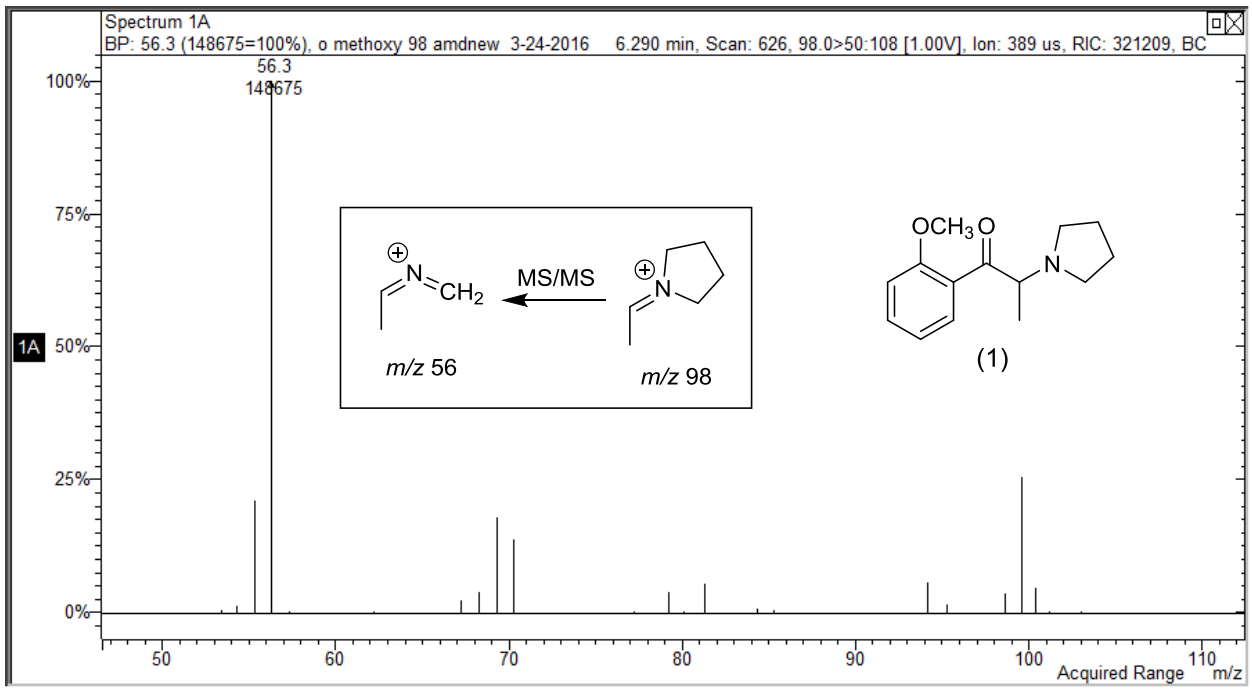
Spectrum 1A
BP: 56.3 (148675=100%), o methoxy 98 amdnew 3-24-2016 6.290 min, Scan: 626, 98.0>50:108 [1.00V], Ion: 389 us, RIC: 321209, BC
56.3
148675
100%
75%
1A 50%
25%
0%
MS/MS
m/z 56
m/z 98
OCH3 O
N
(1)
50
60
70
80
90
100
110
Acquired Range
m/z

B:

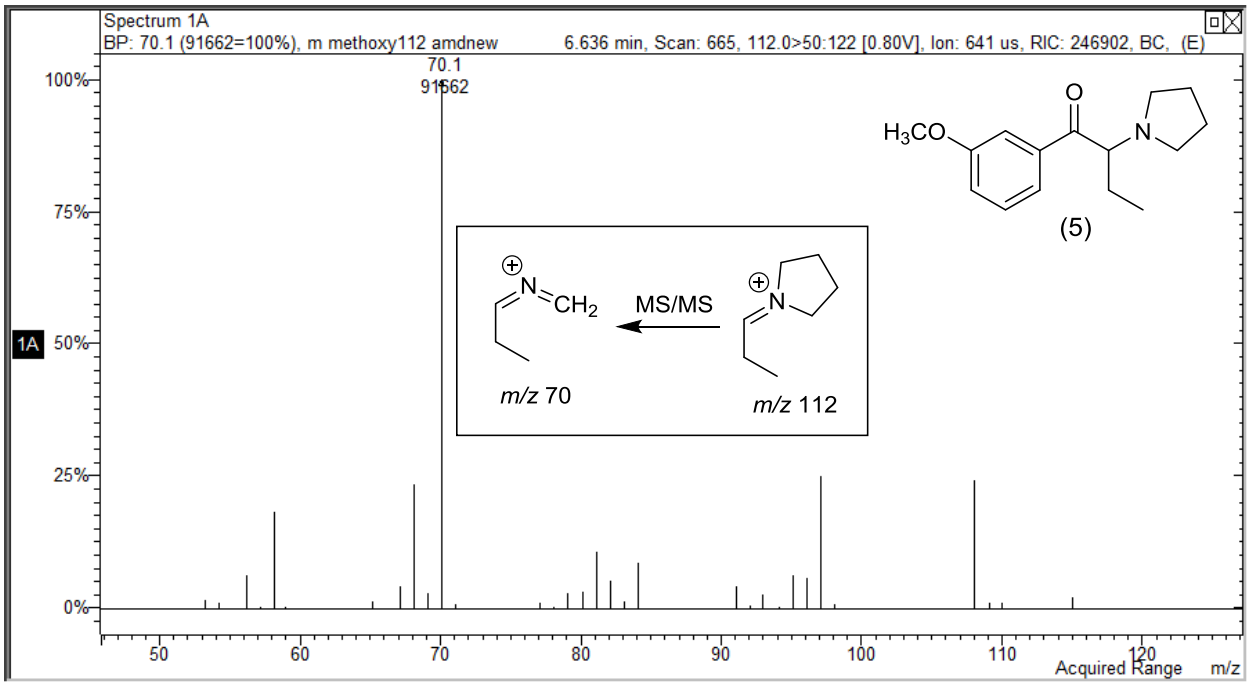
Spectrum 1A
BP: 70.1 (91662=100%), m methoxy112 amdnew 6.636 min, Scan: 665, 112.0>50:122 [0.80V], Ion: 641 us, RIC: 246902, BC, (E)
70.1
91662
100%
75%
1A 50%
25%
0%
MS/MS
m/z 70
m/z 112
H3CO
O
N
(5)
50
60
70
80
90
100
110
120
Acquired Range
m/z

C:

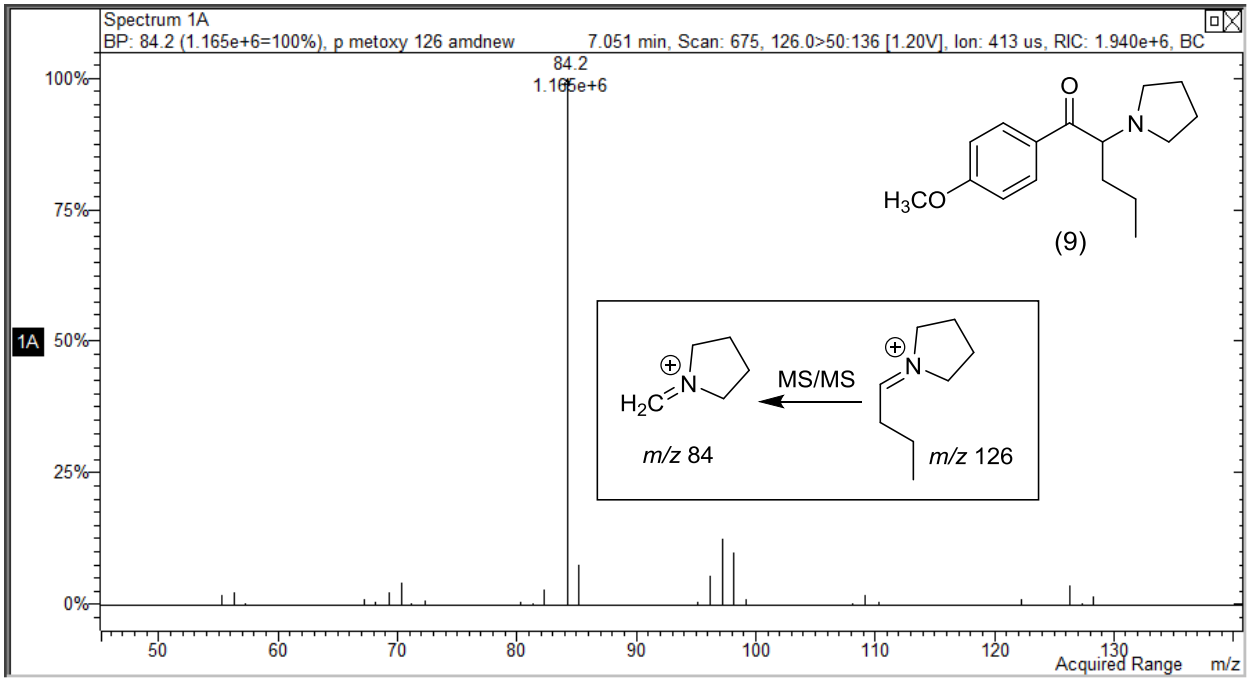

Figure 62. Product ion MS/MS spectra for iminium cation base peaks of Compounds 1, 5 and 9. GC–MS System 2.

2.5.4. Vapor phase infrared spectrophotometry

The vapor phase infrared spectra generated in GC–IR experiments are shown in Figure 63 for an example set of regioisomeric aromatic ring substitution patterns (Compounds 7, 8 and 9). These spectra were generated directly from the chromatography peak as each compound eluted from the capillary GC column. Thus, providing an added level of reliability based on the purity of the chromatography peak generated via the GC analysis. The GC–IR vapor phase infrared spectra were recorded in the range of 4000 – 550 cm^{-1} with a resolution of 8 cm^{-1}. All compounds show a carbonyl band in the 1690 cm^{-1} range and characteristic bands in the 1300 cm^{-1} to 1150 cm^{-1} range. The characteristic bands for aromatic ethers in the 1300 cm^{-1} range provide information concerning the position of the methoxy-group and its relationship to the aminoketone side-chain. The 1300 cm^{-1} to 1150 cm^{-1} range shows a unique and characteristic absorption pattern for each of the three

regioisomeric methoxy-group substitution patterns. The 2-methoxy group for Compound 7 shows a doublet pattern of absorption bands at 1280 cm^{-1} and 1241 cm^{-1} with the 1241 cm^{-1} band having slightly greater intensity. This can be compared to the very intense single absorption band at 1260 cm^{-1} observed in the 3-methoxy substitution pattern for Compound 8. The four absorption bands occurring in the range from 1295 cm^{-1} to 1169 cm^{-1} is characteristic of the 4-methoxy substitution pattern. Compound 9 shows two of these bands, 1251 cm^{-1} and 1169 cm^{-1} as the more intense absorptions for the 4-methoxy- substitution pattern in this compound. The correlations between IR absorption bands and aromatic ring substitution pattern for Compounds 7, 8 and 9 are repeated for the other two sets of compounds (1, 2 and 3 as well as 4, 5 and 6).

A:

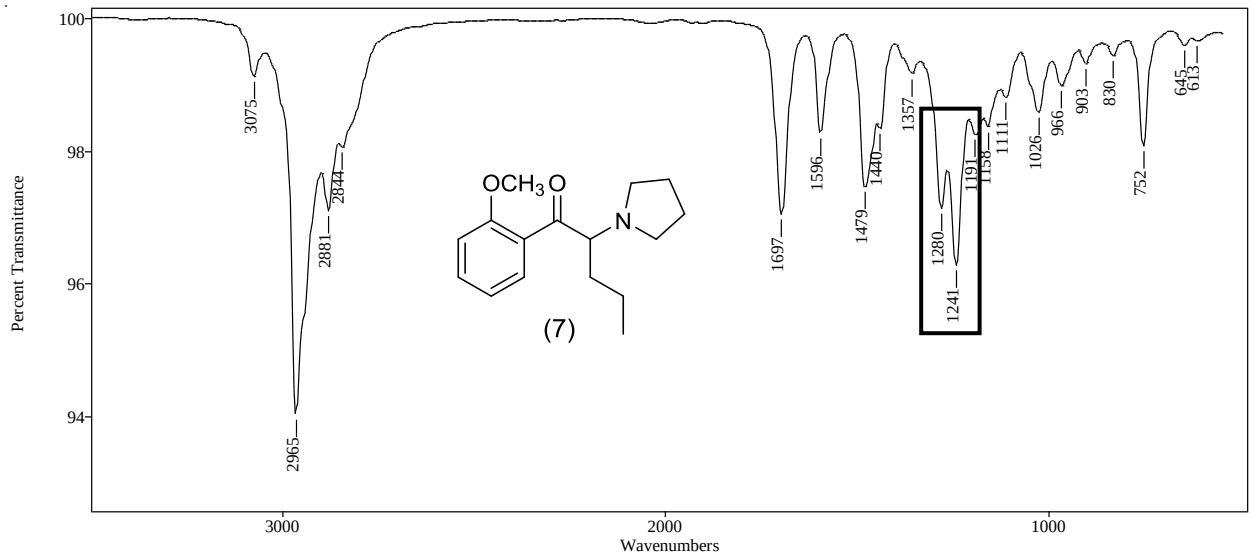

B:

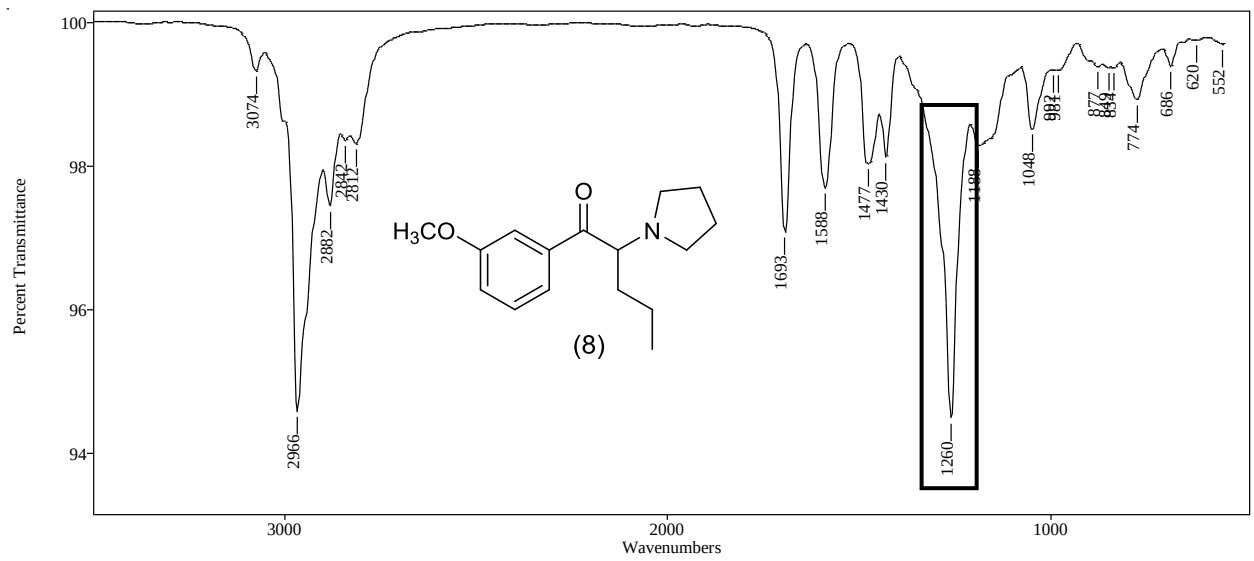

C:

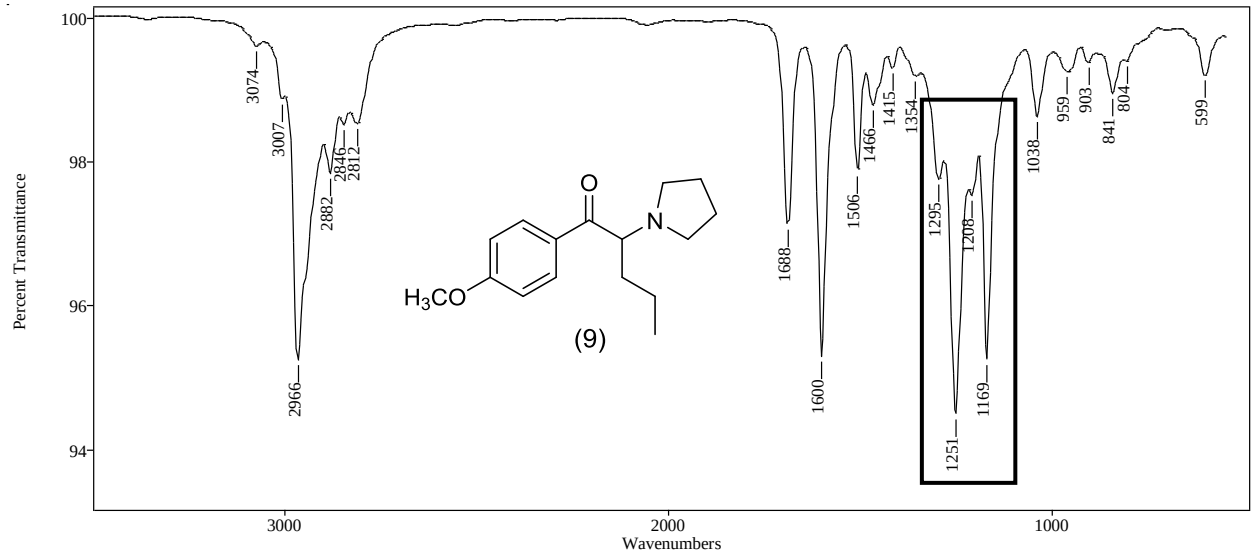

Figure 63. Vapor phase IR spectra of the regioisomeric methoxyaminoketones with *n*-propyl side-chain.

The vapor phase IR spectra in Figure 64 show the consistent absorption pattern in the 1300 cm^{-1} to 1150 cm^{-1} range for a series of 4-methoxyphenyl substituted carbonyl compounds. The commercially available precursor compound 4-methoxybenzaldehyde is compared to the intermediate ketone (c) and the corresponding aminoketone (Compound 3). The four absorption bands occurring in the range from 1294 cm^{-1} to 1169 cm^{-1} are readily observed in all these compounds. Thus, the vapor phase GC–IR infrared absorption spectra provide clear differentiation of the relative position of the methoxy-group in these regioisomeric substances.

A:

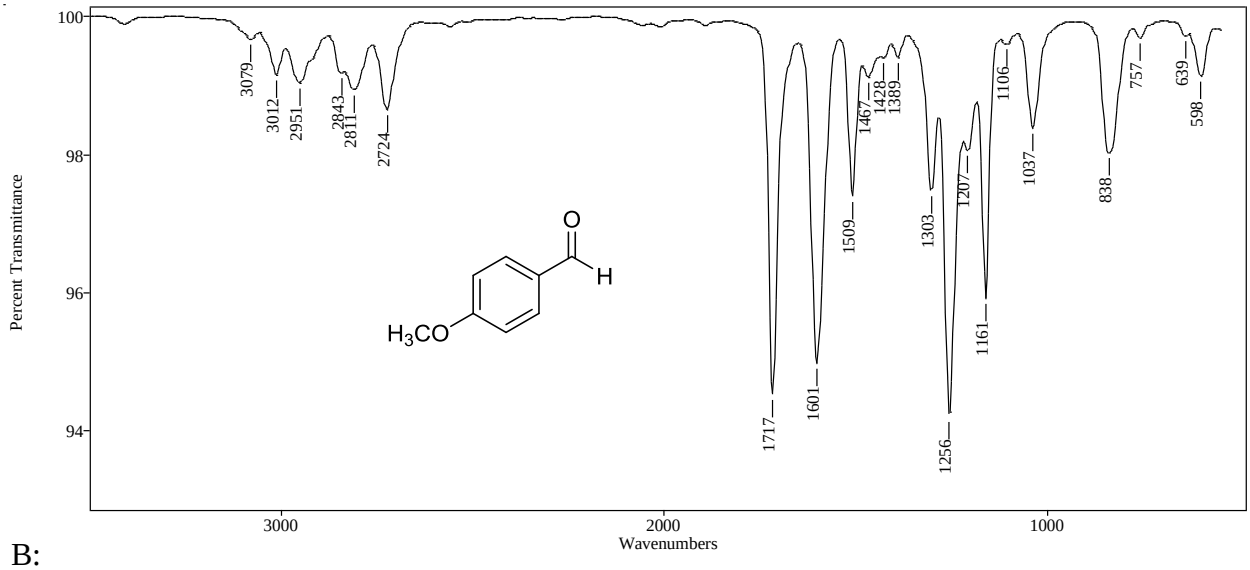

B:

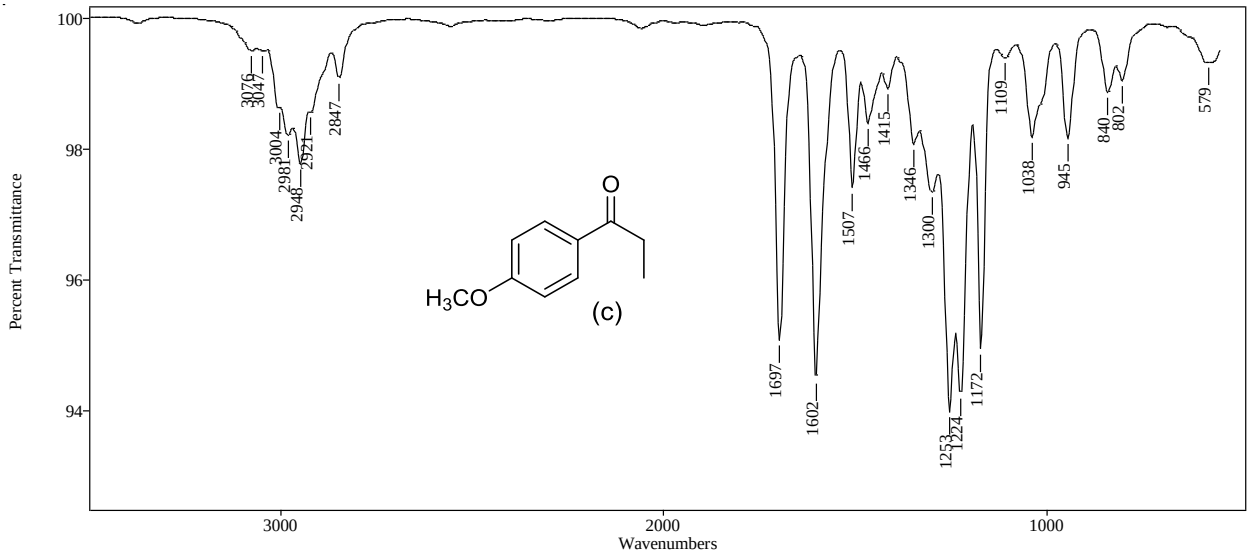

C:

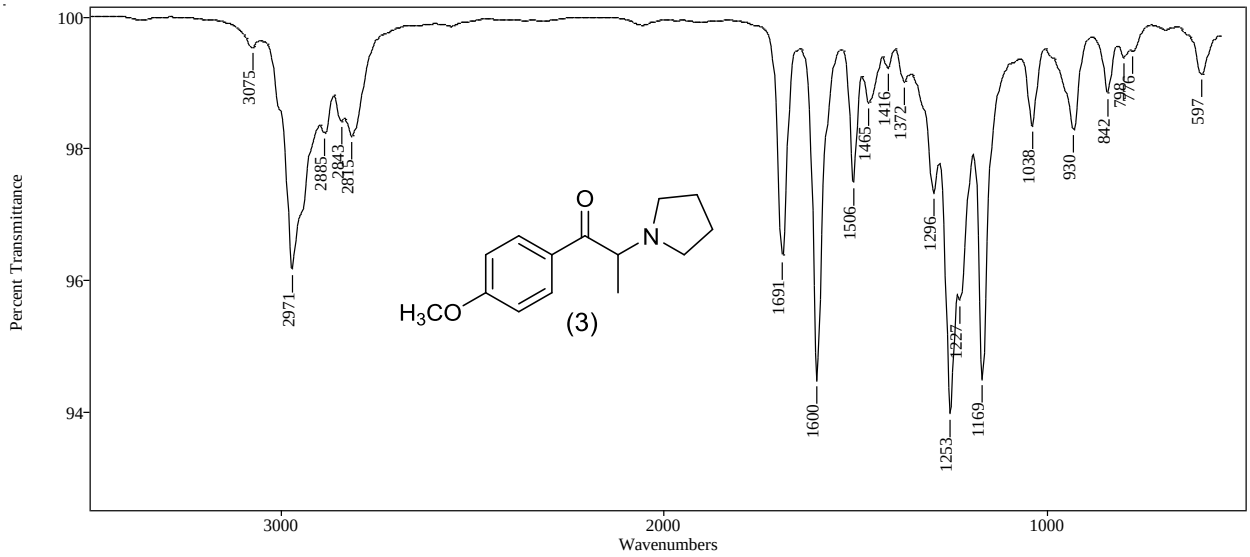

Figure 64. Vapor phase IR spectra of 4-methoxybenzaldehyde, 4-methoxypropiophenone, and 4-methoxyaminoketone.

2.5.5. Conclusion

The regioisomeric aminoketones were resolved on an Rtx®-5 stationary phase column. The iminium cation fragment is the base peak and the dominant feature in all the EI spectra. The spectra show few ions of significance at masses higher than the iminium cation base peak. Thus, the EI-MS spectrum does not provide clear information on the mass of the molecular radical cation due to extensive fragmentation. However, the GC–CI-MS using methanol as the reagent gas provides molecular weight information and these CI spectra show only one major peak occurring at the mass of the protonated $[M+1]^+$ molecular ion. The EI iminium cation base peaks for these compounds occur in a homologous series at *m/z* 98, 112 and 126 depending on the alkyl side-chain of the aminoketone compounds. The MS/MS spectra for the homologous iminium cation species yield a series of product ions each representing the loss of 42 Da from the EI base peaks. The vapor phase infrared absorption spectra provide clear differentiation of the relative position of the methoxy-group in these regioisomeric substances. Thus, this combination of techniques provides

complete differentiation of these regioisomeric and homologous aminoketone designer cathinone derivatives.

2.6. Differentiation of the six dimethoxypyrovalerone (DMPV) regioisomers: GC–MS, GC–MS/MS and GC–IR

Multiple and complementary analytical methods are often necessary for the identification of a specific compound from a series of closely related structural isomers. Gas chromatography-mass spectrometry (GC–MS), gas chromatography-product ion mass spectrometry (GC–MS/MS) and gas chromatography-infrared spectroscopy (GC–IR) were used to differentiate between the six dimethoxypyrrovalerone (DMPV) regioisomers. The six regioisomeric aminoketones were separated on a 50% phenyl stationary phase and the elution order is related to the positioning of substituents on the aromatic ring. These six DMPV regioisomers yield essentially identical mass spectral data in both chemical ionization (CI-MS) and electron ionization (EI-MS) spectra as well as identical product ion MS/MS spectra of the iminium cation base peak (*m/z* 126). These various mass spectral techniques provide data to identify all major structural features of these molecules except the dimethoxy substitution pattern of the aromatic ring. The region of the vapor phase infrared spectra between 1600 cm^{-1} and 1000 cm^{-1} provides a significant number of unique absorption bands characteristic of each individual DMPV regioisomer.

2.6.1. Synthesis of the six regioisomeric dimethoxypyrovalerones

The desired regioisomeric aminoketones (Compounds 1–6) were prepared individually (see Scheme 20) from the six commercially available dimethoxybenzaldehydes using the same procedure prescribed previously in Section 2.1.1. The six final products were isolated by solvent extraction and purified by preparative thin layer chromatography (TLC) using a 20:80 ethyl acetate-petroleum ether solvent and Analtech (Newark, DE) glass backed 20 x 20 cm plates with a 1000 µm layer of silica and an inorganic fluorescent 254 nm indicator.

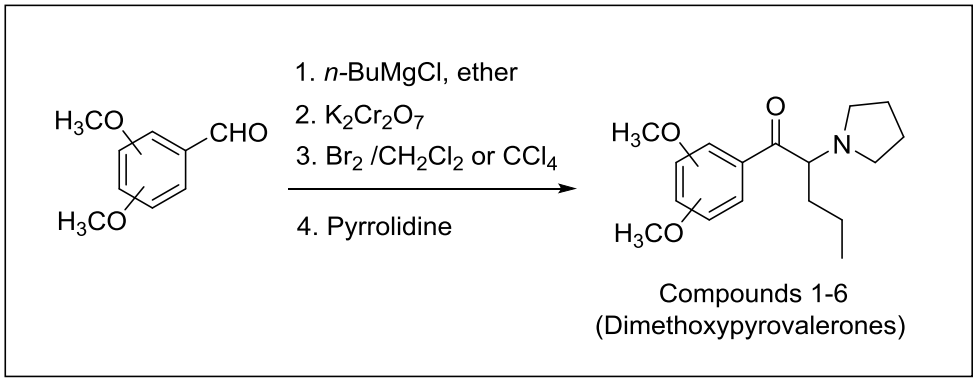

Scheme 20. General synthetic scheme for the six dimethoxypyrovalerones in this study.

2.6.2. Gas chromatographic separation

The chromatogram in Figure 65 shows the capillary gas chromatographic separation of the intermediate dimethoxyvalerophenones. These six regioisomeric ketones elute over approximately a one-minute time window using a column (30 m × 0.25 mm i.d.) coated with 0.25 µm film of midpolarity Crossbond® silarylene phase; similar to 50% phenyl, 50% dimethyl polysiloxane (Rxi®-17Sil MS). The first compound to elute is 2,3-dimethoxyvalerophenone (peak a) followed by the 2,6-isomer (peak d). These two early eluting bands share substitution of all three groups on adjacent carbons of the aromatic ring. The next two compounds to elute are the 2,5-isomer (peak c) and the 3,5-isomer (peak f). The common structural feature for these two isomers

is the 5-methoxy group and this substituent shares a *meta*- relationship with the carbonyl containing side-chain. The remaining two late eluting compounds share a methoxy substituent at the 4-position, *para*- to the carbonyl containing side-chain. Peak b is the 2,4-isomer and the last compound to elute, peak e, represents the 3,4-dimethoxyvalerophenone isomer.

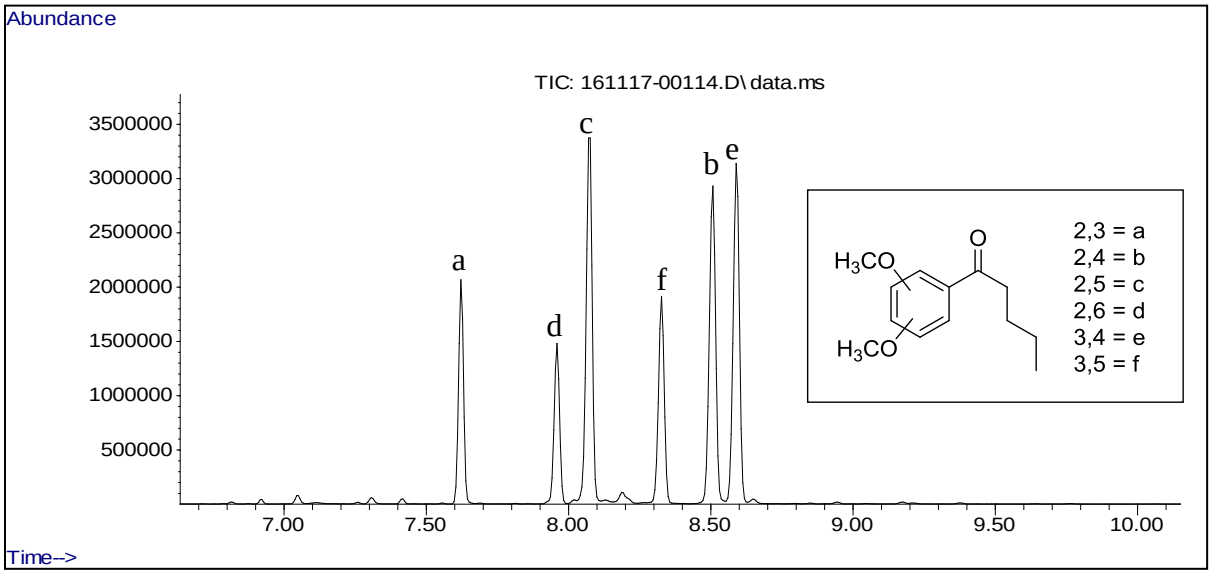

Figure 65. Capillary gas chromatographic separation of the six intermediate regioisomeric dimethoxyphenylketones. GC–MS System 1. Rxi®-17Sil MS stationary phase.

The chromatogram in Figure 66 is a representative of the separation obtained on the Rxi®-17Sil MS stationary phase for the six regioisomeric aminoketones. The compounds elute over approximately a two-minute time window and the elution order based on the aromatic ring substitution pattern is the same as that observed for the intermediate ketones. Compounds 1 and 4 having the most crowded substituent arrangements on the aromatic ring elute first while Compounds 2 and 5 show the highest retention in this chromatographic system. The stationary phase used for these separations was the relatively polar Rxi®-17Sil MS containing a 50% phenyl polymer and this would suggest polar interactions as an important contributor to the retention of these regioisomeric aminoketones. The selectivity of stationary phase polymers in gas chromatography is a complex interplay between steric and electronic forces. The steric and

electronic features of the methoxy groups and their relative positions on the aromatic ring would affect the extended conjugation of the aromatic ring and the carbonyl group, thus altering molecular polarity and relative retention. These two regioisomeric sets of compounds were separated using a temperature program consisting of an initial hold at 70 °C for 1.0 minute, ramped up to 250 °C at a rate of 30 °C/minute followed by a hold at 250 °C for 15.0 minutes.

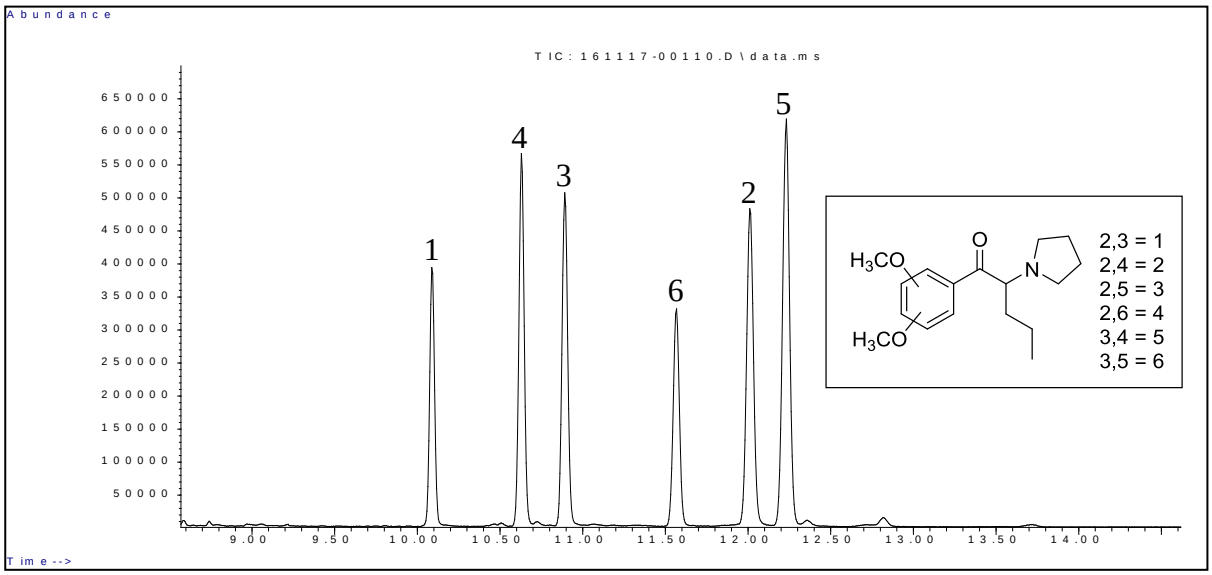

Figure 66. Capillary gas chromatographic separation of the six regioisomeric dimethoxyphenylaminoketones. GC–MS System 1. Rxi®-17Sil MS stationary phase.

2.6.3. Mass spectral studies (EI-MS, CI-MS and MS/MS)

The six DMPV regioisomers yield essentially identical mass spectral data in chemical ionization (CI-MS) and electron ionization (EI-MS) spectra as well as identical product ion MS/MS spectra of the iminium cation base peak (*m/z* 126). The GC–CI-MS (using methanol as the reagent gas) studies for these six regioisomeric DMPV were performed on a column (30 m × 0.25 mm i.d.) coated with 0.10 μm film of Crossbond® 100% dimethyl polysiloxane (Rtx®-1). Chromatographic analysis was performed using a temperature program consisting of an initial hold at 70 °C for 1.0 minute, ramped up to 250 °C at a rate of 30 °C/minute followed by a hold at 250

°C for 15.0 minutes. The GC–MS/MS studies were performed using the same column described for the GC–CI-MS studies (Rtx®-1) with a temperature program consisting of an initial hold at 70 °C for 1.0 minute, ramped up to 250 °C at a rate of 30 °C/minute followed by a hold at 250 °C for 7.0 minutes. The scan type used was the Automated Method Development function (AMD) and the optimum MS/MS excitation amplitude was 1.20 volts. The CI-MS, EI-MS and MS/MS spectra for one example compound of spectra is presented in Figure 67. The CI-MS spectrum in Figure 67A was obtained using methanol as the proton source and it shows the $[M+H]^+$ ion as the only major peak in the spectrum. The $[M+H]^+$ ion confirms the molecular weight of these DMPV regioisomers and this can be compared to the EI-MS spectrum in Figure 67B showing no molecular ion and essentially a complete fragmentation. The EI-MS spectrum shown in Figure 67B is dominated by the iminium cation base peak at *m/z* 126 and the structure for this fragment is shown within that spectrum. This major fragment is the result of elimination of the dimethoxybenzoyl radical species following initial molecular radical cation formation at the basic nitrogen atom.

The mass spectral fragmentation properties for all DMPV aminoketones do not provide any significant information for differentiation between these six regioisomers. These compounds share the identical elemental composition $C_{17}H_{25}NO_3$, identical EI-MS iminium cation base peak at *m/z* 126 which yields the identical MS/MS product ion at *m/z* 84 for each of the six DMPV regioisomers. While these compounds were well resolved in the GC studies, chromatographic data are not considered a confirmation level technique in forensic drug analysis. Other columns, stationary phases or chromatographic conditions could yield a very different separation profile for these compounds. Thus, overlapping chromatography peaks that yield identical mass spectra could lead to misidentification of an individual compound.

A:

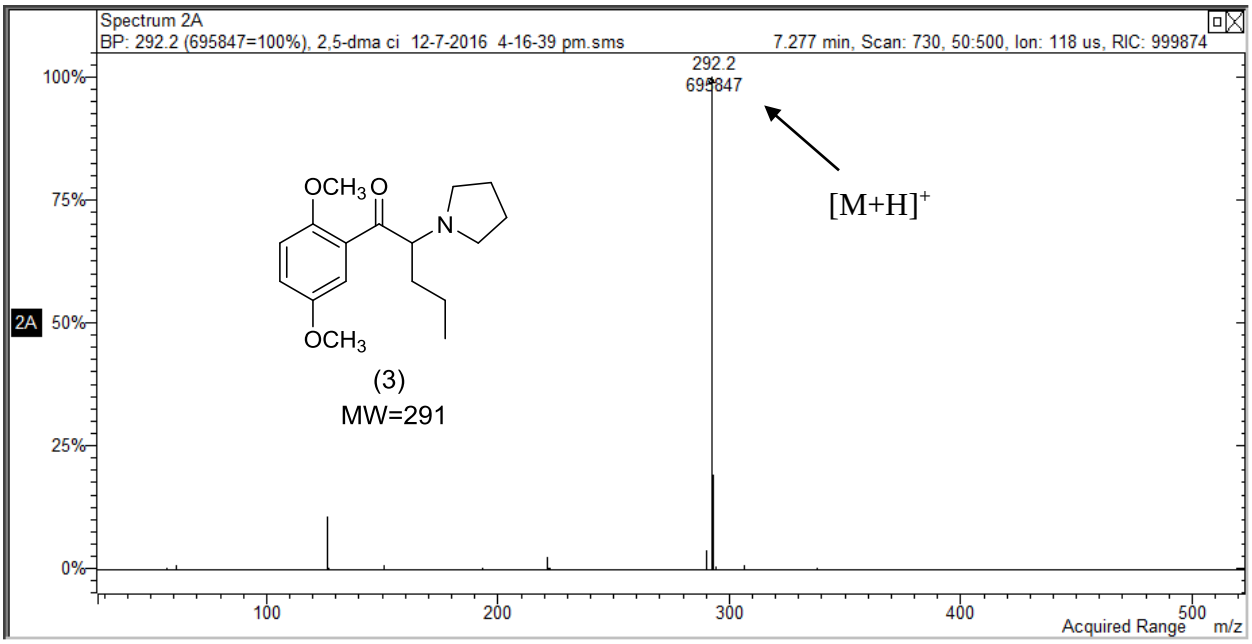
Spectrum 2A
BP: 292.2 (695847=100%), 2,5-dma ci 12-7-2016 4-16-39 pm.sms
7.277 min, Scan: 730, 50:500, Ion: 118 us, RIC: 999874
292.2
695847
100%
75%
2A
50%
25%
0%
100
200
300
400
500
Acquired Range
m/z
OCH3
O
N
OCH3
(3)
MW=291
[M+H]+

B:

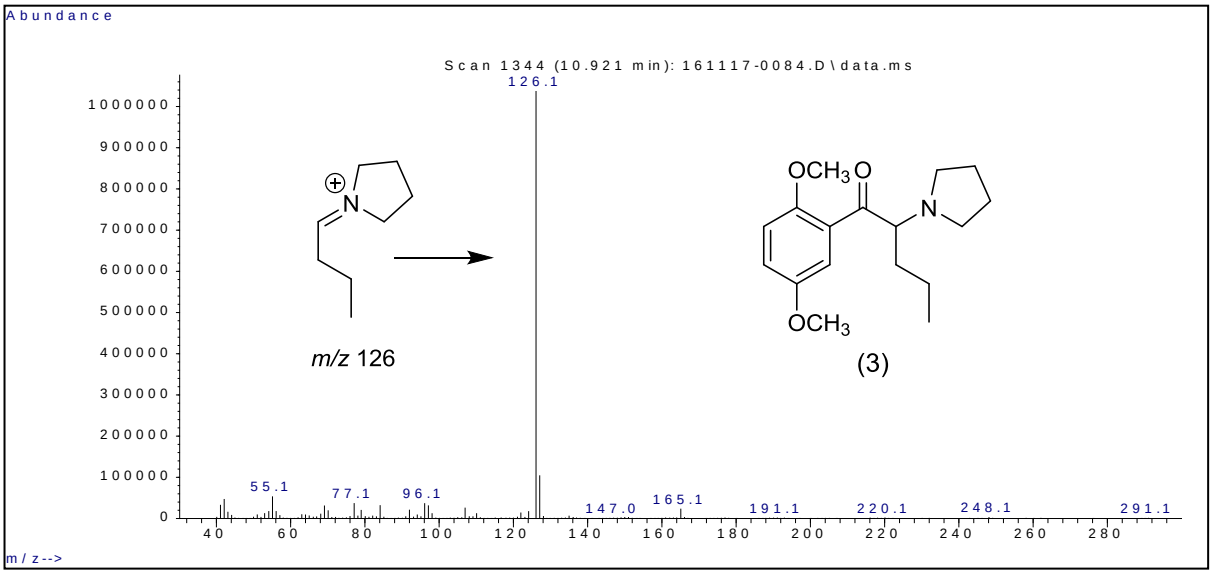
Abundance
Scan 1344 (10.921 min): 161117-0084.D\data.ms
126.1
1000000
900000
800000
700000
600000
500000
400000
300000
200000
100000
0
55.1
77.1
96.1
147.0
165.1
191.1
220.1
248.1
291.1
40
60
80
100
120
140
160
180
200
220
240
260
280
m/z-->
N
m/z 126
OCH3
O
N
OCH3
(3)

C:

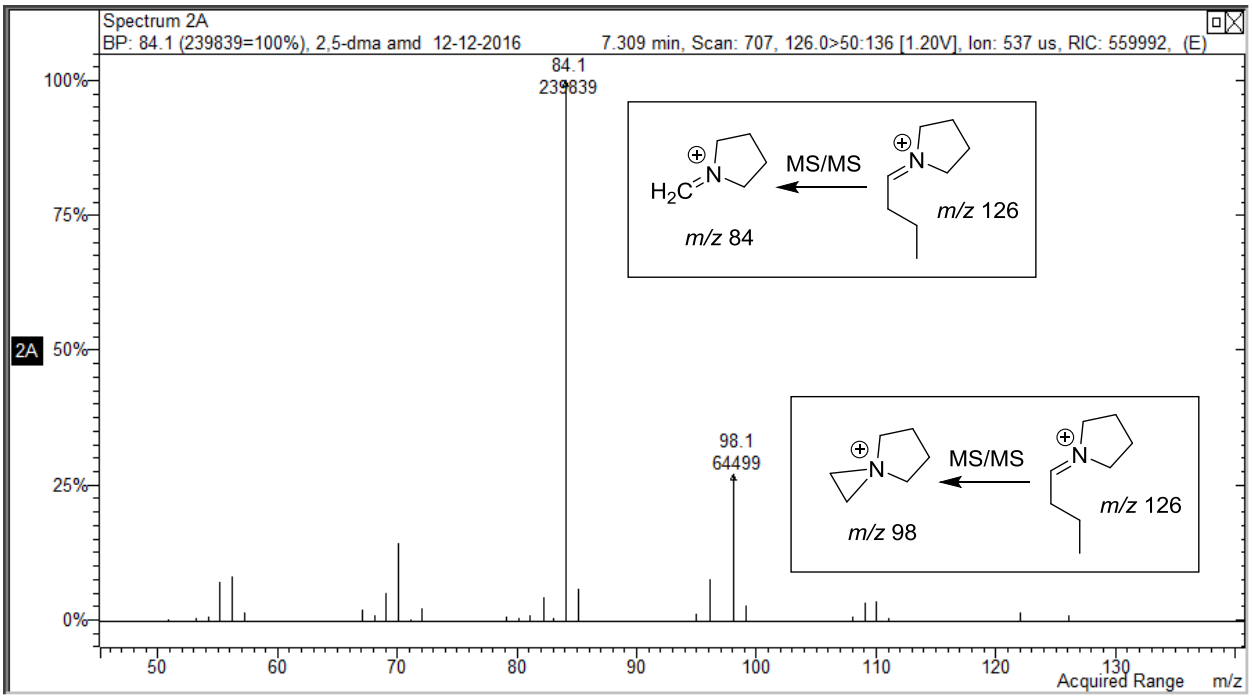

Figure 67. A: CI-MS, B: EI-MS and C: MS/MS spectra for the representative 2,5-dimethoxy substituted isomer (Compound 3).

2.6.4. Vapor phase infrared spectrophotometry

Issues of regioisomerism in drug categories involving totally synthetic drugs require the use of multiple and complementary confirmation level techniques for the identification of a specific compound. The infrared spectrum for an organic molecule provides unique data useful for the characterization of regioisomers especially aromatic ring substitution patterns. The data generated from the various mass spectral techniques described above can be used to identify all major structural features of these molecules except the dimethoxy substitution pattern of the aromatic ring. Once the MS data provide focus on the six regioisomeric dimethoxy pyrovalerones, the vapor phase infrared spectra clearly distinguish each of the aromatic ring dimethoxy substitution patterns. The vapor phase infrared spectra for the six DMPV regioisomers were determined using GC–IR techniques and these spectra are presented in Figure 68. The spectra were

obtained directly as the individual chromatography peaks eluted from the capillary column. The general inspection of the spectra shows a significant degree of similarity in the 3100 cm^{-1} to 2700 cm^{-1} region with the major sharp absorption band occurring at 2965 or 2966 cm^{-1} for all six compounds. This carbon-hydrogen stretching region should be quite similar for all these compounds based on the equivalence of most of the C-H bonding within these regioisomers.

The carbonyl absorption region for these regioisomers shows some variation in frequency likely based on a combination of steric and electronic factors. The spectra for Compounds 1 and 4 (Figure 68) show the highest carbonyl absorption frequencies at 1700 cm^{-1} and 1711 cm^{-1}, respectively. These crowded substitution patterns force the carbonyl group out of the plane of the aromatic ring yielding less through ring conjugation, more carbonyl double bond character and thus a higher carbonyl absorption frequency. Compounds 2 and 5 each have one methoxy group in the 4-position (*para*-) relative to the carbonyl group and this arrangement provides maximum through ring conjugation to the carbonyl group. This maximum conjugation effect enhances the single bond character of the carbonyl group and lowers the absorption frequencies to 1690 cm^{-1} and 1688 cm^{-1}, respectively. Compounds 3 and 6 yield carbonyl absorption frequencies intermediate between these two extremes. This pattern of carbonyl absorption frequencies as a function of dimethoxy group substitution patterns is also observed in the synthetic intermediate ketones (spectra not shown).

The region of the vapor phase infrared spectra between 1600 cm^{-1} and 1000 cm^{-1} provides a significant number of unique absorption bands characteristic for each individual DMPV regioisomer (Figure 68). This region of the IR spectrum includes absorbances of carbon-carbon double bonds, ether functional groups as well as the overall bending and stretching vibrations of

the molecular fingerprint region. This fingerprint region is a composite of interactions among similar energy single bonds and depends on the overall molecular skeleton. Compound 1 is characterized by strong bands at 1470 cm^{-1} and 1264 cm^{-1} while Compound 2 shows a strong single band at 1603 cm^{-1} for the carbon-carbon double bond vibration and a complex of several similar intensity bands from 1293 cm^{-1} to 1121 cm^{-1} in the molecular fingerprint region. Compound 3 has strong absorbances at both 1491 cm^{-1} and 1223 cm^{-1} along with less intense satellite bands at 1408 cm^{-1} and 1273 cm^{-1}. Compound 4 shows three intense fingerprint bands at 1469, 1246 and 1110 cm^{-1} in addition to the strong carbon-carbon double bond absorbance at 1589 cm^{-1}. The strongest absorption band for Compound 5 occurs at 1270 cm^{-1} and it is accompanied by a series of less intense bands at 1507, 1466 and 1411 cm^{-1}. The carbon-carbon double bond absorbance at 1594 cm^{-1} is a significant band for Compound 6 along with a second strong band at 1155 cm^{-1} and a number of absorbances of intermediate strength between 1462 cm^{-1} and 1200 cm^{-1}.

These results demonstrate that vapor phase infrared spectroscopy (GC–IR) clearly differentiates between the six regioisomeric forms of the dimethoxy aromatic ring substitution patterns for the DMPV compounds. The MS data provide focus on the six regioisomeric dimethoxy substitution patterns and the vapor phase infrared spectra clearly distinguish each of the aromatic ring dimethoxy substitution patterns. Thus, these two confirmatory-level techniques used in combination provide a complete identification for any one of these DMPV regioisomers.

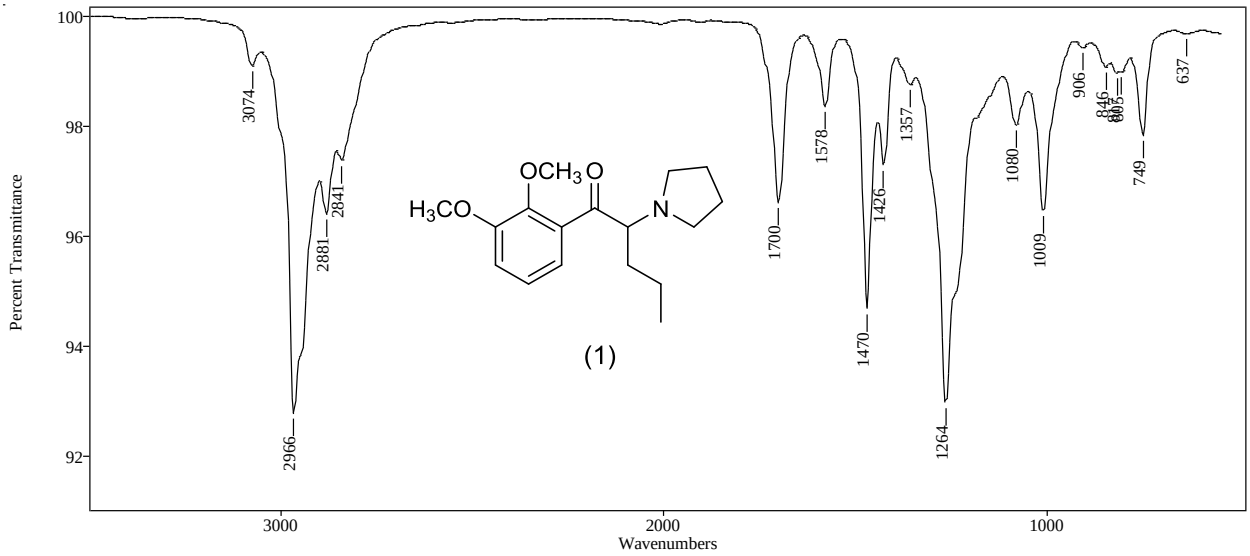
Percent Transmittance
100
98
96
94
92
3074
2966
2881
2841
1700
1578
1470
1426
1357
1264
1080
1009
906
846
749
637
OCH3 O
H3CO
N
(1)
3000
2000
1000
Wavenumbers

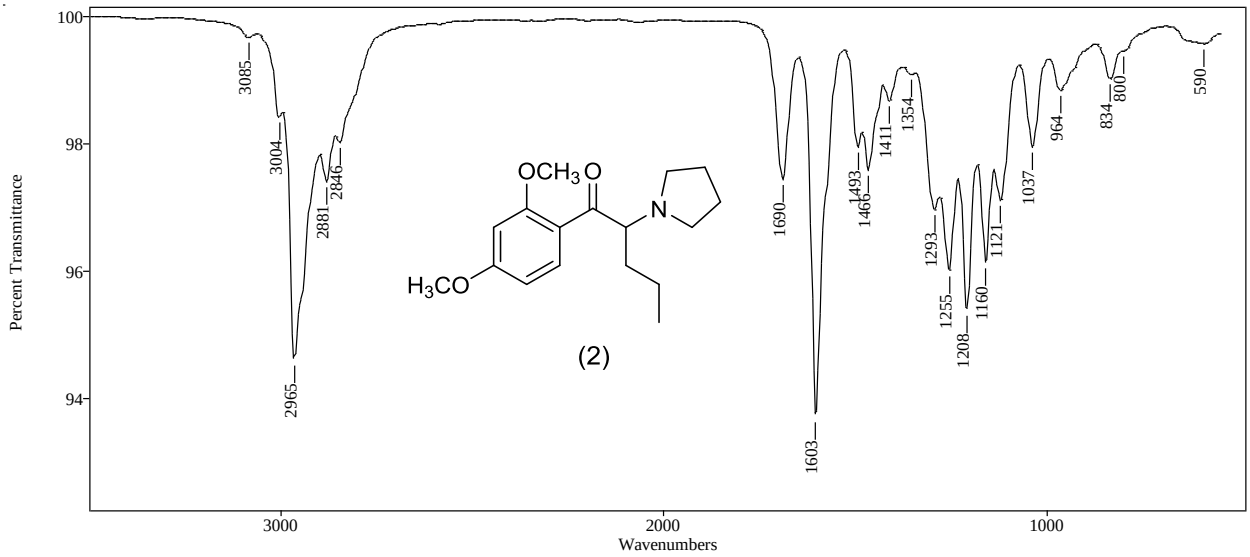
Percent Transmittance
100
98
96
94
3085
3004
2965
2881
2846
1690
1603
1493
1466
1411
1354
1293
1255
1208
1160
1121
1037
964
834
800
590
OCH3 O
H3CO
N
(2)
3000
2000
1000
Wavenumbers

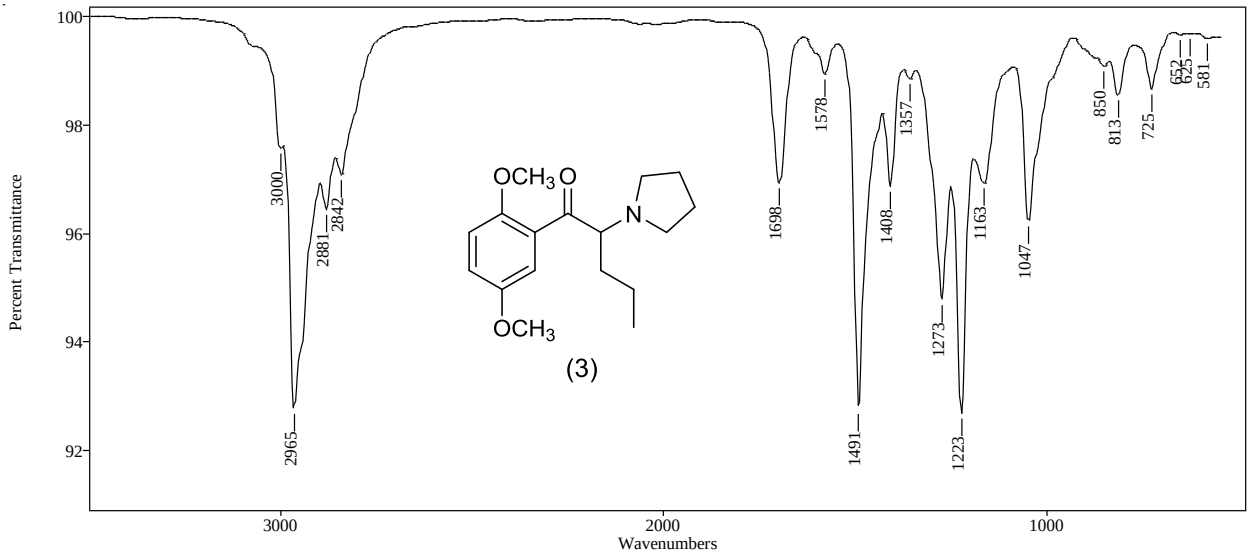
Percent Transmittance
100
98
96
94
92
3000
2965
2881
2842
1698
1578
1491
1408
1357
1273
1223
1163
1047
850
813
725
652
625
581
OCH3
O
N
OCH3
3000
2000
1000
Wavenumbers

(3)

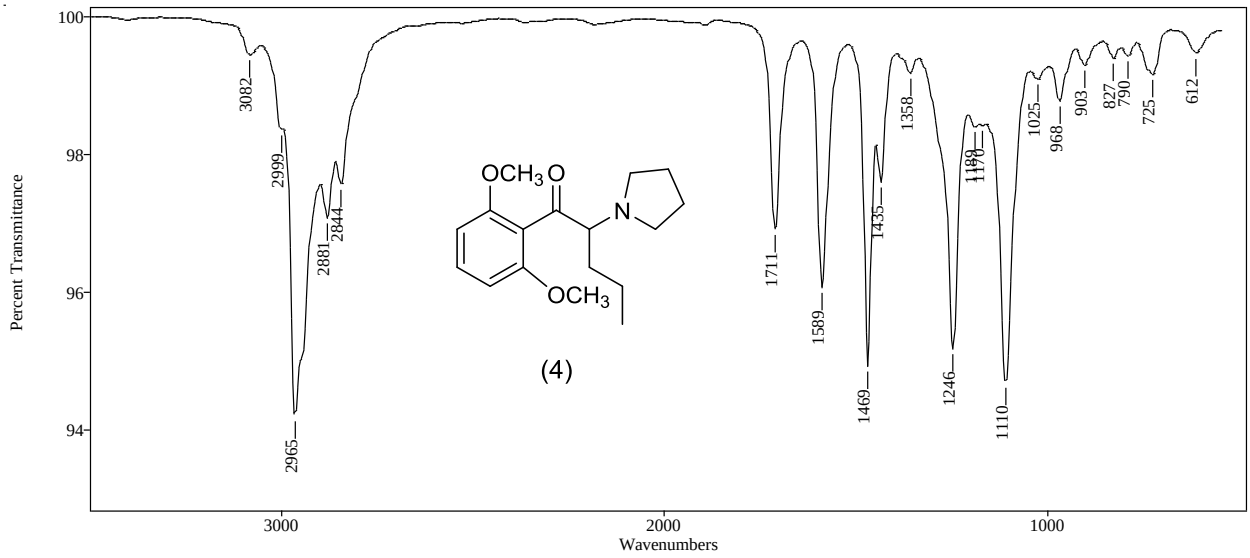
Percent Transmittance
100
98
96
94
3082
2999
2965
2881
2844
1711
1589
1469
1435
1358
1246
1180
1170
1110
1025
968
903
827
790
725
612
OCH3
O
N
OCH3
3000
2000
1000
Wavenumbers

(4)

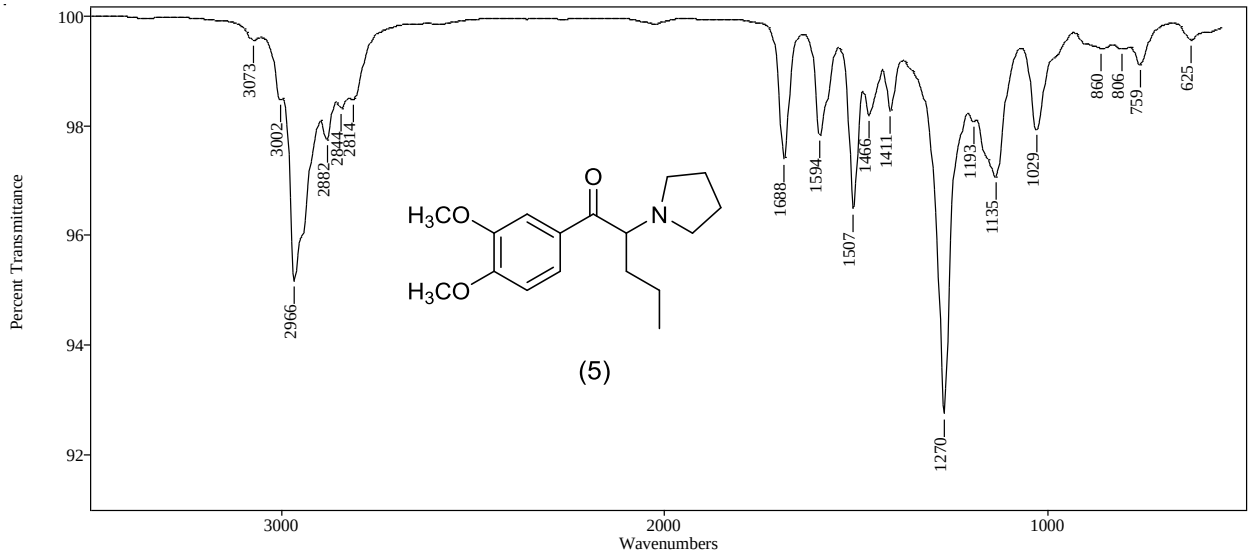

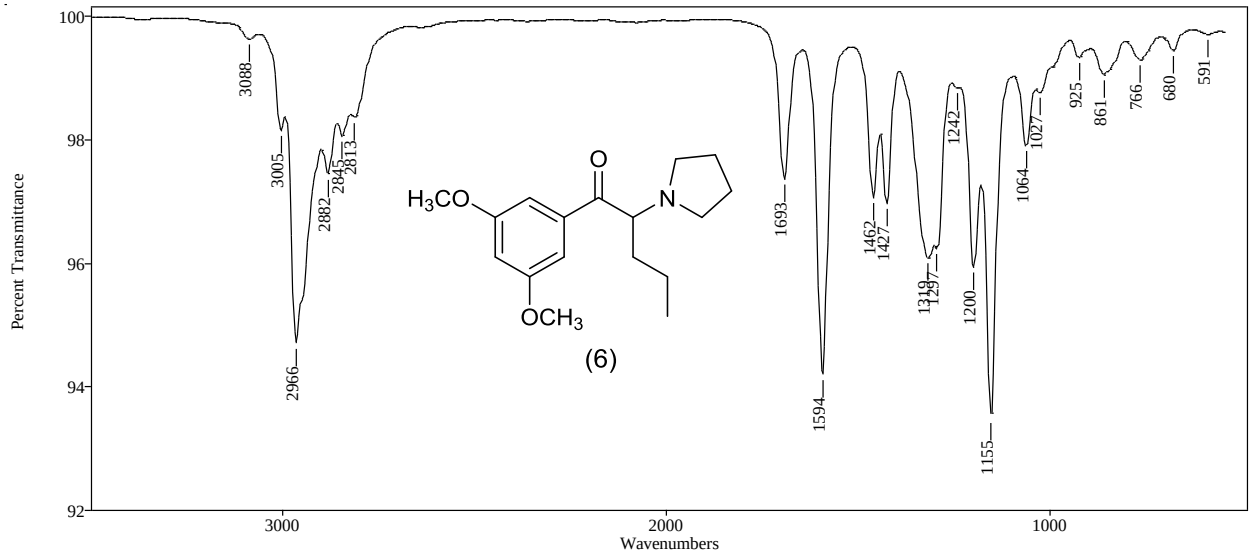

Figure 68. Vapor phase IR spectra (GC–IR) for the six regioisomeric dimethoxyphenylaminoketones.

The consistency of the infrared spectral features based on dimethoxy group substitution patterns is illustrated in Figure 69. The commercially available precursor aldehyde (2,5-dimethoxybenzaldehyde) and the synthetic intermediate ketone having the equivalent 2,5-dimethoxy substitution pattern yield equivalent vapor phase infrared spectra in the 1600 to 1000

cm^{-1} range. Furthermore, the absorption pattern in this range is consistent with that shown in Figure 68 for Compound 3, the 2,5-dimethoxy regioisomer of DMPV. The equivalent consistency for the other dimethoxy substitution patterns was also observed by comparing the remaining spectra in Figure 68 with the appropriate precursor aldehydes and intermediate ketones spectra.

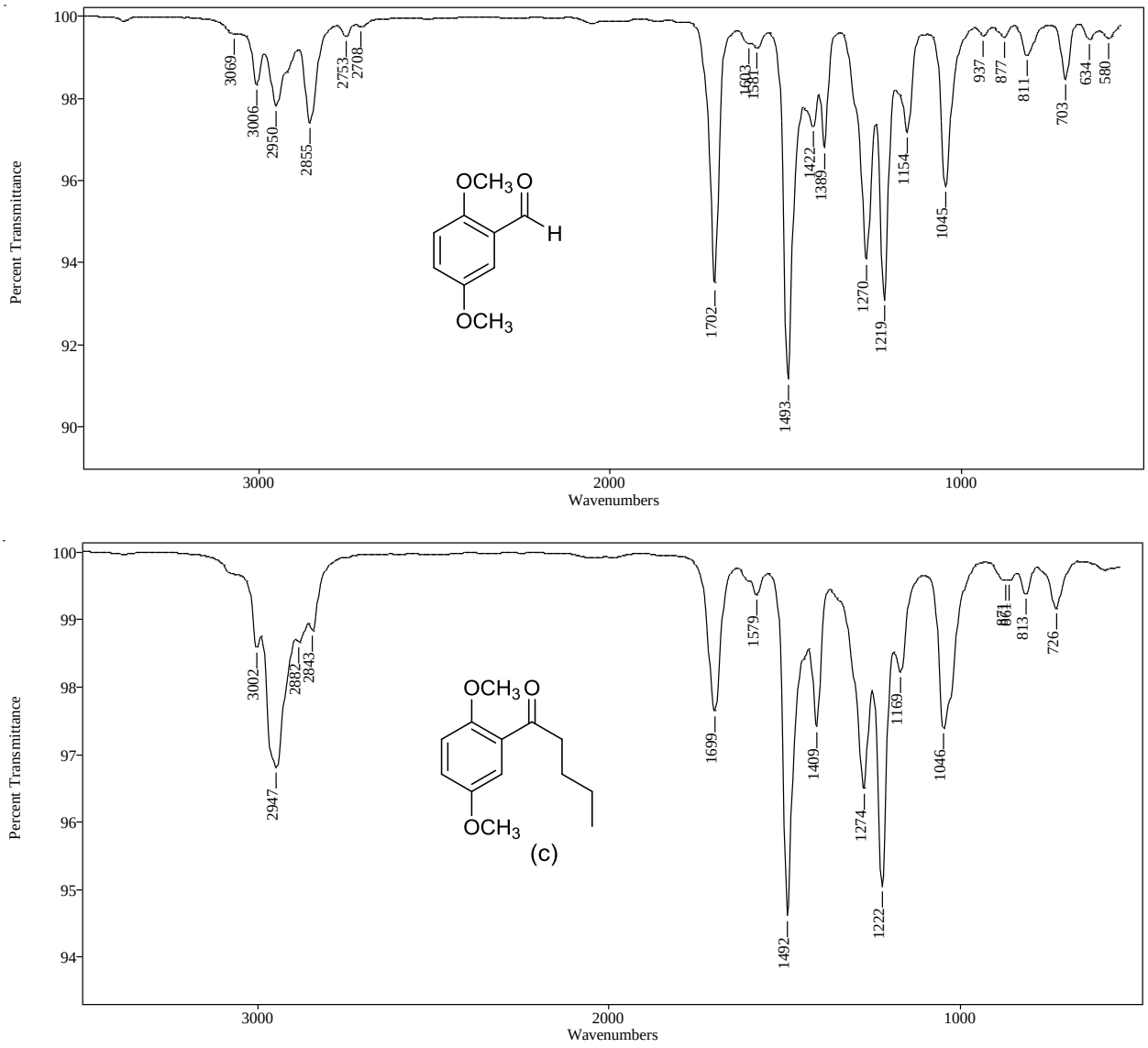

Figure 69. Representative vapor phase IR spectra (GC–IR) of the precursor 2,5-dimethoxybenzaldehyde and the intermediate 2,5-dimethoxyvalerophenone (Compound c).

2.6.5. Conclusion

The six dimethoxypyrovalerones (DMPVs) represent possible designer modifications of the pyrovalerone type cathinone derivatives. These regioisomeric compounds have identical elemental composition and identical functional groups arranged differently within the aromatic ring. The chemical ionization (CI-MS) spectra show the $[M+H]^+$ ion as the only major peak in each spectrum and confirm the molecular weight of these DMPV regioisomers. These six DMPV regioisomers share the identical elemental composition $C_{17}H_{25}NO_3$, identical EI-MS iminium cation base peak at *m/z* 126 which yields the identical MS/MS product ion at *m/z* 84. The six aminoketones and the intermediate ketones were separated on a 50% phenyl stationary phase and the elution order in each case is related to the positioning of substituents on the aromatic ring with the most crowded 2,6- and 2,3-regioisomers eluting first. The MS data provide focus on the six regioisomeric dimethoxy substitution patterns and the vapor phase infrared spectra clearly distinguish each of the aromatic ring dimethoxy substitution patterns. These results demonstrate that the vapor phase infrared spectroscopy (GC–IR) clearly differentiates between the six regioisomeric forms of the dimethoxy aromatic ring substitution pattern for the DMPV compounds. The use of multiple and complementary analytical methods such as GC–MS and GC–IR combine for the specific identification of each regioisomer in the DMPV series.

3. Experimental

3.1. Materials, instruments, GC-Columns and temperature programs

3.1.1. Materials

Precursor materials including piperonal (3,4-methylenedioxybenzaldehyde), 2,3-methylenedioxybenzaldehyde, 3,4-methylenedioxyproiophenone, 3,4-methylenedioxybutyrophenone, benzaldehyde, valerophenone, isovalerophenone, 2-, 3- and 4-methoxybenzaldehydes, 2,3-, 2,4-, 2,5-, 2,6-, 3,4- and 3,5-dimethoxybenzaldehydes, alkylmagnesium halides, 2-bromoalkanoic acid ethyl esters, azetidine, pyrrolidine, piperidine, azepane (hexamethyleneimine, perhydroazepine, hexahydro-1H-azepine), potassium dichromate, bromine, sodium amide, sodium cyanoborohydride, lithium aluminum hydride were obtained from Aldrich chemical company (Milwaukee, WI) or VWR chemical company (Radnor, PA). Samples of 2,2,3,3,4,4,5,5-pyrrolidine-D_8 and 2,2,5,5-pyrrolidine-D_4, piperidine-D_{10} and deuterated bromoalkanes were purchased from CDN Isotopes, Pointe Claire, Quebec, Canada.

HPLC grade acetonitrile, methylene chloride, methanol, tetrahydrofuran were purchased from Fisher Scientific, (Atlanta, GA). Diethyl ether, methylene chloride, carbon tetrachloride, benzene, ethanol, methanol, tetrahydrofuran (THF) were purchased from Fisher Scientific (Fair Lawn, NJ).

3.1.2. Instruments

GC–MS System 1 consisted of an Agilent Technologies (Santa Clara, CA) 7890A gas chromatograph and an Agilent 7683B auto injector coupled with a 5975C VL Agilent mass selective detector. The mass spectral scan rate was 2.86 scans/s. The GC was operated in splitless injection mode with a helium (ultra-high purity, grade 5, 99.999%) flow rate of 0.480 ml/minute and the column head pressure was 10 psi. The MS was operated in the electron ionization (EI) mode with an ionization voltage of 70 eV and a source temperature of 230 °C. The GC injector was maintained at 230, 150 or 250 °C and the transfer line at 280 °C. Samples were dissolved and diluted in high-performance liquid chromatography grade acetonitrile and introduced via the auto injector using an injection volume of 1-µl.

GC–MS System 2 consisted of an Agilent Technologies (Santa Clara, CA) 7890A gas chromatograph and an Agilent 7683B auto injector coupled with a 240 Agilent Ion Trap mass spectrometer (MS/MS). The mass spectral scan rate was 2.86 scans/s. The GC was operated in splitless injection mode (EI-MS and MS/MS) with a helium (ultra-high purity, grade 5, 99.999%) flow rate of 1 ml/minute and the column head pressure was 8.8085 psi. The MS was operated in the electron ionization (EI) mode using an ionization voltage of 70 eV and a trap temperature of 150 °C or 200 °C. The GC injector was maintained at 230 °C and the transfer line at 280 °C. For MS/MS experiments, the scan type used was Automated Method Development function (AMD) and the MS/MS excitation amplitude was ranged from 0.20 to 1.60 volts. CI-MS studies were performed using 99.9% methanol as the reagent gas and split injection mode (split ratio of 20:1). Samples were dissolved and diluted in high-performance liquid chromatography grade acetonitrile and introduced via the auto injector using an injection volume of 1-µl.

GC–IR studies were carried out on a Hewlett-Packard 6890 Series gas chromatograph and a Hewlett-Packard 7683 series auto-injector coupled with an IRD-3 (Infrared detector Model-3) obtained from Analytical Solutions and Providers (ASAP), Covington, KY. The vapor phase infrared spectra were recorded in the range of 4000 to 550 cm^{-1} with a resolution of 16 cm^{-1} and a scan rate 1.50 scans/s. The GC injector was maintained at 250 °C and the transfer line A, the light pipe and the transfer line B temperatures were maintained at 250 °C. The GC was operated in the split injection mode (split ratio of 10:1) with a carrier gas helium (ultra-high purity, grade 5, 99.999%) flow rate of 2 ml/minute and the column head pressure was 2.62 psi.

All IR experiments were performed using the same parameters. The stationary phase used was a 30 m × 0.25 mm i.d. capillary column coated with 0.10 µm film of low polarity Crossbond® silarylene phase; similar to 5% phenyl, 95% dimethyl polysiloxane (Rxi®-5Sil MS) purchased from Restek Corporation (Bellefonte, PA). The temperature program consisted of an initial hold at 70 ºC for 1.0 minute, ramped up to 250 ºC at a rate of 25 ºC/minute followed by a hold at 250 ºC for 6.80 minutes. Samples were dissolved and diluted in high-performance liquid chromatography grade acetonitrile and introduced via the auto injector using an injection volume of 1-µl.

3.1.3. GC-Columns

Different capillary GC columns were evaluated throughout the course of this work. However, only columns showed best compromises between resolution and analysis time are illustrated in Table 2. All columns used were purchased from Restek Corporation (Bellefonte, PA) and have the same dimensions, 30 m x 0.25 mm i.d., and film depth (f.d.) of 0.10, 0.25 or 0.50 µm.

Inlet pressure was converted according to the constant flow mode and the total flow was 60 ml/minute.

Table 2. List of columns used and their composition

Column name	Column composition
Rxi®-35Sil MS	Midpolarity phase; similar to 35% phenyl, 65% dimethyl polysiloxane
Rxi®-17Sil MS	Midpolarity Crossbond® silarylene phase; similar to 50% phenyl, 50% dimethyl polysiloxane
Rtx®-5	Crossbond® 5% diphenyl, 95% dimethyl polysiloxane
Rtx®-1	Crossbond® 100% dimethyl polysiloxane
Rtx®-200	Crossbond® 100% trifluoropropylmethyl polysiloxane
Rxi®-5Sil MS	Low polarity Crossbond® silarylene phase; similar to 5% phenyl, 95% dimethyl polysiloxane

3.1.4. Temperature Programs

Different temperature programs were evaluated throughout the course of this work. However, only programs showing the best compromises between resolution and analysis time are illustrated in Table 3.

Table 3. List of temperature programs used

Temperature program name	Injector temperature °C	Detector temperature °C	Program setup
TP-1 (GC–MS) (System 1)	230	280	Initial hold of column temperature at 70 °C for 1.0 minute, then the temperature was ramped up to 250 °C at a rate of 30 °C/minute followed by a hold at 250 °C for 15.0 minutes
TP-2 (GC–MS) (System 1)	150	280	Initial hold of column temperature at 70 °C for 1.0 minute, then the temperature was ramped up to 250 °C at a rate of 30 °C/minute followed by a hold at 250 °C for 15.0 minutes
TP-3 (GC–MS) (System 2)	230	280	Initial hold of column temperature at 70 °C for 1.0 minute, then the temperature was ramped up to 250 °C at a rate of 30 °C/minute followed by a hold at 250 °C for 7.0 minutes
TP-4 (GC–MS) (System 1)	250	280	Initial hold of column temperature at 70 °C for 1.0 minute, ramped up to 150 °C at a rate of 7.5 °C/minute followed by a hold at 150 °C for 2.0 minutes, then ramped up to 250 °C at a rate of 10 °C/minute followed by a hold at 250 °C for 47.0 minutes
TP-5 (GC–IR)	250	250	Initial hold of column temperature at 70 °C for 1.0 minute, then the temperature was ramped up to 250 °C at a rate of 25 °C/minute followed by a hold at 250 °C for 6.80 minutes

3.2. Synthesis of the regioisomeric and homologous aminoketones

3.2.1. Synthesis of the ring substituted aminoketones

3.2.1.1. Synthesis of the methylenedioxyphenyl-aminoketones

A solution of piperonal or 2,3-methylenedioxybenzaldehyde (0.033 mol) in 50 ml of dry diethyl ether was added to a round bottom flask and maintained under an atmosphere of dry nitrogen. Alkylmagnesium halide solution in diethyl ether (0.033 to 0.05 mol) was added with a syringe and the reaction mixture was stirred in ice-acetone bath for two hours. The reaction mixture was quenched using 1N hydrochloric acid (25 ml) and the ether layer was separated, washed with water and dried over anhydrous sodium sulfate. The ether layer was filtered and evaporated under reduced pressure to yield the 2,3- or 3,4-methylenedioxyphenyl-alcohol.

A solution of 2,3- or 3,4-methylenedioxyphenyl-alcohol (0.022 mol) in dilute sulfuric acid (50 ml) was stirred overnight at room temperature with potassium dichromate (0.022 to 0.033 mol). The reaction mixture was diluted with methylene chloride (150 ml), stirred for 30 minutes then, vacuum filtered on a pad of Celite. The organic layer was separated, evaporated under reduced pressure to yield 2,3- or 3,4-methylenedioxyphenyl-ketone, which was purified by flash chromatography 20:80 ethyl acetate-petroleum ether using Sorbtech (Norcross, GA) purity flash cartridges (granular silica gel, 25 g).

The alcohol derivatives with 2,3-methylenedioxy subsititution pattern and the 3,4-methylenedioxy substituted alcohol derivatives with isopropyl or *n*-butyl side-chain were refluxed overnight with potassium dichromate to yield the intermediate ketones.

The 2,3- or 3,4-methylenedioxyphenyl-ketone (0.011 mol) was dissolved in methylene chloride in a round bottom flask. Bromine (0.013 mol) was dripped slowly into the solution and stirred for one hour. The methylene chloride was then evaporated under reduced pressure to yield a yellow to dark red oil of the alpha brominated 2,3- or 3,4-methylenedioxyphenyl-ketone.

A solution of alpha brominated 2,3- or 3,4-methylenedioxyphenyl-ketone (0.002 mol) in (50 ml) methylene chloride was slowly added to a (50 ml) methylene chloride solution of cyclic amine (azetidine, pyrrolidine, piperidine or azepane) (0.0024 mol) in a round bottom flask and the reaction mixture was stirred at room temperature for 2 hours. The methylene chloride was then evaporated under reduced pressure to yield the oily 2,3- or 3,4-methylenedioxyphenyl-aminoketone product. The product was then isolated by solvent extraction and purified by preparative thin layer chromatography (TLC) 20:80 ethyl acetate-petroleum ether using Analtech (Newark, DE) glass backed 20 x 20 cm plates with a 1000 µm layer of silica and an inorganic fluorescent 254 nm indicator.

The bromoketome derivatives with 2,3-methylenedioxy subsititution pattern and the 3,4-methylenedioxy substituted bromoketone derivatives with isopropyl side-chain were refluxed overnight with pyrrolidine to yield the final product. While the 3,4-methylenedioxy substituted bromoketone derivative with *n*-butyl side-chain was refluxed overnight with azetidine to yield the final product.

3.2.1.2. Synthesis of the monomethoxyphenyl-aminoketones

A solution of 2-, 3- or 4-methoxybenzaldehyde (0.037 mol) in 50 ml of dry diethyl ether was added to a round bottom flask and maintained under an atmosphere of dry nitrogen. Alkylmagnesium halide solution in diethyl ether (0.037 to 0.06 mol) was added with a syringe and the reaction mixture was stirred in ice-acetone bath for two hours. The reaction mixture was quenched using 1N hydrochloric acid (25 ml) and the ether layer was separated, washed with water and dried over anhydrous sodium sulfate. The ether layer was filtered and evaporated under reduced pressure to yield the 2-, 3- or 4-methoxyphenyl-alcohol.

The next steps were accomplished using the same protocol described in the previous section (see Section 3.2.1.1.) and pyrrolidine in the last step. The final nine compounds were purified using acid base extraction to yield the free bases.

3.2.1.3. Synthesis of the dimethoxyphenyl-aminoketones (dimethoxypyrovalerones, DMPV)

A solution of 2,3-, 2,4- 2,5- 2,6- 3,4- or 3,5-dimethoxybenzaldehyde (0.03 mol) in 50 ml of dry diethyl ether was added to a round bottom flask and maintained under an atmosphere of dry nitrogen. Solution of *n*-butylmagnesium chloride in diethyl ether (0.03 to 0.05 mol) was added with a syringe and the reaction mixture was stirred in ice-acetone bath for two hours. The reaction mixture was quenched using 1N hydrochloric acid (25 ml) and the ether layer was separated, washed with water and dried over anhydrous sodium sulfate. The ether layer was filtered and evaporated under reduced pressure to yield the dimethoxyphenyl-alcohol.

The next steps were accomplished using the same protocol described in the previous section (see Section 3.2.1.1.) with minor changes of the conditions. In the oxidation step, the regioisomeric 2,6- and 3,5-dimethoxyphenyl-alcohols were refluxed overnight with potassium

dichromate to yield the intermediate ketones. The alpha bromination of 2,6-dimethoxyphenyl-ketone was performed using carbon tetrachloride. Last, dry tetrahydrofuran was used as a solvent for the neucleophilic substitution reaction with pyrrolidine at room temperature. However, the alpha brominated 2,6-dimethoxyphenyl-ketone was refluxed overnight with pyrrolidine to yield the final product.

The product was then isolated by solvent extraction and purified by preparative thin layer chromatography (TLC) 20:80 ethyl acetate-petroleum ether using Analtech (Newark, DE) glass backed 20 x 20 cm plates with a 1000 µm layer of silica and an inorganic fluorescent 254 nm indicator.

3.2.2. Synthesis of the side-chain regioisomeric cathinone derivatives (flakka and iso-flakka)

These regiosiomers were synthesized from the commercially available intermediate ketones, valerophenone and isovalerophenone or the precursor benzaldehyde. However, the isopropyl side-chain substituted alcohol was refluxed with potassium dichromate to yield the intermediate ketone. Furthermore, the alpha brominated intermediate ketone with isopropyl side-chain was refluxed overnight with pyrrolidine to yield the final product, isoflakka.

The product was then isolated by solvent extraction and purified by preparative thin layer chromatography (TLC) 20:80 ethyl acetate-petroleum ether using Analtech (Newark, DE) glass backed 20 x 20 cm plates with a 1000 µm layer of silica and an inorganic fluorescent 254 nm indicator.

3.2.3. Synthesis of the aminoalcohol regioisomeric compounds

The 2,3- and 3,4-methylenedioxypheny-aminoalcohol derivatives were prepared by lithium aluminum hydride reduction of 2,3-MDPV and 3,4-MDPV, respectively. Dry tetrahydrofuran (30 ml) was added dropwise to a round bottom flask containing lithium aluminum hydride (0.0018 mol) under nitrogen followed by the dropwise addition of 2,3-MDPV or 3,4-MDPV (0.0006 mol) in dry tetrahydrofuran (30 ml). The mixture was refluxed for one hour and then stirred at room temperature overnight. The reaction mixture was quenched using 1 ml of water and 5 ml of tetrahydrofuran, followed by the addition of sodium hydroxide (2 ml, 10%) and 3 ml of water. The mixture was then washed with tetrahydrofuran (10 ml), filtered and evaporated under reduced pressure to yield the oily 2,3- or 3,4-methylenedioxyphenyl-aminoalcohol product. The product was then isolated by solvent extraction and purified by preparative thin layer chromatography (TLC) 20:80 ethyl acetate-petroleum ether using Analtech (Newark, DE) glass backed 20 x 20 cm plates with a 1000 µm layer of silica and an inorganic fluorescent 254 nm indicator.

3.2.4. Synthesis of the desoxy regioisomeric compounds

Sodium amide (0.05 mol) was added dropwise to an ice cooled mixture of piperonal or 2,3-methylenedioxybenzaldehyde (0.033mol) and 2-bromoalkanoic acid ethyl esters (0.033 mol) in dry benzene (50 ml). The mixture was allowed to stir for two hours at 15-20 °C. The reddish colored reaction mixture was then poured over crushed ice and the organic layer was separated. The aqueous layer was washed with benzene (3 x 20 ml). The combined organic extract was washed with distilled water (3 x 30 ml) then dried over anhydrous sodium sulfate. Benzene was filtered and evaporated under reduced pressure to yield crude glycidate ester (β-2,3- or 3,4-methylenedioxyphenyl-α-alkyl glycidic ester) as yellow oils (Darzens reaction).

Crude glycidate ster (0.033mol) was dissolved in ethanol (30 ml) and sodium hydroxide (0.033mol) was added slowly followed by the addition of distilled water (5 ml). The mixture was stirred overnight at room temperature to give white crystals of glycidic acid sodium salt that were collected by filtration under reduced pressure. Crystals were washed with ether and methanol (50 ml each) and air-dried. The glycidic acid sodium salt was added to 50 ml 2N hydrochloric acid solution and the mixture was heated for 1.5 hour. An oily layer of the intermediate ketone was formed. The desired ketone was extracted with ether (70 ml) and the ether layer was washed once with water and dried over anhydrous sodium sulfate. The ether was filtered and evaporated under reduced pressure to give a yellow oil of intermediate ketone.

The intermediate ketone (0.003 mol) along with cyclic amine (azetidine, pyrrolidine, piperidine or azepane) (0.006 mol) and sodium cyanoborohydride (0.009 mol) were dissolved in methanol (50 ml) and the reaction mixture was refluxed overnight. Methanol was evaporated under reduced pressure and the resulting residue was stirred in acidic water (50 ml) at room temperature. The aqueous layer was washed with ether (3 x 20 ml) and was alkalinized using sodium hydroxide pellets. The aqueous layer was then extracted with methylene chloride (3 x 30 ml) and the organic layer was dried over anhydrous sodium sulfate. Methylene chloride was filtered and evaporated under reduced pressure to give a yellow oil of the desired desoxyamine final product. The product was purified by preparative thin layer chromatography (TLC) 20:80 ethyl acetate-petroleum ether using Analtech (Newark, DE) glass backed 20 x 20 cm plates with a 1000 µm layer of silica and an inorganic fluorescent 254 nm indicator.

Summary

This project has focused on issues of resolution and discriminatory capabilities in controlled substance analysis providing data to increase reliability and selectivity for forensic evidence and analytical data on new analytes of the so-called bath salt-type drugs of abuse. The overall goal of these studies was to provide an analytical framework for the identification of individual substituted cathinones to the exclusion of all other possible isomeric and homologous forms of these compounds. A number of aminoketones have appeared on the illicit drug market in recent years including methcathinone, mephedrone, methylone and MDPV (3,4-methylenedioxypyrovalerone). These substances represent a variety of aromatic ring substituent, hydrocarbon side-chain and amino group modifications of the basic cathinone molecular skeleton.

Exploration and designer development in the aminoketone derivatives similar to those reported for amphetamine and related phenethylamines is anticipated to continue for many years. Production of cathinone derivatives can be based on common readily available precursor chemicals. These numerous precursor substances are commercially available and would not prevent the further clandestine/designer exploration of this group of compounds. This suggested a strong need for a thorough and systematic investigation of the forensic chemistry of these substituted aminoketones.

The broad objective of this research was to improve the specificity, selectivity and reliability of analytical methods used to identify ring substituted aminoketones and related compounds. This improvement comes from methods, which allow the forensic analyst to identify specific regioisomeric forms of substituted aminoketones among many isomers of mass spectral equivalence. Mass spectrometry is the most common method of confirmation in forensic drug analysis. This project provides methodology and analytical data to discriminate between those regioisomeric molecules having the same molecular weight and major fragments of equivalent mass (i.e. identical mass spectra). Furthermore, this work has anticipated the future appearance of some designer aminoketones and developed reference data and analytical reference standards for these compounds.

The initial phase of this work was the organic synthesis of aminoketones of varying aromatic ring substituents, hydrocarbon side-chains and amino groups. This included the synthesis of selected deuterium labeled compounds as needed for MS fragmentation confirmation. The analytical phases consisted of chemical characterization, using tools common to forensic science labs such as MS and IR and these studies were carried out on each of the compounds. The chromatographic retention properties for each series of isomers were evaluated by gas chromatographic techniques on a variety of stationary phases to establish a structure-retention relationship for the regioisomeric aminoketones on selected chromatographic stationary phases.

The use of multiple and complementary analytical methods such as GC–MS, GC–MS/MS and GC–IR were necessary for the specific identification of these cathinone derivatives. These techniques were used to differentiate among different groups (regioisomers and homologs) of substituted aminoketone-type drugs (cathinone derivatives). The MS data provided focus on the

dimethoxy, methylenedioxy as well as monomethoxy substitution patterns and the vapor phase infrared spectra clearly differentiated among each of these aromatic ring substitution patterns. The side-chain and cyclic amino group containing regioisomers and the side-chain *n*-propyl and isopropyl containing regioisomers each yielded equivalent iminium cation base peaks and IR spectra. However, these equivalent iminium cation base peaks (*m/z* 126) yielded characteristic product ions in the MS/MS experiments. The product ions from the *m/z* 126 iminium cation produced by the side-chain and cyclic amino group containing regioisomeric desoxy phenethylamines were consistent with the corresponding aminoketone analogues. The vapor phase infrared spectra of the desoxy phenethylamines and the aminoalcohol derivatives displayed characteristic absorption bands specific for those compounds. These studies suggested the strong need for multiple and complementary analytical methods such as GC–MS, GC–MS/MS and GC–IR.

References

AAPCC (2013) American Association of Poison Control Centers: Bath salts. Available in http://www.aapcc.org/alerts/bath-salts/

Aarde, S.M., Angrish, D., Barlow, D.J. *et al*. Mephedrone (4-methylmethcathinone) supports intravenous self-administration in Sprague-Dawley and Wistar rats. Addict. Biol. 18 (2013a) 786–799.

Aarde, S.M., Huang, P.K., Creehan, K.M., Dickerson, T.J., Taffe, M.A. The novel recreational drug 3,4-methylenedioxypyrovalerone (MDPV) is a potentpsychomotor stimulant: Self-administration and locomotor activity in rats. Neuropharmacology 71 (2013b) 130–140.

Abdel-Hay, K.M., DeRuiter, J., Clark, C.R. GC–MS and GC–IRD studies on the six ring regioisomeric dimethoxybenzylpiperazines (DMBPs). Drug Test. Anal. 5 (2013) 560–572.

Aleksandrov, A.L. Oxidation of amines by molecular oxygen, Bull. Acad. Sci. USSR Div. Chem. Sci. 29 (1980) 1740–1744.

Alem, A., Kebede, D., Kullgren, G. The prevalence and socio-demographic correlates of khat chewing in Butajira, Ethiopia. Acta. Psychiatr. Scand. Suppl. 397 (1999) 84–91.

Al-Motarreb, A., Baker, K., Broadley, K.J. Khat: Pharmacological and medical aspects and its social use in Yemen. Phytother. Res. 16 (2002) 403–413.

Al-Mugahed, L. Khat chewing in Yemen: Turning over a new leaf. Bull. World Health Organ. 86 (2008) 741.

Archer, R.P. Fluoromethcathinone, a new substance of abuse. Forensic Sci. Int. 185 (2009) 10–20.

Arunotayanun, W., Gibbons, S. Natural product ‘legal highs’. Nat. Prod. Rep. 29 (2012) 1304–1316.

Awad, T., Belal, T., DeRuiter, J., Kramer, K., Clark, C.R. Comparison of GC–MS and GC–IRD methods for the differentiation of methamphetamine and regioisomeric substances. Forensic Sci. Int. 185 (2009) 67–77.

Balint, E.E., Falkay, G., Balint, G.A. Khat—a controversial plant. Wien Klin Wochenschr 121 (2009) 604–614.

Baumann, M.H., Ayestas Jr, M.A., Partilla, J.S. *et al*. The designer methcathinone analogs, mephedrone and methylone, are substrates for monoamine transporters in brain tissue. Neuropsychopharmacol. Off. Publ. Am. Coll. Neuropsychopharmacol. 37 (2012) 1192–1203.

Baumann, M.H., Partilla, J.S., Lehner, K.R. Psychoactive "bath salts": Not so soothing. Eur. J. Pharmacol. 698 (2013a) 1–5.

Baumann, M.H., Partilla, J.S., Lehner, K.R. *et al*. Powerful cocaine-like actions of 3,4-Methylenedioxypyrovalerone (MDPV), a principal constituent of psychoactive 'bath salts' products. Neuropsychopharmacol. Off. Publ. Am. Coll. Neuropsychopharmacol. 38 (2013b) 552–562.

Bentur, Y., Bloom-Krasik, A., Raikhlin-Eisenkraft, B. Illicit cathinone ("Hagigat") poisoning. Clin. Toxicol. 46 (2008) 206–210.

Brandt, S.D., Sumnall, H.R., Measham, F., Cole, J. Second generation mephedrone. The confusing case of NRG-1. Bmj. 341 (2010a) c3564.

Brandt, S.D., Wootton, R.C., De Paoli, G., Freeman, S. The naphyrone story: The alpha or beta-naphthyl isomer? Drug Test. Anal. 2 (2010b) 496–502.

Brenneisen, R., Fisch, H.U., Koelbing, U., Geisshusler, S., Kalix, P. Amphetamine-like effects in humans of the khat alkaloid cathinone. Br. J. Clin. Pharmacol. 30 (1990) 825–828.

Brenneisen, R., Geisshusler, S., Schorno, X. Metabolism of cathinone to (−)-norephedrine and (−)-norpseudoephedrine. The Journal of pharmacy and pharmacology 38 (1986) 298–300.

Bretteville-Jensen, A., Tuv, S., Bilgrei, O., Fjeld, B., Bachs, L. Synthetic cannabinoids and cathinones: Prevalence and markets. Forensic Sci. Rev. 25 (2013) 7–26.

Cameron, K.N., Kolanos, R., Solis Jr, E., Glennon, R.A., De Felice, L.J. Bath salts components mephedrone and methylenedioxypyrovalerone (MDPV) act synergistically at the human dopamine transporter. Br. J. Pharmacol. 168 (2013) 1750–1757.

Canning, H., Goff, D., Leach, M.J., Miller, A.A., Tateson, J.E., Wheatley, P.L. The involvement of dopamine in the central actions of bupropion, a new antidepressant [proceedings]. Br. J. Pharmacol. 66 (1979) 104P–105P.

Casale, J.F., Hays, P.A., Klein, R.F.X. Synthesis and characterization of the 2,3-methylenedioxyamphetamines, J. Forensic Sci. 40 (1995) 391–400.

Chapman, M.H., Kajihara, M., Borges, G. *et al*. Severe, acute liver injury and khat leaves. N. Engl. J. Med. 362 (2010) 1642–1644.

Clark, C.R., DeRuiter, J., Valaer, A., Noggle, F.T. Gas chromatographic-mass spectrometric and liquid chromatographic analysis of designer butanamines related to MDMA. J. Chromatogr. Sci. 33 (1995) 328–337.

Collins, M. Some new psychoactive substances: Precursor chemicals and synthesis-driven end-products. Drug Test. Anal. 3 (2011) 404–416.

Concheiro, M., Anizan, S., Ellefsen, K., Huestis, M.A. Simultaneous quantification of 28 synthetic cathinones and metabolites in urine by liquid chromatography-high resolution mass spectrometry. Anal. Bioanal. Chem. 405 (2013) 9437–9448.

Coppola, M., Mondola, R. Synthetic cathinones: chemistry, pharmacology and toxicology of a new class of designer drugs of abuse marketed as "bath salts" or "plant food". Toxicol. Lett. 211 (2012) 144–149.

Corkery, J.M., Schifano, F., Oyefeso, A. *et al.* 'Bundle of fun'or'bunch of problems'? Case series of khat-related deaths in the UK. Drugs Educ. Prev. Policy 18 (2011) 408–425.

Cox, G., Rampes, H. Adverse effects of khat: A review. Adv. Psychiatr. Treat. 9 (2003) 456–463.

Cozzi, N.V., Sievert, M.K., Shulgin, A.T., Jacob 3rd, P., Ruoho, A.E. Inhibition of plasma membrane monoamine transporters by beta-ketoamphetamines. Eur. J. Pharmacol. 381 (1999) 63–69.

Dal Cason, T.A. The characterization of some 3,4-methylenedioxycathinone (MDCATH) homologs. Forensic Sci. Int. 87 (1997) 9–53.

Dal Cason, T.A., Young, R., Glennon, R.A. Cathinone: An investigation of several *N*-alkyl and methylenedioxy-substituted analogs. Pharmacol. Biochem. Behav. 58 (1997) 1109–1116.

Davies, S., Wood, D.M., Smith, G. *et al.* Purchasing 'legal highs' on the Internet–is there consistency in what you get? QJM. Mon. J. Assoc. Phys. 103 (2010) 489–493.

de Castro, A., Lendoiro, E., Fernández-Vega, H., Steinmeyer, S., López-Rivadulla, M., Cruz, A. Liquid chromatography tandem mass spectrometry determination of selected synthetic cathinones and two piperazines in oral fluid. Cross reactivity study with an on-site immunoassay device. J. Chromatogr. A 1374 (2014) 93–101.

Deluca, P., Schifano, F., Davey, Z., Corazza, O., Di Furia, L. Group PWMR (2009) Mephedrone report. Available at http://www.psychonautproject.eu/

Dhaifalah, I., Santavy, J. Khat habit and its health effect. A natural amphetamine. Biomedical papers of the Medical Faculty of the University Palacky, Olomouc, Czechoslovakia 148 (2004) 11–15.

Drug Enforcement Administration DoJ Schedules of controlled substances: Temporary placement of three synthetic cathinones in Schedule I. Final order. Fed. Reg. 76 (2011) 65371–65375.

Drug Enforcement Administration DoJ Schedules of controlled substances: Extension of temporary placement of methylone into schedule I of the controlled substances Act. Final order. Fed. Reg. 77 (2012) 64032–64033.

EMCDDA (2012) The EMCDDA annual report 2012: The state of the drugs problem in Europe. Euro. Surveill. doi:10.2810/64775. Available at http://www.emcdda.europa.eu/

EMCDDA (2018) The EMCDDA annual report 2018: Trends and developments. Euro. Surveill. doi:10.2810/688395. Available at http://www.emcdda.europa.eu/

EMCDDA-Europol (2009) EMCDDA–Europol 2008 annual report on the implementation of council decision 2005/387/JHA. Available at http://www.emcdda.europa.eu/

EMCDDA-Europol (2010) EMCDDA–Europol 2009 annual report on the implementation of council decision 2005/387/JHA. Available at http://www.emcdda.europa.eu/

EMCDDA-Europol (2011) EMCDDA–Europol 2010 annual report on the implementation of council decision 2005/387/JHA. Available at http://www.emcdda.europa.eu/

Emerson, T.S., Cisek, J.E. Methcathinone: A Russian designer amphetamine infiltrates the rural midwest. Ann. Emerg. Med. 22 (1993) 1897–1903.

Fasanmade, A., Kwok, E., Newman, L. Oral squamous cell carcinoma associated with khat chewing. Oral Surg. Oral Med. Oral Pathol. Oral Radiol. Endod. 104 (2007) e53–e55.

Fass, J.A., Fass, A.D., Garcia, A.S. Synthetic cathinones (bath salts): Legal status and patterns of abuse. Ann. Pharmacother. 46 (2012) 436–441.

Fluckiger, F.A., Gerock, J.E. Contribution to the knowledge of catha leaves. Pharm. J. Transvaal. 18 (1887) 221–224.

Gardos, G., Cole, J.O. Evaluation of pyrovalerone in chronically fatigued volunteers. Curr. Ther. Res. Clin. Exp. 13 (1971) 631–635.

Garrett, G., Sweeney, M. The serotonin syndrome as a result of mephedrone toxicity. BMJ. Case Rep. (2010) 1–5.

German, C.L., Fleckenstein, A.E., Hanson, G.R. Bath salts and synthetic cathinones: An emerging designer drug phenomenon. Life Sci. 97 (2014) 2–8.

Gezon, L.L. Drug crops and food security: The effects of khat on lives and livelihoods in northern madagascar. Cult. Agric. Food Environ. 34 (2012) 124–135.

Gibbons, S., Zloh, M. An analysis of the ‘legal high’ mephedrone. Bioorg. Med. Chem. Lett., 20 (2010) 4135–4139.

Gorun, G., Dermengiu, D., Curcă, C., Hostiuc, S., Ioan, B., Luta, V. Toxicological drivers issues in “legal highs” use. Romanian J. Legal Med. 18 (2010) 272.

Hyde, J., Browning, E., Adams, R. Synthetic homologs of d, l-ephedrine. J. Am. Chem. Soc. 50 (1928) 2287–2292.

Iqbal, M., Monaghan, T., Redmond, J. Manganese toxicity with ephedrone abuse manifesting as Parkinsonism: A case report. J. Med. Case Rep. 6 (2012) 52.

James, D., Adams, R.D., Spears, R. *et al*. Clinical characteristics of mephedrone toxicity reported to the U.K. National Poisons Information Service. Emerg. Med. J. EMJ. 28 (2011) 686–689.

Jerry, J., Collins, G., Streem, D. Synthetic legal intoxicating drugs: The emerging ‘incense’ and ‘bath salt’ phenomenon. Clevel. Clin. J. Med. 79 (2012) 258–264.

Kalix, P. A comparison of the catecholamine releasing effect of the khat alkaloids (−)-cathinone and (+)-norpseudoephedrine. Drug Alcohol Depend. 11 (1983) 395–401.

Kalix, P. The pharmacology of psychoactive alkaloids from ephedra and catha. J. Ethnopharmacol. 32 (1991) 201–208.

Kalix, P. Cathinone, a natural amphetamine. Pharmacol. Toxicol. 70 (1992) 77–86.

Kalix, P., Braenden, O. Pharmacological aspects of the chewing of khat leaves. Pharmacol. Rev. 37 (1985) 149–164.

Kalix, P., Khan, I. Khat: An amphetamine-like plant material. Bull. World Health Organ. 62 (1984) 681–686.

Kamata, H.T., Shima, N., Zaitsu, K. *et al*. Metabolism of the recently encountered designer drug, methylone, in humans and rats. Xenobiotica. Fate Foreign Compd. Biol. Syst. 36 (2006) 709–723.

Karila, L., Reynaud, M. GHB and synthetic cathinones: Clinical effects and potential consequences. Drug Test. Anal. 3 (2011) 552–559.

Katz, D.P., Bhattacharya, D., Bhattacharya, S., DeRuiter, J., Clark, C.R., Suppiramaniam, V., Dhanasekaran, M. Synthetic cathinones: “A khat and mouse game”. Tox. Letters 229 (2014) 349–356.

Kavanagh, P., O’Brien, J., Fox, J., O’Donnell, C., Christie, R., Power, J.D., McDermott, S.D. The analysis of substituted cathinones. Part 3. Synthesis and characterisation of 2,3-methylenedioxy substituted cathinones, Forensic Sci. Int. 216 (2012) 19–28.

Kelly, J.P. Cathinone derivatives: A review of their chemistry, pharmacology and toxicology. Drug Test. Anal. 3 (2011) 439–453.

Khreit, O.I., Grant, M.H., Zhang, T., Henderson, C., Watson, D.G., Sutcliffe, O.B. Elucidation of the Phase I and Phase II metabolic pathways of (±)-4′-methylmethcathinone (4-MMC) and (±)-4′-(trifluoromethyl)methcathinone (4-TFMMC) in rat liver hepatocytes using LC-MS and LC-MS(2). J. Pharm. Biomed. Anal. 72 (2013) 177–185.

Klein, A., Jelsma, M., Metaal, P. Chewing over Khat prohibition. In: The globalisation of control and regulatio.n of an ancient stimulant. Transnational Institute Series on Legislative Reform of Drug Policies No. 17. Transnational Institute, Amsterdam, 2012.

Kriikku, P., Wilhelm, L., Schwarz, O., Rintatalo, J. New designer drug of abuse: 3,4-Methylenedioxypyrovalerone (MDPV). Findings from apprehended drivers in Finland. Forensic Sci. Int. 210 (2011) 195–200.

Levine, M., Levitan, R., Skolnik, A. Compartment syndrome after "bath salts" use: A case series. Ann. Emerg. Med. 61 (2013) 480–483.

Lewin, A.H., Seltzman, H.H., Carroll, F.I., Mascarella, S.W., Reddy, P.A. Emergence and properties of spice and bath salts: A medicinal chemistry prospective. Life Sci. 97 (2014) 9–19.

Lindsay, L., White, M.L. Herbal marijuana alternatives and bath salts—"barely legal" toxic highs. Clin. Pediatr. Emerg. Med. 13 (2012) 283–291.

Lopez-Arnau, R., Martinez-Clemente, J., Pubill, D., Escubedo, E., Camarasa, J. Comparative neuropharmacology of three psychostimulant cathinone derivatives: Butylone, mephedrone and methylone. Br. J. Pharmacol. 167 (2012) 407–420.

Marinetti, L.J., Antonides, H.M. Analysis of synthetic cathinones commonly found in bath salts in human performance and postmortem toxicology: Method development, drug distribution and interpretation of results. J. Anal. Toxicol. 37 (2013) 135–146.

Marusich, J.A., Grant, K.R., Blough, B.E., Wiley, J.L. Effects of synthetic cathinones contained in "bath salts" on motor behavior and a functional observational battery in mice. Neurotoxicology 33 (2012) 1305–1313.

Mas-Morey, P., Visser, M., Winkelmolen, L., Touw, D. Clinical toxicology and management of intoxications with synthetic cathinones ("bath salts"). J. Pharm. Pract. 26 (2012) 353–357.

Mathys, K., Brenneisen, R. Determination of (S)-(−)-cathinone and its metabolites (R, S)-(−)-norephedrine and (R, R)-(−)- norpseudoephedrine in urine by high-performance liquid chromatography with photodiode-array detection. J. Chromatogr. 593 (1992) 79–85.

Meltzer, P.C., Butler, D., Deschamps, J.R., Madras, B.K. 1-(4-Methylphenyl)-2-pyrrolidin-1-yl-pentan-1-one (Pyrovalerone) analogues: A promising class of monoamine uptake inhibitors. J. Med. Chem. 49 (2006) 1420–1432.

Meng, H., Cao, J., Kang, J. *et al*. Mephedrone, a new designer drug of abuse, produces acute hemodynamic effects in the rat. Toxicol. Lett. 208 (2012) 62–68.

Meyer, M.R., Du, P., Schuster, F., Maurer, H.H. Studies on the metabolism of the alpha-pyrrolidinophenone designer drug methylenedioxy-pyrovalerone (MDPV) in rat and human urine and human liver microsomes using GC–MS and LC-high-resolution MS and its detectability in urine by GC–MS. J. Mass Spectrom. JMS. 45 (2010a) 1426–1442.

Meyer, M.R., Vollmar, C., Schwaninger, A.E., Wolf, E., Maurer, H.H. New cathinone-derived designer drugs 3-bromomethcathinone and 3-fluoromethcathinone: Studies on their metabolism in rat urine and human liver microsomes using GC–MS and LC-high-resolution MS and their detectability in urine. J. Mass Spectrom. JMS. 47 (2012) 253–262.

Meyer, M.R., Wilhelm, J., Peters, F.T., Maurer, H.H. Beta-keto amphetamines: Studies on the metabolism of the designer drug mephedrone and toxicological detection of mephedrone, butylone, and methylone in urine using gas chromatography-mass spectrometry. Anal. Bioanal. Chem. 397 (2010b) 1225–1233.

Motbey, C.P., Clemens, K.J., Apetz, N. *et al*. High levels of intravenous mephedrone (4-methylmethcathinone) self-administration in rats: Neural consequences and comparison with methamphetamine. J. Psychopharmacol. 27 (2013) 823–836.

Nencini, P., Amiconi, G., Befani, O., Abdullahi, M.A., Anania, M.C. Possible involvement of amine oxidase inhibition in the sympathetic activation induced by khat (Catha edulis) chewing in humans. J. Ethnopharmacol. 11 (1984) 79–86.

Nichols, D.E., Hoffman, A.J., Oberlender, R.A., Jacob III, P., Shulgin, A.T. Derivatives of 1-(1,3-benzodioxol5-yl)-2-butanamine: Representatives of a novel therapeutic class. J. Med. Chem. 29 (1986) 2009–2015.

Noggle, F.T., DeRuiter, J., Valaer, A., Clark, C.R. GC–MS analysis of methcathinone and its major decomposition product, Microgram 27 (1994) 106–118.

Osorio-Olivares, M., Rezende, M.C., Sepulveda-Boza, S., Cassels, B.K., Fierro, A. MAO inhibition by arylisopropylamines: The effect of oxygen substituents at the beta-position. Bioorg. Med. Chem. 12 (2004) 4055–4066.

Paul, B.D., Cole, K.A. Cathinone (Khat) and methcathinone (CAT) in urine specimens: A gas chromatographic-mass spectrometric detection procedure. J. Anal. Toxicol. 25 (2001) 525–530.

Pawlik, E., Plasser, G., Mahler, H., Daldrup, T. Studies on the phase I metabolism of the new designer drug 3-fluoromethcathinone using rabbit liver slices. Int. J. Legal Med. 126 (2012) 231–240.

Pedersen, A.J., Reitzel, L.A., Johansen, S.S., Linnet, K. *In vitro* metabolism studies on mephedrone and analysis of forensic cases. Drug Test. Anal. 5 (2013) 430–438.

Peters, F.T., Meyer, M.R., Fritschi, G., Maurer, H.H. Studies on the metabolism and toxicological detection of the new designer drug 4′-methyl-alpha-pyrrolidinobutyrophenone (MPBP) in rat urine using gas chromatography-mass spectrometry. J. Chromatogr. B Anal. Technol. Biomed. Life Sci. 824 (2005) 81–91.

Prosser, J.M., Nelson, L.S. The toxicology of bath salts: A review of synthetic cathinones. J. Med. Toxicol. Off. J. Am. Coll. Med. Toxicol. 8 (2012) 33–42.

Regester, L.E., Chmiel, J.D., Holler, J.M., Vorce, S.P., Levine, B., Bosy, T.Z. Determination of designer drug cross-reactivity on five commercial immunoassay screening kits. J. Anal. Toxicol. 39 (2015) 144–151.

Roelandt, P., George, C., d'Heygere, F. *et al*. Acute liver failure secondary to khat (< i > Catha edulis </i >)–induced necrotic hepatitis requiring liver transplantation: Case report. Transpl. Proc. 43 (2011) 3493–3495.

Saal, C. Pharmaceutical Salts Optimization of Solubility or Even More? American Pharmaceutical Review, (hhttp://www.americanpharmaceuticalreview.com/Fea- tured-Articles/117009-Pharmaceutical-Salts-Optimization-of-Solubility-or- Even-More/). 2010.

Sakitama, K., Ozawa, Y., Aoto, N., Nakamura, K., Ishikawa, M. Pharmacological properties of NK433, a new centrally acting muscle relaxant. Eur. J. Pharmacol. 273 (1995) 47–56.

Sammler, E.M., Foley, P.L., Lauder, G.D., Wilson, S.J., Goudie, A.R., O'Riordan, J.I. A harmless high? Lancet 376 (2010) 742.

Sauer, C., Peters, F.T., Haas, C., Meyer, M.R., Fritschi, G., Maurer, H.H. New designer drug alpha-pyrrolidinovalerophenone (PVP): Studies on its metabolism and toxicological detection in rat urine using gas chromatographic/mass spectrometric techniques. J. Mass Spectrom. JMS. 44 (2009) 952–964.

Schifano, F., Albanese, A., Fergus, S. *et al*. Mephedrone (4-methylmethcathinone; 'meow meow'): Chemical, pharmacological and clinical issues. Psychopharmacology 214 (2011) 593–602.

Shima, N., Katagi, M., Tsuchihashi, H. Direct analysis of conjugate metabolites of methamphetamine, 3,4-methylenedioxymethamphetamine, and their designer drugs in biological fluids. J. Health Sci. 55 (2009) 495–502.

Shortall, S.E., Green, A.R., Swift, K.M., Fone, K.C., King, M.V. Differential effects of cathinone compounds and MDMA on body temperature in the rat, and pharmacological characterization of mephedrone-induced hypothermia. Br. J. Pharmacol. 168 (2013) 966–977.

Siegel, G.J., Agranoff, B.W., Albers, R.W., Fisher, S.K., Uhler, M.D. (1999) Storage and release of catecholamines. In: Siegel, G.J., Fisher, S.K., Uhler, M.D., Albers, R.W., Agranoff, B.W. (eds) Basic neurochemistry: Molecular, cellular and medical aspects, 6th edn. Lippincott Williams & Wilkins, Philadelphia.

Simmler, L.D., Buser, T.A., Donzelli, M. *et al*. Pharmacological characterization of designer cathinones *in vitro*. Br. J. Pharmacol. 168 (2013) 458–470.

Smith, L.W., Thaxton-Weissenfluh, A., Abiedalla, Y., DeRuiter, J., Smith, F., Clark, C.R. Correlation of vapor phase infrared spectra and regioisomeric structure in synthetic cannabinoids. Spectrochim. Acta A 196 (2018) 375–384.

Soine, W.H., Shark, R.E., Agee, D.T. Differentiation of 2,3-methylenedioxyamphetamine from 3,4-methylenedioxyamphetamine. J. Forensic Sci. 28 (1983) 386–390.

Sparago, M., Wlos, J., Yuan, J. *et al*. Neurotoxic and pharmacologic studies on enantiomers of the *N*-methylated analog of cathinone (methcathinone): A new drug of abuse. J. Pharmacol. Exp. Ther. 279 (1996) 1043–1052.

Spyker, D.A., Thomas, S., Bateman, D.N. *et al*. International trends in designer amphetamine abuse in UK and US, 2009–2012. Clin. Toxicol. 50 (2012) 141.

Strano-Rossi, S., Cadwallader, A.B., de la Torre, X., Botre, F. Toxicological determination and *in vitro* metabolism of the designer drug methylenedioxypyrovalerone (MDPV) by gas chromatography/mass spectrometry and liquid chromatography/quadrupole time-of-flight mass spectrometry. Rapid Commun. Mass spectrum. RCM. 24 (2010) 2706–2714.

Swortwood, M.J., Hearn, W.L., deCaprio, A.P. Cross-reactivity of designer drugs, including cathinone derivatives, in commercial enzyme-linked immunosorbent assays. Drug Test. Anal. 6 (2014) 716–727.

Toennes, S.W., Kauert, G.F. Excretion and detection of cathinone, cathine, and phenylpropanolamine in urine after kath chewing. Clin. Chem. 48 (2002) 1715–1719.

Truscott, S.M., Crittenden, N.E., Shaw, M.A., Middleberg, R.A., Jortani, S.A. Violent Behavior and Hallucination in a 32-Year-Old Patient. Clin. Chem. 59 (2013) 612–615.

Tsujikawa, K., Kuwayama, K., Kanamori, T., Iwata, Y.T., Inoue, H. Thermal degradation of α-pyrrolidinopentiophenone during injection in gas chromatography/mass spectrometry. Forensic Sci. Int. 231 (2013a) 296–299.

Tsujikawa, K., Mikuma, T., Kuwayama, K., Miyaguchi, H., Kanamori, T., Iwata, Y.T., Inoue, H. Identification and differentiation of methcathinone analogs by gas chromatography-mass spectrometry, Drug Test. Anal. 5 (2013b) 670–677.

Tsujikawa, K., Yamamuro, T., Kuwayama, K., Kanamori, T., Iwata, Y.T., Inoue, H. Instability of the hydrochloride salts of cathinone derivatives in air. Forensic Sci. Int. 248 (2015) 48–54.

United Nations. Etudes sur la composition chimique du khat: Recherches sur la fraction phénylalkylamine. UN document MNAR/11/1975.

United Nations Office on Drugs and Crime, World Drug Report 2016 (United Nations publication, Sales No. E.16.XI.7). ISBN: 978-92-1-148286-7, 52–61.

U. S. Department of Justice, National Drug Intelligence Center (NDIC), Situation report, synthetic cathinones (bath salts): An emerging domestic threat, July 2011.

Valente, M.J., Guedes de Pinho, P., Bastos, M., Carvalho, F., Carvalho, M. Khat and synthetic cathinones: A review. Arch. Toxicol. 88 (2014) 15–45.

Van Hout, M.C., Brennan, R. Plant food for thought: A qualitative study of mephedrone use in Ireland. Drugs Educ. Prev. Policy 18 (2011) 371–381.

Varlibas, F., Delipoyraz, I., Yuksel, G., Filiz, G., Tireli, H., Gecim, N.O. Neurotoxicity following chronic intravenous use of "Russian cocktail". Clin. Toxicol. 47 (2009) 157–160.

Wang, C.C., Hartmann-Fischbach, P., Krueger, T.R., Wells, T.L., Feineman, A.R., Compton, J.C. Rapid and sensitive analysis of 3,4-methylenedioxypyrovalerone in equine plasma using liquid chromatography–tandem mass spectrometry, J. Anal. Toxicol. 36 (2012) 327–333.

Warrick, B.J., Wilson, J., Hedge, M., Freeman, S., Leonard, K., Aaron, C. Lethal serotonin syndrome after methylone and butylone ingestion. J. Med. Toxicol. Off. J. Am. Coll. Med. Toxicol. 8 (2012) 65–68.

Westphal, F., Junge, T., Rosner, P., Fritschi, G., Klein, B., Girreser, U. Mass spectral and NMR spectral data of two new designer drugs with an alpha-aminophenone structure: 4′-methyl-alpha-pyrrolidinohexanophenone and 4′-methyl-alpha-pyrrolidinobutyrophenone. Forensic Sci. Int. 169 (2007) 32–42.

Westphal, F., Junge, T., Rosner, P., Sonnichsen, F., Schuster, F. Mass and NMR spectroscopic characterization of 3,4- methylenedioxypyrovalerone: A designer drug with alpha-pyrrolidinophenone structure. Forensic Sci. Int. 190 (2009) 1–8.

Westphal, F., Rosner, P., Junge, T. Differentiation of regioisomeric ring-substituted fluorophenethylamines with product ion spectrometry. Forensic Sci. Int. 194 (2010) 53–59.

Wolfes, O. Über das Vorkommen von d-nor-iso-Ephedrin in *Catha edulis*. Arch. Pharm. 268 (1930) 81–83.

Wood, D.M., Davies, S., Greene, S.L. *et al*. Case series of individuals with analytically confirmed acute mephedrone toxicity. Clin. Toxicol. 48 (2010) 924–927.

Wright Jr, M.J., Vandewater, S.A., Angrish, D., Dickerson, T.J., Taffe, M.A. Mephedrone (4-methylmethcathinone) and d-methamphetamine improve visuospatial associative memory, but not spatial working memory, in rhesus macaques. Br. J. Pharmacol. 167 (2012) 1342–1352.

Yohannan, J.C., Bozenko Jr, J.S. The characterization of 3,4-methylenedioxypyrovalerone (MDPV). Microgram J. 7 (2010) 5–15.

Young, R., Glennon, R.A. Cocaine-stimulus generalization to two new designer drugs: Methcathinone and 4-methylaminorex. Pharmacol. Biochem. Behav. 45 (1993) 229–231.

Zaitsu, K., Katagi, M., Kamata, H., Kamata, T., Shina, N., Miki, A., Tsuchihashi, H., Mori, Y. Determination of the metabolites of the new designer drugs bk-MBDB and bk-MDEA in human urine. Forensic Sci. Int. 188 (2009) 131–139.

Zaitsu, K., Katagi, M., Tatsuno, M., Sato, T., Tsuchihashi, H., Suzuki, K. Recently abused β-keto derivatives of 3, 4-methylenedioxyphenylalkylamines: A review of their metabolisms and toxicological analysis. Forensic Toxicol. 29 (2011) 73–84.